Max-Planck-Institut für Astronomie

Heidelberg-Königstuhl

Annual Report 2002

MAX-PLANCK-GESELLSCHAFT

Cover Picture:
The Max Planck Institute for Astronomy on top of the Königstuhl. In the background downtown Heidelberg and the Neckar valley. (Photo: Walter Rauh und Axel M. Quetz)

Max-Planck-Institut für Astronomie

Heidelberg-Königstuhl

Annual Report 2002

Max-Planck-Institut für Astronomie

Staff:
The MPIA currently employs a staff of 205 (including externally funded positions). There are 40 scientists and 53 junior and visiting scientists. Students of the Faculty of Physics and Astronomy of the University of Heidelberg work on dissertations at the degree and doctorate level in the Institute. Apprentices are constantly undergoing training in the Institute's workshops.

Address: MPI für Astronomie, Königstuhl 17, D-69117 Heidelberg
Telephone: 0049-6221-5280, *Fax:* 0049-6221-528 246
E-mail: sekretariat@mpia.de
Anonymous ftp: ftp.mpia.de
Isophot Datacenter: phthelp@mpia.de
Internet: www,mpia.de

Calar Alto Observatory
Address: Centro Astronómico Hispano Alemán,
Calle Jesús Durbán 2/2, E-04004 Almería, Spain
Telephone: 0034-50-230 988, - 632 500, *Fax:* 0034-50-632 504
E-mail: name@caha.es

Masthead

Editors: Jakob Staude, Thomas Henning
Text: Thomas Bührke
Translation: Margit Röser
Illustrations: MPIA and others
Graphik und picture editing: Axel M. Quetz, Martina Weckauf, Karin Meißner-Dorn
Layout: Marita Beyer, Modautal
Printing: Koelblin Fortuna, Baden-Baden
ISSN 1437-2924; *Internet:* ISSN 1617 – 0490

Contents

I General

I.1 The Max Planck Institute for Astronomy – Past, Present, and Future

Since it was established in 1967, the Max Planck Institute for Astronomy (MPIA, Fig. I.1) is dealing with the formation and evolution of stars and galaxies. According to its foundation statute, research is focused on the optical and infrared wavelength range. It is the goal of MPIA to significantly advance astrophysical research by building telescopes and their auxiliary instruments, by direct observations, and by interpretation of the data obtained. In addition to the home institute in Heidelberg, MPIA operates the German-Spanish Astronomical Center (DSAZ), generally known as the **Calar Alto Observatory** (Fig. I.2). It is situated on the Calar Alto Mountain (height 2168 meters), in the province of Almería in southern Spain, where good climatic and meteorological conditions for astronomical observations are found.

The instruments developed and built at the Institute are used for ground-based as well as for satellite-borne observations. Both kinds of observation are ideally complementing each other. Ground-based telescopes mostly have larger primary mirrors and therefore a larger light-gathering power than space telescopes. By using modern techniques like adaptive optics and interferometry – in the development of which MPIA plays a leading role –, they achieve higher angular resolution. Space telescopes are compulsory for observations in wavelength regions where the atmosphere absorbs the radiation or generates a perturbing background.

In developing instruments for the infrared, MPIA has been very successful in the past. It was participating significantly in the world's first Infrared Space Observatory (ISO) of the European Space Agency ESA: ISOPHOT, one of four scientific instruments on board of ISO, was built under the coordinating leadership of the Institute. From 1996 to 1998, ISO provided excellent data, particularly in the hitherto inaccessible far-infrared range. The valuable

Fig. I.1: The Max Planck Institute for Astronomy on the Königstuhl Mountain in Heidelberg.

Fig. I.2: The Calar Alto Observatory.

know-how gained this way will be exploited by the Institute's scientists in future projects like the HERSCHEL space telescope and the Next Generation Space Telescope (recently re-named James Webb Space Telescope, JWST). Based on ISO data, meanwhile more than thausand scientific papers have been published.

With the Calar Alto Observatory, MPIA commands one of the two most efficient observatories in Europe. Three telescopes with apertures of 1.2, 2.2, and 3.5 m are operating there. About half of the time they are available to all German astronomers. Furthermore, about 75% of the observing time of a 2.2 m telescope working on La Silla, Chile, has been loaned by MPIA to the European Southern Observatory (ESO).

In addition, the Institute is participating in a series of international collaborations for building new large telescopes and scientific instruments, thereby gaining access to the world's most important observatories. In the southern hemisphere, this is the ESO Very Large Telescope (VLT) in Chile, with its four 8 m telescopes being the world's most powerful observatory. In the northern hemisphere, MPIA is participating in the Large Binocular Telescope (LBT) in Arizona, which will be put into full operation in 2005. By then, this extraordinary telescope will be equipped with two mirrors of 8.4 m diameter each, fixed on a common mount, making it the world's largest single telescope. These two collaborations enable MPIA's astronomers to observe the northern and the southern sky with first-class telescopes.

I.2 Scientific Goals

Two main research fields have crystallized at the Institute, on the one hand the formation of stars and planets, on the other hand cosmology, particularly the formation and evolution of galaxies. Although these two fields are clearly separated in terms of their research subjects, there are nevertheless many common points of contact. Star formation in the early Universe, e.g., is closely related to the formation and evolution of galaxies. Observations with the best instruments available as well as computer simulations carried out by a theory group also working at the Institute are the foundations of scientific progress.

Formation of Stars and Planets

The first stages of star formation take place in the interiors of dust clouds, and hence remain hidden from our view in visible light. Infrared and submillimeter radiation, however, can penetrate the dust, which is why the early stages of star formation are being studied preferentially in this wavelength range. For this reason, the focus of astronomical observation at MPIA has in the recent past shifted more and more from the optical to the infrared spectral range.

Using ISOPHOT as well as sub-millimeter telescopes very cold and dense regions have been detected within large dust clouds – protostellar cores which are on the verge of collapse or already contracting to form stars. In a later stage, the central (proto-) star is already taking shape. It is surrounded by a disk of gas and dust where planets can form. But there is also a possibility of forming a binary or multiple stellar system. What are the conditions for either process to take place? This is one of the questions astronomers at MPIA want to answer, for example by using the NACO (NAOS and CONICA) high-resolution camera and the MIDI interferometer for the mid-infrared range, both at the VLT.

Recently, the investigation of brown dwarfs has also gained significance. These are "failed" stars with masses too low to provide enough pressure within their cores for hydrogen to fuse continuously into helium. They are distinguished from planets with even lower masses by the fact that in the first instance they are formed like other stars. The first brown dwarf had been discovered as late as 1995; meanwhile a little over hundred are known.

But many questions still remain open. How do brown dwarfs form precisely? Which properties do they have and how common are they? Are they too, like stars, initially surrounded by a disk of gas and dust? Scientists at MPIA recently made important contributions to answer these questions. A few years ago they found free floating planetary objects with a few Jupiter masses. This discovery shed new light on the formation of stars and planets and brought up the issue of re-defining stars, brown dwarfs and planets.

Studying massive stars is also of growing interest. Here, for one thing, questions about their formation are yet unanswered: How do their early stages differ from those of low-mass stars? Are they, too, surrounded by disks where planets can form? Massive young stars are very hot, driving strong particle winds that affect the formation of other stars in their neighborhood. How this happens is another important issue. Finally this is the only kind of star formation, which we can observe in other galaxies.

These problems can best be studied in nearby star formation regions in our own Milky Way while the observation of star formation regions in other galaxies offers the opportunity to tackle other problems. Here, galaxies are seen as a whole, thus allowing to measure star formation rates, for example. So it is possible to determine the rates in different galaxy types or as a function of the surroundings of the respective galaxies. Another question of current interest is how UV emission and particle winds affect the interstellar medium and thereby the entire morphology of galaxies. Observations will be complemented by a close collaboration with colleagues at the Universität Jena who do experimental "laboratory astrophysics". A small group residing there will form a branch of MPIA, investigating spectroscopic properties of dust particles with sizes in the nano- and micrometer range as well as performing spectroscopy of molecules in the gaseous phase. Findings obtained here under controlled conditions can be used to interpret astronomical observations.

Galaxies and Cosmology

The second research field at MPIA deals with the formation and evolution of galaxies as well as with their structure. How did the first galaxies form? What was the star formation rate in the early Universe? Did galaxies merge, thereby reducing their total number over the billions of years? What effect does dark matter have on these processes? These are only some of the questions studied at MPIA. In the recent past, interest has focused more and more on the role of massive black holes residing at the centers of active galaxies. To get a clear picture of what is going on there, astronomers at the Institute have access to the data of the Sloan Digital Sky Survey (SDSS). In the future, detailed studies will use mainly the NACO and

MIDI instruments, which allow to investigate the immediate vicinity of the black holes.

The study of the formation of galaxies and their evolution in the early Universe makes extreme demands on current observation techniques. Great progress was recently made thanks to deep sky surveys such as the Faint Infrared Extragalactic Survey (FIRES). It combines images of the HUBBLE Space Telescope in visible light with new near-infrared images obtained with the VLT. These are the deepest and best images in this wavelength region to date. The goal is, among other things, to determine the magnitude distribution, sizes and shapes of galaxies over a wide redshift range and the evolution of their stellar components.

Pursuing a similar goal is the COMBO 17 (Classifying Objects by Medium-Band Observations with 17 Filters) survey which is conducted at the MPG/ESO 2.2 m telescope on La Silla. Here, a wide-field camera developed at MPIA is used. The data already obtained will be complemented in the near future by infrared observations on Calar Alto. On a medium-term basis, the PRIME mission will yield further valuable data.

The structure of galaxies can be studied in detail only in nearby galaxies like those of the Local Group or in the Milky Way itself. Here too, the Institute makes great efforts. So, for instance, it was possible for the first time to determine the orbit of a globular cluster (Palomar 5) with high accuracy (Chapter II). From these data and additional information on the structure of the cluster the gravitational potential of the Milky Way system can be deduced – which in turn gives interesting information about the distribution of dark matter within the halo of our Galaxy.

Ground-based Astronomy

During the last years, MPIA has made great efforts in developing **adaptive optics systems**. Construction of the ALFA adaptive optics system for Calar Alto has been completed; including experiments with an artificial laser guide star. For the first time, also a new coronograph could be tested, based on the phase masking technique. Currently, this field of research is carried on, by developing a multiconjugate adaptive optics system. Experience gained in this work will be incorporated into the development of new instruments for the VLT and LBT.

Participation of the Institute in the VLT (Fig. I.3) is of major importance. While in 2001 the CONICA high-resolution infrared camera combined with the NAOS adaptive optics system was successfully put into operation (Fig. I.4), MIDI saw first light at the end of 2002 (Chapter II). It is the first large interferometric instrument at the VLT and is used in the mid-infrared range. From 2003 on, the trend-setting MIDI instrument is planned to allow interferometric observations with a resolution of only a few hundredths of an arc second.

At the end of 2001, ESO called upon all institutes of its member countries to present proposals for second-generation instruments for the VLT. Thereupon a consortium of 12 institutes in Germany, Italy, Switzerland, the Netherlands and Portugal was founded at MPIA proposing the PLANET FINDER project. PLANET FINDER is supposed to be an adaptive optics system for direct detection, spectroscopy and polarimetry of extrasolar planets. For this project, MPIA can rely particularly on its experience with the construction of the ALFA adaptive optics system.

Together with the University of Arizona and Italian institutes, MPIA is a partner in an international consortium, which is building the **Large Binocular Telescope** (LBT, Fig. I.5). This large telescope consists of two mirrors of 8.4 m diameter each, fixed on a common mount. Together, the two mirrors have a light-gathering power equivalent to a single 11.8 m mirror. This will make the LBT the world's most powerful single telescope. Furthermore, the unique structure of the double mirror is especially well suited for interferometric observations. Its spatial resolution will correspond to that of a single mirror 22.8 m in diameter. First light with only one primary mirror is currently planned for mid-2004. One year later, the entire telescope will be put into operation.

Under the leadership of the Landessternwarte Heidelberg, the German partners are building the LUCIFER near-infrared spectrograph for the LBT (Chapter IV). MPIA will supply the entire detector package and develop the overall design of the cryogenic system. Integration and tests of the instrument will also be carried out in the laboratories of MPIA. Simultaneously, planning of the LBT interferometer, which will be equipped with an adaptive optics system, is in full swing. For this instrument, MPIA is developing the optics of the LINC beam combiner, which finally will allow interferometry over a wavelength range between 0.6 and 2.2 μm. This requires an extremely ambitious optical design. For this project, an informal consortium with colleagues from the Universität Köln and the Astrophysical Observatory in Arcetri near Florence was formed.

Fig. I.3: The Very Large Telescope, situated in the Chilean Andes. (Image: ESO)

Fig. I.4: The NACO high-resolution camera with adaptive optics at the VLT.

Fig. I.5: The building of the Large Binocular Telescope in summer 2002.

Extraterrestrial Research

Since it was established, MPIA has been involved in space-based astronomy. In particular, an early start in infrared astronomy associated with these activities has been of great significance for the later development of the Institute as a whole. In the 1970's, two photometers were developed and built at MPIA which flew successfully on board the two solar probes HELIOS 1 and 2. Around the same time, the THISBE infrared telescope (Telescope of Heidelberg for Infrared Studies by Balloon-borne Experiments) was developed. It was carried by a high-altitude research-balloon up to an altitude of 40 km, where for short times excellent infrared observations are already possible.

MPIA is also participating significantly in the ISO project of the European Space Agency ESA: ISOPHOT, one of four scientific instruments on board of ISO, was built under the coordinating leadership of the Institute. For over two years, ISO collected excellent data. It was switched off on 8 April 1998, after its coolant supply had been exhausted. Meanwhile, numerous papers in all fields of astronomy have been published, documenting the efficiency of this space telescope.

At present, MPIA runs the ISOPHOT data center where first of all programs and calibration procedures for the automatic data analysis were developed. The final software that created the ISO Legacy Archive is now running at the ISO data center at VILSPA, Spain. An active archive phase, during which the data will be calibrated with high accuracy, will last for a period from 2002 to 2006. The goal is to expand the ISO database to be part of a globally accessible "virtual observatory" for all wavelength ranges.

The experience gained with ISOPHOT was decisive for the MPIA's significant participation in the construction of the PACS imaging spectrometer for the far-infrared spectral range. This instrument will operate on board the European HERSCHEL infrared observatory (Chapter IV). The launch of this 3.5 m space telescope is scheduled for 2007.

The Institute will also participate in the successor to the HUBBLE space telescope, the James Webb Space Telescope (JWST) (Fig. I.6). The JWST will be equipped with a folding primary mirror about 6 m across as well as three focal-plane instruments. As part of a European consortium, MPIA will develop the cryo-mechanics for the positioning of the optical components in one of the three focal-plane instruments called MIRI (Chapter IV). This instrument designed for the mid-infrared range from 5 - 28 μm consists of a high-resolution camera and a spectrometer of medium resolving power. MIRI will be built half by American and half by European institutes, which will be granted guaranteed observation time in exchange for their contributions.

At the same time, MPIA is partaking in the development of the second focal-plane instrument of the JWST, a near-infrared-multi-object spectrograph called NIRSPEC. Here too, the Institute is supposed to deliver the cryo-mechanics. Such a contribution would provide the astronomers at MPIA with further excellent possibilities for high-resolution infrared observations. Thanks to the successful development of ISOPHOT and PACS, the Institute is well prepared for both tasks, MIRI and NIRSPEC.

Furthermore, MPIA is participating in a satellite experiment proposed to NASA by Johns Hopkins University, Baltimore. This telescope, known as PRIME (Primordial Explorer), is intended to map a large part of the sky down to a magnitude of 24.5 in the wavelength range between 0.9 and 3.4 μm. It would consist of a 75 cm telescope,

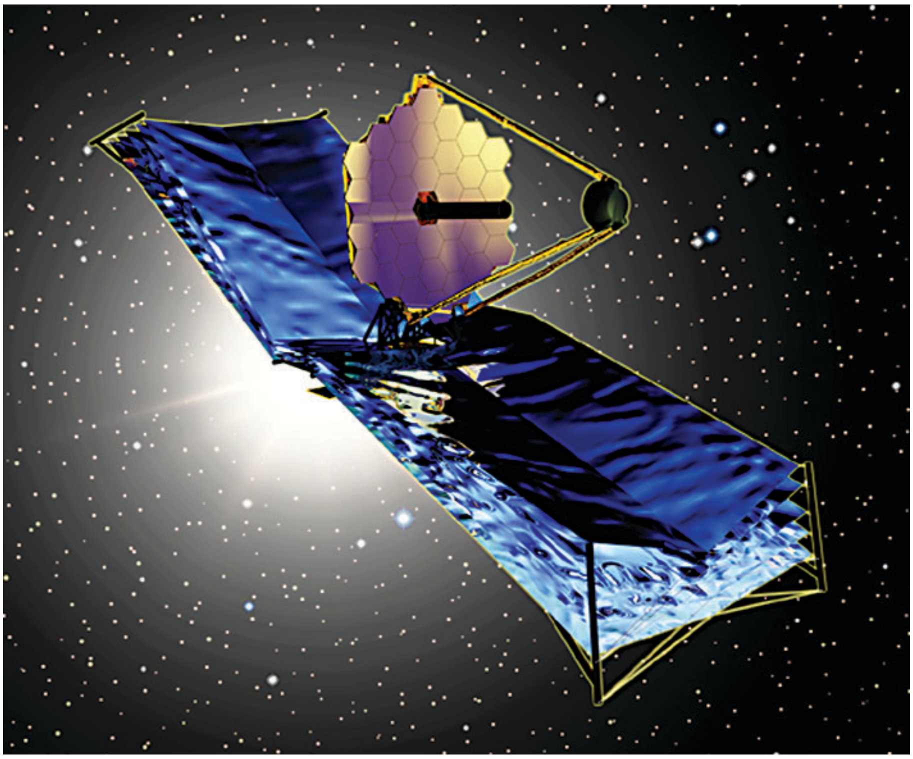

Fig. I.6: Possible structure of the NGST, with the large primary mirror and the characteristic solar screen. (Image: TRW)

which could scan a quarter of the entire sky within three years with unprecedented accuracy.

PRIME successfully passed the scientific and technical reviews. In summer 2002, however, NASA decided that the project could not be realized within the scope of their small-size missions (SMEX). Together with their colleagues at Johns Hopkins University, scientists at MPIA are currently looking for possibilities either to cut down costs or to develop an expanded version of PRIME, which then could be carried out as a NASA medium-size mission (MIDEX).

Since 1998, MPIA represents Germany within the DARWIN Science Advisory Group. DARWIN (Fig. I.7) is a space interferometer to be launched by the European Space Agency ESA between 2012 and 2015. According to current plans it will comprise up to eight telescopes orbiting the sun at the Lagrangian point L2 in 1.5 million kilometers distance from Earth. This observatory will be used for imaging and spectroscopy of extrasolar planets in the mid-infrared range. At present, the Institute is participating in preparatory technology studies.

MPIA is also contributing to ESA's GAIA project, a space observatory scheduled for launch between 2010 and 2015. GAIA will be the successor of the HIPPARCOS astronomy satellite, exceeding the latter's sensitivity by several orders of magnitude. GAIA is planned to measure positions, magnitudes and radial velocities of one billion stars plus numerous galaxies, quasars and asteroids. The telescope will provide photometric data in 15 spectral bands as well as spectra in a selected spectral range. Unlike HIPPARCOS, however, GAIA will not be provided with an input catalogue. An automatic object classification will thus be of major importance for data analysis. This problem is currently dealt with at the Institute. In addition, a representative of the Institute is part of the GAIA Science team and fellow coordinator of the GAIA Classification Working Group.

Figure I.8 gives an overview of the major instruments which are already working or are about to be put into operation. Sensitivity is shown as a function of wavelength (above), and spatial resolution as a function of the size of the image field (below).

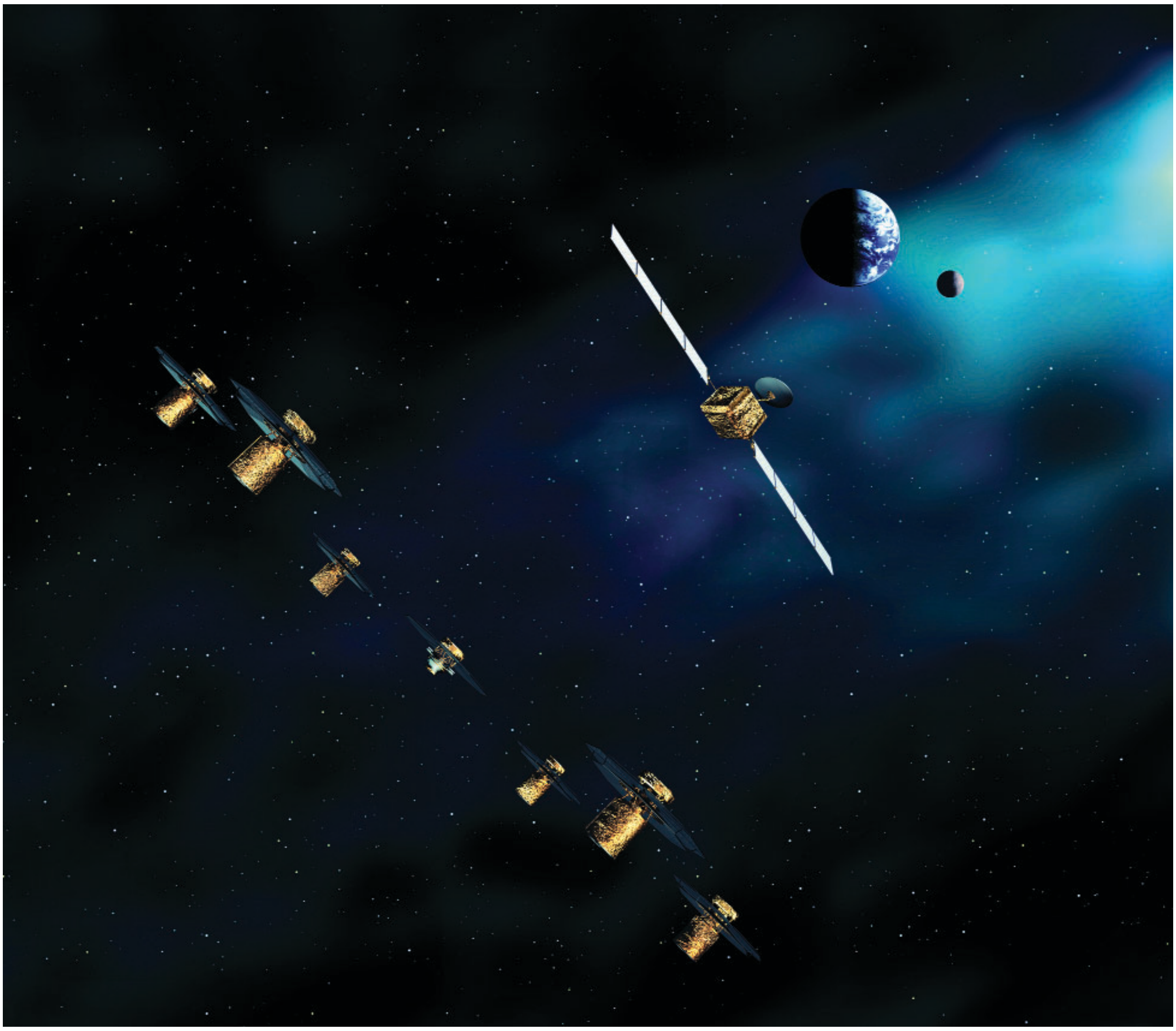

Fig. I.7: Possible concept of the DARWIN space interferometer with eight free-flying individual telescopes. (Image: ESA/ALCATEL)

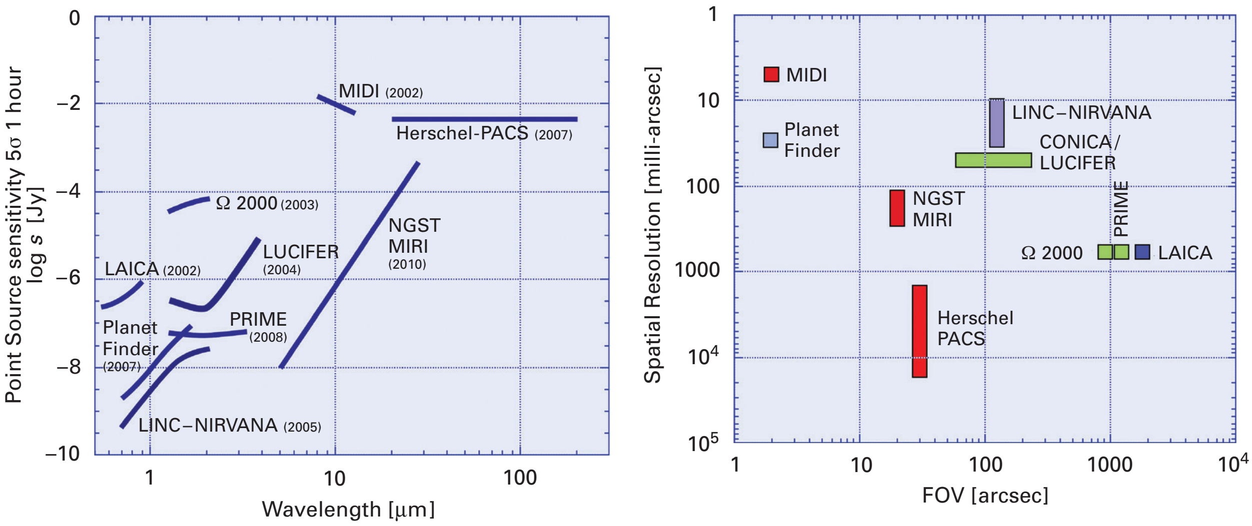

Fig. I.8: The Institute's major instruments. Above: the sensitivity as a function of wavelength; below: the spatial resolution as a function of the size of the field of view.

I.3 National and International Cooperation

Thanks to its location in Heidelberg, the Institute is able to work within an especially active astronomical environment. Cooperation with the Landessternwarte, the Astronomische Rechen-Institut, the Institut für Theoretische Astrophysik der Universität or the department Kosmophysik of the MPI für Kernphysik occurs over and over again in manifold ways. Presently, this is especially true for the Sonderforschungsbereich 439, "Galaxies in the young Universe", in which all Heidelberg institutes named above are participating. Moreover, the Astronomische Rechen-Institut and the Landessternwarte cooperated with MPIA in the DIVA project.

Collaboration with the MPI für extraterrestrische Physik in Garching and the MPI für Radioastronomie in Bonn as well as with institutes of German universities is quite common. Examples for such a collaboration are the ALFA adaptive optics system and the future PARSEC laser-guide-star project in which the MPI für extraterrestrische Physik is participating.

The establishment of the **German Center for Infrared and Optical Interferometry** (Frontiers of Interferometry in Germany, or FRINGE for short), located at MPIA, emphasizes the Institute's leading role in Germany in this trend-setting astronomical technique. The goal is to coordinate efforts made by German institutes in this field. FRINGE will gather tools and software developed by participating institutes. Another concrete goal is the definition of the next generation of interferometric instruments. This includes the extension of MIDI up to 20 μm wavelength and the design of MIDI II, participation in the definition of new imaging capabilities of the VLT interferometer, and participation in preparing the DARWIN space mission. FRINGE will seek to establish cooperation with

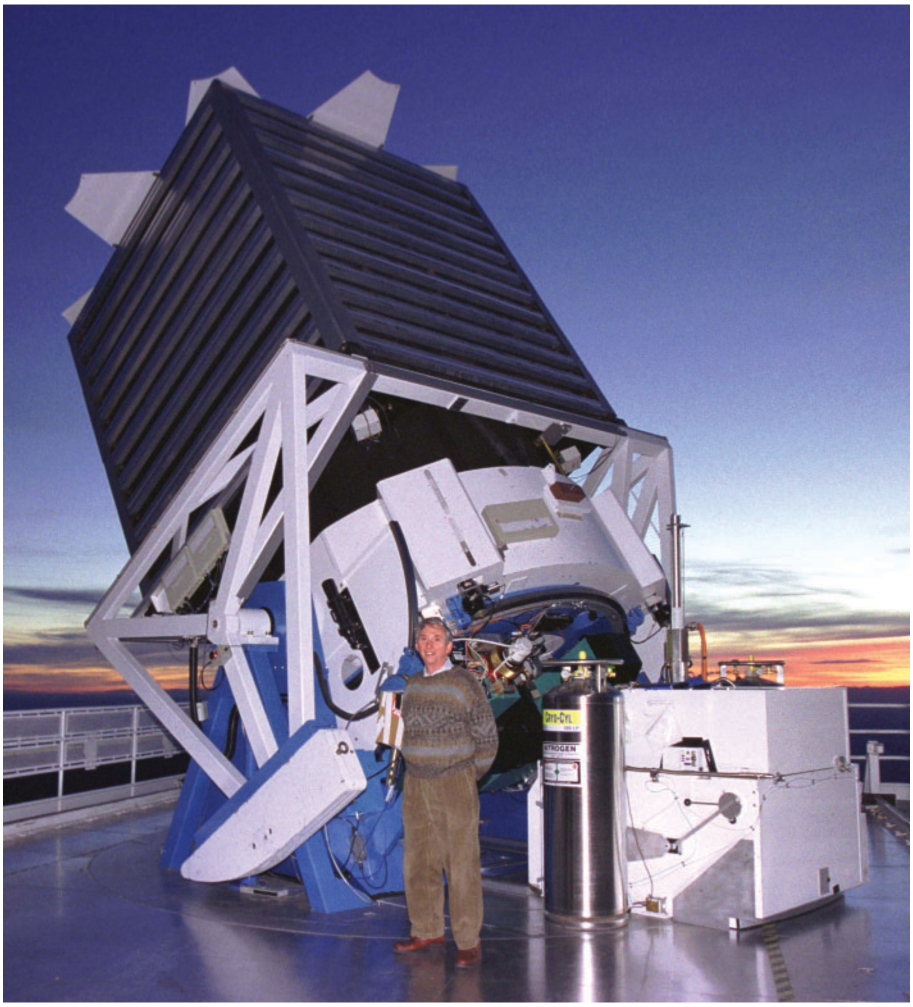

Fig. I.9: The 2.5 m telescope of the Sloan Digital Sky Survey. (Image: SDSS) other interferometric centers in Europe. The long-term perspective is to establish a European interferometric center for the optical and infrared wavelength region. Apart from MPIA, the following institutes are participating in FRINGE: the Astrophysikalische Institut Potsdam, the Astrophysikalische Institut and Universitätssternwarte der Universität Jena, the Kiepenheuer-Insitut für Sonnenphysik in Freiburg, the MPI für extraterrestrische Physik in Garching, the MPI für Radioastronomie in Bonn and the I. Physikalische Institut der Universität zu Köln.

MPIA is participating in a number of **EU-networks**, partly in a leading position. This includes:

- OPTICON: Network of all operators of major telescopes in Europe. The goal is to increase scientific results and reduce costs.
- PLANETS: Program to study theoretical and experimental aspects of planet formation.
- Adaptive Optics for Extremely Large Telescopes: Funding of an adaptive-optics simulator. Here, MPIA can contribute its rich experience with ALFA.
- SISCO: Study of the evolution of galaxies by means of sky surveys. Here too, the Institute was already able to contribute significantly with CADIS and COMBO 17.
- SIRTF Legacy Program: The NASA SIRTF infrared telescope is to be launched in August 2003. Within the scope of a so-called Legacy program, collaborations are enabled to carry out large observation programs. MPIA is participating in such a program, which is already approved, which is devoted to the question, how long it takes, until planetary systems are formed.

At the international level, participation in the **Sloan Digital Sky Survey** (SDSS) is of major importance (Fig. I.9). This, is the hitherto most extensive sky survey, imaging about a quarter of the entire sky in five filters. The final catalogue will provide positions, magnitudes, and colors of an estimated one hundred million celestial objects as well as redshifts of about one million galaxies and quasars. The observations are made with a 2.5 m telescope specially built for this purpose at the Apache Point Observatory, New Mexico. The project is conducted by an international consortium of US-American, Japanese, and German institutes. In Germany, MPIA in Heidelberg and the MPI für Astrophysik in Garching are involved. In exchange for material and financial contributions to the SDSS from MPIA, a team of scientists at the Institute gets full access to the data.

Teaching and Public Relations

Although students from all over the world are coming to the Institute to do their Diploma or doctoral thesis, a majority of the scientific recruits complete their studies at the University of Heidelberg. For that reason, a number of scientists at MPIA give lectures there.

The Institute's tasks also include informing the general public about results of astronomical research. So members of the Institute give talks at schools, adult education centers and planetaria. They also appear at press conferences or on radio and television programs, in particular on the occasion of astronomical events, which attract major public attention. Numerous groups of visitors come to the MPIA on the Königstuhl and the Calar Alto Observatory. A one-week teacher training course, which is very popular among teachers of physics and mathematics in Baden-Württemberg is held regularly in autumn at MPIA.

Finally, the monthly astronomical journal **Sterne und Weltraum** (Stars and Space), co-founded 1962 by Hans Elsässer, founding director of MPIA, is published at MPIA. This journal is intended for the general public but also offers a lively forum both for professional astronomers and for the large community of amateurs in this field.

II Highlights

II.1 Formation and Evolution of Brown Dwarfs

In recent years, astronomical research has focused increasingly on brown dwarfs. Because of their nature as a connecting link between stars and planets they are of special interest. Are they more similar to stars or rather to planets? How do they form? In the year under report, astronomers at the Institute were following up these questions. For the first time they were able to show that young brown dwarfs, like stars, are surrounded by dusty disks. On the other hand, brown dwarfs do not seem to exist in binary systems as frequently as stars do – this may indicate differences in the evolution history of stars and brown dwarfs. In a third investigation, it was possible to measure brightness variations of a putative brown dwarf that can be explained by temporary dust clouds within its atmosphere.

With respect to their masses, brown dwarfs are ranking between stars and planets. If the mass of a celestial body is below about 0.07 solar masses (corresponding to 75 Jupiter masses), temperature and pressure in its central region do not get high enough to start nuclear hydrogen burning. Only the fusion of deuterium and tritium can be ignited for a short period of time, but is turned off again soon after. Then the body cools down. If its mass is smaller than about 13 Jupiter masses, even deuterium-tritium burning is no longer possible. The masses of planets, asteroids and moons of the solar system are within this range.

The presence of brown dwarfs had already been predicted 40 years ago. But due to the low luminosities of these objects and their maximum intensity lying in the infrared range because of their low temperature, the first brown dwarf was not detected until 1995. During the past years, other objects of this kind have been found using different strategies. Near-infrared sky surveys have proved to be very effective, but only spectroscopy can confirm the nature of the candidates detected. To date, a total of several hundred brown dwarfs has been detected that can be used for comparative and statistical studies.

How do brown dwarfs form?

Three possible ways of forming brown dwarfs are currently discussed.

1) Brown dwarfs form like stars as a result of gravitational collapse of interstellar clouds. If this were true, brown dwarfs, like stars, should be surrounded initially by an equatorial disk of gas and dust. Within such disks, planets are forming within a period of a few hundred million years. This has to take place before the disks are dissolved by particle winds and energetic radiation from their central stars. So, if brown dwarfs are forming like stars, at least the youngest of them should be surrounded by circumstellar disks.

2) Another possibility has come to be known as the concept of “stellar embryos”. According to it, brown dwarfs are forming like stars, but are stopped growing before reaching their possible final size. Such a scenario is conceivable in large interstellar clouds where large numbers of single stars and multiple systems are forming within a small volume. As these stars are constantly moving close encounters are bound to happen. Simulations performed at MPIA have shown that during such “near collisions” individual members of multiple systems can be ejected due to strong tidal forces. If this occurs in an early evolutionary phase their growth is interrupted before they have accumulated enough mass for hydrogen burning to ignite. A brown dwarf that forms this way should have an incompletely developed equatorial disk at most.

3) But brown dwarfs might also form like planets within circumstellar disks around more massive stars. In a densely populated star formation region, they would then be ejected from their system because of gravitational interactions with other stars. In this case, no isolated brown dwarfs surrounded by circumstellar disks should to be found.

Brown dwarfs with circumstellar disks

Therefore, an obvious strategy to solve the question of the formation of brown dwarfs is to search for evidence of circumstellar disks. As brown dwarfs are rather cool the dust of the disks should have temperatures between 100 and 400 K and thus should be best detectable in the mid-infrared range. A few brown dwarfs could be observed in this spectral range with the European ISO Infrared Observatory. But those data were insufficient to confirm or discard the presence of circumstellar disks.

For their study, astronomers at the Institute selected an object that had already been detected by ISO. It is lying in the Chameleon I star-formation region and is called Cha Hα2. At an age of 2 to 4.5 million years, it is still very young. Its mass could not be determined definitely so far: It may be a very low-mass main-sequence star or a massive brown dwarf.

In addition, another seven brown dwarfs as near to us as possible were selected that are not members of a star cluster and that are considerably older. Astronomers observed these objects in the mid-infrared region around 10 μm with the ESO 3.6 m telescope.

Among the seven brown dwarfs only one was detected: LP 944-20, which has a distance of five parsec (16 light years) and an estimated age of about 500 million years (Fig. II.1). The radiation flux measured, however, can easily be explained by emission of the brown dwarf itself if its temperature is assumed to be 2300 K. So the observations do not indicate the presence of circumstellar dust. Quite a different result was obtained for the young object Cha Hα2. It shows strong emission that cannot come from the brown dwarf alone (Fig. II.2).

These are the first ground-based observations of brown dwarfs in the thermal mid-infrared at all. And both objects probably are the faintest sources ever observed with the instrument TIMMI 2 at the ESO 3.6 m telescope – two facts that elucidate the difficulties of this research area.

The new measurements are complementing the older ISO data in an ideal way making it possible now to compare them to numerical models of the thermal emission from circumstellar disks. So far, experts had preferred the so-called flared-disk model, a standard model of the disks of young stars scaled down to the conditions of brown dwarfs. This kind of disk has an optically thin surface layer that is excited by the star's radiation and produces a clear silicate emission feature around 9.7 μm (Fig. II.3, above).

But the fluxes measured in Cha Hα2 are much lower than predicted by this model and do not show any evidence of the silicate emission (Fig. II.2). Astronomers at MPIA therefore modeled a simple disk that is optically thick throughout (Fig. II.3, below). Previous observations have shown a very low extinction of the light from Cha Hα2 excluding the presence of a dense layer of dust in

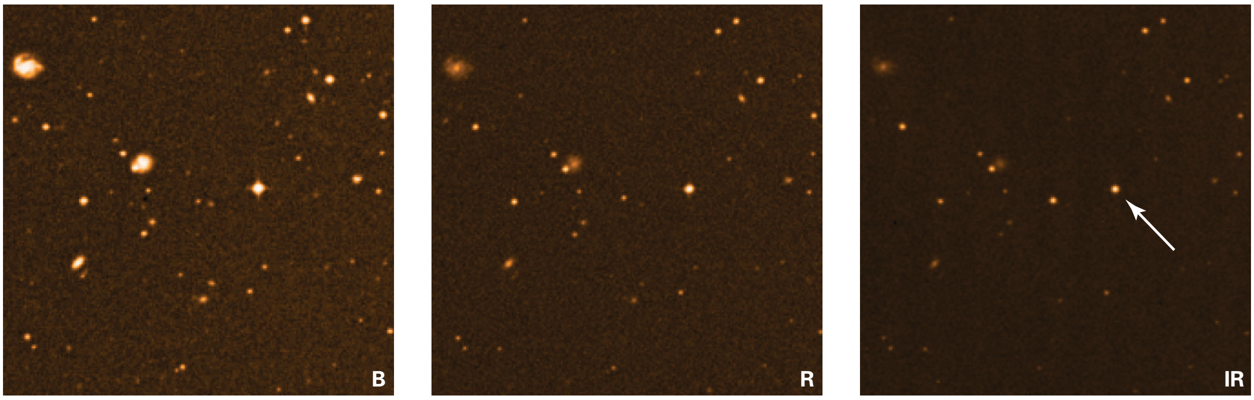

Fig. II.1: Three images of the same field of sky in the blue, red, and near-infrared spectral range. Because of its low temperature the brown dwarf LP 944-20 only appears in the IR-image. (Images: SDSS)

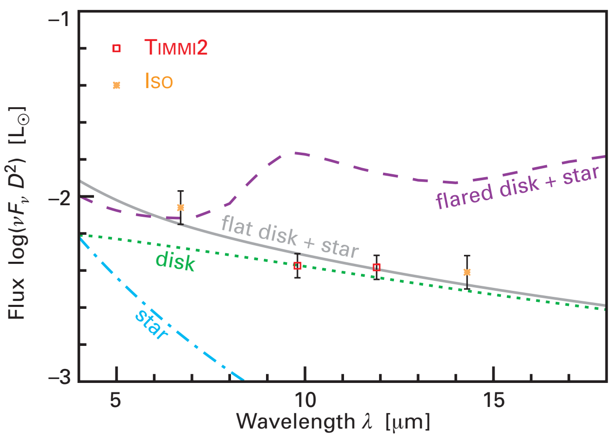

Fig. II.2: Near-infrared measurements of the young brown dwarf Cha Hα2. Models of a flared disk as well as of the star without disk are excluded. But the simple model of an optically thick flat disk matches the data very well.

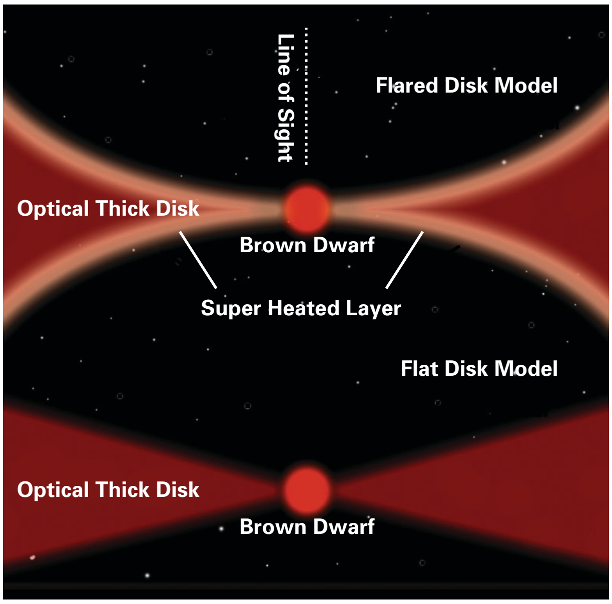

Fig. II.3: Diagram of the flared disk (above) and the optically thick disk of a brown dwarf. (Image: ESO)

front of the brown dwarf. This means that we are seeing the disk nearly face-on. Assuming standard runs for density and temperature yields an emission function that is in very good agreement with the observational data (Fig. II.2).

These data thus give new clues to solve the above-mentioned problem of brown dwarf formation. Observations indicate that young brown dwarfs are surrounded by disks, thereby suggesting that they have formed the same way as normal stars and will loose their disks within a period of a few hundred million years. But it is not possible yet to distinguish between scenario 1 (like a normal star) and 2 ("stellar embryo"); for this, further statistical studies are necessary, wich will besome feasible only with SIRTF.

This has been a first step to solve this important issue. But scientists at the Institute already have gone further by observing brown dwarfs in the millimeter and sub-millimeter regime, too. These data that have not been fully analyzed yet will yield information on the masses of the disks. Other brown dwarfs of different ages will also be examined for dust emission in order to put better constraints on the disks' lifetimes.

Brown dwarfs within binary systems

There is another, completely different approach to reveal information on the formation and evolution of brown dwarfs. About half of the lower- and medium-mass stars in the vicinity of the sun are known to be members of binary or multiple systems. Thus the question arises if this is also true for brown dwarfs.

To answer this question, astronomers at MPIA selected a sample of 134 brown dwarfs that had been detected in infrared sky surveys. The data available up till then suggested that the objects lie at distances between 7 and 105 pc (23 and 340 light years). Astronomers observed these objects with the Wide Field Planetary Camera 2 onboard the HUBBLE Space Telescope. In these images it was possible to detect binary systems with separations down to 0.06 arc seconds, corresponding to projected real separations between 0.4 and 6 Astronomical Units (AU).

The following example illustrates typical conditions found in these systems. For a brown-dwarf binary with characteristic components of 0.045 and 0.02 solar masses the orbital period would be between 1 and 100 years, respectively. Thus, it will be possible to determine the orbits and thereby the masses for at least some pairs of brown dwarfs within the next 5 to 10 years.

Observations showed that 26 of the 134 objects are multiple systems (Fig. II.4). One of it, though, is associated to a G-dwarf in a triple system and was excluded from further analysis. Thus, on first sight, 25 binaries were found in a sample of 133 brown dwarfs, corresponding to a fraction of 19 percent. But for several reasons this value cannot be compared yet to that of stars in the solar neighborhood.

For one thing, only components with differences of magnitudes less than 3 mag could be separated. Therefore, preferentially pairs with similar luminosities were detected. For another thing, all these brown dwarfs were selected from the sky surveys on the basis of their color and brightness. This results in an overrepresentation of distant binaries since the brightnesses of both components (which are not separated on the survey images) add up, thereby passing the detection limit more easily. Nonetheless, it can be concluded from the characteristics of the survey that the data are unbiased with respect to this effect up to a distance of 20 pc (65 light years). This is corroborated by the fact that up to this distance the number density of objects is proportional to the observed volume of space, as expected. Finally, in comparing the binary fraction to that of normal stars it has to be taken into account that due to the camera's resolving power the detections are limited to systems with angular separations wider than of 0.06 arc seconds. Within the observed distance range of up to 20 pc this limit corresponds to a minimum physical separation of 0.04 to 1.2 AU.

The widest possible pair separation that can be detected is limited, too. It is about 4 arc seconds, corresponding

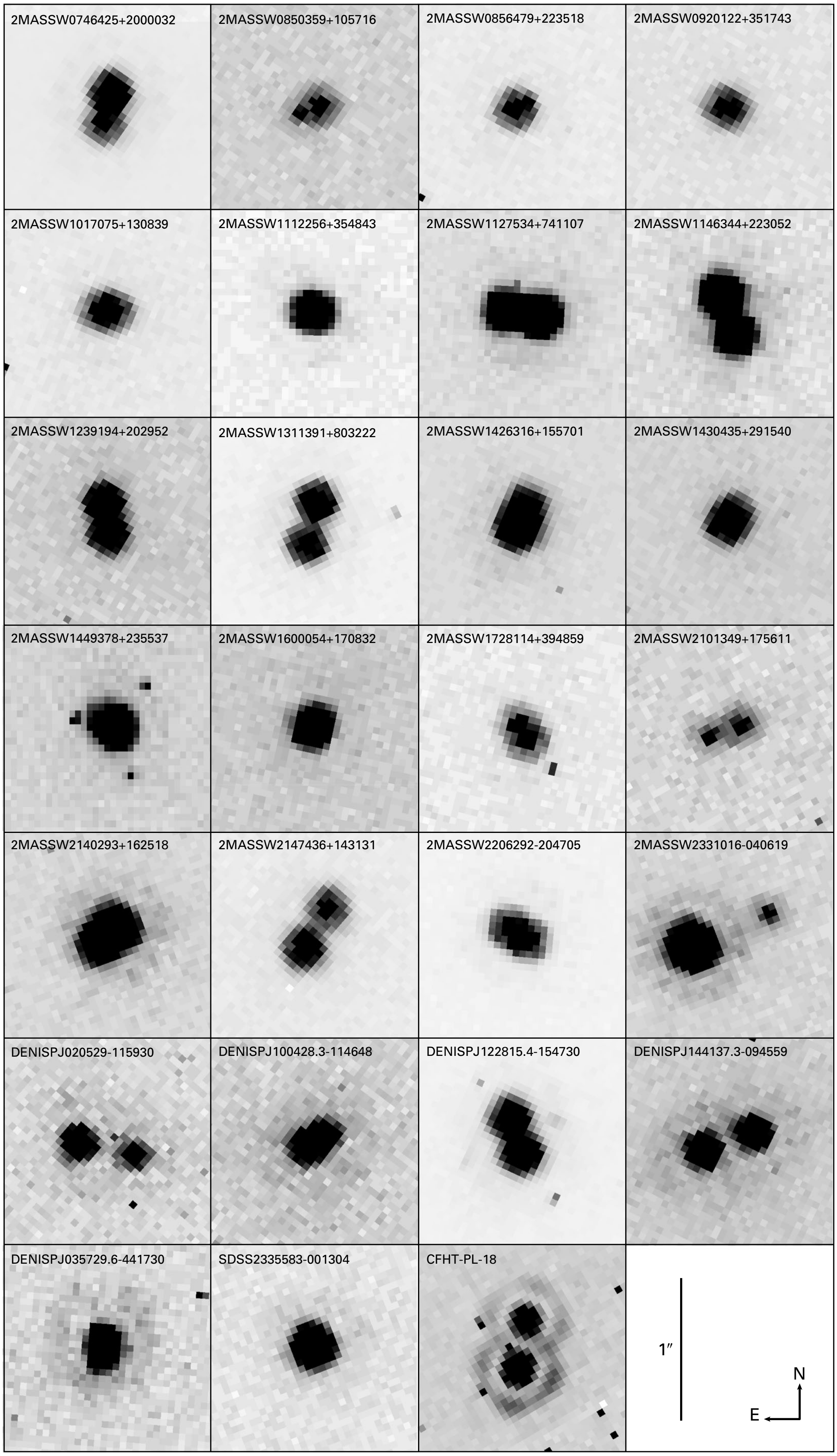

Fig. II.4: Some examples of brown dwarfs in binary systems.

to 28 to 80 AU. However, this is not a serious constraint since binaries with separations wider than 4 arc seconds would already have been found in the sky surveys mentioned above.

In spite of these limitations some very important conclusions can be drawn. Comparing the binary frequency of brown dwarfs to that of G- and M-stars within the same range of separations of their components (0.06 to 4 arc seconds) yields about 10 percent for brown dwarfs in contrast to 33 percent for the stars. This large difference cannot be attributed to a selection effect caused by the named limitations of the sample of brown dwarfs studied, but must be real. As is shown in Fig. II.5 there is a lack of systems with separations wider than 0.6 arc seconds. In addition, the mean separation for brown-dwarf binaries is 4 to 8 AU while it is about 30 AU for double stars. On average, brown dwarfs seem to form closer pairs than stars (Fig. II.6). Both results, too, cannot be explained as a consequence of the limitations of the data.

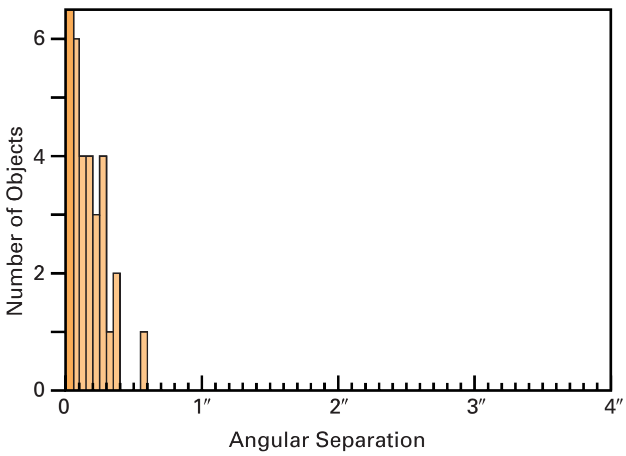

Fig. II.5: Distribution of angular separations of the binary components.

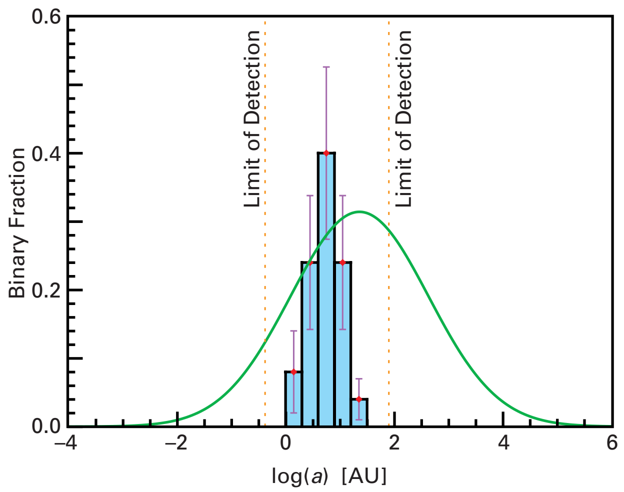

Fig. II.6: Distribution of separations of brown dwarfs (histogram), compared with that of G-dwarfs in the solar neighborhood.

Brown dwarfs seem to have a tendency to form pairs with small differences in brightness and thus also in mass. Fig. II.7 shows that there are almost no systems with brightness differences between the components larger than 1.5 mag. This, too, has to be considered as a real phenomenon. Since the two components of a binary system can be assumed to be coeval, similar luminosities mean that brown dwarfs in binaries are forming preferentially with similar masses. This may be illustrated by the following example: In a 1 billion years old system with a primary of 0.07 solar masses, a companion with a 3 mag lower luminosity still would have 0.06 solar masses.

How do these new findings fit into the formation scenarios of brown dwarfs? First of all, the binary fraction of 10 percent is too high to be explained by hypothesis 3 (planet-like formation). Thus this investigation, too, like that of circumstellar disks, confirms that brown dwarfs form in a way similar to stars.

Hypothesis 2 (stellar embryos being ejected from the star formation region before reaching their final mass) is in contradiction with the presence of bound pairs of brown dwarfs. Such pairs would be disrupted during the close encounters that cause the ejection of brown dwarfs from star forming clouds. Therefore it can be assumed that at least the pairs found here have not formed as stellar embryos. So hypothesis 1 (formation mechanism like stars) is the most likely one to be in agreement with the presence of binary brown dwarfs. However, the lack of binaries with wide separations is still not understood. Theoretical calculations of the formation of brown dwarfs currently carried out at the Institute may help to solve this problem.

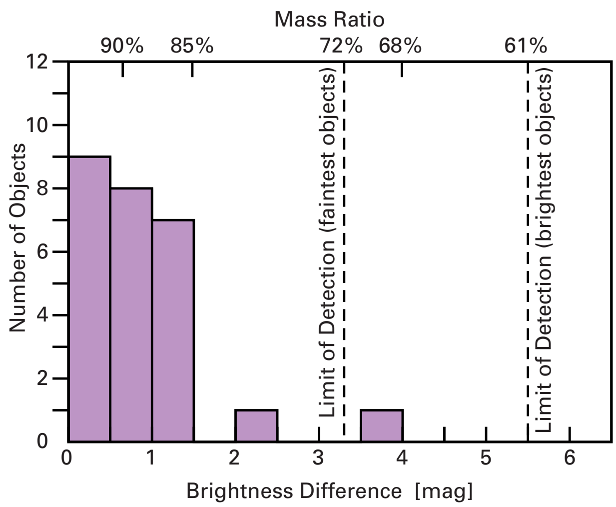

Fig. II.7: Distribution of brightness differences between both components of brown dwarf binary systems.

Dust clouds or magnetic spots?

As demonstrated above, questions concerning the formation of brown dwarfs can be tackled by statistical analysis of as large numbers of objects as possible. But if one wants to learn more about the properties of these objects individual observations are needed, too. Astronomers at the Institute have monitored the brightness variations of 21 ultra-cool dwarf stars using the telescopes on Calar Alto. Ultra-cool dwarfs are objects of spectral type M8 or later. Thus they are candidates for brown dwarfs although in many cases a definite classification is still missing.

In some of these dwarfs variations with timescales of a few hours were found. In general, periodical intensity variability is causally related to the rotation period. Irregular variations, however, can originate from surface phenomena that may evolve on timescales shorter than a rotation period. In very cool objects like brown dwarfs, there are two plausible sources for this kind of variability. For one thing, star spots can cause intensity variations. But up to now it is not known if ultra-cool dwarfs and brown dwarfs develop sufficient magnetic activity at all in order to produce such cool spots. For another thing, it is conceivable that dust clouds are forming at different times within the atmospheres, which also cause brightness variations. In addition, dust is able to affect the spectrum. How this does happen depends on the properties of the dust such as the size distribution of the particles. These properties vary with the temperature of the ultra-cool star or brown dwarf but also can change on shorter timescales.

There are different model predictions for this kind of objects. Within a static atmosphere, tiny dust particles are forming, growing slowly, thereby getting heavier and more massive, and finally sinking down. Thus a dust-free photosphere is created which in addition is deprived of elements that are bound within the dust. The lower the temperature, the lower the dust will sink. Completely static atmospheres, however, seem to be unrealistic for brown dwarfs.

In a dynamical atmosphere, convection occurs which

Fig II.8: Two theoretical spectra of ultra-cool dwarf stars with an effective temperature of 1900 K. The following cases were calculated: Dust cloud in a clear atmosphere (blue solid line), cool magnetic spot in a clear atmosphere (blue dashed), clear region in a dusty atmosphere (red solid), and cool magnetic spot in a dusty atmosphere (red dashed).

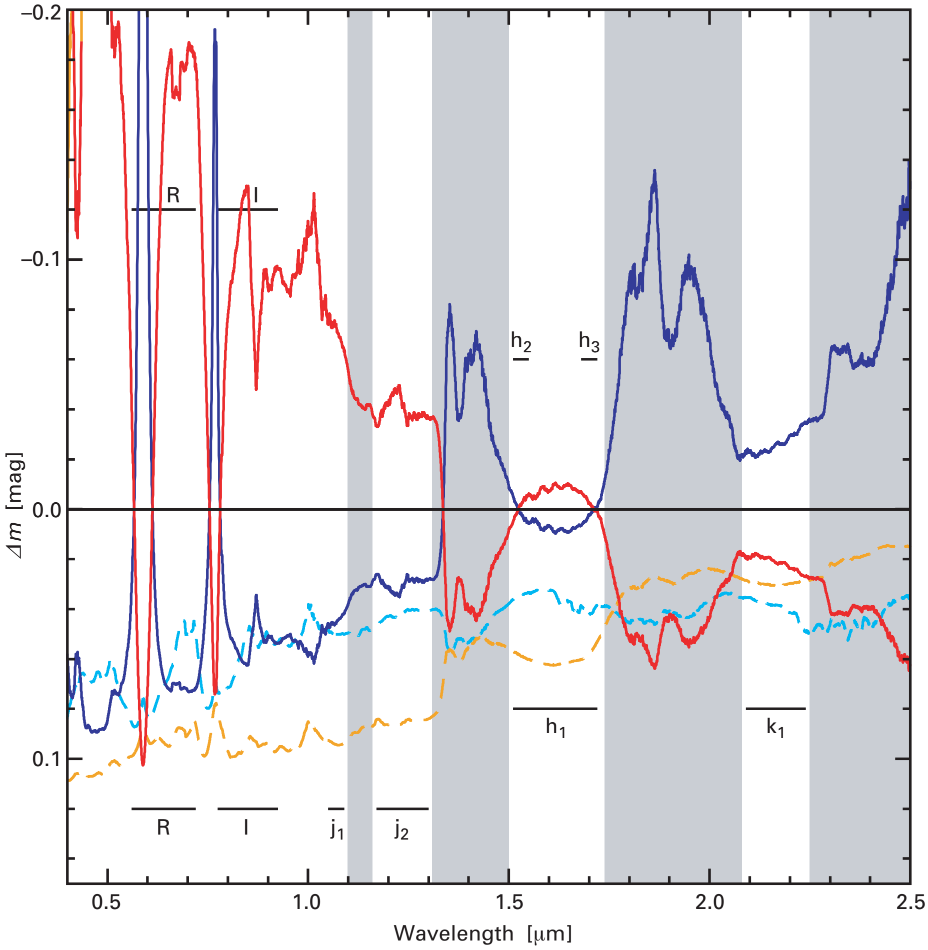

transports dust upwards into the upper photospheric layers. The altitude at which the dust mainly resides within the atmosphere depends on the effective temperature. In such dynamical models also horizontal inhomogeneities occur. Simply put: Clear regions can form in a dusty atmosphere or dust clouds can form in an almost clear atmosphere.

Dust clouds as well as magnetic spots have an effect on the spectrum of an ultra-cool dwarf. In Fig II.8, theoretical model spectra of four different cases are shown: dust clouds in a clear atmosphere, cool magnetic spot in a clear atmosphere, clear region in a dusty atmosphere and cool magnetic spot in a dusty atmosphere. As is clearly evident, significant modifications are expected in specific wavelength regions from which the causes of intensity variations can be determined. But it has always to be kept in mind that theoretical predictions depend on the largely unknown properties of the particles like their sizes and on the characteristics of the convection.

From the 21 brown dwarf candidates, the astronomers selected an object named 2M 1145. It is a dwarf star of spectral type L1.5 with an effective temperature of 1900 K and 0.075 to 0.08 solar masses – characteristics that put it at the borderline to brown dwarfs. The idea was to spectrophotometrically monitor the object 2M 1145 and subsequently look for variations in specific wavelength regions marked by j, h, and k in the Figure.

On each of three successive nights, 2M 1145 was observed in the near infrared at wavelengths from 1 µm to 2.4 µm for several hours with the Omega Cass Spectrograph at the 3.5 m telescope. Data analysis had to be meticulous since the expected intensity variations were of the order a few hundredths of a magnitude only. At first the data for four spectral ranges were combined. No convincing variability was found in any one of these bands. But a significant correlation is found if the differences (h_1-h_2) are plotted against (j_1-j_2) (Fig. II.9).

Such a correlation is more consistent with the model of a ultra-cool star or brown dwarf with a dynamical dusty atmosphere and temporally variable clear regions. But cool magnetic spots in a dusty atmosphere could also produce these effects. The strength of the variation indicates a coverage of the surface by clear atmospheric regions or magnetic spots of not more than 15 to 20 percent.

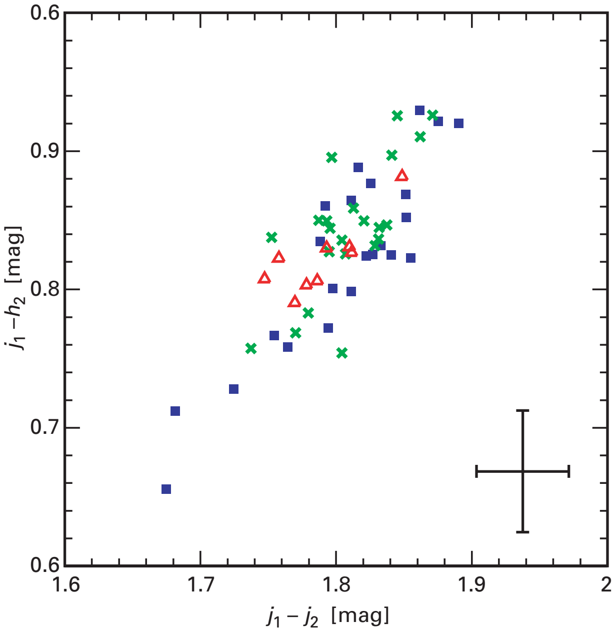

Fig. II.9: Correlation between two relative color ranges in the near infrared.

This is a first step to learn more about the atmospheric characteristics of brown dwarfs. But there are numerous other methods. Currently, spectrophotometric observations in the optical region and spectroscopic measurements of the Doppler shift are planned.

(Daniel Apai, Coryn Bailer-Jones, Wolfgang Brandner, Thomas Henning, Reinhard Mundt, Ilaria Pascucci, Stefan Umbreit

II.2 Palomar 5 – an Archetype of Dissolving Globular Clusters

For two years already, astronomers at MPIA are studying a very faint globular cluster named Palomar 5. During its past passages through the Galactic disk it has lost a great many of its stars and might be disrupted completely next time. New observations reveal two very long tidal tails that together contain more stars than the cluster itself. Further investigations should make it possible, among other things, to determine the gravitational potential of the Milky Way System and thereby the distribution of its dark matter.

The Milky Way is surrounded by about 150 globular clusters that contain ten thousands to some million stars each and that are 13 pc (40 light years) to 130 pc (400 light years) across. They are occupying an extended halo with a diameter of more than 100 kpc (300 000 light years) and move around the Galactic center on elliptical orbits. Globular clusters are generally thought to have formed as the first objects in a giant primordial gas cloud that was still contracting to form a rotating galaxy. Because of its angular momentum the remaining gas cloud later flattened into an equatorial disk. Within this disk the second stellar population of the galactic plane formed, including our Sun.

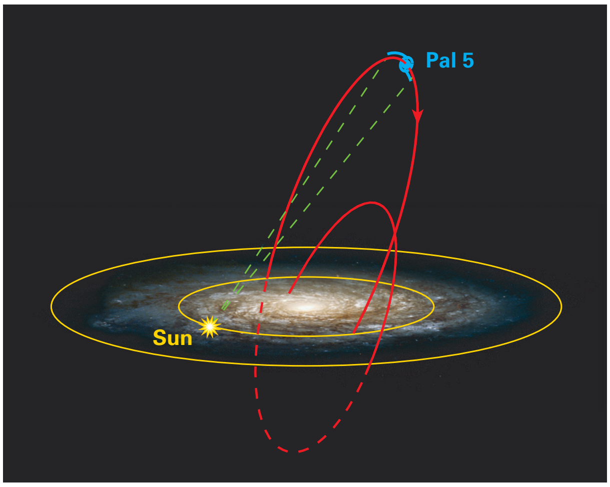

Fig. II.10: Three-dimensional view of the Galactic orbit of Palomar 5, for a period from 500 million years ago until the next passage through the Galactic disk. At present, Palomar 5 is on the far side of the Galaxy and almost at its largest distance to the Galactic center. In about 100 million years from now, it will cross the Galactic disk again, at a distance of only 7 kpc from the center.

Reconstructing the dissolution

Palomar 5 is an old globular cluster presently being at a distance of 23 kpc (75 000 light years) from the Sun and 18.5 kpc (60 000 light years) from the Galactic center (Fig. II.10). With an absolute visual magnitude of -4.8 mag, a total mass of about 5000 solar masses, and a core diameter of 48 pc (156 light years) it is one of the least concentrated, lowest-mass, and least luminous globular clusters known. These characteristics suggested that Palomar 5 may have been shaped by substantial mass loss.

Using the data of the Sloan Digital Sky Survey (SDSS), astronomers of MPIA for the first time found direct evidence that the cluster actually suffers a severe dissolution process. The SDSS is the most extensive sky survey so far: Since April 2000, about a quarter of the entire sky is imaged in five wavelength ranges using a mosaic CCD camera on a 2.5 m telescope at the Apache Point Observatory in New Mexico. The final catalogue will contain positions and colors of an estimated one hundred million celestial bodies as well as the redshifts of about one million galaxies and quasars. The project is conducted by an international consortium of US, Japanese, and German institutes, including MPIA (see Chapter I).

The region containing Palomar 5 was already imaged during the commissioning phase of the SDSS (Fig. II.11). The cluster members which are scattered over a wide area on the sky could be distinguished from the numerous foreground stars due to their position in a color-magnitude diagram (cf. Annual Report 2000, page 57). In this way, clear indications of the presence of tidal tails were found.

Since these first investigations researchers at MPIA have analyzed more data from the SDSS and extended their search for member stars of Palomar 5 over an area of 87 square degrees. In addition, they were able to distinguish cluster members more clearly from other objects using an optimized selection method and thereby to determine more precisely the spatial distribution of the member stars. These new data show the northern tidal tail to extend over an arc of 6.5 degrees. The southern tail is traced over 3.5 degrees till the border of the currently available field. It is probably as long as its northern counterpart (Fig. II.12).

The total length measured corresponds to a size of about 4 kpc (13 000 light years). Both tails are very prominent and with a width of 18 arc minutes, corresponding to 120 pc or 390 light years, relatively thin. Already at a first glance a slightly clumpy structure of the tails is noticed. This implies that the mass loss had been episodic and can be explained as a result of several passages through the Galactic disk, which Palomar 5 has to suffer every 150 to 250 million years.

Fig. II.11: Multicolor composite image of Palomar 5 from the Sloan Digital Sky Survey. The loosely distributed stars of this cluster appear yellowish and blue. They are mainly subgiants and main-sequence stars.

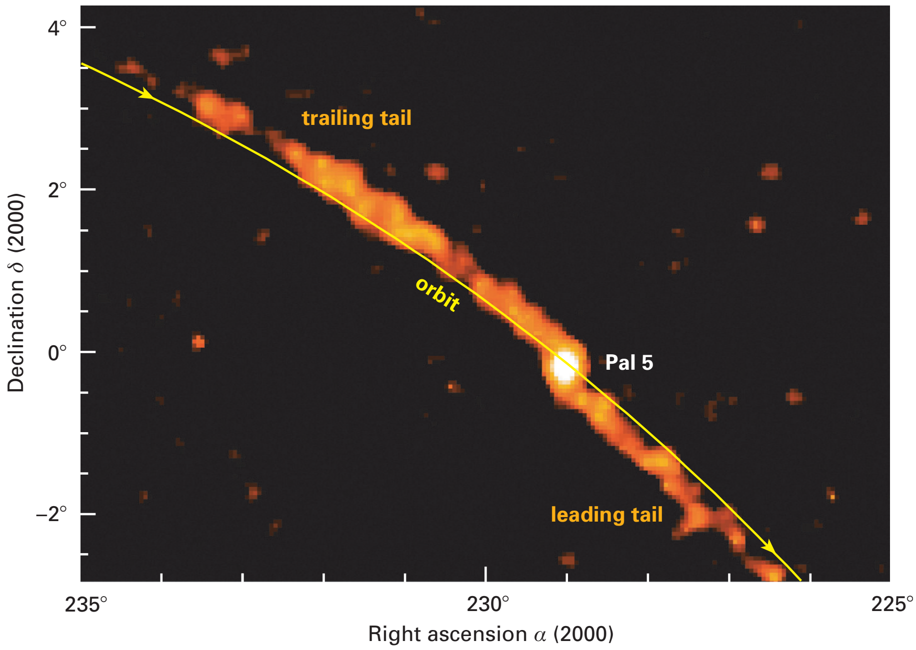

Fig. II.12: Palomar 5 and its two tidal tails in a false-color map illustrating the surface density of the cluster stars in the sky (white corresponds to the highest density in the central region of the cluster).

The boundary between the cluster and its tidal tails is marked by a characteristic break in the radial profile of the stellar surface density. As is shown in Figure II.13 this density decreases as r^{-3} inside a radial distance of about 16 arc minutes from the center. Beyond this distance, which corresponds to the cluster's boundary radius, the profile is flatter and the surface density decreases approximately as $r^{-1.4}$. The decrease of the density profile of the tidal tails thus is somewhat steeper than generally predicted by models in the literature that expect a profile proportional to r^{-1}.

From the number of stars found inside the tails and in the cluster it can be inferred that the tails contain at least 20 percent more mass than the cluster itself. Palomar 5 thus has lost a substantial fraction of its stars during its previous passages through the Galactic disk. The current data already allow to draw some conclusions about its earlier history.

When a globular cluster passes through the Galactic plane it experiences strong, temporally variable tidal forces. These forces supply energy to the cluster stars, thereby changing the stellar orbits. As a result, some stars can leave the immediate gravitational field of the cluster and move towards its outskirts where the gravitational field of the Milky Way dominates. This process eventually leads to the formation of symmetric tails, consisting of stars that are no longer bound to the cluster but still follow its orbit.

Computer simulations also conducted at MPIA allowed to reconstruct the cluster's orbit from the observed location and curvature of the tidal tails together with a model of the Galactic potential. This is shown as a dashed line in Figure II.10. Here, it can also be recognized that both tails are slightly offset from the cluster orbit.

This offset is caused by the following: When stars, driven by the Galactic tidal field, are escaping from the cluster they are either leaving it in the direction of the Galactic center or in the opposite direction. Because of the Galaxy's differential rotation (the orbital velocity decreases with increasing distance to the Galactic center) the trajectories of the "runaways" bend and eventually follow their own orbits around the Galactic center, which are quite similar to that of the cluster.

From the observed offset (about 75 pc in projection, corresponding to an actual offset within the orbital plane of about 240 pc), the velocity of the escaping stars can be estimated and from this in turn follows the mean mass loss of Palomar 5. These computations yielded a mean mass-loss rate of 5 solar masses per million years. Numerical simulations of the dissolution of globular clusters suggest this rate to be more or less constant over long periods of time.

Fig. II.13: Radial profile of the stellar surface density in Palomar 5 and its two tidal tails.

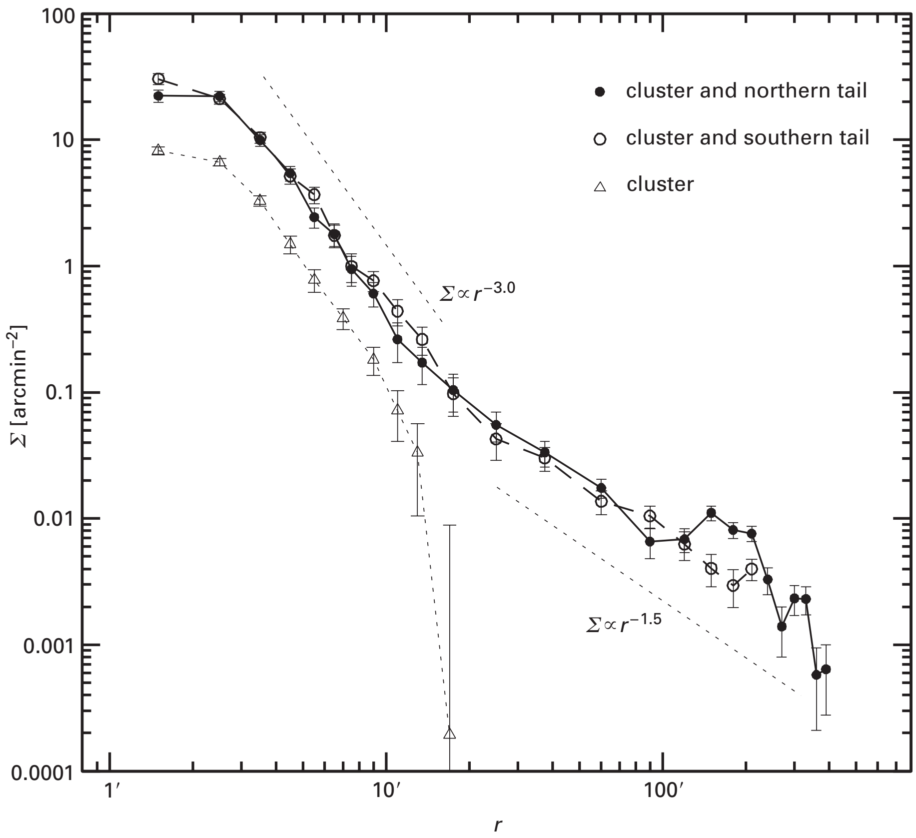

Assuming the cluster to move in its present orbit around the Galaxy for about ten billion years, it has lost a total of 50 000 solar masses during this period of time. This is about ten times its remaining current mass. But compared to other globular clusters the mass of Palomar 5 had been relatively low already in its early stages.

Luminosity function

The fact that some globular clusters have rather flat luminosity functions, i.e., a lower fraction of faint stars than the majority of globulars, is generally thought to be an indirect clue to significant mass loss in these clusters. Such a flat luminosity function was also found some time ago for the core of Palomar 5. The discovery of the tidal tails of Palomar 5 allowed for the first time an observational test of the basic assumption that the lack of low-luminosity stars is due to their escape from the cluster. For this test, however, deeper observations than that of the SDSS were required. Therefore, astronomers at MPIA obtained deep images of some selected fields in the region of Palomar 5 using the wide field camera at the ESO/MPG 2.2 m telescope on La Silla in Chile.

Analysis of these images showed the luminosity functions for the cluster and for the tidal tails to differ at low luminosities (i.e. for low-mass stars). This is illustrated in Figure II.14. A larger fraction of faint stars is indeed found among the members that have left the cluster than among those stars that are staying within the cluster core. The trend to loose mainly low mass stars is explained by the fact that in close encounters of stars inside the cluster the lighter ones are gaining higher velocities and move towards the outskirts where they are subject to the influence of tidal forces. The assumed correlation between mass loss and luminosity function has thus been corroborated by the observations of Palomar 5.

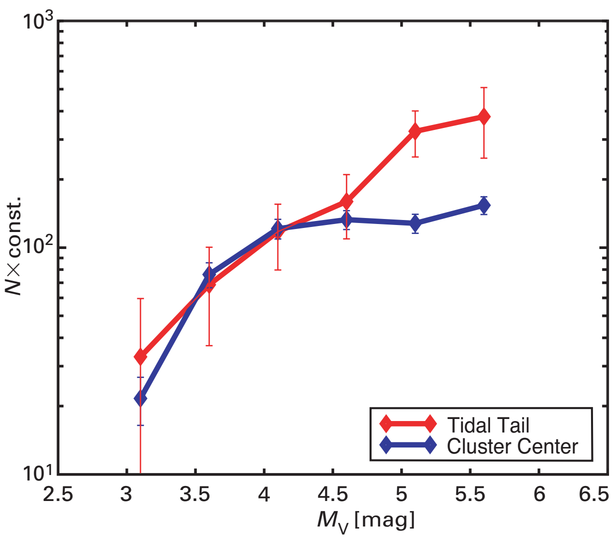

Fig. II.14: Luminosity function of the stars in Palomar 5 (blue) and in the northern tidal tail (red).

The internal dynamical state

One of the goals of future work will be to reconstruct the history of this globular cluster in more detail in order, for instance, to better interpret the observed structures within the tidal tails. An important boundary condition for such studies is the present kinematical structure of the cluster, respectively the velocity distribution of the stars in its interior. In order to determine these, spectra of high quality have to be obtained which provide radial velocities of the stars. This is not an easy task in a star cluster 23 000 pc away.

From the SDSS data, the astronomers selected 18 red giants located within 6 arc minutes of the center of Palomar 5, i.e., within the cluster's core. Excellent spectra of these stars were obtained using the UVES instrument at one of the 8 m telescopes of the Very Large Telescope. These spectra provided radial velocities with an accuracy of about 0.15 km/s. With 14 km/s, one of the giants showed a large deviation from the average velocity of the cluster. It is probably a member of a binary system, whose fast orbital motion adds to and falsifies its radial velocity. Therefore it was excluded from further analysis.

The remaining stars all showed a mean deviation of only 1.14 km/s with respect to the cluster. But this is most likely not the true value as some of the stars are probably members of binary systems. Their orbital motions broaden the velocity dispersion. It is not possible to correct for this effect individually since the binaries cannot be resolved observationally and their orbital periods cannot be measured because they are to long. Therefore the sample of stars was analyzed statistically by calculating several models with differing assumptions on the binary characteristics such as masses of the components and distributions of the orbits.

These simulations showed that about 40 percent of the stars are members of binaries that are broadening the velocity dispersion. Taking this into account, the real velocity dispersion turns out to be 0.12 to 0.42 km/s. This is the lowest value that has so far been measured for a globular cluster. What does that mean for the dynamical state of the cluster?

From the absolute magnitude of Palomar 5 astronomers infer a mass of 4500 to 6000 solar masses. A star cluster this size is in virial equilibrium if the velocity dispersion of its members is between 0.32 and 0.39 km/s. Thus it can be concluded that at present Palomar 5 is most likely in a state of dynamical equilibrium and presents a stable, bound system. This is in agreement with the orbit of the cluster and the results of numerical simulations. The last passage of the globular cluster through the Galactic disk took place about 140 million years ago and the cluster is presently located near the orbital point farthest from the Galactic Center. So there has been enough time for the stars accelerated during the passage to leave the cluster and the increased velocity dispersion of the system to settle down again.

100 million years from now Palomar 5 will again pass through the Galactic plane. As it will then be only about 7 kpc (23 000 light years) away from the Galactic Center, tidal forces may get so strong as to completely dissolve the cluster. Palomar 5 is certainly not special in this respect, but it is the only known example and thus the archetype. Such dissolution processes, that, by the way, can also affect entire dwarf galaxies, are generally believed today to play a major role in the evolution of large galaxies like the Milky Way.

Because of this great significance astronomers at MPIA will continue to study Palomar 5. Currently, an investigation of the radial velocities of stars inside the tidal tails is conducted. First results suggest that the velocity dispersion in the tails is low too but that the run of the mean radial velocity along the cluster orbit differs from that predicted by simple models of the Galactic potential. A longer-term goal will be to determine also proper motions and thereby the complete spatial motion of the cluster and its tidal tails. Should this be achieved it would be possible to determine the gravitational potential of the Milky Way system at a distance of about 20 kpc. This would allow us to learn more about the distribution and maybe the nature of the dark matter that is assumed to occupy the Galaxy's halo.

(Michael Odenkirchen, Eva K. Grebel, Walter Dehnen, Andreas Koch, Hans-Walter Rix)

II.3 »First Fringes« for MIDI – a revolution in spatial resolving power

On 15 December 2002, the beams of two of the four 8.2 m reflectors of the ESO Very Large Telescope (VLT) were successfully combined coherently for the first time to create an interference image within a scientific instrument called MIDI. MIDI (Mid-Infrared Interferometric Instrument) is the first instrument worldwide enabling such observations in the spectral range around 10 μm at large telescopes. The instrument built by a European consortium under the leadership of MPIA will be put into regular operation at the VLT interferometer in fall 2003. It will then be possible to observe celestial objects in the mid-infrared range around 10 μm with a resolution of a few hundredths of an arc second.

Because of their large mirrors the four large telescopes of the VLT have an enormous light gathering power. Equipped with sensitive cameras and adaptive optics, they also achieve their highest possible, diffraction-limited - spatial resolution. This was demonstrated by the NAOS-CONICA infrared camera, that had also been built under the leadership of MPIA, and put into operation in 2001 (the adaptive optics system for it had been delivered by colleagues from France) (cf. Annual report 2001, p. 13).

Fig. II.15: Schematic light path at the VLT interferometer. Two light beams are led from the telescopes (here ANTU and MELIPAL) into the underground tunnel (delay line) and then are coherently combined within the interferometric instrument.

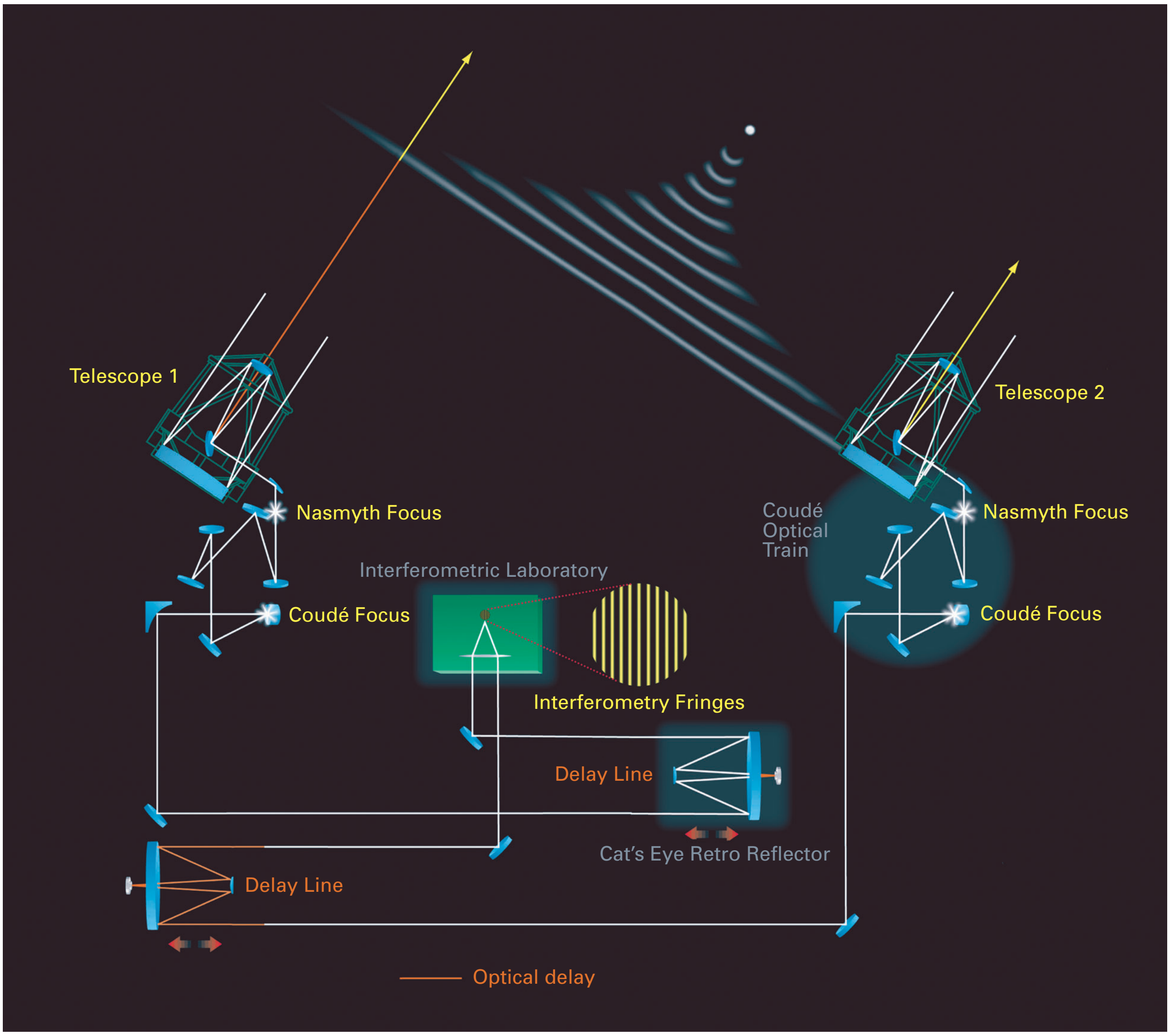

The resolving power of the VLT, however, can be increased by more than a factor of ten by interferometric coupling of two (or more) telescopes (Fig. II.15). To this end, light beams arriving from both telescopes are led into an underground tunnel where they are combined coherently in a focus. Since 2001, the optical coupling of the telescopes has been realized step by step. In fall 2002, all four large telescopes finally were successfully coupled interferometrically two at a time. These experiments were all conducted with the VINCI testing and experimental instrument. Now MIDI is the first scientific instrument to allow astronomical interferometric observations.

In 1997, astronomers at MPIA had suggested to ESO to build this instrument. Soon after, institutes from Germany, the Netherlands and France joined in (see below). Under the leadership of MPIA, more than two dozens engineers, astronomers and students were working intensely for three and a half year planning, designing and building all parts until the assembly of the instrument could be started at MPIA in 2001.

Control electronics, read-out electronics for the detector as well as computer programs for detector control and communication between MIDI and the telescope control system were created in the laboratories at MPIA. In addition, assembly of the instrument and optical alignment of all components were done at MPIA. Colleagues from the Netherlands also contributed considerably. They built the cold optics inside the cryostat and were responsible for planning the software and for the programs that control the data quality and for the interface to the astronomers. A total of about 60 person years was invested into the 6 million Euro instrument. About two thirds of time and costs fell to MPIA.

Following the final acceptance by ESO the instrument was shipped to Chile in September 2002, packed up in 32 big boxes with a total weight of 8 tons. First tests were

Fig. II.16: The MIDI team during the first successful run (»first fringes«). The two project leaders at MPIA are Uwe Graser (standing, 4th from left) and Christoph Leinert (standing, 6th from left).

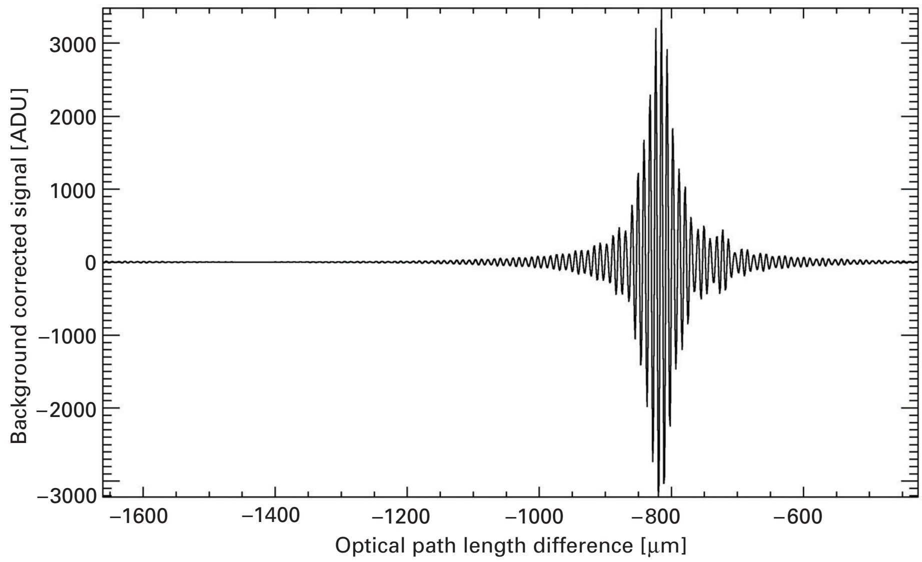

Fig. II.17: »First fringes« – the interference pattern of the star Epsilon Carinae.

conducted in early December and interferometric fringes of a star were obtained for the first time on 15 December (Fig II.16 and II.17). For this purpose, astronomers had observed the bright star Epsilon Carinae using the 8 m telescopes ANTU and MELIPAL that are 102 m apart.

MIDI – a technical masterpiece

Interferometry with MIDI in the thermal mid-infrared range makes heavy demands on technology. For one thing, the difference in path length of the light beams arriving from the telescopes must not exceed a tenth of the wavelength, corresponding to about 1 µm; otherwise coherence is lost and the fringes vanish. Enormous precision is compulsory for this technique.

The path difference changes during the observations due to the rotation of the celestial sphere. This problem is resolved by an optical system moving on a cart on rail tracks within the underground tunnel. The light beams arriving from the telescopes are reflected by this system and their path lengths corrected by shifting the cart (delay line). The path difference of the two incoming beams, which is mainly geometric, will be compensated in this way before the light enters the measuring instrument. The final fine correction is done inside MIDI where both light beams eventually combine to produce the fringes.

Astronomical observations in the mid-infrared range have to deal with quite specific problems since in this spectral region bodies that are not cooled emit strong thermal radiation. Therefore, the design of MIDI had to make sure that the detector will not be blinded by the instrument's own emission. To avoid this, a complex cooling system was needed. This in turn created the problem to maintain the alignment of all optical components – a critical task on its own – also at low temperatures. Even the smallest flexure of the cooled parts during the cooling period would thwart the measurements. This could be avoided by manufacturing all metal parts of the optical system in the environment of the detector from pieces of a single, especially selected block of aluminum. In addition, MIDI has to be positioned and aligned with respect to both incoming light beams with an accuracy of at least 0.1 millimeter and 0.01 degrees, respectively. The MIDI electronics was accommodated in a neighboring room to the interferometry laboratory to minimize thermal and mechanical perturbations.

The MIDI cryogenic system has several stages. Most optical components are working inside a cold box (cryostat) at temperatures around 40 Kelvin. An outer radiation shield protects the cryostat from the surrounding thermal radiation. Inside the cryostat, there is a second radiation shield at 77 Kelvin. The detector itself operates at 5 to 10 Kelvin. Moreover, external thermal radiation from around the field of view has to be blocked from the detector. This is achieved by two cold pupils or cold field stops that baffle the field.

Fig. II.18: Schematic optics of MIDI. The multiple cooling systems is not shown.

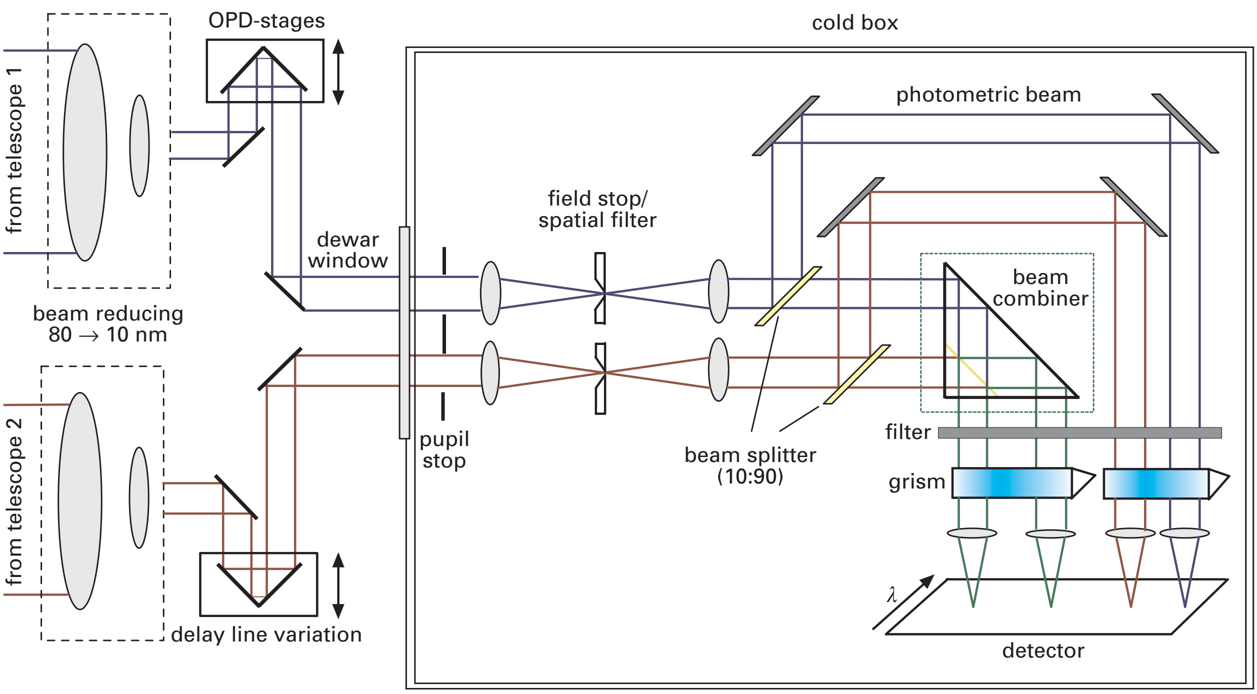

Technically, the cooling is realized with a »closed cycle cooler«. In it, helium gas is expanded within a closed cycle, thereby cooling down. This device, however, uses moving pistons that create significant vibrations. To avoid any disturbances of the interference measurements, the cooler rests on a separate pedestal, which is connected to the cryostat by a movable bellows. The cooling takes place via a flexible copper litz wire.

The light path inside MIDI is illustrated by Figure II.18, Figure II.19 shows the instrument in the VLTI laboratory. Both telescope beams come in from the left. Their initial diameter is 80 mm. At the tunnel exit they are reduced to 18 mm. After that, the beams pass the entrance pupils. Next, an intermediate focus is formed where additional components, e.g. for additional suppression of background radiation, or filters can be inserted. Beyond, the beams are recollimated and then encounter a beamsplitter. This component is necessary to measure the degree of coherence between the beams with extreme accuracy. Here, the beams that have been made coherent by means of movable piezo-electrically driven mirrors are combined to create the fringe pattern.

However, this complex system alone is not sufficient for interferometry in the mid-infrared range. This is because of the intense thermal background radiation from the sky which is, moreover, temporally changing due to atmospheric turbulences. This thermal background is about ten times brighter than an object of 0 mag! Therefore it is mandatory to subtract the background signal from the actually measured signal during the observation. This is done with a so-called chopper. A tilting mirror inside the telescope allows to measure alternately the flux from the object and from a nearby empty field of sky.

At the same time one has to take into account that the flux of the object observed is varying itself, mostly due to atmospheric turbulences and water vapor. MIDI therefore allows to determine the flux of the object in a separate photometric light path. This additional information increases the measuring accuracy of the interference. But this additional light path uses 30 percent of the incoming light, thereby reducing the sensitivity.

A particular feature of MIDI is its broadband sensitivity in the spectral range from 8 to 13 μm. Thus spectroscopy is possible with the instrument, although the resolution obtained is relatively low. A prism that can be inserted into the light path yields a spectral resolution of $\Delta\lambda/\lambda = 25$; with a grism (a combination of prism and grating), a higher resolution of even 230 is possible. This observational mode uses a slit or a triple pinhole (Fig. II.20 and II.21). In addition, narrowband observations are possible by inserting filters.

Measuring the interference signal also turned out to be very complex. So two different methods were developed for this task. Which one is the most suitable depends on the kind of observation and will later generally be specified for the astronomer during operation.

The detector read-out and the development of the software for it also proved to be critical. The large thermal background requires a full frame readout time of 5.6 ms or faster. This has to be done strictly in step with a modu-

Fig. II.19: MIDI in the underground VLTI laboratory. The instrument weighing 1.5 tons is resting on a 1.5m × 2.1m high-precision optical bench. The big golden box is the cryostat containing the detector and the cold optics. The incoming telescope beams fall onto the optical components seen at the left edge of the table.

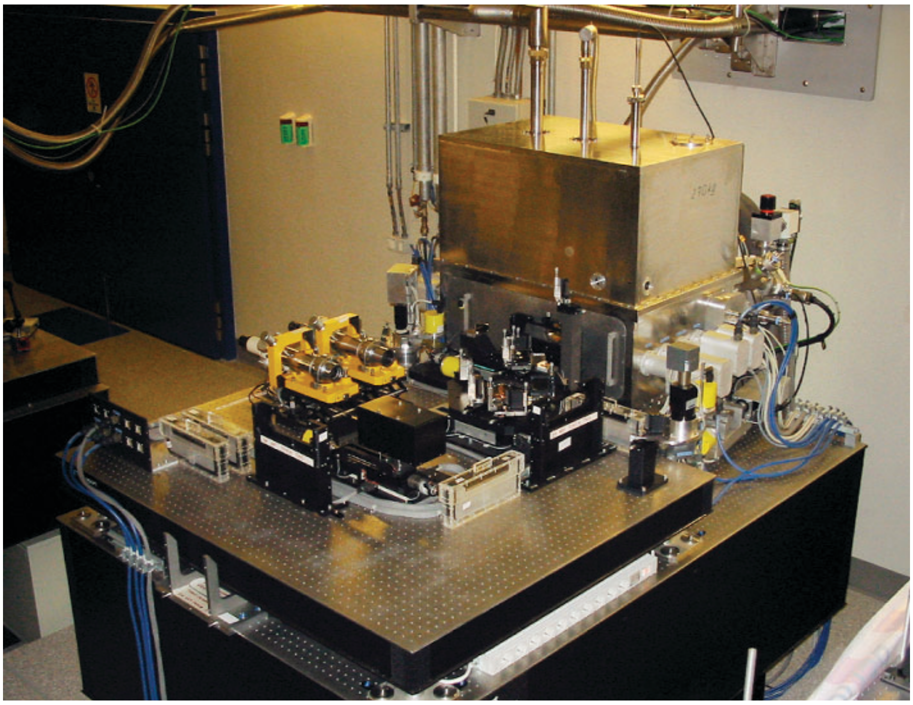

Fig. II.20: Channel layout on the detector in the spectroscopic mode with the prism (left) or the grism (right). Two interferometric (middle) and two photometric (outside) channels are to be seen. In this mode, each channel itself consists of three single channels allowing simultaneous flux measurements of the object and the sky background for calibration purposes.

lation of the entire measuring process. For this end, a sophisticated, efficient, highly specialized but flexible electronics was developed over the years at MPIA.

Doing astronomy with MIDI

Operating MIDI will be different from other observing instruments at VLT. Because of the instrument's complexity a guest observer will largely have to rely on the experienced ESO staff for choosing the working mode suitable for his or her particular needs. Moreover, computer simulations at MPIA show that the observing mode as well as the selection of the telescopes (the baseline) of the VLTI have to be specially laid out for the "geometry" expected for the object to be observed. Therefore, the success of an interferometric observation will also depend on how well the astronomer anticipates the appearance of the object to be observed. This significantly distinguishes interferometry from traditional spectroscopy or direct imaging.

Of importance is the limiting magnitude obtainable with MIDI. During the first attempts 1 to 5 mag were obtained. Thus bright nuclei of active galaxies, T Tauri stars and Ae/Be stars as well as red giants are already observable. In 2003, though, MIDI will be supplied with a so-called external fringe tracker, allowing stable fringe tracking without the pattern itself being visible. Thereby the fringe patterns of individual short observations can be added blindly, thus improving the sensitivity by up to a factor of 100 (corresponding to 5 mag).

In general, MIDI will be perfectly suited to study objects rich in dust. Heated by other celestial bodies, dust emits thermal infrared radiation. It can be found in dust tori in the nuclei of quasars and radio galaxies just as in disks of gas and dust around young stars where planets may form. The environs of giant stars where dust particles are formed for the first time are also interesting observing objects.

In return for building and allocation of the instrument, the MIDI team was granted 300 hours of observing time. A preliminary observing program for this guaranteed time

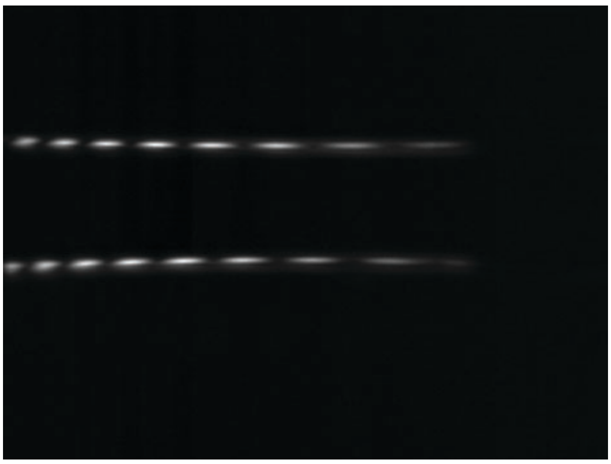

Fig. II.21: Dispersed fringes measured in the laboratory. Within each spectrum the wavelength increases from left to right. For astronomical objects, the contrast between constructive and destructive interference fringes yields information on the geometry of the objects.

contains just the kinds of astronomical objects mentioned above. In addition, the team will use about 25 hours for the direct detection of extrasolar planets although everybody is aware that this attempt will be at the very edge of feasibility.

Next steps

In spring 2003, the commissioning phase is taking place on Paranal during which functional performance and reliability are tested. MIDI will then be put into regular operation and offered to all guest astronomers from October 2003 on. At this time, the external fringe tracker will also get installed. From spring 2004 on, the addition of the 1.8 m auxiliary telescopes will be tested and by the end of 2004 the wavelength coverage is planned to be extended beyond 20 µm. In 2005, finally, an attempt will be made to extend the angular distance inside which reference stars can be used from presently 2 arc seconds up to 60 arc seconds. If this attempt would succeed one could look for a bright reference star for guiding within this field – quite similar to adaptive optics. This would again considerably improve the limiting magnitude.

(Ch. Leinert, U.Graser, A. Böhm, O. Chesneau, B. Grimm, Th. Henning, T. M. Herbst, S. Hippler, R. Köhler, W. Laun, R. Lenzen, S. Ligori, R. J. Mathar, K. Meisenheimer, W. Morr, R. Mundt, U. Neumann, E. Pitz, F. Przygodda, Th. Rabzah, R.-R. Rohloff, P. Schuller, C. Storz, K. Wagner, K. Zimmermann.
Participating institutes: Eso, Kiepenheuer-Institut für Sonnenphysik, Freiburg, Thüringer Landessternwarte, Tautenburg, Astronomisches Institut, Universität Amsterdam, Sterrewacht Leiden, Kapteyn Astronomical Institute, Netherlands Foundation for Research in Astronomy, ASTRON, Observatoire de la Côte d'Azur, Observatoire de Paris/Meudon, National Radio Astronomy Observatory

Tabelle 1: Einige Daten zu MIDI

Verfügbare Basislängen mit 8-m-Teleskopen:	47 bis 130 m
Verfügbare Basislängen mit 1.8-m-Teleskopen:	8 bis 200 m
Auflösung bei 10 µm Wellenlänge:	0.″25 bis 0.″01
Empfindlichkeit:	8 bis 13 µm
Blickfeld (Durchmesser) mit 8-m-Telskopen:	2″
Blickfeld (Durchmesser) mit 1.8-m-Telskopen:	10″
Grenzgröße (8-m-Tel., ohne Fringe tracker):	3-4 mag
Grenzgröße (1.8-m-Tel., ohne Fringe tracker):	0-0.8 mag
Grenzgröße (8-m-Tel., mit Fringe tracker):	8-9 mag
Grenzgröße (1.8-m-Tel., mit Fringe tracker):	5-5.8 mag

III Scientific Work

III.1 Formation of Stars and Planets

Molecular Clouds under the Influence of External Radiation

Although stars form inside dense clouds of gas and dust, external effects such as radiation from nearby hot stars can decisively affect this process: The outskirts of the clouds get heated up to 10 000 Kelvin and can rapidly dissolve. On the other hand, the UV radiation produces shock waves within the clouds that considerably affect the star formation process. Computer simulations performed by theorists at the Institute show how this happens.

One of the best-known examples of such dust clouds heated from the outside are found in the Eagle Nebula M16. They are also called »Pillars of Creation« after the sensational images by the HUBBLE Space Telescope. Images taken with the Very Large Telescope show an infrared overview of this spectacular star formation region (Fig. III.1). The three elongated dust clouds, also called elephant trunks, are located at the edge of a dense molecular cloud that is lying near a young star cluster. The UV radiation of the massive stars within this cluster is heating and ionizing the outer regions of the clouds, which can be seen in the images as a bluish glow. At the same time, more than ten young low-mass stars were detected in the outer regions of the clouds. Several reddish stars are also discernable in the region of the clouds. At least some of them may have formed only very recently.

Fig. III.1: Three dust clouds (elephant trunks) inside the Eagle Nebula M16, imaged in the near infrared with the Very Large Telescope. (Image: ESO)

From images like this, however, no conclusions can be drawn about the conditions inside the dense clouds. This is only possible at longer wavelengths. Here, some examples were found recently where young stars inside some clouds are aligned along the axis towards the outer star or star cluster. Moreover, there are indications that the age of the newly formed stars is decreasing with increasing distance to the edge of the cloud. In other words: Star formation proceeds along the axis from the outside inwards. Therefore it seems possible that the outer stars affect the processes within the cloud via their UV radiation, thereby initiating sequential star formation.

Using analytical models and computer simulations, astrophysicists already tried to find out how this can happen. They came up with the following qualitative scenario: While the UV radiation ionizes the outer regions of the cloud high pressure is generated within this hot envelop driving a shock front inwards. The front sweeps up a thin, dense layer of cool material immediately underneath the hot envelop. This compressed layer is unstable and disintegrates into smaller fragments, which under certain circumstances may condense into stars. In the further course of events the surrounding material evaporates, now exposing the individual compressed fragments to the ionizing stellar radiation. What happens next?

Theorists at the Institute tried to answer this question through computer simulations. The results were the first three-dimensional calculations of such radiation driven implosions of dust clouds including dynamics as well as self-gravity of the matter. The virtual cloud comprising

220 000 gas particles was assumed to be a Bonnor-Ebert sphere, that is, the gravitational force is balanced by the pressure everywhere inside the sphere. The maximum particle density in the center was assumed to be 1000 cm^{-3} and the temperature 10 Kelvin. These are values typically found in the interiors of molecular clouds.

The core of this cloud has one Jeans mass, just the mass at which a cloud starts to contract under the effect of its own gravitation. Assuming these basic conditions, the theorists ran several simulations, changing certain physical parameters in order to identify their effects on the cloud's evolution.

Case A was calculated without self-gravity. As is shown in Figure III.2, at first an ionization front is driven into the cloud (Fig. III.2, panel 1), having a diluting effect on the material. So after about 1500 years, the denser core region of the cloud is excavated and surrounded by hot, ionized gas. The once spherical cloud slowly assumes an elongated, cometary shape (2). Due to the pressure imbalance a new shock front forms which compresses the material in the outer regions of the cloud. This matter converges towards the longitudinal axis forming an elephant trunk. After 130 000 years (3), the cloud reaches a stage of maximum compression. But in this phase, the internal pressure exceeds the external and the material starts to re-expand. Now more and more hot, ionized gas leaves the surface, exposing the internal density enhancements aligned along the symmetry axis (4). Without self-gravity, the condensations inside the cloud cannot stay bound and disintegrate. Now, knots also form at the tip of the cloud (5 and 6). This layer is dynamically instable and disintegrates after about 600 000 years. Finally, the remaining fragments are completely ionized, too. Because of the lack of gravity no stars can form.

For case B, the same initial conditions were chosen, but now self-gravity is included. The evolution during the first 130 000 years is indistinguishable from that in case A. In this phase of maximum compression condensations with densities above a critical value of 5×10^{-17} g/cm^{-3} have masses of about 5.3 solar masses. This corresponds to twice the Jeans mass. So gravitational collapse sets in that can result in the formation of stars.

However, the Jeans mass criterion is not a reliable indicator of the collapse of cloud fragments since it only takes into account the balance between internal energy and gravity. Internal gas motion and turbulences are neglec-

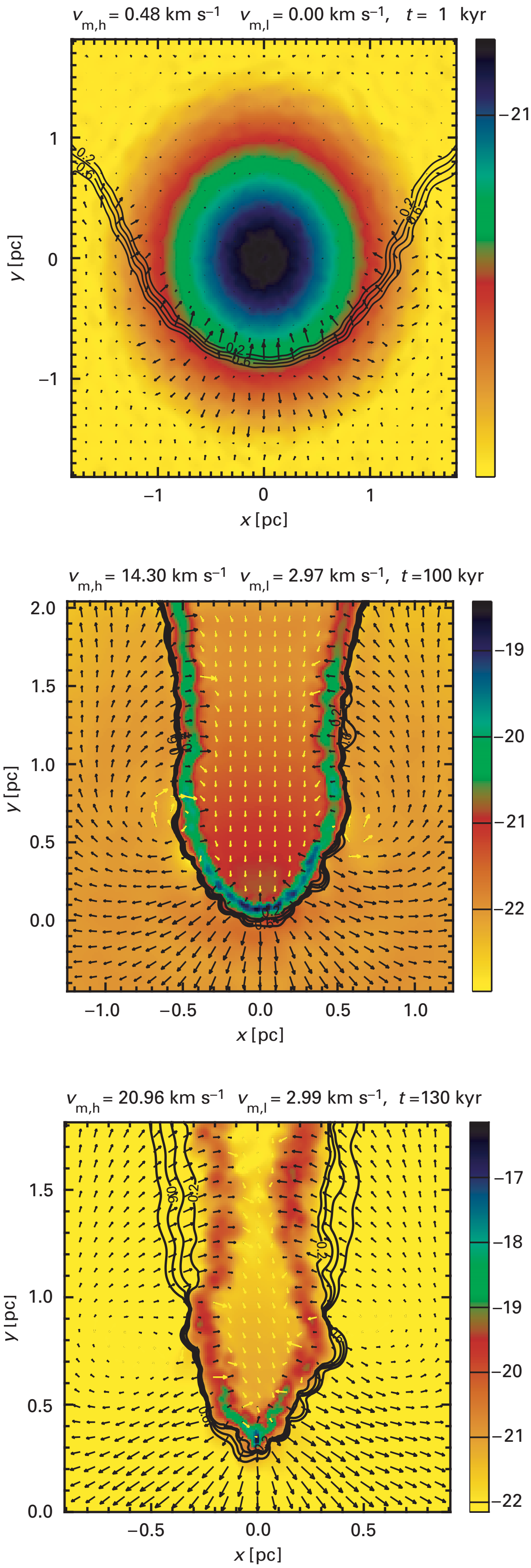

Fig. III.2: Time evolution of the simulated cloud in case A. Density is shown in g/cm^3. Contour lines mark the degree of ionization, arrows the velocity field.

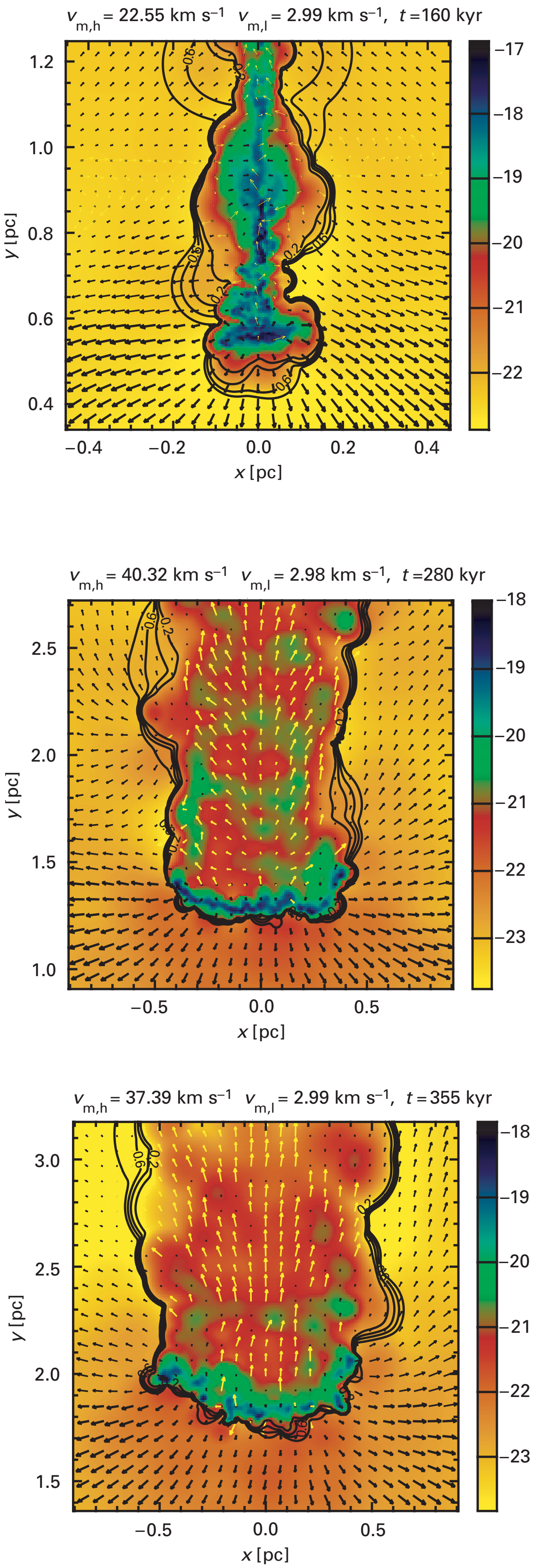

ted, though. How these affect the cloud's behavior, is demonstrated by models C and D.

Cases C and D included density perturbations of the cloud medium. In case C, mainly large-scale perturbations were assumed, in case D rather small-scale ones. Both models were calculated including self-gravity. Figure III.3 shows the time evolution of model C. Compared to model B, density enhancements are amplified further in the shock front at the edge of the cloud, similar to what is observed in the Eagle Nebula. Contrary to case B, however, the denser fragments do not continue to collapse because of their internal turbulent pressure. The evolution then is more analogous to case A. Although self-gravity is included, the collapse is much delayed. After 300 000 years, the fragments slowly disintegrate. The same behavior is observed in model D.

In cases C and D, the fragments stop to collapse because of the kinetic energy of the gas. The simulations show the material to be strongly accelerated during the compression phase. Thus the kinetic energy continues to increase steadily. It is mainly converted into undirected gas motion within the globules, preventing further collapse. In cases A, C, and D, all fragments again disintegrate in the end; in C and D, the initial density perturbations only delay this process but do not prevent it.

Figures III.4 and III.5 show the radiation emitted from the cloud during the initial and the final stages of models A and C, respectively. Both pictures roughly correspond to the impression obtained from an astronomical image. Figure III.6 shows the time evolution of the regions of maximum density for all four cases. In cases A, C, and D, the density of the fragments obviously never exceeds the critical value for gravitational collapse. Only in case B, the fragments continue to collapse, indicated by the dotted line that increases steeply after about 100 000 years.

The simulations very impressively demonstrate that the evolution of an interstellar cloud under the influence of an external radiation field does strongly depend on the internal condition of the gas. However, these simulations lack a detailed heating and cooling model of the gas. Instead, the simplifying assumption was made that the neutral material has a constant temperature of 10 Kelvin, whereas the ionized gas is at 10 000 Kelvin. The cooling properties, however, significantly affect the contraction.

But even these simplified simulations corroborate the idea that inside a dust cloud stars are forming along an axis pointing towards the outer, hot star. An age gradient in star formation can be explained in this model by sequential star formation initiated by a shock front driven inwards.

(O. Kessel-Dynet, A. Burkert)

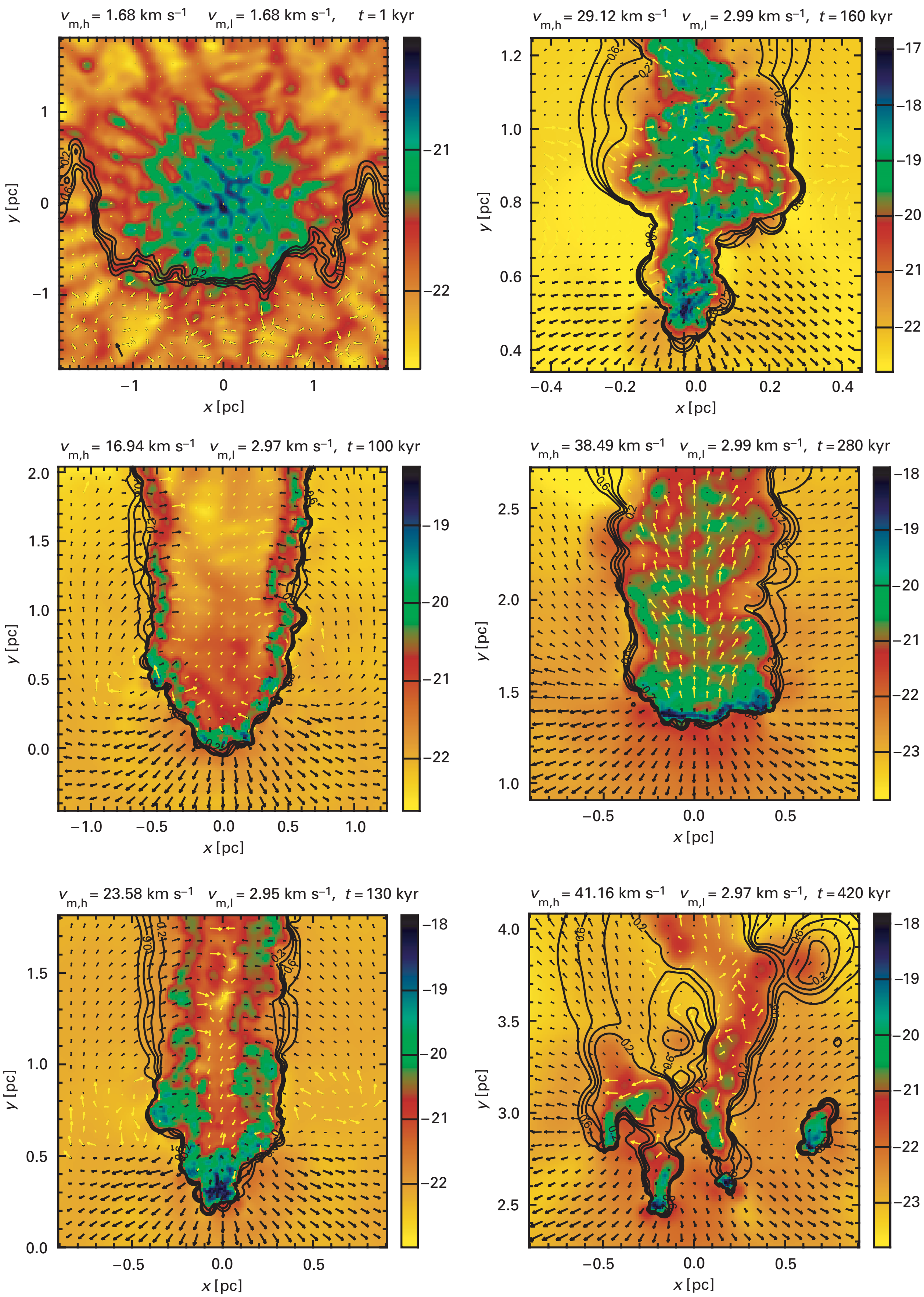

Fig.III.3: The same as in Fig. III.2, but for case C.

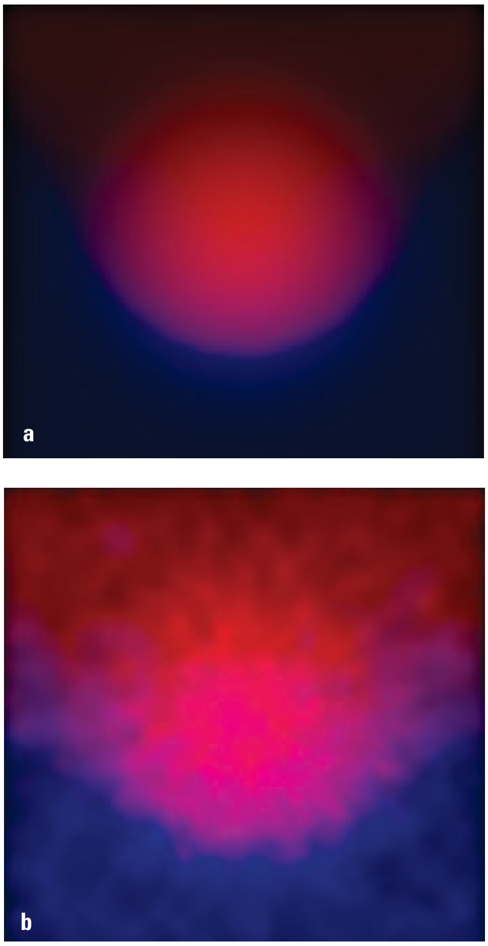

Fig. III.4: Radiation emitted by the cloud during the initial **(a)** and final stages **(b)** of case A. Both pictures roughly correspond to the impression obtained from an astronomical image.

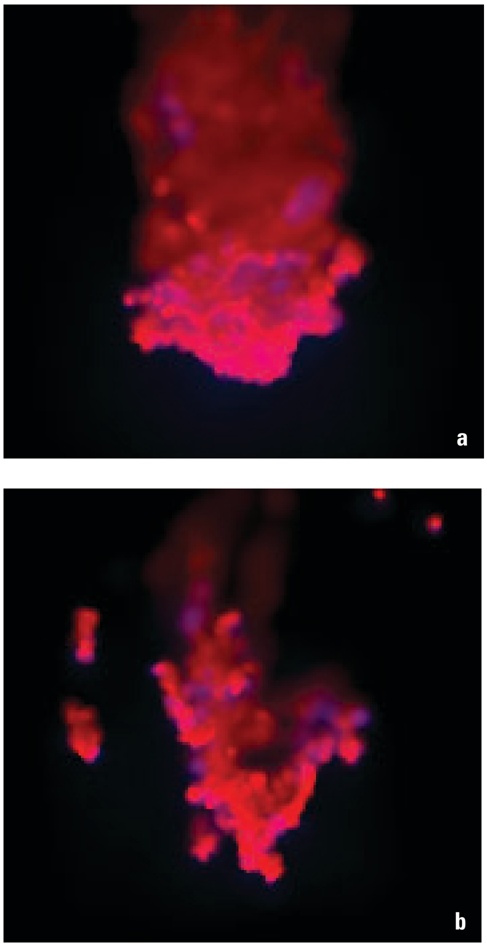

Fig. III.5: The same as in Fig. III.4, but for case C.

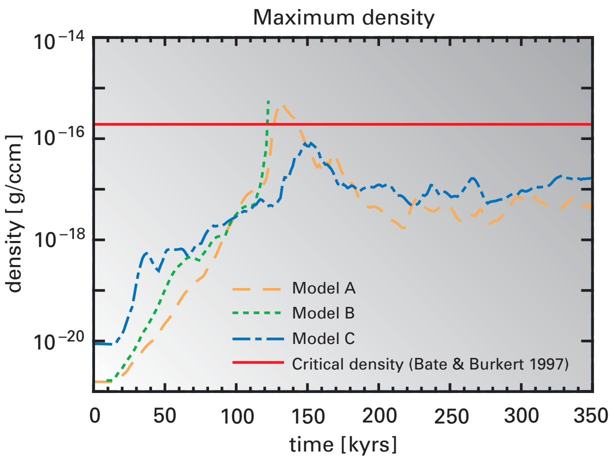

Fig. III.6: Time evolution of the density within the fragments. Only in case B, gravitational collapse sets in after about 100 000 years.

Isophot and the Realm of Star Formation

The first stages of the star formation process take place deeply inside dense clouds of gas and dust and hence are not observable in visible light. Long-wavelength radiation from the infrared to the millimeter range, however, can penetrate the dust and is thus excellently suited for this purpose. Astronomers at the Institute used the large data base gathered by the Isophot camera, built at MPIA and flown onboard the Iso Infrared Satellite, in order to investigate pre-protostellar condensations in the interiors of such clouds. These measurements were complemented by observations in other wavelength regions. This multi-wavelength analysis provides an extensive picture of these objects that are in an early evolutionary stage on the verge of collapsing to form stars. Another great success of this project has been the generation of the first far-infrared map of the Small Magellanic Cloud showing a wealth of details that allow far-reaching conclusions about star formation within our neighboring galaxy.

The condensations inside interstellar clouds are the coldest objects in the universe for the following reason: Although the outer regions of the clouds are heated by the surrounding general star light, particularly by its ultraviolet and blue components, this radiation cannot penetrate deeply into the cloud. So the innermost regions are shielded from the heating through stellar radiation and cool down considerably.

If a critical density is exceeded in some part of a cloud, the interstellar matter in this region contracts under the influence of its own gravity. Only when this stage is attained the condensation starts to warm up due to contraction until the central temperature finally reaches several million degrees. At this point, nuclear fusion sets in and a star is born. When reaching this phase, the stars frequently have already shed their surrounding dusty envelops and are visible now also in optical light.

The theory of star formation can be tested to a large extent by observations. The very first stages, however, in which the condensations are still very cold, remained hidden from view for a long time. Only in the radio spectral range molecules had been detected within presumed prestellar cores.

Then, with the advent of Isophot, an excellently suited instrument to identify these initial condensations in the interiors of dust clouds became available. It was one out of four scientific instruments onboard the European Iso space telescope, which observed selected astronomical sources for about 29 months, till April 1998. Isophot, built under the direction of MPIA, worked as a photopolarimeter, camera, and spectrophotometer in the wavelength range from 2.5 μm to 240 μm. Thus thermal emission of dust at temperatures as low as about 8 Kelvin could be detected.

Iso was designed to selectively observe individual sources. But the slewing time when the satellite was pointed from one object in the sky to another was also utilized. Isophot was kept turned on during the slews. During a total of 12 000 random slews across the sky astronomers were able to obtain 550 hours of observing time with the far-infrared camera. The result was a »strip map« covering about 15 percent of the entire sky at 170 μm wavelength, called the Iso Serendipity Survey (IsoSS). This is the most extensive sky survey in this wavelength region to date.

Cygnus X

Over the last years, researchers at MPIA developed computer programs to automatically identify sources from the strip maps in the far infrared. Thereby they noticed several very cold objects within a long known giant molecular cloud called Cygnus X (Fig. III.7). This is a very young star formation region about 1800 pc (6000 light years) away. To get to know the evolutionary state of the knots, the astronomers observed the region with several telescopes at numerous wavelengths in the spectral range from 0.3 μm to 1200 μm. In addition, they studied the area at radio wavelengths in order to measure the emission of ammonia (NH_3) as this molecule is a good indicator of the gas temperature and density. Even a 70 cm telescope at the Institute on the Königstuhl was used.

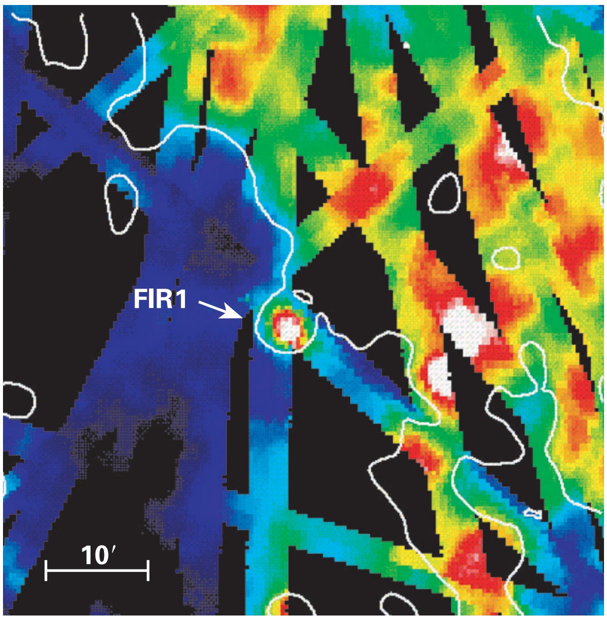

Fig. III.7: Strip map from the Isophot Serendipity Survey at 170 μm wavelength. The star formation region is discernable as a bright point source (FIR 1) in the center of the image. The image gives an impression of the typical sky coverage in a region frequently crossed by the telescope's field of view.

From these extensive data important conclusions were drawn.

Among the ISOSS data the astronomers discovered a condensation of matter that was called FIR 1. It is a star formation complex containing a total of about 120 solar masses of gas and dust. Since the measurements cover a wide wavelength range the spectral energy distribution could be derived (Fig. III.8). It can be described very well as emission from an optically thin medium at two temperatures, 13 and 19 Kelvin. Moreover, the temperature in FIR 1 was found to decrease from the outside inwards down to 11 Kelvin. Presumably the cloud is heated from the outside. The cloud's core region of 50 solar masses is elliptical in shape and has a size of 0.5 pc × 0.3 pc. Its extinction in the visible spectral range is 30 magnitudes.

Radio observations of ammonia molecules allowed to estimate the kinetic energy of the particles and to compare it to the potential energy of the cloud complex. This estimation showed the core region to be roughly in virial equilibrium and thus gravitationally bound. There is a future possibility for this cloud to contract and form one or several stars. Thus FIR 1 would represent the first stage of a star formation process. Such objects are also called pre-protostellar cores.

Within FIR 1, three compact condensations with temperatures between 13 and 19 Kelvin were found in the sub-millimeter range using the James-Clerk-Maxwell Telescope on Mauna Kea, Hawaii (Fig. III.9). Two of them have masses of about 8 and 3.5 solar masses and temperatures of 18 and 21 Kelvin, respectively. Most probably they are protostars in their first evolutionary stage, so-called Class 0 objects.

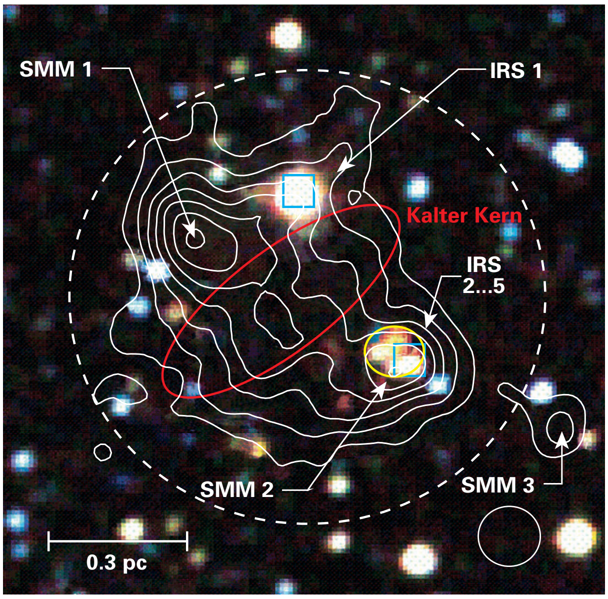

Fig. III.9: Map of the 2MASS sky survey with several infrared sources (IRS). IRS 1 is a Herbig Be star. Sub-millimeter data of sources SMM 1, 2, and 3 appear as overlaid contours. The red ellipse marks the region of the cold core which may be the presumed pre-protostellar core. Here, the point source FIR 1 shown in Fig. III.7 corresponds to the region within the dashed circle.

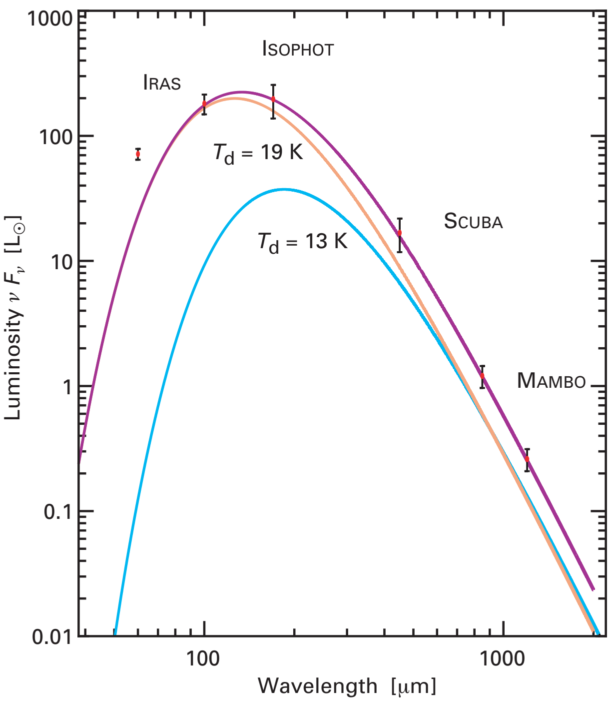

Fig. III.8: Spectral energy distribution of the pre-protostellar core FIR 1. It can be explained as a superimposition of two optically thin bodies with temperatures of 13 and 19 Kelvin, respectively.

In addition to these objects, astronomers found eight sources in the same region in the data of the 2MASS infrared sky survey that probably are young stars or protostars. One of it is a Herbig Be star. Comparison of the measurements with theoretical stellar evolutionary tracks showed this object to have 6.5 solar masses, 2200 solar luminosities, and an age of less than 40 000 years (Fig. III.10). Moreover, spectra suggest that the star is surrounded by an accretion disk, accumulating matter from its vicinity with a rate of 10^{-5} solar masses per year. Because of their fast evolution, such objects are rarely known so far.

Thus, all data indicate that the astronomers have identified an unusually young star formation region in the ISOSS catalog. In the future, it will be interesting to study each of these objects in greater detail, for instance in the millimeter range using ALMA or in the far infrared with HERSCHEL.

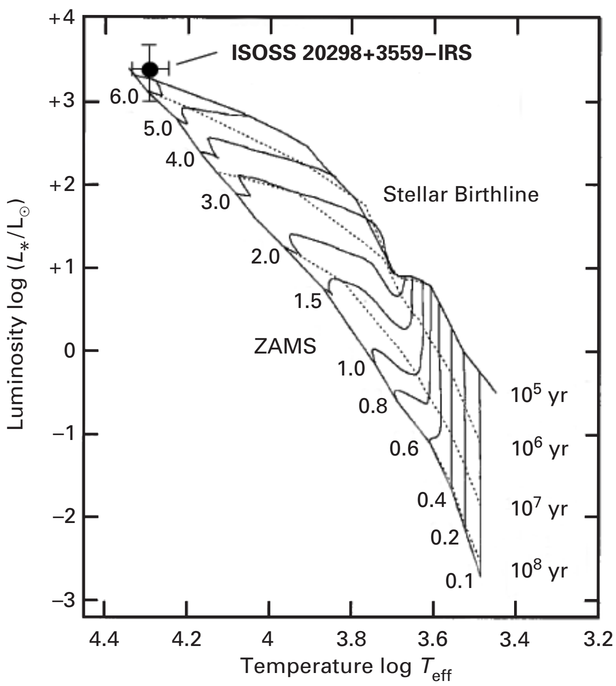

Fig. III.10: Hertzsprung-Russell diagram showing theoretical evolutionary tracks of stars with masses between 0.1 and 6 solar masses and evolution times between 10^5 and 10^8 years. Accordingly, the mass of the newly found Herbig B2 star is about 6 solar masses and its age less than 40 000 years.

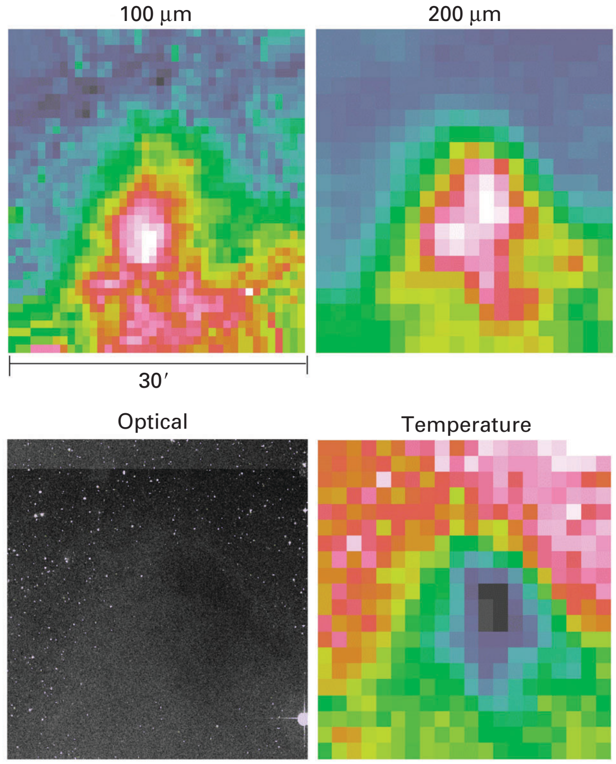

Fig. III.11: Lynds 183 in the far infrared (above) and in the visible spectral range. The panel to the lower right shows the temperature decreasing towards the cloud's center. (Cfr. Fig. III.13)

Lynds 183

Great progress was made observing the dark cloud Lynds 183, sometimes also cited as Lynds 134 North, using ISOPHOT among other instruments. The cloud has been known for a long time and is regarded as a prototypical molecular cloud, not least because of its short distance of 110 pc (360 light years). Together with the clouds L 134, L 169, and L 1780, it belongs to a large complex located at a rather high Galactic latitude of 36 degrees. Thus no »infrared cirrus« along the sight of line contaminates the observations.

So far, no evidence of star formation (e.g. the presence of T Tauri stars or infrared sources) was found. It is impossible to look far into the cloud in the optical, anyhow, since extinction toward the center is about 17 magnitudes. In the sub-millimeter range, however, a small extended core had been detected in the center. More emission in this spectral range was found later coming from a region 1.5 arc minutes south of the core.

Astronomers at the Institute, together with colleagues from the University of Helsinki, observed the entire cloud in the far infrared. At 200 µm, they found the two condensations (FIR 1 and 2) already detected in the sub-millimeter range. In addition, they identified two previously unknown emission knots (FIR 3 and 4). One of them was not detectably at 100 µm, indicating a very low temperature for this condensation (Fig. III.11). Other observational data available confirm this presumption.

From the resulting energy distributions dust temperatures of the four condensations between 8.4 Kelvin and 12.8 Kelvin were derived (Fig. III.12, 13). These values together with further observations in the sub-millimeter range provided masses for FIR 1 and FIR 2 of 1.4 and 2.4 solar masses, respectively. These masses are at least as

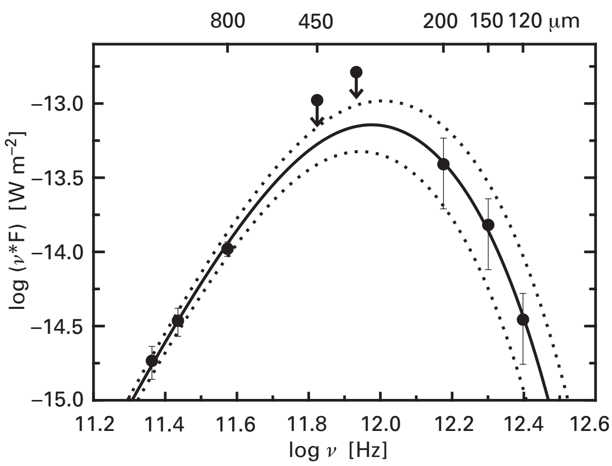

Fig. III.12: Spectral energy distribution of the source FIR 1.

high as the corresponding virial masses, probably even higher. Thus, these condensations, too, appear to be gravitationally bound and perhaps on the verge of collapse. Like those in Cygnus X, they are probably pre-protostellar cores. According to their early evolutionary stage their bolometric luminosities are still very low, namely 0.04 and 0.06 solar luminosities.

With 0.2 solar masses and 0.03 solar luminosities, FIR 3 was found to be of low mass and luminosity. For the faint source FIR 4 no mass could be derived as it was only detected at 200 µm. So it was impossible to determine its evolutionary stage. This region, too, will be of great interest for observations with future telescopes.

Small Magellanic Cloud

The Small and Large Magellanic Cloud (SMC and LMC hereafter) are two companion galaxies of the Milky Way system (Fig. III.14). Over the past, several close encounters between these three star systems took place during which gravitational interactions should have strongly affected the evolution of the Magellanic Clouds. Due to its low mass, the SMC is likely to have suffered most from the consequences of these interactions. The most recent encounter about 200 million years ago is believed to be responsible for the present irregular shape of the SMC.

Fig. III.13: Far-infrared map of L 183 as well as spectral energy distributions and temperatures at three selected locations.

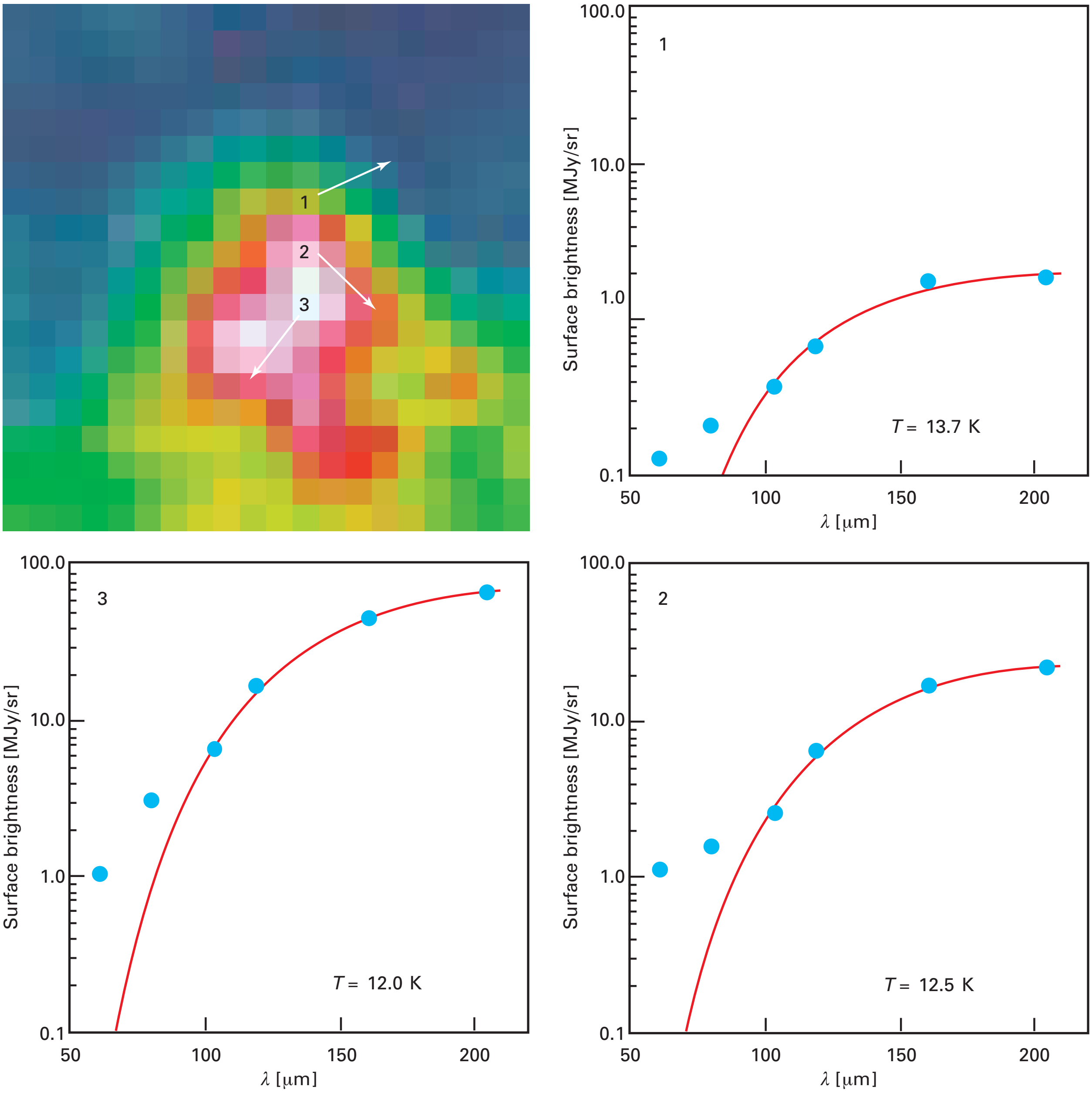

A bridge of material connecting the SMC and LMC as well as a wide gaseous arc called the Magellanic stream are also interpreted as a consequence of the gravitational interactions.

Heavy-element abundances in both the SMC and the LMC are only about one tenths of the solar values. The fraction of interstellar dust is low too in both objects. Yet the star formation rate is high enough to lead to significant infrared emission from warm and cool dust. Far-infrared observations providing information on the actual amount of cool dust were not available until recently. Using ISOPHOT, a group of scientists at MPIA made the first complete map of the SMC at 170 μm wavelength. Because of the SMC's extended size of 6 × 8 degrees the observations had to be split into nine fields and the images then put together in a mosaic. The total exposure time was almost 20 hours.

At 170 μm wavelength, the map shows a wealth of structure (Fig. III.15). Several bright star formation regions (dark blue and white) that had been known before attract attention and can be identified with HII regions. Furthermore, an extended emission is to be seen to the north east: it is the bridge to the LMC. The south west region towards the Magellanic stream is not covered by the observations.

Fig. III.14: The Small Magellanic Cloud imaged in the visible spectral range. (CTIO/NOAO)

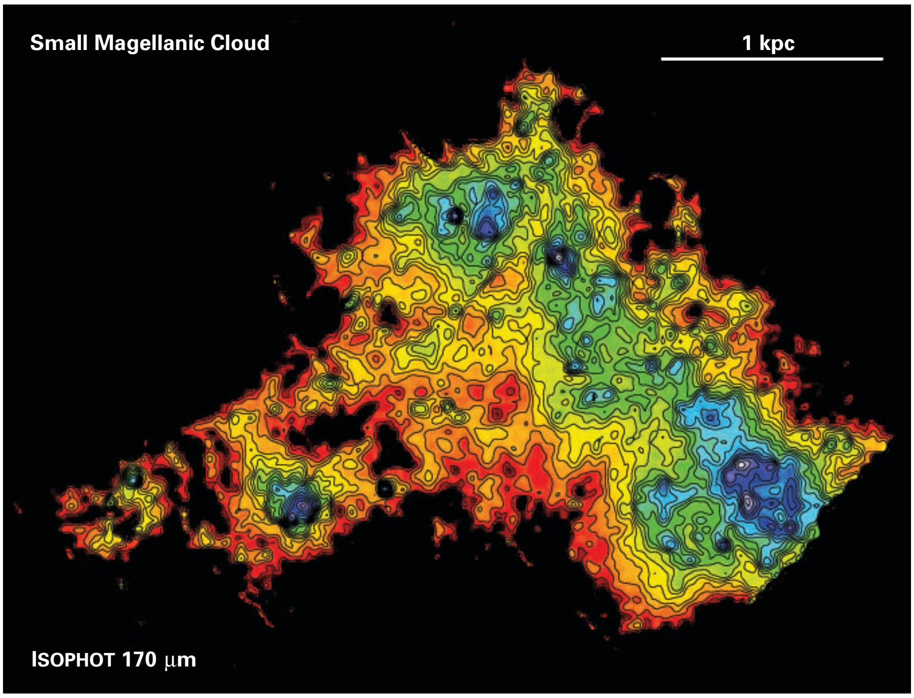

Fig. III.15: The SMC imaged with ISOPHOT at 170 μm wavelength.

Analysis of this map is just beginning. But even the preliminary results are indicating its great potential. The software used enables a search for individual sources in the SMC based on objective parameters. The same computer program was used to re-analyze the earlier data obtained by the IRAS satellite at 12, 25, 60, and 100 μm wavelengths. Up till then sources in the IRAS data had to be identified with the naked eye.

Resulting from this new analysis are several maps of the SMC in the wavelength region from 12 to 170 μm generated for the first time according to a uniform standard. The IRAS maps show the warm dust residing mostly in HII regions where it is heated by hot stars. Now, with ISO, the cooler dust became detectable too.

In the four wavelength regions of the IRAS catalogue, a total of about 800 sources was found, many of them appearing in several maps. In the ISO map at 170 μm, 243 sources were found, 153 of which could also be identified in the new IRAS maps at 60 and 100 μm. In the mid-infrared range, mainly isolated point or extended sources are to be seen which are not related to each other. In the far infrared, the emission traces the extended, diffuse emission along the bar and the bridge. Furthermore, the sources in the mid infrared differ significantly from those in the far infrared with respect to source statistics, brightness distribution and other criteria. About one hundred of these objects have temperatures below 30 Kelvin and can be associated with dust and molecular clouds. Seven other sources are warm regions ($T > 30$ K) associated with HII regions. One of the future tasks will be to correlate the sources with one another.

The diffuse far-infrared radiation is emitted by dust which is heated by the interstellar radiation field to temperatures below 20 Kelvin. This cool dust occupies 45 percent of the total area. Further 42 percent come from somewhat warmer dust in the vicinity of HII regions. The rest can be attributed to the warm dust in individual HII regions mentioned above with maximum temperatures of about 40 Kelvin.

Through comparison with the IRAS data some global properties of the SMC can be derived. The mass of the dust totals 3.7×10^5 solar masses, its bolometric luminosity is 8.5×10^7 solar luminosities. The star formation rate is estimated to be 0.015 solar masses per year. For comparison: in the Milky Way system being about one hundred times more massive the star formation rate is one to two solar masses per year. Next thing to do will be a comparison of these values with star formation rates in other dwarf galaxies for which ISO data are also available. Eventually, astronomers will try to obtain more information about the physical properties of the dust they have detected in the IRAS and ISO maps.

(Martin Haas, U. Herbstmeier, Ulrich Klaas, Oliver Krause, Dietrich Lemke, Manfred Stickel, L. Victor Toth, R. Vavrek, Karsten Wilke)

The Rotating Jet of a Young Star

Early in the 1980s, astronomers unexpectedly discovered strongly confined particle winds emanating in opposite directions from some young stars. The gas within these so-called jets is streaming away from the central object with velocities between 200 and 400 km/s. Since its discovery, in which astronomers at MPIA had a significant part, this phenomenon has remained a research focus at the Institute. So, for instance, the jets could be shown to reach a length up to ten light years and dynamical ages of more than 10 000 years. In spite of many further observational facts it is not clear yet beyond any doubts how the bipolar streams get accelerated. Now astronomers at MPIA for the first time found evidence of a jet rotating about its longitudinal axis, suggesting magnetic fields to be at work.

Young stars initially are surrounded by a disk of gas and dust in which planets can form. The jets have an important function during the star formation process: They remove angular momentum from the accretion disk thereby enabling the star to continue to grow for a long time by accreting matter from the disk.

To date, more than 50 jets are known, about twenty of them discovered at MPIA. The jets originate in T Tauri stars and Herbig Ae/Be stars which frequently are still deeply embedded within their parental clouds. These stars represent the transition stage between the collapsing protostellar clouds and the main sequence stars. T Tauri stars have 0.1 to 2 solar masses and Herbig Ae/Be stars more than two solar masses.

The formation process of jets, however, is still mostly unknown, especially since their point of origin has to be very close to the star. In most of the models collimation of the gas streams occurs within a few Astronomical Units (AU) from the star. But there are conceptions suggesting that the range of acceleration and collimation may extend to about one hundred AU from the star.

Astronomers at the Institute together with colleagues from the Astrophysical Observatory in Arcetri, Italy, the Thüringer Landessternwarte Tautenburg, and the Dublin Institute for Advanced Studies had selected the jet of the young star DG Tauri to investigate the processes in the near vicinity of the star. The jet of DG Tauri is one of the first jets detected (Fig. III.16). Because of its small distance of about 150 pc (500 light years) it has been studied intensely since then. So, the mass of DG Tauri is known to be 0.7 solar masses and the jet to be inclined 38 degrees to the line of sight.

For the high-resolution observations, the team used the STIS spectrograph onboard the HUBBLE Space Telescope. The observing strategy was to align the slit of the spectrograph along the jet axis and shift it perpendicular to the axis in steps of 0.07 arc seconds. The goal was to measure the velocity field of the jet back to the immediate vicinity of the star through the Doppler shift of several spectral lines. The data allowed a spatial resolution of 0.1 arc seconds, corresponding to 15 AU, within 2 arc seconds (300 AU) from the star.

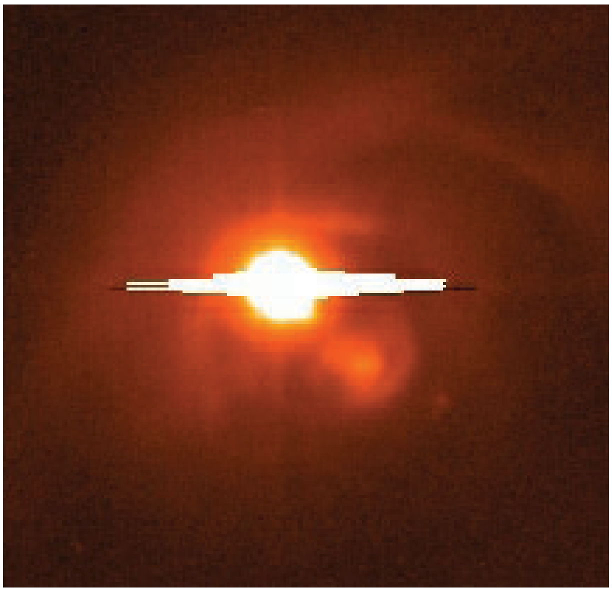

Fig. III.16: DG Tauri and its jet, imaged with the 3.5 m telescope on Calar Alto. The smearing of the stellar image (white) is due to the saturation of the CCD pixels. The jet extends to the southwest and ends in a bow shock.

The spectra showed several emission lines allowing measurements of both the particle density within the jet and the radial velocity. Two interesting facts were revealed.

For one thing, two components were detected within the jet that are clearly distinguishable through their radial velocities: a high-velocity component with radial velocities between -60 km/s and -200 km/s and a low-velocity component with -5 to -20 km/s (the minus indicating that the gas is flowing towards the observer). These data are with respect to the star. Both components had already been observed earlier but it had been impossible yet to decide if they indeed are two spatially separated streams and where they originate.

The new data now showed the gas density within the jet to decrease with increasing distance from the star. At the same time the density is highest along the central axis, decreasing towards the edges. Thus the jet has a dense central region surrounded by a thin envelop. Moreover, the high-velocity gas could be traced back to 0.1 arc seconds (15 AU) from the star. So the collimation and acceleration probably occurs even closer to the star. In the vicinity of the star the jet is not resolved perpendicular to the longitudinal axis and therefore has to be narrower than 15 AU. The slower gas flow, on the other hand, is not collimated so strongly and could be spatially resolved. In 0.2 arc seconds distance from the star, for instance, it is 0.2

arc seconds wide. So the total picture shows a dense high velocity gas spatially separated from a low velocity gas with low density.

From these data the mass flux within the jet could be determined to be about 2.4×10^{-7} solar masses per year, corresponding to about one tenth of the star's mass accretion rate through the surrounding disk. This value is in reasonable agreement with predictions made by models including magnetic fields.

According to these models, the star and the disk each have a magnetic field, both fields interacting in a complicated way (Fig. III.17). The magnetic field presumably is "frozen" to the disk matter and gets coiled up to a certain degree due to the rotation. Similar in shape to a corkscrew, it extends into the space above and below the disk. Along these field lines charged particles (ions) can be accelerated. If this model is correct the matter along the jet channel should rotate about the longitudinal axis while moving away from the star.

For the first time astronomers now were able to support this hypothesis. They found the south-western side of the DG Tauri jet to move towards us with respect to its north-eastern side (Fig. III.18). This can be interpreted simply as a rotation of the jet channel with toroidal velocities of 5 km/s to 15 km/s. These values are consistent with the rotation velocities derived theoretically for a disk rotating about DG Tauri. With a derived stellar mass of 0.67 solar masses Kepler's law provides velocities for the disk ranging between 4.5 km/s and 8 km/s within a distance range of 30 and 10 AU from the star.

One team member tried to measure the so far unobserved rotation of the DG Tauri disk. He studied the object in the light of the CO emission line using the millimeter-interferometer of the Owens Valley Radio Observatory, California. He succeeded to detect a disk that is orientated perpendicular to the jet axis and rotating in the same direction as the jet. This identical sense of rotation found both in the radio range and in visible light significantly supports the interpretation of the optical data as a rotation of the jet.

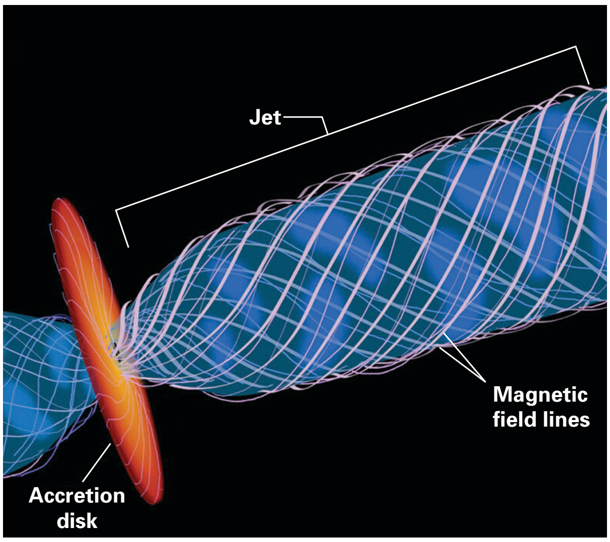

Fig. III.17: Schematic view of a jet with its particles moving away from the star along magnetic field lines.

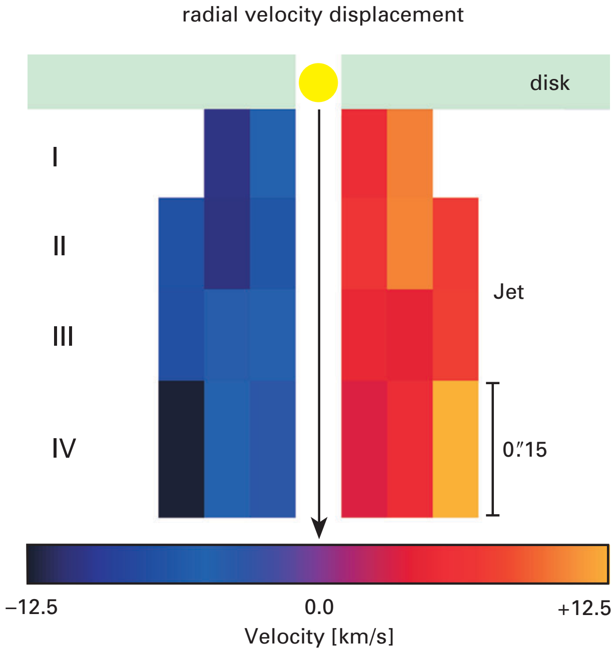

Fig. III.18: Radial velocity field within the jet close to DG Tauri. The blue part is moving towards us, the red one away from us.

Thus the connection between accretion disk and jet is confirmed for the first time by direct observations. Further information should be obtained in the near future using for instance the MIDI infrared interferometer at the VLT (Chapter II.3). With this instrument it should be possible to observe the immediate vicinity of the jet sources. Much progress is also expected from observations with the planned ALMA millimeter interferometer because the velocity field within the disk can be measured in greater detail using this instrument. This could also be done in the jet if in it molecular gas is flowing.

(Reinhard Mundt)

Star Formation in Spiral Galaxies

Spiral galaxies are among the most esthetic objects in the universe, resembling giant fire wheels. Our Milky Way, too, belongs to this galaxy type. Although spiral galaxies have been intensely studied for decades there are still many questions left open. Two studies carried out at the Institute are dealing with star formation within these galaxies. Using data of the ISO infrared observatory, astronomers found the star formation rates in spiral galaxies showing strongly pronounced arms and faint cores to be higher than in those with dominating cores. Only in the first type star formation occurs over the entire disk. These properties can be explained by different amounts of interstellar gas and by its distribution within the disk. Interestingly, the light profiles of all spiral galaxies are decreasing exponentially from the center outwards. Computer simulations performed by the Institute's theory group prove this typical feature to be a natural consequence of star formation.

Spiral galaxies are thought to be active star forming systems while the second large galaxy type, the ellipticals, are old systems showing much less activity. Since the work of Edwin Hubble in the 1920s, galaxies are classified according to their appearance. Three main types are distinguished: Sa, Sb, and Sc (also called early, medium, and late type). Sa spirals are those with tightly wound spiral arms around a large, prominent central bulge while Sc systems have an insignificant or no central bulge at all and only loosely wound arms. Sb spirals occupy an intermediate position. In addition, there are barred spiral galaxies, designated as SB. They are characterized by a bar-like structure running through the nucleus. It is defined by bright stars and huge masses of gas. More or less prominent spiral arms originate at both ends of this bar. As with ordinary spirals, barred spirals are classified into SBa, SBb, and SBc according to the tightness of their spiral windings. Midway in appearance between elliptical and spiral galaxies are the S0 galaxies, having a strongly pronounced bulge surrounded by a more or less uniform disk without any spiral arms.

Up to now, the cause of these different morphologies has not been clearly identified. But star formation certainly plays a major role. So the large star formation regions with bright, massive stars and their surrounding nebulae are found within the arms. The question whether the intensity of star formation is related to the galaxy type of the Hubble sequence is disputed for 20 years now. Studies in the visible wavelength range are of limited indicative value since dust absorbs a major part of the radiation. But as young, hot stars heat the surrounding dust, infrared observations offer the opportunity to detect the total extent of star formation in spiral galaxies.

The IRAS infrared satellite provided the data for the first extensive studies of this kind. However, it often did not have the spatial resolution needed to distinguish between emission from the central regions and the disks. Much better possibilities were provided by ISO: The ISOCAM mid-infrared camera and the ISOPHOT far-infrared camera developed at the Institute achieved a spatial resolution four times higher than IRAS and had a higher sensitivity. Moreover, ISOPHOT for the first time allowed observations up to 200 μm which are needed to record the total mass of the heated dust. In addition, ISO was able to perform pointed observations while IRAS had scanned the entire sky.

Astronomers at the Institute together with colleagues from the USA and the United Kingdom used these possibilities to observe a large sample of spiral galaxies of various morphological types. The data were complemented by near-infrared observations with a 2.2 m telescope on Hawaii. The galaxies were chosen from a catalogue that is complete to a blue magnitude B = 13 mag. During 27 hours observing time, the astronomers observed a total of 74 galaxies at distances up to about 30 Mpc (100 million light years).

As is shown in Figure III.19, the majority of the galaxies observed in this study emits about 10^9 to 10^{11} solar luminosities in the far infrared range. So, no unusually luminous galaxies were among them. From which region within the galaxies does the emission emerge? In the mid-infrared range, the study revealed a significant correlation with the Hubble type. In S0 and Sa galaxies, the emission

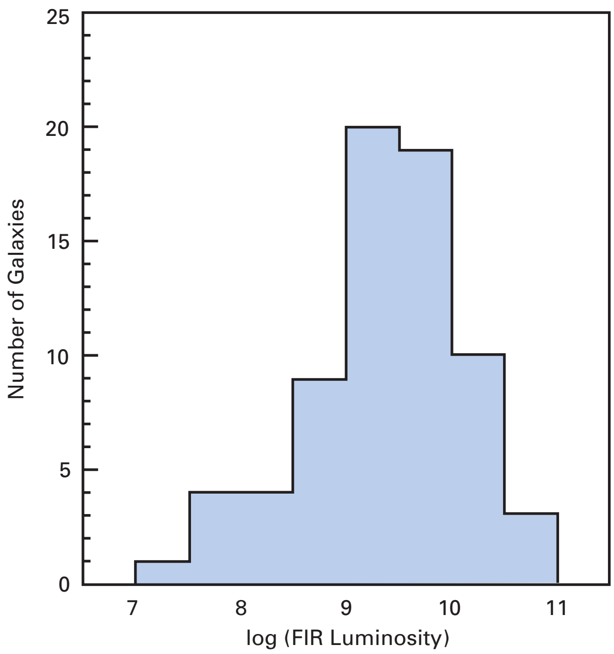

Fig. III.19: Distribution of the far-infrared luminosities of spiral galaxies, determined from ISOPHOT measurements in the wavelength range between 60 μm and 180 μm. The luminosities of most of the systems range between 10^9 and 10^{11} solar luminosities.

Fig. III.20: Spiral galaxies NGC 5236 (M 83) and NGC 5364, imaged in visible light with the ESO VLT and in the near infrared at 12 μm with ISO. The infrared images only show the inner region with a size of 150 arc seconds.

is concentrated to the central regions. In the late types, however, emission regions are distributed over the entire disks. But here, too, the central region provides the major portion of the total emission. Two examples are shown in Figure III.20.

The emission in the mid-infrared and far-infrared range can be assumed to originate mainly from star formation regions. Thus the new study indicates that the star formation activity is changing with the Hubble type: In early types it is strongly centralized, while in late-type galaxies it is increasingly spreading over the disks (Figure III.21). This result can be interpreted in relation with another well-known fact. In the late 1980s, the star-formation rate was found to increase with increasing gas density, the latter obviously having to exceed a certain minimum value for star formation to set in. Observations of molecular gas confirm the increase of the overall surface density of interstellar gas from early- to late-type galaxies and an increasing spread of the molecular gas over the disk along the Hubble sequence.

Under certain assumptions star formation rates can be calculated from the radiation fluxes measured in the near- to far-infrared spectral region. They range from a few thousandths up to eight solar masses per year and galaxy. The mean value of 1.4 solar masses per year is in reasonable agreement with the star formation rate of the Milky Way. These data could be used to test the so-called Schmidt law suggested already in the 1950s. It claims that there is a unique relation between the star formation rate and the gas density within the star formation region. As is shown in Figure III.22, the new data, averaged over the entire galaxy, follow a power law. This relation still holds if the central regions and the disks are considered separately.

The new study reveals interesting relations between both the intensity and the spatial distribution of star formation and the Hubble type of spiral galaxies. But the physical cause for this is still unknown. Maybe another investigation just started at MPIA will provide further information. It is based on the so-called ISOPHOT Serendipity Survey at 170 µm containing data of more than 2000 spiral galaxies. This data base will be screened, calibrated, and analyzed in the near future.

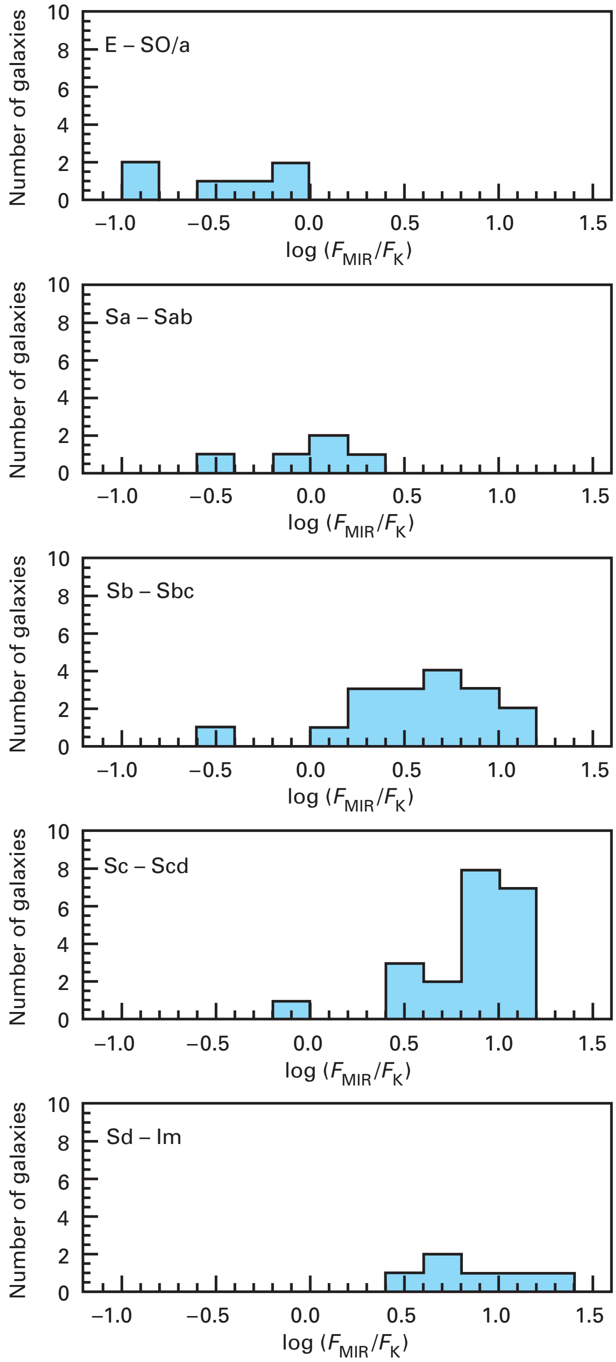

Fig. III.21: Number of galaxies as a function of the star formation rate in the disk represented by the mid-infrared flux as a function of Hubble type. For better comparison, the data are normalized to the total stellar population of each galaxy whose radiation is measured through the K-band flux (2.2 µm). The diagram shows the portion of the emission coming from the disk compared to that coming from the center. The disk portion is increasing with the Hubble type.

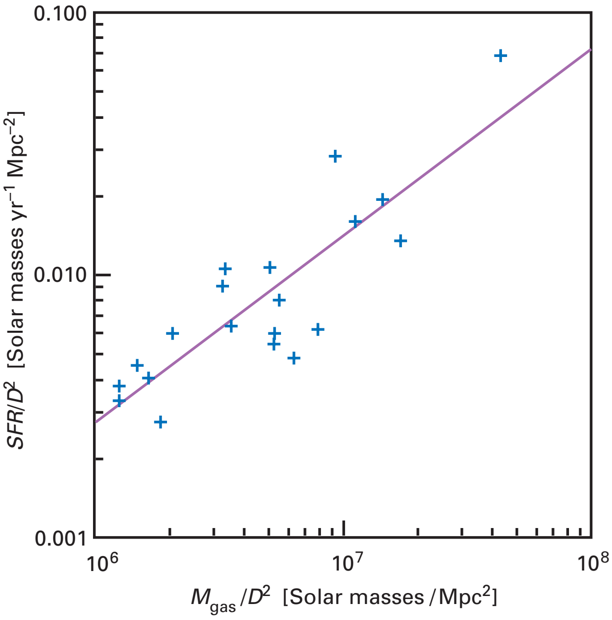

Fig. III.22: The integrated star formation rate derived from the infrared luminosity is increasing with the gas mass. This relation, described by a power law, is called Schmidt law. As both quantities are derived from the luminosity (which is proportional to the square of the distance D) the distance term has to be removed by dividing by D^2 in order to eliminate an alleged correlation based only on distance.

Turbulence in spiral galaxies and the exponential light profile

It is known for decades that spiral galaxies have a characteristic radial light profile: The intensity is decreasing exponentially from the center to the edge. For a long time, the so-called ín situ scenario has been discussed as the cause of this phenomenon. This scenario probably is based on an observation made 40 years ago. It was noticed then that the distribution of angular momentum in spiral galaxies is very similar to that of a uniform, rigidly rotating body. Spiral galaxies thus were thought to form through contraction of spherical gas clouds with the angular momentum being conserved. Recent calculations mostly confirmed this hypothesis. If the galaxies were assumed to form within the gravitational potential of a dark matter halo, the decrease of the intensity is exponential at least over three scale lengths. In addition, further properties such as the shape of the rotation curves and the Tully-Fisher relation could be explained within this scenario.

The in situ scenario, however, vitally depends on the conservation of angular momentum and ignores any process that could redistribute major gas masses through turbulent motions. In our current view, this seems to be unrealistic.

In the current hierarchical paradigm, large spiral galaxies did not form from a single cloud but by accumulation of several smaller building blocks. Therefore, it seems plausible to look for models that produce the exponential intensity profile in spiral galaxies regardless of the initial density distribution of the proto-cloud.

An essential element of such models is friction or viscosity in the interstellar gas. It is caused by turbulences driven by energy that is supplied from supernovae, stellar winds, and ionizing radiation from young stars. In this so-called viscous scenario, star formation therefore plays a crucial role.

Theorists at the Institute, together with colleagues at the University of Oxford, have performed simulations to look for conditions leading to an exponential light profile in a turbulent star-forming medium. However, present-day computers are by far not powerful enough to simulate all major processes accompanying star formation in an entire galaxy. Moreover, the calculations were not intended to include the full-scale cosmological model of hierarchical galaxy formation or even to confirm it. The purpose of this first approach only was to demonstrate that the initial density profile of the proto-cloud need not be exponential, to lead to the formation of a spiral galaxy with an exponentially decreasing light profile.

Turbulence in the interstellar medium is the crucial factor. Goal of the two-dimensional hydrodynamical simulations was to detect the effects of a turbulent interstellar medium on galaxy evolution. The physical causes and sources of the turbulence, however, remained unidentified.

In the simulations, the galaxy was assumed to be a disk-shaped aggregation of gas with a total mass of 5×10^{10} solar masses. The initial density profile could be varied. The system evolved in the constant gravitational potential of a dark matter halo of 10^{12} solar masses. For simplicity, the gas was assumed to have a constant temperature of 10 000 Kelvin and a constant viscosity. The radius of this model spiral galaxy was chosen to be 20 kpc (65 000 light years).

Because of the extent of the system the size of each simulation cell was 200 pc (630 light years) per side. Individual star formation processes cannot be simulated on this scale. Therefore, star formation and the turbulence within the interstellar medium generated by it was characterized by certain parameters. This turbulence causes the gas to no longer move on Keplerian orbits around the center but also to flow radially in- and outwards. The result is a redistribution of angular momentum. The simulations followed the evolution of the disk system over a period of 12 billion years, checking the effects of various parameters.

Of prime importance was the effect of viscosity. The typical viscous timescale t_{visc} is defined as the time it takes a gas clump to move a radial distance r. This time can be related to a star formation timescale t_*. Of great importance for the simulations was the fact that the star formation process itself causes viscosity and thereby radial gas motions. But from the moment a star has formed, it moves on a Keplerian orbit and does no longer contribute to the redistribution of angular momentum.

A set of three simulation runs was performed under these assumptions, varying the ratio of the star formation timescale to viscous timescale t_*/t_{visc} (Fig. III.23). As it turned out, almost no redistribution of angular momentum occurs if the star formation timescale is ten times shorter than the viscous one. In that case star formation is converting gas into stars so rapidly (Fig. III.23, left), that after 12 billion years more than 98 percent of the gas is gone. But this case is inconsistent with reality. Our Galaxy, e.g., still has a supply of gas of about 15 percent in its interstellar medium. If, at the other extreme, the star formation rate is ten times slower, the medium becomes very turbulent without many stars being formed (Fig. III.23, right). As a consequence, too much angular momentum is redistributed. The resulting radial density profile is too steep to be exponential and rather resembles a power law. Moreover, only a few percent of the gas have been converted into stars, which is unrealistic, too.

An interesting case is the third one where stars are forming on the viscous timescale (Fig. III.23, middle). Here, indeed, the stellar density and thereby the light profile become approximately exponential as is observed in spiral galaxies. This stage is already established after six billion years, the evolution proceeding much faster at early times than later. The results for the amount of gas converted into stars and the stellar density in the solar neighborhood also correspond to present-day observations. Further simulation runs confirmed that exponential stellar density profiles are obtained for ratios t_*/t_{visc} ranging between 0.5 and 2.

Thus, these calculations support the hypothesis that a proto-galaxy can develop an exponential intensity profile through star formation and the accompanying gas viscosity. In further simulations it was checked how different initial conditions would change the results for the $t_*/t_{visc} = 1$ case.

Fig. III.23: Time evolution of gas density, radial velocity, tangential velocity and stellar density (from top to bottom) for the three cases : $t_*/t_{visc} = 0.1, 1$, and 10 (from left to right).

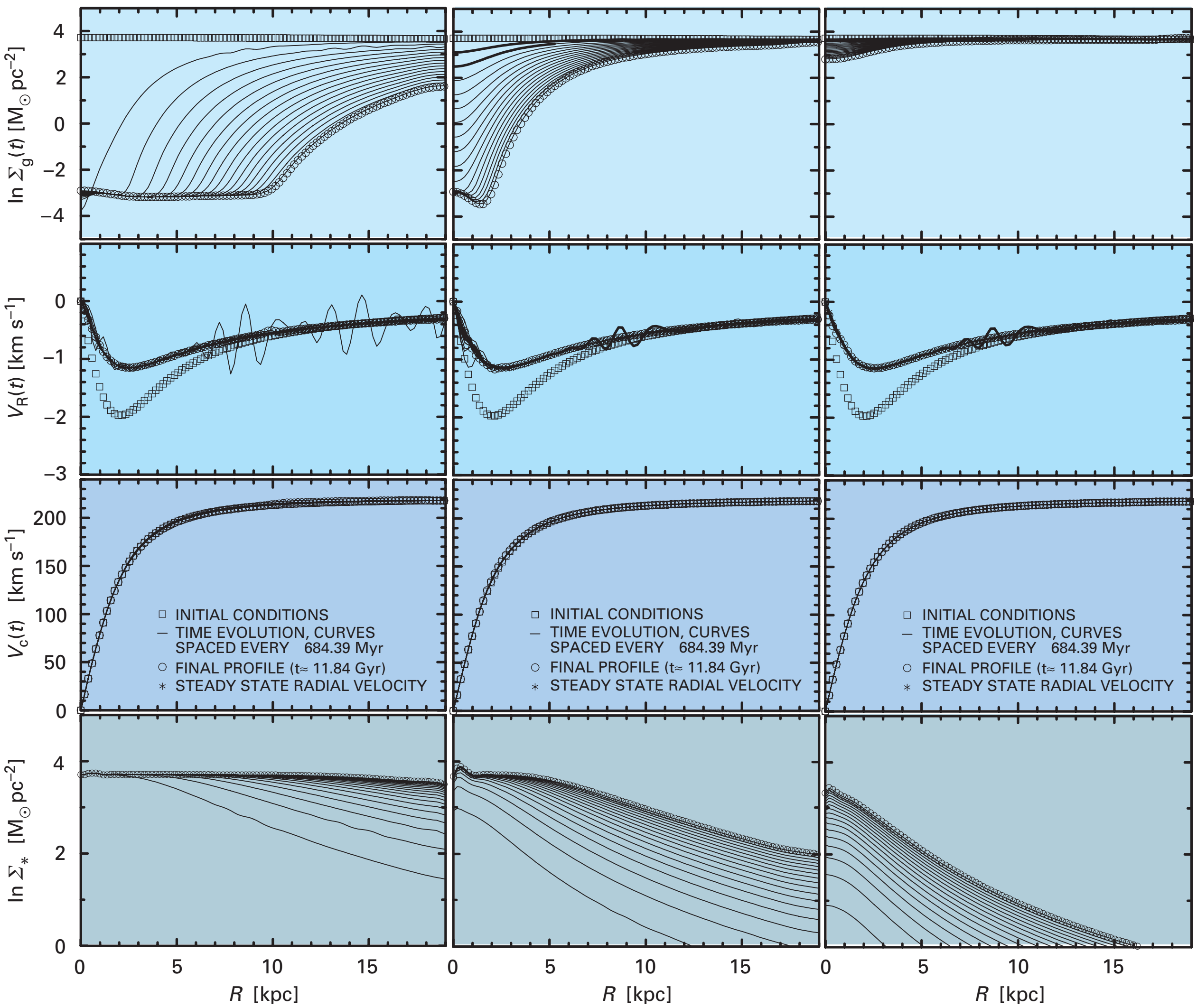

So, the initial gas profile was varied between an exponential law and power laws with various steepness. Several initial profiles indeed led to an exponential intensity profile. Interestingly, agreement with the present-day interstellar gas fraction, observed in the Galaxy, of about 15 percent was best obtained for initial density profiles that follow a very steep power law. Based on this steep density profile the time and spatial evolution of star formation can be estimated. Figure III.24 demonstrates the good agreement between gas density (above) and the star formation rate in the disk, compared to Milky Way data. (In the central region out to about 4 kpc, the simulations are not very reliable because they do not include self-gravity, which is of significance there due to the rather high matter density.)

Moreover, star formation turned out to proceed from the center outwards (Fig. III.25). This is a consequence of the given initial gas density and the fact that in the simulation star formation commences primarily in regions with strong radial gas flows. In the vicinity of the sun, the star formation rate has achieved its present-day value already after about two billion years, remaining constant since then. The implications of this result are difficult to judge since present-day observations do not provide a clear picture of the star formation history in the solar neighborhood.

Because of the simplifications that had to be made, some details of these simulations should be considered with care. Nonetheless, they strongly suggest the hypothesis that the present-day exponential intensity profiles of spiral galaxies could be caused by star formation and the turbulent, viscous gas motions generated by this process. Thus, the formation of spiral galaxies within modern hierarchical scenarios is much better understood. In further steps, there will be attempts to make the simulations more realistic by extending the code to three dimensions and including physical effects such as self-gravity of both the disk and the halo.

(Observations: M. Haas, U. Klaas, D. Lemke; Theory: A. Burkert, A.D. Slyz)

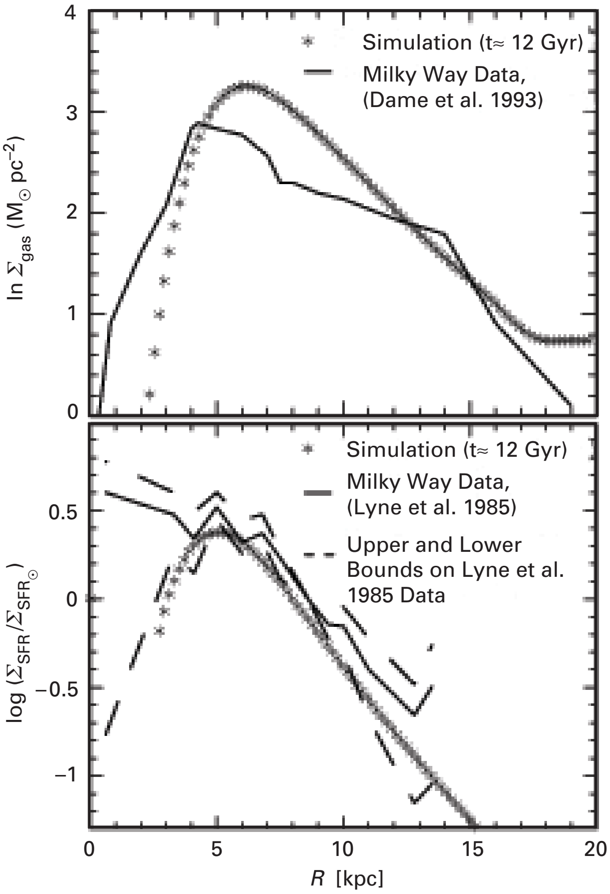

Fig. III.24: Comparison between the simulations (asterisks) and observational data for radial profiles of gas density (above) and star formation rate (below).

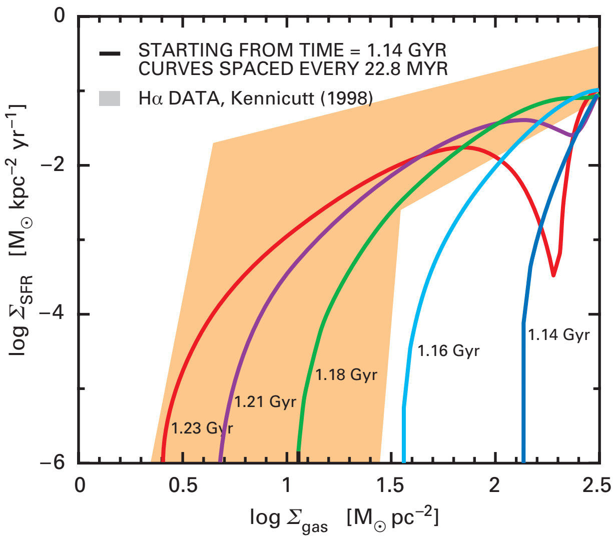

Fig. III.25: Time evolution of the star formation rate in the period between 1.14 and 1.23 billion years after galaxy formation as a function of the gas density decreasing from the center outwards.

III.2. Galaxies and Cosmology

Luminosity Evolution of 25 000 Galaxies

The goal of cosmological research is to trace the formation and subsequent evolution of galaxies by looking back into the past. Only extended sky surveys using sensitive detectors have recently led to major breakthroughs in this difficult field. Scientists at MPIA have initiated such a project, called COMBO-17, and conducted it together with colleagues at the Universität Bonn and at the Institute for Astronomy in Edinburgh. This sky survey allowed to classify 25 000 galaxies and to determine their redshifts (distances) and luminosity functions. Currently, this is the most extensive and deepest survey worldwide. The data impressively demonstrate how the fractions of the various types of galaxies have shifted over the last six to eight billion years. Initially, irregular and starburst-galaxies dominated the total luminosity in the universe while at present, elliptical and spiral galaxies are contributing the major part.

The onset of galaxy formation takes place soon after the big bang so that this very first phase cannot be observed directly. Since recently, however, it is possible to trace the further evolution of large samples of galaxies. Due to limited observation time available at big telescopes, two different strategies are followed for this purpose. Either a very small field on the sky is observed with very long exposure times. In this case, one can peer very deeply into space and very far back into the past, but the field of view contains only a relatively small number of galaxies. Or a very large area on the sky is observed with short exposure times. In this case, one cannot look quite as far out but gets data on a large sample of galaxies that is representative of the entire universe. This second strategy is followed by astronomers at the Institute with their COMBO-17 sky survey.

The Strategy of COMBO-17

The name of the survey, COMBO-17 (Classifying Objects by Medium-Band Observations with 17 Filters), already indicates the course of action: A large area on the sky is imaged through 17 different filters, measuring the galaxy magnitudes in the corresponding color ranges. Thus it is possible to classify the galaxies and determine their redshifts.

The key requirement for the project is the large field of view of the wide field camera (Wide Field Imager, WFI, cf. Annual Report 1998, p. 33). It had been developed under the leadership of MPIA and was built together with ESO. Since the end of 1998, it is operating at the MPG/ESO 2.2 m telescope on La Silla. It has a field of view of 34 × 33 arc minutes, a little bit more than the size of the full moon. The CCD array consisting of eight individual chips with 8.3 million pixels each is sensitive over a wide spectral range, from UV (350 nm) to the near infrared (950 nm).

In the course of COMBO-17, a total of five widely separated fields on the sky is imaged through 17 filters (Fig. III.26), including five broad-band filters (standard ranges *U, B, V, R, I*) and 12 medium-band filters (relative width about 3 percent). With the help of sophisticated software first the point-like stars and quasars are distinguished from the extended galaxies in the images. Based on the magnitudes in the various color ranges, the remaining objects then can be classified very precisely. Intensities

Fig. III.26: Transmission curves of the COMBO-17 filter set. The five broad-band and the twelve medium-band filters are easily recognized.

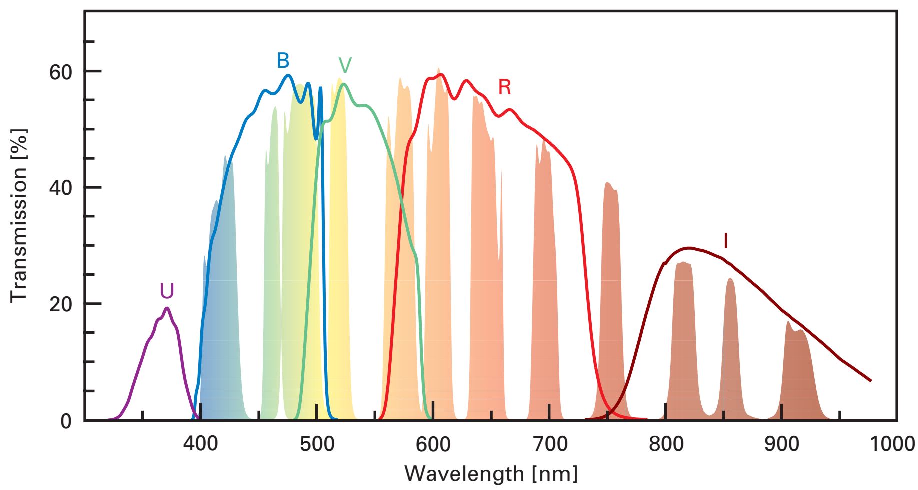

measured though the 17 filters are compared with characteristic spectra of the corresponding object classes (templates) taken from existing catalogues (Fig. III.27). For stars, spectral types A to M8, for galaxies, classes E (elliptical) to Sc (spiral galaxy with high star formation rate) as well as starburst galaxies with extraordinary high star formation rates can be identified. Moreover, for each galaxy down to an R-magnitude of 24 mag, a redshift can be determined, with an uncertainty varying according to magnitude and type between 0.005 and 0.1. Quasars, too, are identified and their redshifts measured with an accuracy better than ± 0.1.

When the COMBO-17 survey will be finished, a field of sky of almost one and a half square degrees will be completely searched for stars, galaxies, and quasars. For comparison: Both HUBBLE Deep Fields, the deep images taken with the HUBBLE Space Telescope in the northern and southern sky, only cover one hundredth of the WFI's field of view. COMBO-17 will provide more reliable information on the evolution of galaxies because it includes a significantly larger and therefore more representative volume of space. COMBO-17 will determine redshifts and spectral energy distributions of a total of approximately 50 000 galaxies brighter than 24 mag and about a thousand quasars. A comparison with X-ray data will also be very interesting. This will soon be possible as COMBO-17 also covers the CHANDRA Deep Field (about 15 × 15 square arc minutes) that was obtained from an image taken with the US-American CHANDRA X-ray telescope with an exposure time of 278 hours.

In the year under report, observations and data analysis were completed for three fields covering a total area of 0.78 square degrees. Each field was imaged with a total exposure time of 44 hours and contains 200 000 objects down to an R-magnitude of 26 mag. From these, the team selected 25 000 galaxies suitable for classification. In or-

Fig. III.27: Comparison of the intensities measured through the 17 filters (black crosses) with the best-fit spectrum from a template library. Above, the spectrum of an elliptical galaxy; below, that of an Sc spiral galaxy.

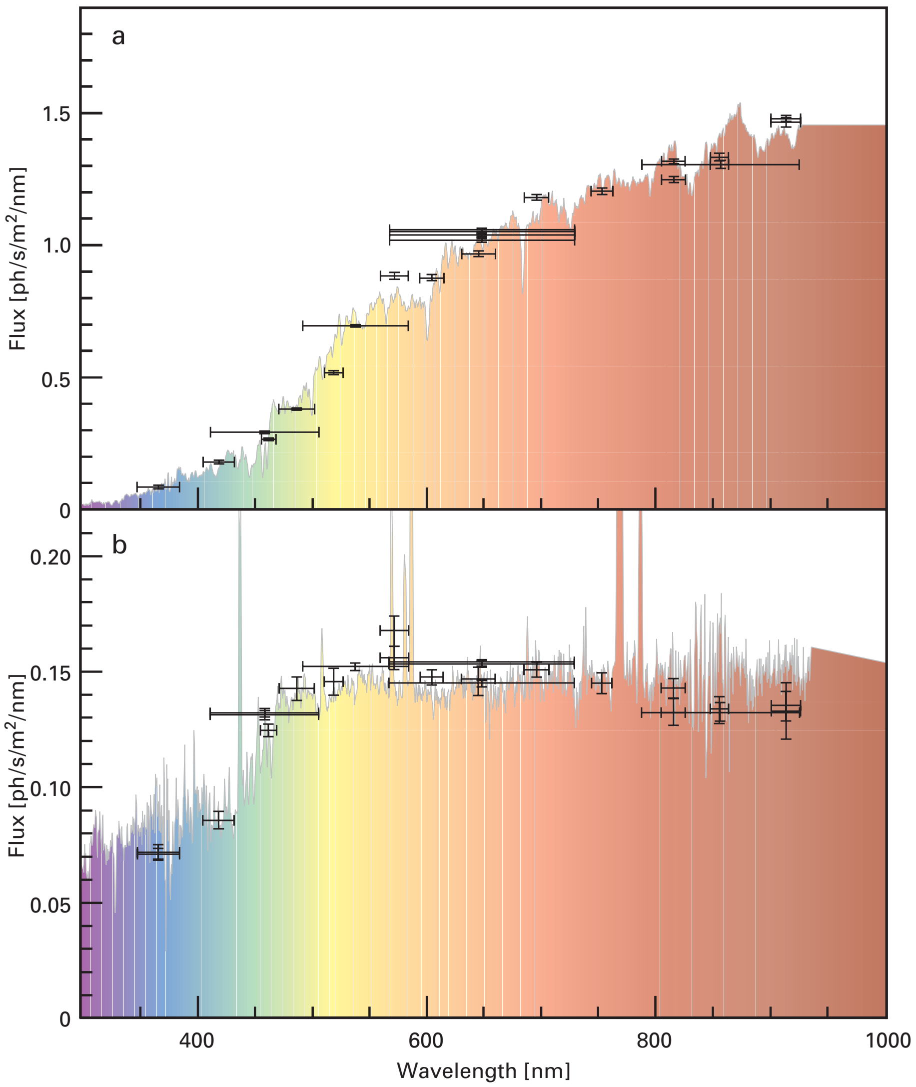

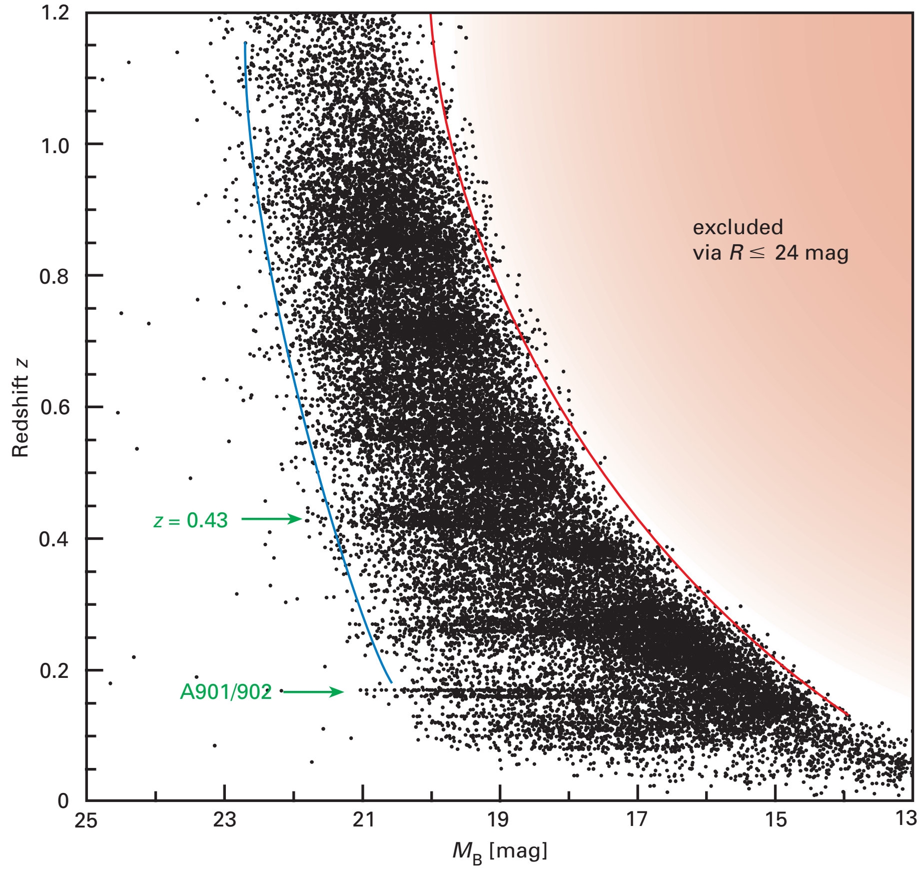

Fig: III.28: Distribution of the absolute magnitudes of all 25 000 galaxies as a function of redshift. The strip-like horizontal concentrations, e.g. at $z = 0.2$, correspond to individual galaxy clusters.

der to get sub-groups containing statistically relevant numbers of objects for later analysis, the galaxies were classified into only four galaxy types: type 1: elliptical galaxies, type 2: spiral galaxies, type 3: irregular galaxies, and type 4: starburst-galaxies with unusually high star formation rates.

The redshifts of all galaxies range from $z = 0.2$ to $z = 1.2$. Galaxies with lower redshifts are not found in the COMBO-17 fields in sufficient numbers to allow statistical analysis, and for more distant galaxies, no accurate redshift could be derived. The selected sample is estimated to be 90 percent complete (depending on the type) down to an R-magnitude of 23.0 mag and 50 percent down to $R = 23.8$ mag.

Figure III.28 shows the distribution of the four galaxy types as a function of redshift. The empty region to the right is excluded by magnitudes beyond 24 mag. Several horizontal strip-like features representing local overdensities can be recognized, the most conspicuous one being that at $z = 0.2$. It represents the galaxy cluster Abell 901/902 comprising about one thousand members.

Time Evolution of the Luminosity Function

The luminosity function is defined as the number density of galaxies per luminosity interval; the luminosity can also be characterized by absolute magnitude. In comparing values at various redshifts one has to allow for the expansion rate of the universe: The unit volume is increasing over time, the time evolution depending on the world model. The scientists based their study on a “flat” universe with the critical density in which the total energy density comprises 30 percent matter (baryonic and dark matter) and 70 percent dark energy.

The luminosity function of 5674 galaxies in the redshift range $0.2 < z < 0.4$ was assumed to be quasi-local. The number of galaxies is too small to determine significant evolutionary effects within this interval. Among these relatively nearby objects, the major part of the total luminosity density is provided by the fainter galaxies (to the right in Fig. III.29). A detailed view reveals differences. The bright section of the luminosity function is dominated by elliptical galaxies (type 1), while at its faint end starburst galaxies (type 4) prevail (at least in the blue and red spectral region). At intermediate magnitudes, all four galaxy types contribute about equally to the luminosity function.

Of special interest was the question how this luminosity function has evolved since a redshift of $z = 1.2$, corresponding to a look-back time of about eight billion years.

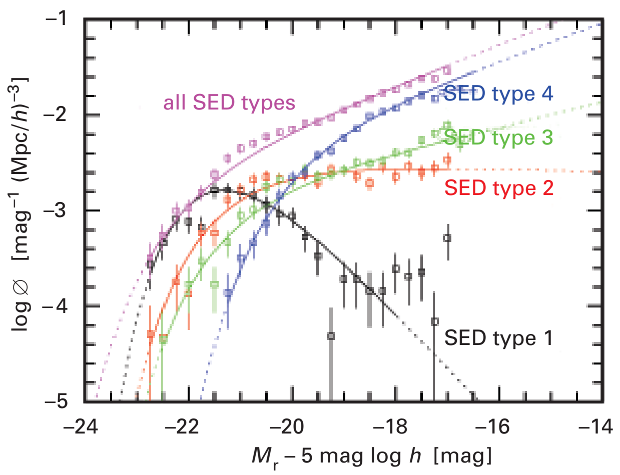

Fig. III.29: Luminosity function of the four galaxy types in the quasi-local redshift-range from $z = 0.2$ to $z = 0.4$.

For this purpose redshift intervals each with a width of Δz = 0.2 were considered, centered at z = 0.3, 0.5, 0.7, 0.9, and 1.1. Figure III.30 shows the changes of the luminosity functions for the four galaxy types over this redshift range. Remarkable is the fact that the number of elliptical galaxies (type 1) has increased until today by a factor of ten. The steep increase indicates that the maximum is not reached yet. The spiral galaxies (type 2) show a time evolution with a maximum density at z = 0.6, i.e. about eight billion years ago. The density of the irregular galaxies (type 3) seems to have remained nearly constant for a long time until it decreased by a factor of two in the recent past. The starburst galaxies show a continuous decrease over the entire redshift range. The data suggest the maximum luminosity of this type of galaxy to lie in the early universe beyond the upper redshift limit of the survey at z = 1.2.

This evolution appears even clearer if one looks at the luminosity density in a unit volume instead of the luminosity function. Figure III.31 demonstrates the increasing contribution of the elliptical galaxies up to now. The slight maximum of the spiral galaxies around redshift z = 0.6 to 0.8 is also noticeable while the fractions of the other galaxy types have decreased over the past eight billion years (since z = 1.2). The total luminosity density of all four galaxy types taken together has declined over the period of time covered by the data.

Figure III.32 illustrates the change of the contributions of the various galaxy types to the luminosity density: In the early universe, irregular and starburst galaxies with intensive star formation (types 3 and 4) dominate the luminosity density. In the blue and red spectral region, their fraction amounts to 70 percent and 90 percent, respectively. In the course of time, however, the relative frac-

Fig. III.30: Evolution of the luminosity function of the four galaxy types in the red spectral range as a function of redshift. The blue graph represents the nearest group, the red graph the most distant one, and the green graphs those in between.

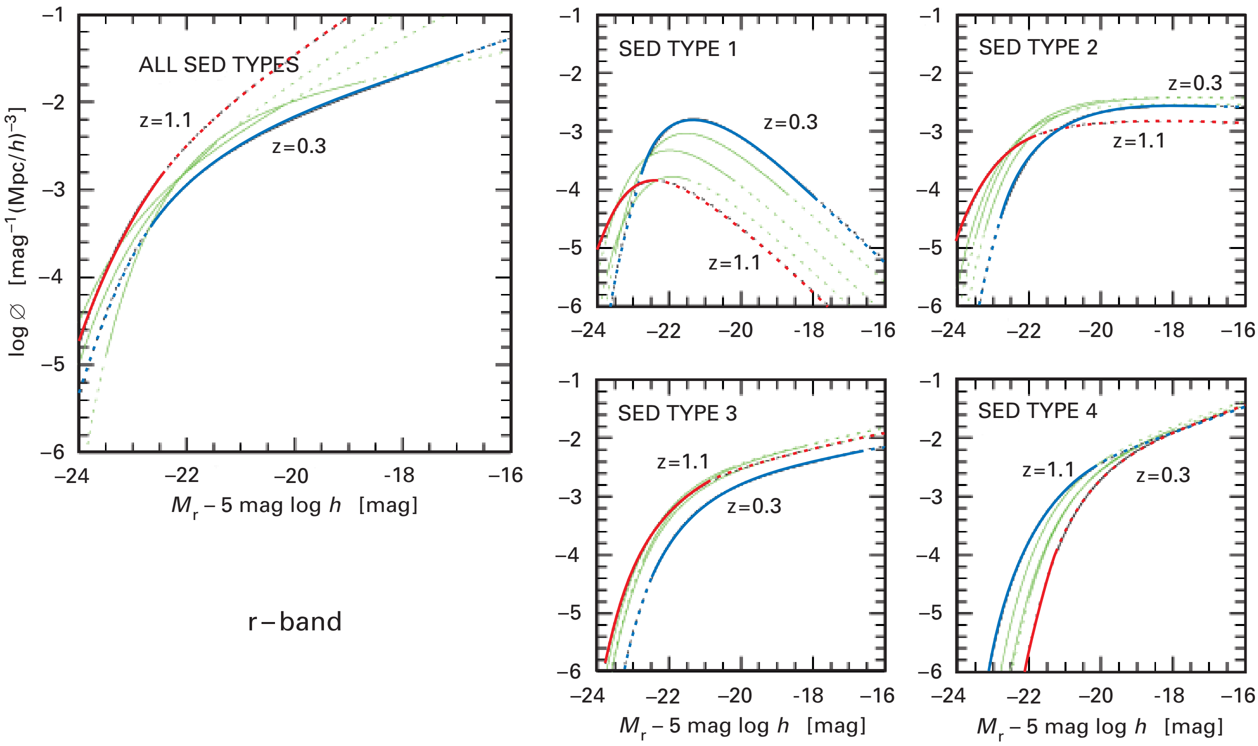

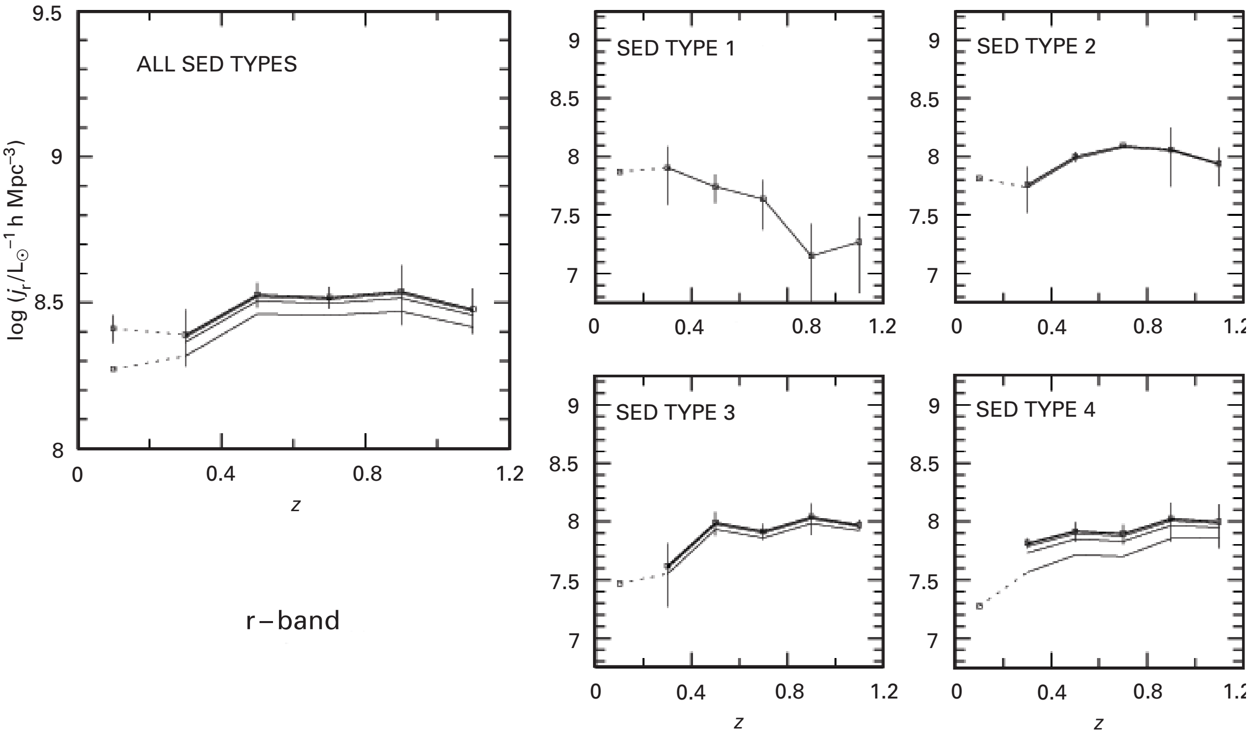

Fig. III.31: Evolution of the luminosity density in the red spectral region as a function of redshift.

tions have shifted significantly. At present, types 3 and 4 contribute only about 20 percent to the luminosity density while elliptical and spiral galaxies dominate.

Compared to previous sky surveys with good redshift accuracy, the data of COMBO-17 go deeper by about two magnitudes and the number of galaxies is about ten times larger. Thus this study was able to draw a much clearer picture of the evolution of galaxies over the observed distance range.

Future studies will have to show how these new findings can be incorporated into present-day cosmological theories. The data support previous suggestions that elliptical galaxies have formed by mergers of spirals. These theories are also confirmed by numerical simulations carried out at the Institute. Particularly, they qualitatively agree with models where the star formation rate in the early universe was considerably higher than today. This important issue had been investigated in greater detail in another observational project named CADIS as is shown in the next chapter.

(C. Wolf, K. Meisenheimer, A. Borch, S. Dye, M. Kleinheinrich, S. Phleps, H.-W. Rix, H.-J. Röser)

Fig. III.32: Contributions of the various galaxy types to the luminosity density in the UV as well as in the blue and red spectral region as a function of redshift. Types 1 to 4 are plotted from bottom to top.

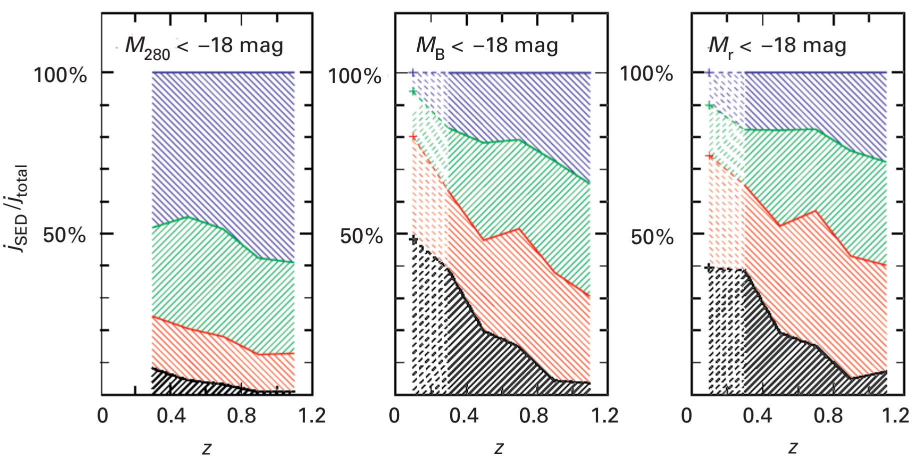

Star Formation History in the Early Universe

In the big bang, almost exclusively the elements hydrogen and helium were created. Heavier elements, such as oxygen, nitrogen, and carbon, were formed later through nuclear fusion processes in the interiors of stars. After being distributed throughout the interstellar medium by stellar winds and supernovae explosions, these elements then provided the basic material for new stars and planets. The question, when the first generation of stars did light up in the universe and at which rate subsequent generations did form is of central importance for cosmology. Within the scope of the CADIS sky survey carried out at Calar Alto, astronomers at the Institute detected several primordial galaxies and found the star formation rate to have decreased by a factor of 20 over the past eight billion years. This program is part of the DFG-Sonderforschungsbereich "Galaxies in the Young Universe".

According to current theories, already one billion years after the big bang giant gas clouds contracted under the influence of gravity to form the first galaxies. It is not clear, though, whether the present-day large galaxies such as the Milky Way did form from a single cloud or whether smaller proto-galaxies formed first and then merged to build a large one (building-block scenario). Which course took the further evolution? Did the galaxies form first and then accumulated over billions of years into large galaxy clusters (bottom-up model)? Or did gas clouds the size of galaxy clusters contract as a whole and then broke apart into smaller fragments that subsequently formed galaxies (top-down model)? Many questions are still open since very distant galaxies are extremely difficult to detect even with present-day large telescopes.

Only in the last few years it was possible to find a small number of star systems from this very early epoch. In many cases, the discovery was made entirely by chance. Only since recently, programs exist worldwide to search systematically for galaxies with redshifts $z > 4.5$ using sophisticated strategies. These redshifts correspond to a period till about two billon years after the big bang.

Since the mid-1990s, the extremely ambitious CADIS (Calar Alto Deep Imaging Survey) observation program has been conducted using the 2.2 and 3.5 m telescopes on Calar Alto. Within the scope of this program the astronomers search for distant galaxies and trace back the history of star formation in the universe to the primordial epoch. The project is one of the most ambitious in this research field in the world. Each year, more than ten percent of the observation time at both telescopes is granted to the CADIS team. One of the prerequisites for successful work was the building of the new CAFOS and MOSCA focal reducers that widen the field of view to the extraordinary size of 120 square arc minutes (Fig. III.33). In addition, the scientists developed a sophisticated technique of multicolor photometry that enables them to identify promising candidates for very distant star systems among the large number of foreground galaxies.

The major goal of the project is to detect galaxies in their state of formation at redshifts of $z = 4.7$, 5.7, and 6.6. These redshifts correspond to an age of the universe of 1.2, 1.0, and 0.8 billion years, respectively. These data are based on a universe with critical density, in which matter provides 30 percent and dark energy 70 percent of the total energy density.

The Strategy of CADIS

The search strategy of CADIS is based on the reasonable assumption that the very first galaxies show intense radiation of hydrogen at certain wavelengths. This radiation is caused by massive young stars that heat the surrounding gas to ten thousand degrees. The strongest hydrogen emission line is the so-called Lyman-α-line at 122 nm in the UV spectral range. In present-day galaxies, dense interstellar dust clouds absorb the light in this spectral region, making the Lyman-α-emission rather faint in these objects. The first galaxies, however, barely contained any heavy elements so that no dust could form within them. Therefore only primordial galaxies should make themselves conspicuous by intense Lyman-α-emission. In addition, primeval galaxies contained only a small number of stars compared to present-day galaxies so that the continuum radiation, too, should be very low. The strategy applied by CADIS is based on these two conditions.

Several fields on the sky are imaged in various spectral bands. One of these bands will then contain the Lyman-α-line. Of course it has to be taken into account that the line's rest wavelength of 122 nm has been shifted to longer wavelengths according to the redshift of the observed galaxy. The CADIS project therefore requires filters that transmit in exactly defined spectral bands (Fig. III.34). For this purpose, the astronomers are using a Fabry-Perot filter. It essentially exists of two mirrored glass plates that let pass only light of a particular wavelength. This is accomplished by multiple reflections and deconstructive and constructive interference, respectively. The pass band can be varied by varying the distance between the glass plates. A Fabry-Perot filter thus is acting like a tunable narrow-band filter.

Principally, a Lyman-α-galaxy can be identified by imaging an area on the sky in the range of the Lyman-α-line and then a second time in the range of the neighboring continuum. However, a strong Lyman-α-emission can also be faked. For instance, there are numerous dwarf galaxies resembling very distant large galaxies due to their low luminosity. The gas they contain can also emit strong line radiation. For instance, in addition to Lyman-α, hydrogen emits at 656 nm (Hα) and 486 nm (Hβ), and oxygen shows emission lines at 501 nm and 372 nm. So, if one finds a galaxy with an emission line at 820 nm, e.g.,

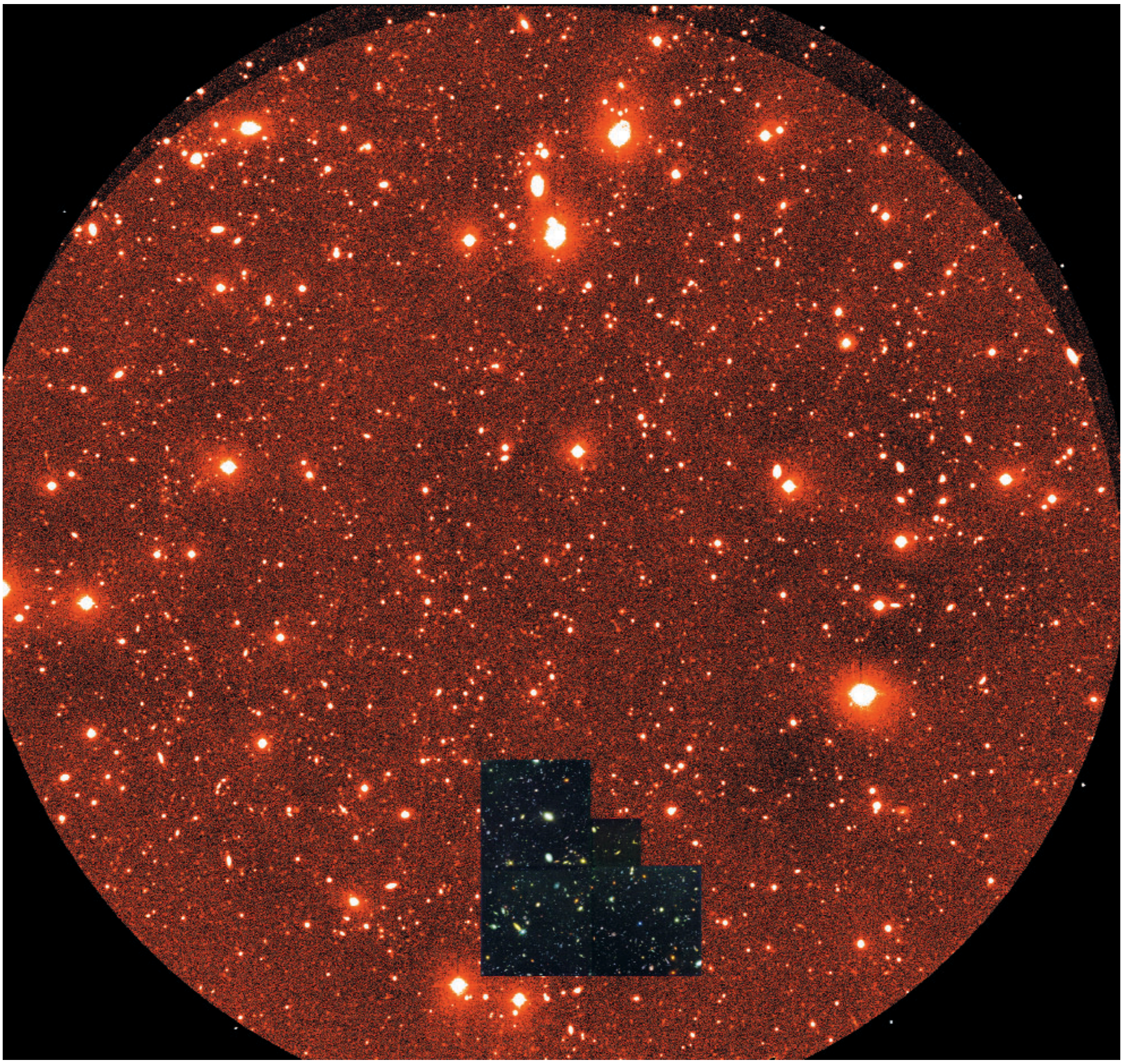

it can be Lyman-α-emission at $z = 5.7$ or Hα-emission at $z = 0.25$ or Hβ-emission at $z = 0.69$, and so on.

This ambiguity, however, can be eliminated based on the following empirical fact: If a galaxy emits strong Hα-radiation, it normally also emits the oxygen lines [OII] at 373 nm and [OIII] at 501 nm. Therefore, additional exposures of the same area on the sky have to be made using so-called veto filters. These filters transmit exactly in the spectral bands occupied by these oxygen lines (Fig. III.34). A galaxy appearing in both filters is a low-redshift dwarf galaxy. But if a galaxy is only detected in the Fabry-Perot image it may be one of the distant Lyman-α-galaxies searched for. For each galaxy, the intensity ratios in the various filter bands are determined, and by estimating the probabilities of the line identifications a redshift is attributed to the galaxy. All in all, exposures through 16 medium- and broad-band filters are made in the spectral range between 400 and 2200 nm.

Fig. III.33: The section on the sky covered by the wide field camera (red field) compared to the HUBBLE Deep Field imaged with the HUBBLE space telescope (blue field).

To search for young galaxies with Lyman-α-emission, the astronomers selected three wavelength bands with a width of 10 to 16 nm for the Fabry-Perot filter, lying at 700nm, 820 nm, and 918 nm. These wavelengths correspond to redshifts of the Lyman-α-line of $z = 4.75$, $z = 5.74$, and $z = 6.53$, respectively.

The observations cover six fields on the sky with a total area of 0.2 square degrees, corresponding to almost the size of the full moon. For each field and redshift interval about 400 exposures are needed. All in all, CADIS requires more than 3000 individual exposures with a total exposure time of 1400 hours. Until the end of 2002, 90 percent of the observations had been completed.

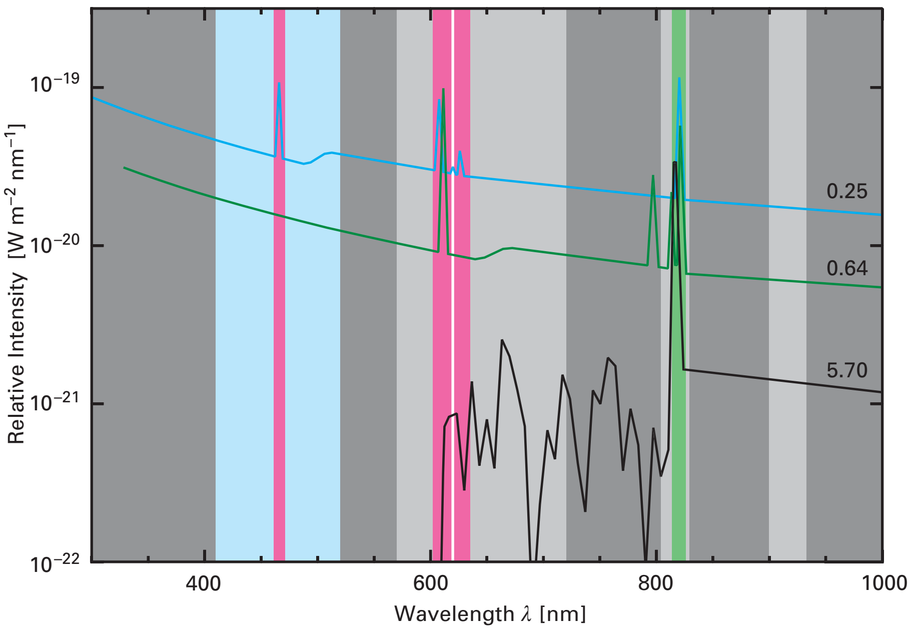

Fig. III.34: The CADIS observation method. The pass band of the Fabry-Perot filter for the Lyman-α-line at $z = 5.7$ is plotted in green, those of the veto-filters in red and light blue. Three spectra with redshifts $z = 0.25$, 0.64, and 5.7 are represented schematically.

First Lyman-α-Galaxies Discovered

In the year under report, the astronomers could announce for the first time the definite detection of two Lyman-α-galaxies. This was preceded by an intense analysis of the data obtained in four fields on the sky in two redshift windows at $z = 4.75$ and $z = 5.74$. Within these data, the computer program found a total of 614 emission-line galaxies. Almost 600 of them could be excluded because they were identified, for instance, as foreground galaxies, leaving 16 candidates for Lyman-α-galaxies. In order to verify their nature, spectroscopy with the largest telescopes available was necessary.

Four out of the 16 candidates were observed using the FORS 2 spectrograph at the VLT, three of them at $z = 5.7$ and one at $z = 4.8$. While the two faintest objects could not be detected, the search proved successful for the two other candidates. The hoped for Lyman-α-lines showed up yielding redshift values of $z = 5.735$ and $z = 4.803$. So these two galaxies belong to a handful of presently known objects of this kind from the early universe. Figure III.35 shows the discovery image and spectra of the galaxy at $z = 5.7$.

From the measured redshifts and intensities of the Lyman-α-lines a star formation rate of 14 and 10 solar masses per year, respectively, was deduced. These values are obtained assuming continuous star formation. But if it is a short-time starburst, which seems more probable, the value can be larger by a factor of five. For comparison: in our Milky Way, presently only one to two solar masses per year are converted into stars from the interstellar medium.

Presumably the phase in which the Lyman-α-galaxies lit up was very short. It started with the first generation of stars and ended when these had produced enough heavy elements to allow the formation of large amounts of dust. Models predict a period of the order of one hundred million years. Afterwards, interstellar clouds significantly absorbed the Lyman-α-radiation. The exciting question is: When did the young universe pass through this Lyman-α-phase?

The astronomers found a qualitative answer to this question by fitting a model to the distribution of the known Lyman-α-galaxies at $z = 3.5$. They then shifted this graph to $z = 4.8$ and $z = 5.7$, taking into account the decreasing brightness of the objects at the larger distances and the decrease of the observed volume of space due to the expansion of the universe. In this case, the Lyman-α-emission of the galaxies is assumed to remain unchanged. As Figure III.36 demonstrates, the number of galaxies at $z = 4.8$ and $z = 5.7$ is lower than predicted by this model. This means that the peak of Lyman-α-emission was already past at this redshift. In other words: The first generation of stars has formed between $z = 3$ and $z = 6$, i.e., 0.9 to 2.1 billion years after the big bang. This redshift range is already accessible to observation with present-day techniques. This analysis, though, is based on a very small number of galaxies. Therefore it will be of major significance in the near future to detect as many additional young galaxies as possible. In doing so it will be very important to observe large areas on the sky. Only that way it will be possible to avoid random variations that arise due to the large-scale structure of the universe in the form of galaxy clusters.

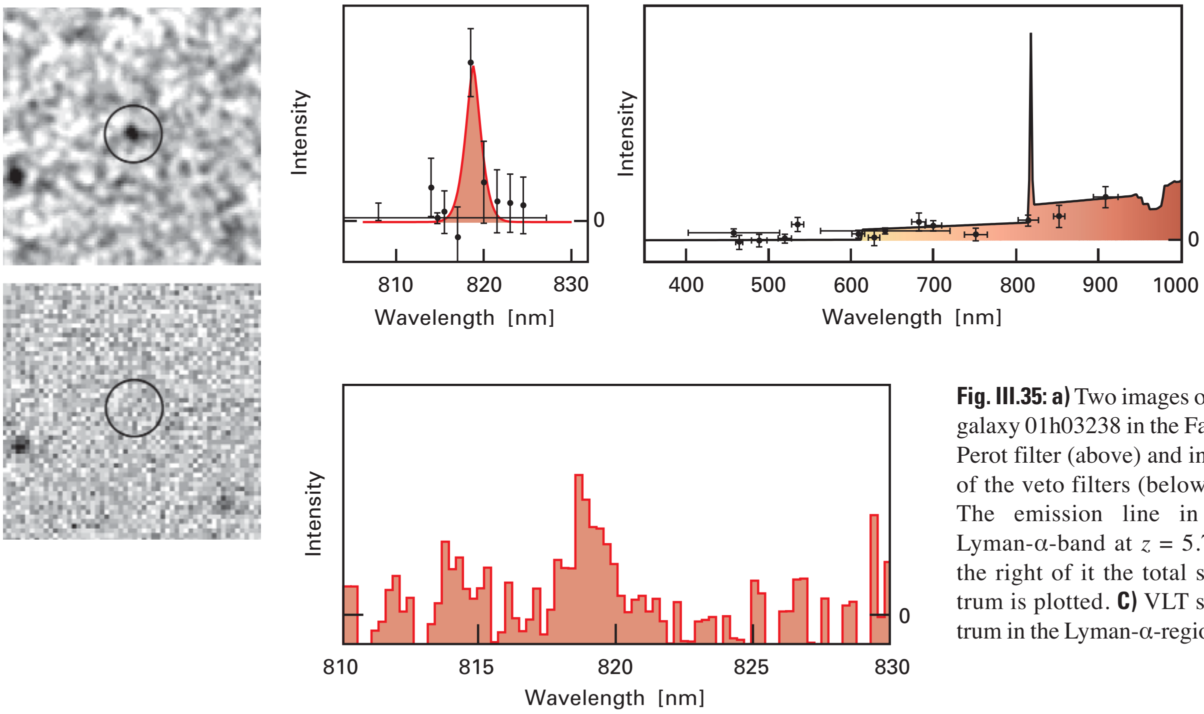

Fig. III.35: a) Two images of the galaxy 01h03238 in the Fabry-Perot filter (above) and in one of the veto filters (below). **b)** The emission line in the Lyman-α-band at z = 5.7; to the right of it the total spectrum is plotted. **C)** VLT spectrum in the Lyman-α-region.

Fig. III.36: Cumulative number of galaxies per square degree which are brighter than a certain magnitude limit, at $z = 4.8$ (left panel) and $z = 5.7$ (right panel). Circles denote galaxies at z = 3.5, the distribution of which is given by the upper solid model graph. When this curve is shifted according to the redshift (dashed line) it lies above the measured data. This indicates that the Lyman-α-phase has attained its peak after $z = 5.7$.

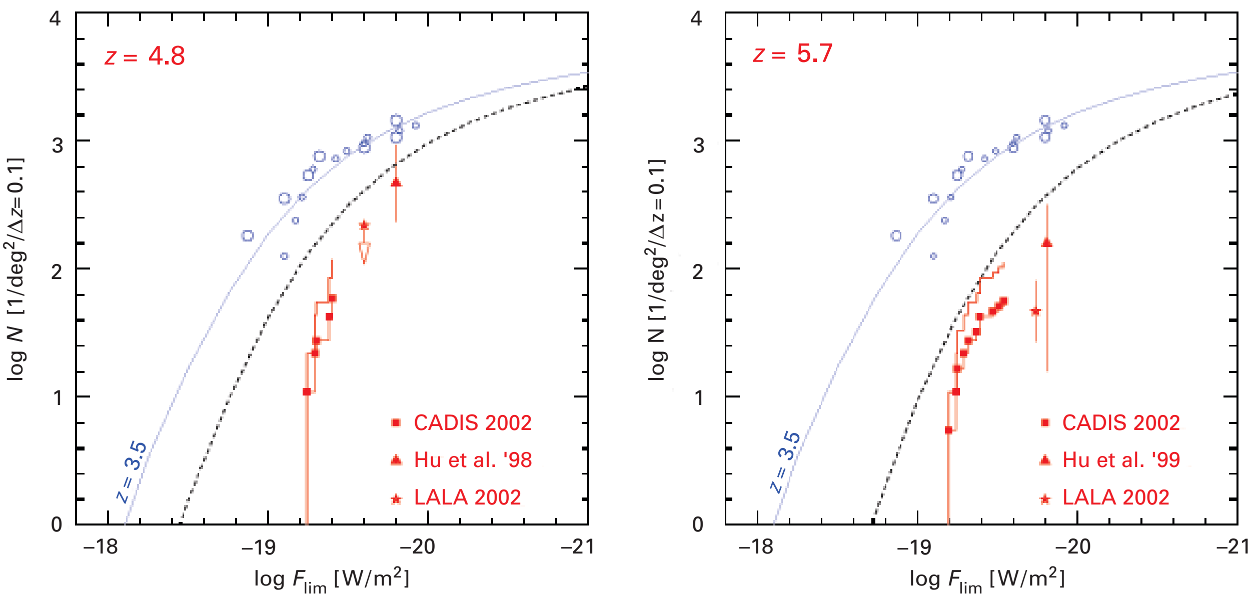

Exponential Decline of the Star Formation Rate

What happened after the first stars had lit up? Numerous studies attempted to determine the evolution of the star formation rate with progressive age of the universe, i.e., with decreasing redshift. This can be done with various methods: Intensities of emission lines such as the Hα hydrogen line, the emission in the UV spectral range, or the infrared emission of dust are useful tracers of star formation activity in galaxies.

The large CADIS data-base provides the opportunity to determine star formation rates of galaxies in two redshift windows at $z = 0.25$ and $z = 1.2$. Here the fact is utilized that at certain redshift values some emission lines are falling into the transmission bands of the Fabry-Perot filter. In particular, these are Hα at $z = 0.25$, the oxygen lines of [OIII] at $z = 0.4$ and $z = 0.64$, and the [OII]-lines at $z = 0.88$ and $z = 1.2$.

The images are classified by a computer-program using three criteria: the intensity distribution of the emission line in the Fabry-Perot filter, the intensities in the remaining emission line bands and in the continuum. The former can be done because the transmission band of the Fabry-Perot filter is scanned in several steps (Fig. III.35b). To optimize the criteria of this method, several galaxies were observed spectroscopically in follow-up studies at the 3.5 m telescope on Calar Alto using MOSCA as well as at the Keck telescope and at the VLT.

Using this elaborate method more than 400 emission-line galaxies were found in five redshift intervals lying between $z = 0.24$ and $z = 1.2$. This redshift range corresponds to a period of time of about four billion years. In a first step, the astronomers deduced the luminosities of the galaxies in the respective emission lines. Here the difficulty occurs that dust may obscure the line emission. It was not possible to determine the degree of this extinction for each individual galaxy. Instead, a correction based on the observation of nearby galaxies was applied. This correction affects distant galaxies more strongly than nearby ones because, as we know from experience, extinction increases with increasing mass and luminosity of the galaxies. At high redshifts, though, increasingly more luminous galaxies are observed. In a second step, emission-line luminosities had to be converted into star formation rates. Here, a correction had to be applied since at increasing redshifts the number of detectable faint galaxies decreases.

Despite the necessary corrections, it can be said that CADIS reaches deeper than similar studies performed up to now and that the derived star formation rates are hardly affected by incompleteness. The resulting time evolution of the star formation rate is shown in Figure III.37. The rate declines from 0.23 solar masses per cubic Megaparsec and year at $z = 1.2$ to 0.024 solar masses per cubic Megaparsec and year at $z = 0.25$. This evolution is in very good agreement with other studies. A peak was reached about eight billion years ago (Fig. III.38), i.e., six billion years after the Big bang. Following this peak, the star formation rate declined exponentially with the rate decreasing by a factor of two every 2.6 billion years. In other words: Within the period of six billion years the star formation rate has decreased by a factor of ten. And from the time of maximum activity about eight billion years ago until today, the rate went down to about one twentieth.

Cosmological theories offer two explanations for the exponential decline of the star formation rate. For one thing, the gas content of the galaxies shrinks, reducing the raw material for newly forming stars. But there could be another effect: Simulations have shown the frequency of gravitational interactions between galaxies or mergers to decrease strongly in the course of time due to the expansion of the universe. These interactions, however, initiate star-formation activity within the galaxies involved. Simulations of these processes calculated by theorists at MPIA support the exponentially declining star formation rate.

(K. Meisenheimer, H. Hippelein, C. Maier, H.-J. Röser, E. Thommes, J. Fried, M. Kümmel, B. v. Kuhlmann, S. Phleps, C. Wolf)

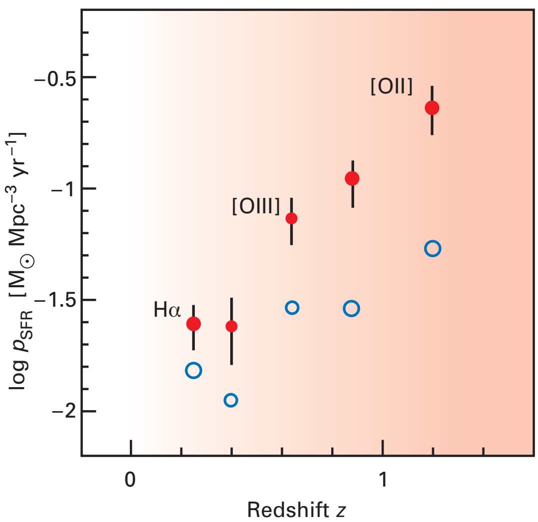

Fig. III.37: Star formation rate as a function of redshift. CADIS data are shown uncorrected and corrected for extinction (filled circles).

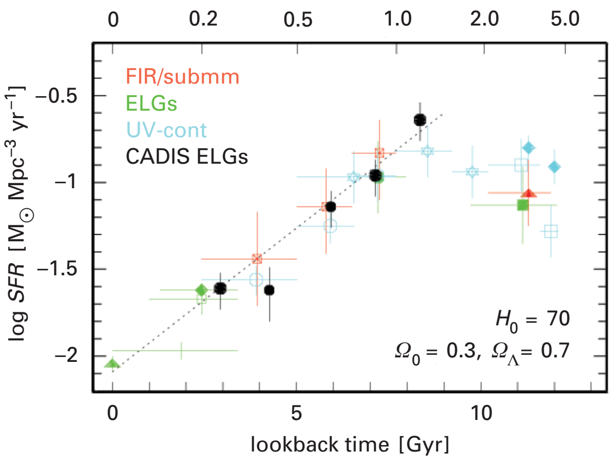

Fig. III.38: Star formation rate as a function of redshift and lookback time, respectively.

Intergalactic Dust within the Virgo Cluster

Some while ago, X-ray observations showed the intergalactic space within galaxy clusters to be filled with hot gas. Galaxies moving around in this medium with high velocities should be interacting with this gas. This led to the assumption that gas as well as dust might be swept from the galaxies by dynamic pressure. This so-called »ram pressure stripping« would have significant influence on galaxy evolution. For instance, in this way the galaxies would lose the raw material needed for star formation. The loss of neutral hydrogen gas has repeatedly been established by radio observations. For some time, astronomers consider the giant galaxy M 86 located in the Virgo cluster as an outstanding example for the loss of dust by stripping. However, observations with the ISO European infrared space observatory do not corroborate this hypothesis.

The Virgo cluster is the nearest large galaxy cluster, representing the center of the local supercluster. It has several thousand members, among them the massive elliptical galaxies M 86 and M 87. Both are surrounded by a halo of hot gas at temperatures of some ten millions degrees. M 86 is assumed to be the most massive member of a smaller galaxy cluster plunging into the Virgo cluster from behind. This is supported by the galaxy's high radial velocity of -1364 km/s with respect to the entire cluster (Fig. III.39).

Because of this high velocity with respect to the intergalactic gas M 86 is regarded as a candidate for »ram pressure stripping«. ROSAT had observed extended X-ray emission not coincident with the center of the galaxy. Recent observations made with CHANDRA confirmed these findings. The X-ray emission is clearly asymmetric around M 86: To the north, the intensity shows a sudden, quite steep decline. Some astronomers interpreted this morphology as a shock front within a gas streaming from the galaxy due to stripping. Three-dimensional simulations, however, did not agree with this explanation leaving the cause of the asymmetric shape of the X-ray emitting gas still unclear. At the end of the 1980s, two dust components were found in images obtained with the IRAS infrared satellite. One seemed to coincide with the galaxy while the other one was located near the X-ray emission. This led to the hypothesis that even dust was swept from the interior of M 86.

On the other hand, radio observations of atomic hydrogen suggested another interpretation. The material could have been pulled out of the galaxy NGC 4402 as a result of its tidal interaction with M 86. The suggestion that gravitational interaction plays an important role in M 86 is supported by recent observations in the optical spectral range as well. These images indicate that matter is being stripped of the dwarf galaxy VCC 882 (NGC 4406B) while it is moving along its bound orbit around M 86.

ISOPHOT Observations of M 86

So, despite many observational results it is not clear yet whether dust stripping really plays a role in M 86. And so far, there is no direct evidence for this phenomenon in any other large galaxy. The ISOPHOT instrument onboard ISO provided the opportunity to study the whole area around M 86 with higher resolution and sensitivity up to a wavelength of about 180 μm.

All in all, M 86 was observed in three channels at 60, 90, and 180 μm for about two and a half hours. Figure III.40 shows a superimposition of all three spectral bands. Seven sources are recognizable. The IRAS image, on which the dust-stripping hypothesis is based in the end, shows only two objects: M 86/ M 86-SE as an unresolved single source and M 86-NW.

On the new ISOPHOT image, the position of the condensation M 86 is about coincident with that of the galaxy. This emission thus probably comes from a central dust disk in the core of M 86 that was detected only recently. The two sources FIR 5 and FIR 6 match the positions of the two companion galaxies VCP 463 and VCP 479. The identification of the remaining objects proved to be difficult.

Interestingly, the object M 86-NW has a totally different spectral energy distribution than all the other objects. While, for instance, a temperature of about 18 Kelvin can be assigned to the dust in M 86, the dust in M 86-NW is much warmer with a temperature around 100 Kelvin. Moreover, images in the blue spectral range show a point source at this position. So it seems that just the only infrared source in the vicinity of M 86 that was known until then and on which the dust-stripping hypothesis is based is not a member of the Virgo cluster at all but a far more distant active galaxy or quasar.

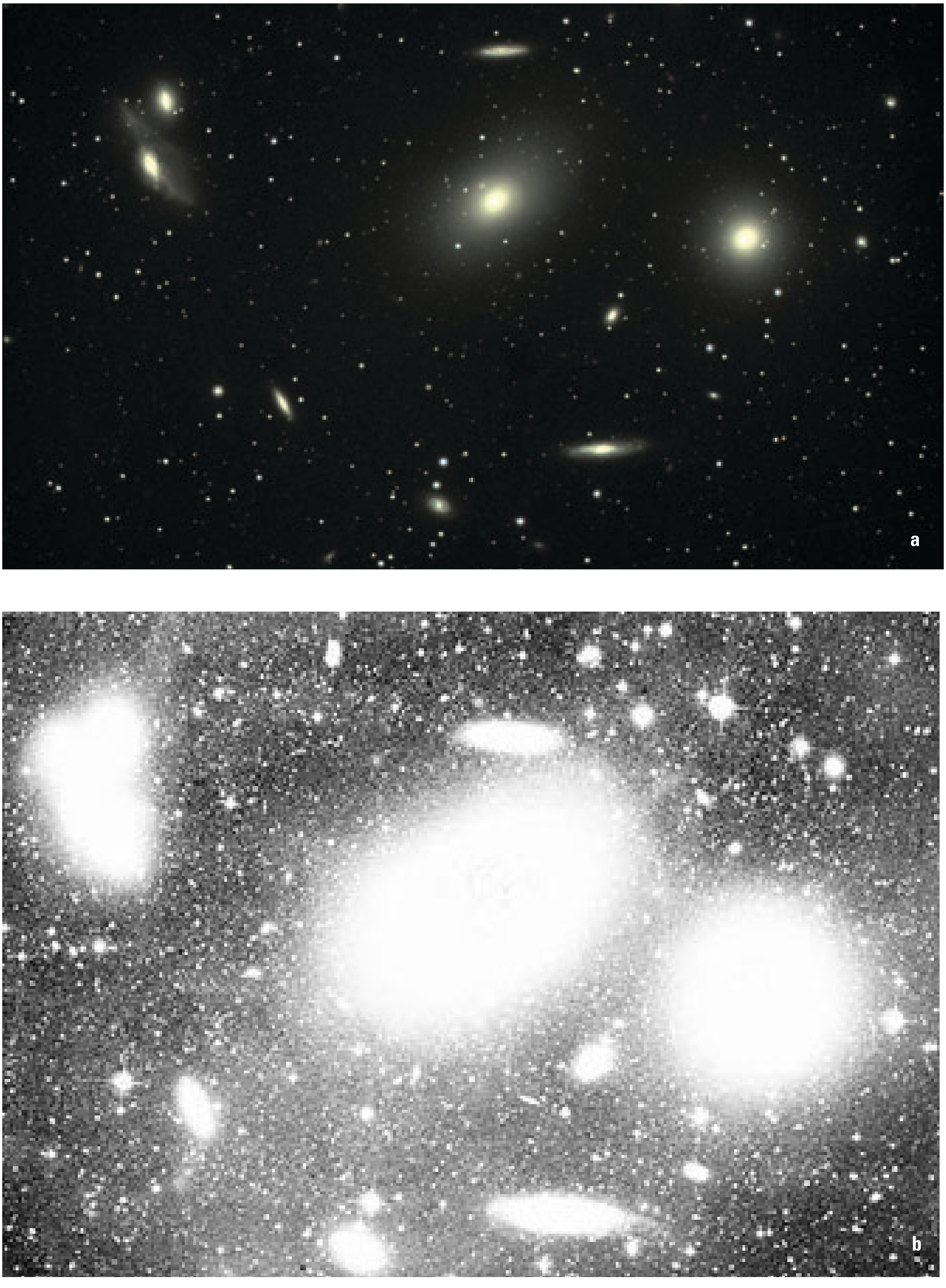

Fig. III.39: a) Part of the Virgo cluster in the vicinity of the elliptical galaxies M 86 (brightest galaxy near the center) and M 84 (to the right of it). Above M 86, the spiral galaxy NGC 4402 is seen. **b)** This very deep exposure reveals extended halos around the galaxies that even partly overlap.

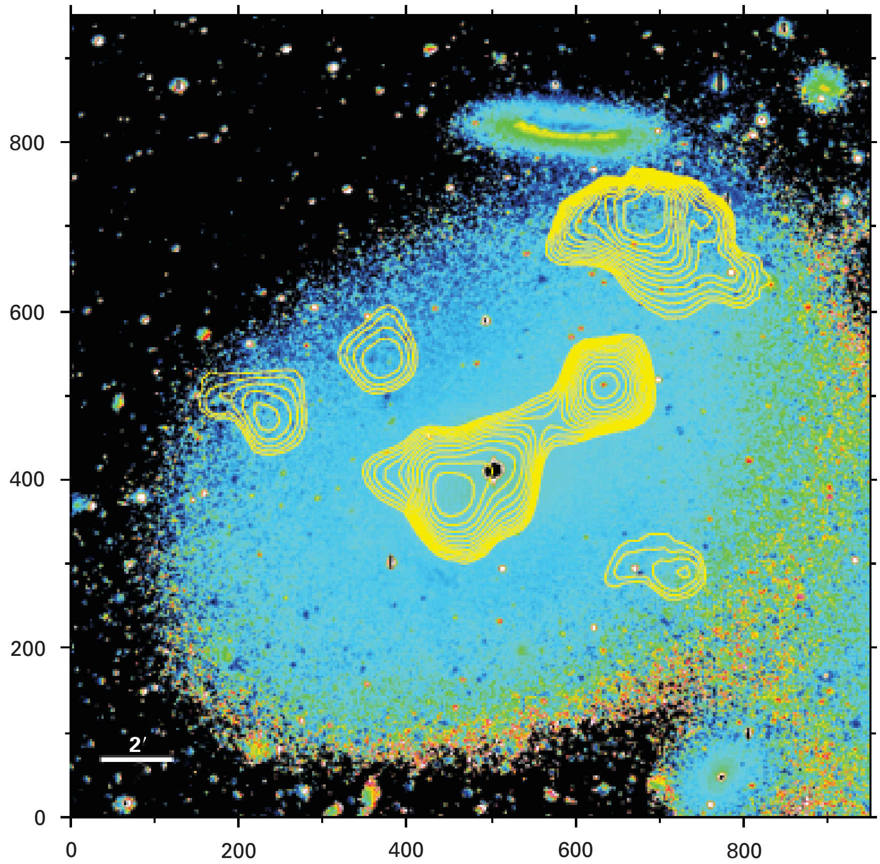

The source M 86-SE could be associated with dust filaments that had already been detected in optical images. As indicated above, they are attributed to tidal interactions with the companion galaxy VCC 882. Moreover, the position of this infrared source does not agree with the direction in which one would expect material that has been stripped from M 86 due to the galaxy's motion through the intergalactic gas.

In connection with the opening question about interaction or stripping, only the bright objects M 86-SE and M 86-FIR 4 seem to be relevant. Assuming that they lie at the distance of M 86 (19.5 Mpc, corresponding to 64 million light years), their dust masses can be estimated from the measured far-infrared fluxes to be 5×10^6 (M 86), 7.5×10^6 (M 86-SE), and 1.5×10^7 (FIR 4) solar masses. The value derived for M 86 is quite typical for elliptical galaxies.

The source FIR 4 is clearly extended, showing a core surrounded by a halo. Although FIR 4 is the brightest far-infrared source in this field, no optical counterpart was found on images taken in the visible spectral region. Nor did radio observations of neutral hydrogen reveal a corresponding object. Deep optical images of M 86 (Fig. III.41) give a clue to its nature. A detailed analysis shows a slight distortion of the shape of M 86 pointing towards the nearest neighboring galaxy NGC 4402 (outside the ISOPHOT field). NGC 4402 is a very dusty spiral galaxy with a warped disk or even a ring-like structure. But this

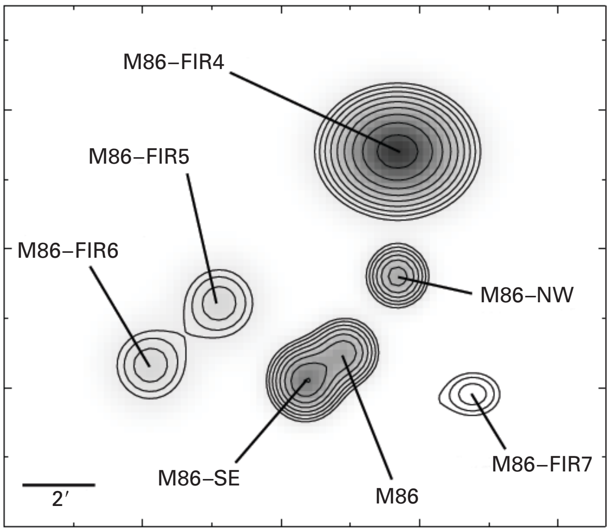

Fig. III. 40: Top: An ISOPHOT color map (60 µm – 180 µm, contour lines) of the region around M 86, superimposed on a color map ($B-I$) in the optical range. **Bottom:** A schematic map of the seven infrared sources and their designations.

is difficult to verify as we see the galaxy edge-on. However, there are some arguments supporting the idea of FIR 4 being dust stripped from either M 86 or NGC 4402 as a result of tidal interactions between both galaxies. This issue will only be settled when far-infrared images of the entire field around M 86 become available.

In the light of this interpretation, a different explanation can be given for the above-mentioned asymmetric structure of the X-ray gas. As shown in Fig. III.41, the X-ray intensity in the ROSAT image is strongly decreasing in the vicinity of FIR 4. The fact that the decline is steeper at low X-ray energies than at higher ones can be taken as evidence that the shape is rather due to absorption within the FIR 4 dust cloud than to the X-ray emitting gas itself. If this interpretation were correct, this would be the first known case of intergalactic dust affecting the morphology of the X-ray gas within a galaxy cluster.

Although the galaxy M 86 is showing a very complex overall morphology in the far infrared, it does not fit into the dust-stripping picture. Thus, the question if this phenomenon is playing a significant role at all in the evolution of large galaxies is open again. Maybe only statistical studies can demonstrate whether galaxies within galaxy clusters contain systematically less dust than those in the field. The first direct detection of an intergalactic dust cloud, however, is still an outstanding result of the ISOPHOT-observations of M 86.

(M. Stickel)

Fig. III.41: ROSAT image of the region around M 86. Crosses denote the infrared objects M 86, M 86-SE, and M 86-FIR 4. Absorption by the latter could cause the steep decline of the X-ray emission.

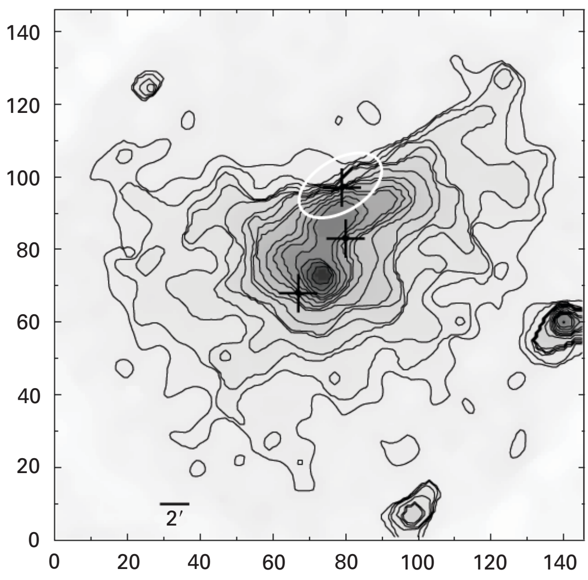

Puzzling Element Abundances in Globular Cluster 47 Tucanae

Globular Clusters are among the oldest objects in the universe. They reside in the halos of large galaxies and move around their centers on bound orbits. In cosmological standard scenarios, globular clusters formed right at the beginning from large proto-galactic clouds. As a consequence, all stars within a cluster should have about the same initial chemical composition. But this is not the case. In some clusters, significant abundance variations of certain elements are observed. The reason for these variations is debated for three decades. Now, a new study of the globular cluster 47 Tucanae carried out by astronomers at MPIA and colleagues from Lick Observatory suggests that massive stars in binary systems may have "polluted" their companions with heavy elements.

According to present-day cosmological theories, globular clusters formed even before the large galaxies did. Large proto-galactic clouds contracted under the influence of gravitation. In some regions of such a cloud, the gas condensed into globular clusters while the remaining matter continued to contract and finally formed a large galaxy that is surrounded by a halo in which the globulars are moving around. Our Milky Way, for instance, is orbited by 150 known globular clusters. In this simple scenario, all members of a cluster should have the same chemical composition.

As early as 1971, however, the atmospheres of two red giants in the globular clusters M 5 and M 10 were found to show a significantly enhanced abundance of the CN molecule compared to other stars in these clusters. Similar studies followed, being at first limited to the brightest stars for observational reasons. Only recently, with the advent of new large telescopes, fainter main-sequence stars could also be observed spectroscopically, for instance in M 13, in M 3, and in 47 Tucanae.

But even with the present-day 10-m-class telescopes very long exposure times would be necessary to obtain the high-resolution spectra needed for the analysis of atomic absorption lines. A more promising approach therefore is the observation of molecular absorption bands. For instance, the intensities of CN and CH bands can be measured with medium-resolution spectroscopy or even with photometry using narrow-band filters.

CN Abundance in 47 Tucanae

The globular cluster 47 Tucanae is very well suited to such observations (Fig. III.42). It is only 4500 pc (15 000 light years) away and after Omega Centauri the second-brightest cluster in the Milky Way, with an absolute visual magnitude of M_V = -9.4 mag. Moreover, due to its angular diameter of 47 arc minutes the cluster is resolved very easily into individual stars. Consequently, 47 Tuc has been studied intensely over the last 30 years. These studies led to a surprising result: There is a very broad CN abundance spread detectable in stars along the main sequence till its upper end. Particularly, there is an obvious bimodal distribution: The stars either show very weak or very strong CN absorption bands while at the same time no inhomogeneities of very heavy elements, such as iron for instance, are found.

Such a result is inconsistent with the simple formation scenario. Therefore explanations for the abundance inhomogeneities were sought. Today, essentially three models are under consideration:

Stellar evolution: Deep within the interiors of stars nuclear reactions take place that generate the energy needed. In low-mass stars, the most important reaction is hydrogen fusion (pp-reaction). Depending on the star's mass, the CNO-cycle of nuclear fusion also takes place. Although carbon, nitrogen, and oxygen act only as catalysts in this process, it is able to modify the ratios of element abundances. The processed elements can reach the surface through convection and be detected spectroscopically.

"Pollution": Giant stars generate particle winds that carry elements such as carbon, oxygen, and nitrogen into the interstellar medium. If other stars take in matter from those winds, the chemical abundances within their atmospheres change.

Primordial variations: The material from which the stars of the cluster formed may not have been chemically homogeneous. Various reasons for such a situation are conceivable. For instance, two large clouds of different chemical composition could have collided before stars started to form. Incomplete mixing of the gas of both clouds would explain the stars' chemical inhomogeneities. Or supernova explosions may have chemically enriched the gas locally making the whole cloud chemically inhomogeneous. And last not least, 47 Tuc may have formed as the merger of two globular clusters with different chemical compositions.

Up to now it was unclear whether the chemical inhomogeneities of stars in globular clusters bear information on the formation of these objects or whether they are due to evolutionary effects. The first of the above-mentioned hypotheses may be tested by measuring the CN abundance also in low-mass stars, since the CNO-cycle is only significant in massive stars. Below 0.8 solar masses it is neglectable. If the CN variation were a consequence of an internal mixing process, the effect should ever decrease towards lower-mass stars. Until recently, this could not be tested because of the low luminosities of these stars.

In their new study, astronomers at the Institute utilized the capabilities of the FORS2 multi-object spectrograph at the VLT to spectroscopically observe a large number of stars in 47 Tuc down to about 0.6 solar masses. First they imaged the cluster through several filters using the wide field camera at the ESO/MPG 2.2 m telescope on La Silla. This way they were able to find suitable stars and determine their positions. In follow-up observations using FORS2, 115 stars were studied spectroscopically, with a total exposure time of about ten hours (Figs. III.43 and 44).

A surprising picture emerged when the astronomers plotted the strength of the CN absorption versus the stars' apparent magnitudes (and thereby their mass): An obvious bimodal distribution was found (Fig. III.45). The fact that this bimodality becomes more pronounced towards lower masses may be a consequence of lower surface temperatures since the probability of molecule formation is increasing with decreasing temperatures. Nevertheless, the effect is unmistakable and cannot be explained by the hypothesis of element enrichment through the CNO-cycle.

Thus the second and the third of above-mentioned scenarios are left to explain the abundance inhomogeneities: primordial variation and pollution. The former, however, also encounters a problem. It can explain the inhomogeneity of the CN abundance, but not so the homogeneity of the iron abundance that is found at the same time. One hardly can imagine two merging clouds having identical iron abundances but completely different CN abundances.

The most likely scenario therefore is that of external "pollution" according to which the low-mass stars have incorporated nitrogen-rich gas from their surroundings. But how did the bimodal distribution arise? One possibility would be that all CN-strong stars are members of binary systems the second component of which had been a red giant some time ago. Through its nitrogen-rich wind, this giant could have enriched the smaller companion. If this were true, the CN-strong stars should also show abundance enhancements in other elements such as sodium, magnesium or aluminum since the winds of red giants are rich in these too. The crucial test might be performed with high-resolution spectroscopy.

(D. Harbeck, E. K. Grebel)

Fig. III.42: Part of the globular cluster 47 Tucanae, imaged with the HUBBLE Space Telescope. (image: NASA / ESA)

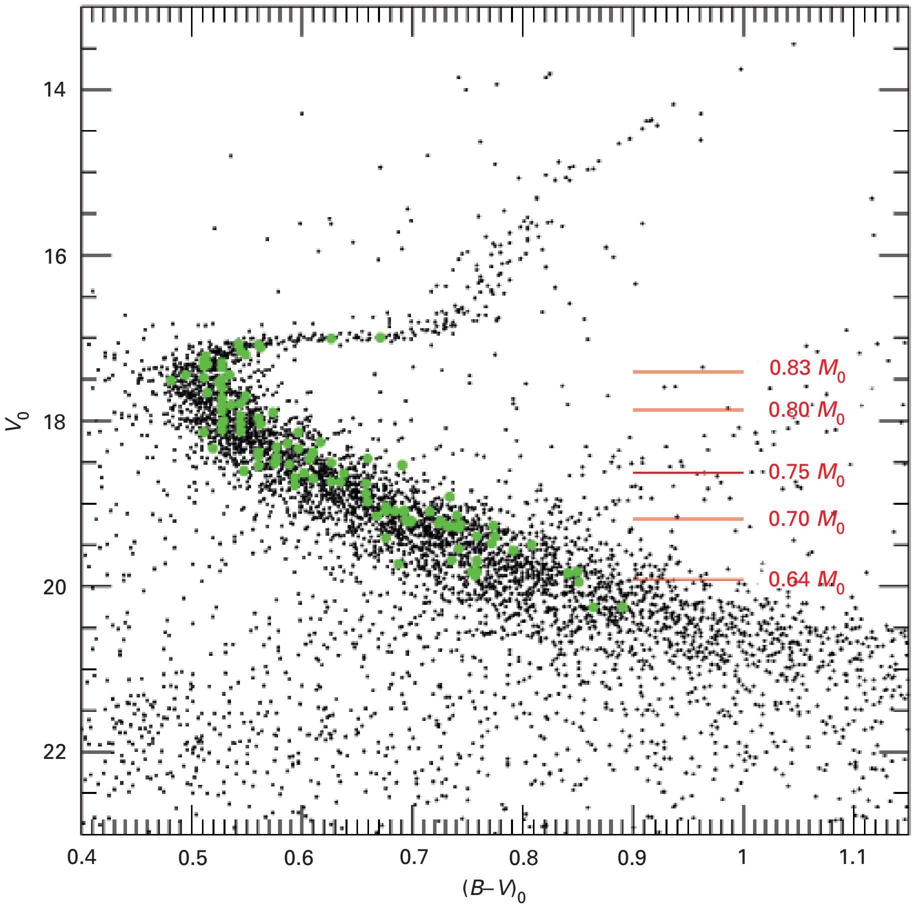

Fig. III.43: Color-magnitude diagram of 47 Tuc, obtained from images taken with the Wide Field Camera. The spectroscopically observed stars are marked in green.

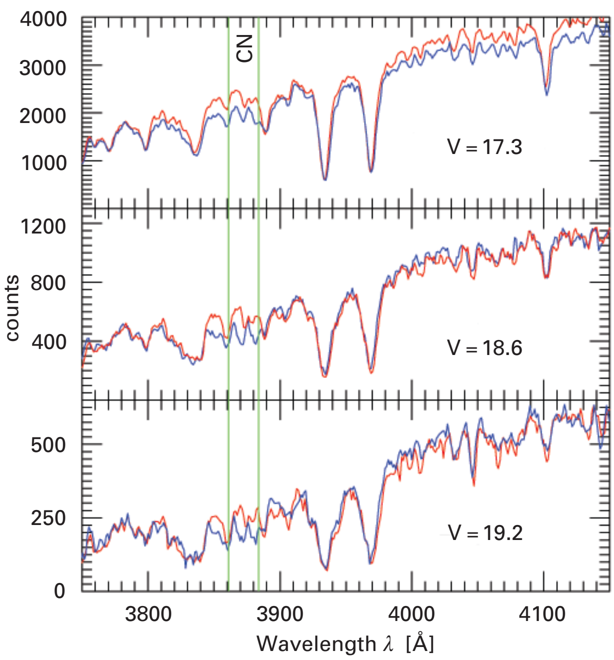

Fig. III.44: Spectra of six stars. Plotted are two stars at a time having the same magnitude, but one showing strong (blue) and one weak (red) CN absorption.

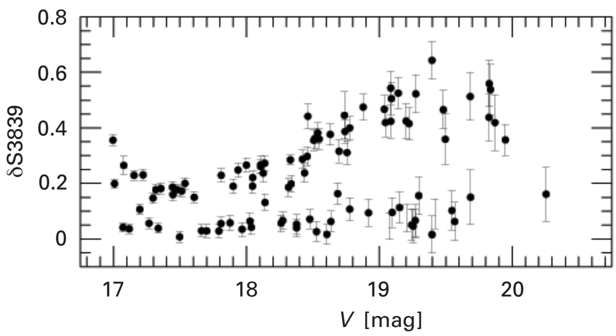

Fig. III.45: The strength of the CN absorption (in terms of the parameter ΔS(3839)) plotted versus the apparent visual magnitude shows a clear bimodal distribution.

Dark-Matter Halos of Dwarf Galaxies

For about 30 years, there is increasing evidence that galaxies are imbedded within extended clouds of dark matter. However, so far only the gravitational influence of these halos is known while other physical properties of this invisible kind of matter are still unidentified. Indirect information about those properties are expected from observations of dwarf galaxies whose kinematics are dominated by dark matter. Astronomers at MPIA have studied rotation curves of six dwarf galaxies in detail. The results are suggesting a density distribution within the dark-matter halos that is inconsistent with current cosmological models.

In the 1970s, observations of spiral galaxies led to the hypothesis that these stellar systems are imbedded within giant clouds of invisible matter. This was implied by the shape of their rotation curves. If all stars and all gas clouds in a galaxy were moving on Keplerian orbits around the dominating central mass, the orbital velocities of the stars should decrease with increasing distance to the galactic center beyond a certain radius. However, the velocity is found to be nearly constant up to the outskirts of the galaxies. Our Milky Way, too, has this kind of rotation curve. This is interpreted as the gravitational effect of an extended dark-matter halo.

This dark matter must have played a crucial role already in the formation of galaxies. In the early universe, it formed potential wells in which ordinary baryonic matter accumulated and then further condensed into galaxies. Present-day computer simulations allow for this effect of dark matter while its physical properties are mostly unknown. Quite recently, however, a problem occurred in these cosmological simulations: Theory predicts the density and thus the gravitational potential of a dark-matter halo to increase very steeply (as r^{-1} to $r^{-1.5}$) towards the center. This model is called “cuspy core”. But the rotation curves of galaxies are best explained by a more moderate central density. These observational results are consistent with a density profile suggested by theorists at MPIA already in 1995. Accordingly, the density of the dark-matter halo is almost constant within the central region or increases only slightly towards the center. This model is called “soft core”.

Late-type dwarf galaxies whose kinematics are dominated essentially by dark matter provide an excellent laboratory to investigate the gravitational effect of dark matter on galaxies. Because of their low brightness, though, their rotation curves are rather difficult to observe. Several years ago, radio astronomers had measured the rotation curves of five dwarf galaxies by observing the radial velocity of atomic hydrogen (HI) at 21 cm wavelength. These observations supported the soft-core model. Some astronomers, however, argued that the spatial resolution of the radio data had been too low to map the particularly important central regions of the galaxies. This shortcoming would have prevented the detection of a strong central mass concentration.

To settle this controversy, astronomers at the Institute together with colleagues from Italy spectroscopically observed six dwarf galaxies in the optical spectral range using the Telescopio Nazionale Galileo (3.6 m aperture) on Roque de los Muchachos, La Palma. Rotation curves were derived from the Hα line of neutral hydrogen. As these galaxies had already been observed in the radio range a direct comparison with the 21 cm radio results was possible. The stellar systems are located at distances between 6.8 and 48 Mpc (22 to 160 million light years) and have a surface brightness in the red spectral range of about 21 mag per square arc second.

Fig. III.46 shows examples of the data obtained from the new Hα and the older 21 cm observations: In five out of six cases the data are in very good agreement; evidence of beam smearing of the 21 cm radio data, particularly in the central region of the galaxies, was found only in one galaxy, which therefore was excluded from further analysis. The combined data sets now provide an excellent possibility to determine the gravitational potential of the dark-matter halos: While the Hα data define the central region particularly well, the 21 cm data reach out to large distances from the center.

The observational data were compared to the predictions of three halo models, two with cuspy cores and one with a soft core. In the modeling, the rotation curves were assumed to be determined exclusively by the gravity of the halo. The gravitational influence of the disk was neglected, which seems to be justified because of the large mass-to-light ratios of the galaxies. The result (Fig. III.47) clearly shows that the observational data only match the model with a flat potential well (soft core). They are inconsistent with those suggested by cosmological scenarios (cuspy core).

The analysis described above referred to the present-day condition of the galaxies and their halos. In a second step, the theorists wanted to identify the possible density distribution of the halos at the time of their formation. For when gas is accumulating in the inner regions, the gravitational force increases which in turn causes the dark-matter halos to contract.

Starting out from two different density distributions, the theorists traced the contraction of the dark-matter halos and then compared the results in order to decide which initial density profile causes the halo to evolve in a way that can explain the present-day rotation curves. Again, dark-matter halos with an initially steep density peak at the center do not match the data well. In particular, the present-day velocities in the central region should rise much faster. The best fit was achieved with a so-called King profile, showing a moderate density increase in the central region. This profile usually describes the density distribution of stars in globular clusters.

In this way it was possible to infer a certain new property of dark matter from the rotation curves observed in galaxies. This hitherto unknown property obviously affects the density distribution in the centers of the halos and thereby the formation of structure in the universe. It might also be of major importance for the identification of the putative dark-matter particles.

(E. d'Onghia)

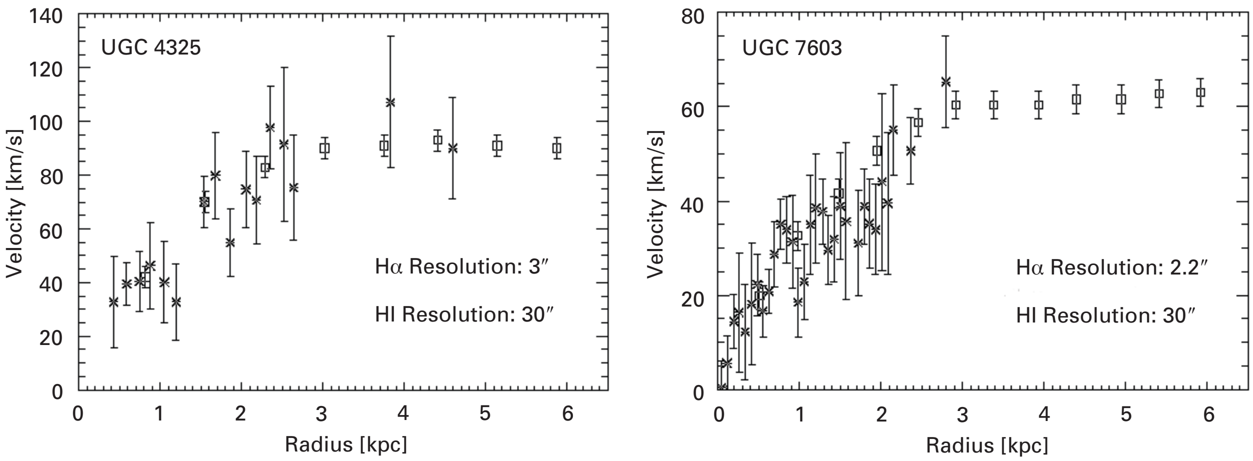

Fig. III.46a,b: Two examples of rotation curves deduced from the 21 cm data (squares) and the Hα observations (asterisks). ▲

Fig. III.47a,b: Comparison between the deduced rotation curves and the three models. Solid line: soft-core model; dashed lines: cuspy-core models. ▼

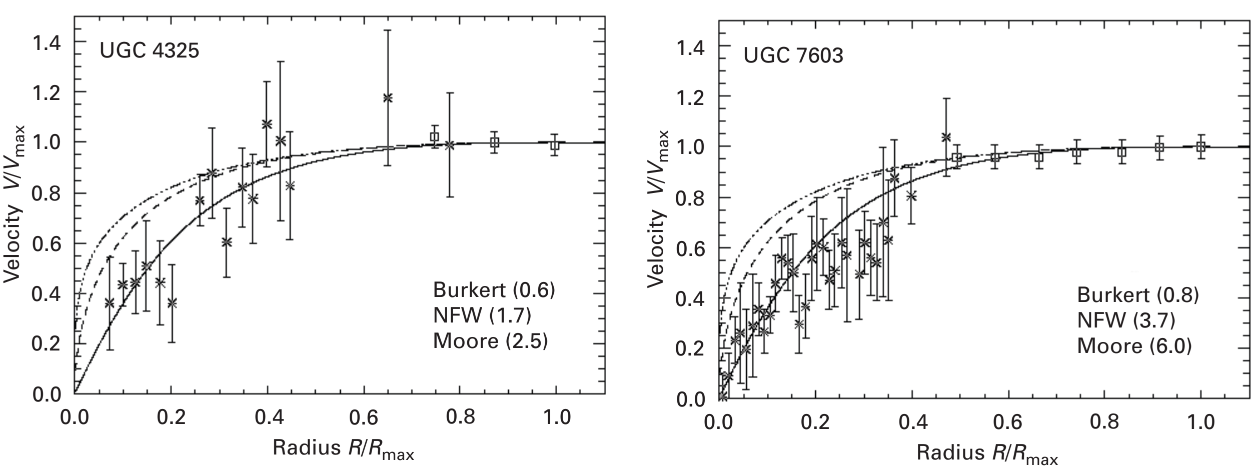

White Dwarfs and the Dark-matter Halo of the Milky Way

It is generally accepted now that stars and interstellar matter only constitute a minor fraction of the total mass of the Milky Way. The major portion of the mass is in an invisible component surrounding our stellar system in an approximately spherical halo. This component is called dark matter. What it consists of is still completely unclear. Two years ago, very faint white dwarfs were detected for the first time which were presumed to be located within the halo, providing at least two percent of the dark matter there. Theorists at the Institute together with colleagues from Spain now reexamined the observational data, concluding that the majority of these white dwarfs apparently is not located in the halo at all and so contributes much less to the dark matter than previously thought.

The total mass of the Milky Way system is only known very poorly. The mass of the visible component consisting of stars, dust, and gas amounts to no more than 1.2×10^{11} solar masses. From the rotation of gas and stars within the galactic disk, however, the dynamical mass can be determined. It is calculated under the assumption that these objects are moving on Keplerian orbits around the galactic center. The mass derived from such analyses is 2.2 to 3×10^{11} solar masses. Considering the motion of the Milky Way and its neighboring galaxies a mass of even 1.2×10^{12} solar masses is deduced. Dark matter therefore constitutes between 35 and 90 percent of the Galaxy's total matter.

Which kind of matter is located in the halo, making itself conspicuous only by gravitation, we do not know. It definitely cannot consist of baryonic matter alone. Such high a baryon density would be inconsistent with cosmological models that account for the element abundances created in the big bang. It is possible, though, that part of the dark matter consists of hitherto undetected cosmic bodies.

This was first indicated by observations of so-called gravitational microlensing events, which are interpreted as deflection and magnification of light in the gravitational field of a cosmic body. If an invisible object located in the halo of the Milky Way crosses in front of a distant star, one located in the Large Magellanic Cloud, e.g., the brightness of the star increases for a short period. In the 1990s, special observational programs succeeded in detecting dark cosmic bodies within our Galactic halo. Yet their nature remained unclear. Brown dwarfs or faint white dwarfs appeared to be the most likely candidates.

In 2001, very faint, ultra-cool white dwarfs were found that were believed to populate the halo of the Milky Way. According to this study, these stars would contribute at least two percent to the dark matter there. Thus, for the first time, part of the dark matter within the halo of our Galaxy seemed to be identified.

But there are serious problems with this hypothesis. White dwarfs represent the final stages of stars that started out with initial masses up to eight solar masses. If white dwarfs really were contributing that much to the mass of the halo, the proportion of their progenitors had to be significantly larger than observed in present-day stellar populations.

The question whether a white dwarf is located within the halo or in the Galactic disk is not easy to decide. In their study, the astronomers had correctly assumed halo objects to have a considerably higher tangential velocity than those within the Galactic disk. Based only on this criterion, 38 white dwarfs had been attributed to the halo. The tangential velocity of a star, however, can only be calculated from the measured proper motion if the distance to the star is known; but the distance is hard to determine. Theorists at the Institute now reexamined the observational data, analyzing them very critically.

The distance determination is based on an evolutionary model for white dwarfs. At their formation, these stars are very hot. Subsequently, they are slowly cooling down since the generation of energy by nuclear fusion in their interiors has ceased. In order to determine the distance of a sample of white dwarfs from their apparent magnitude and color, if possible, a cooling-model is needed as well as an estimation of the group's age.

In their model, the theorists assumed the star formation within the disk to decline exponentially over the billions of years, as observational data suggest. In the halo, though, all stars are assumed to have formed within the first billion years, the star formation rate then being zero afterwards. Also of prime importance was the use of a new cooling-model for white dwarfs based on recent observations and theories. In these two assumptions, the new model differed significantly from that used in 2001 to analyze the data of the white dwarfs observed. At that time, the astronomers had applied a model appropriate for white dwarfs in the Galactic disk but not for those in the halo.

The new analysis revealed that in the older work, the data had been calibrated incorrectly, which significantly affected the distance determination: In the older analysis, the distances had been underestimated for bright white dwarfs and overestimated for low-luminosity white dwarfs. Consequently, for the major part of the white dwarfs, the tangential velocities derived from the proper motions were too high. So per definition, these stars do not belong to the halo but to the disk.

The question how many of the white dwarfs detected actually belong to the halo can only be answered statistically. The number of the observed white dwarfs, though, is too small to obtain a reliable result. Therefore, the theorists at MPIA and their colleagues performed so-called Monte Carlo simulations. In these calculations, they defi-

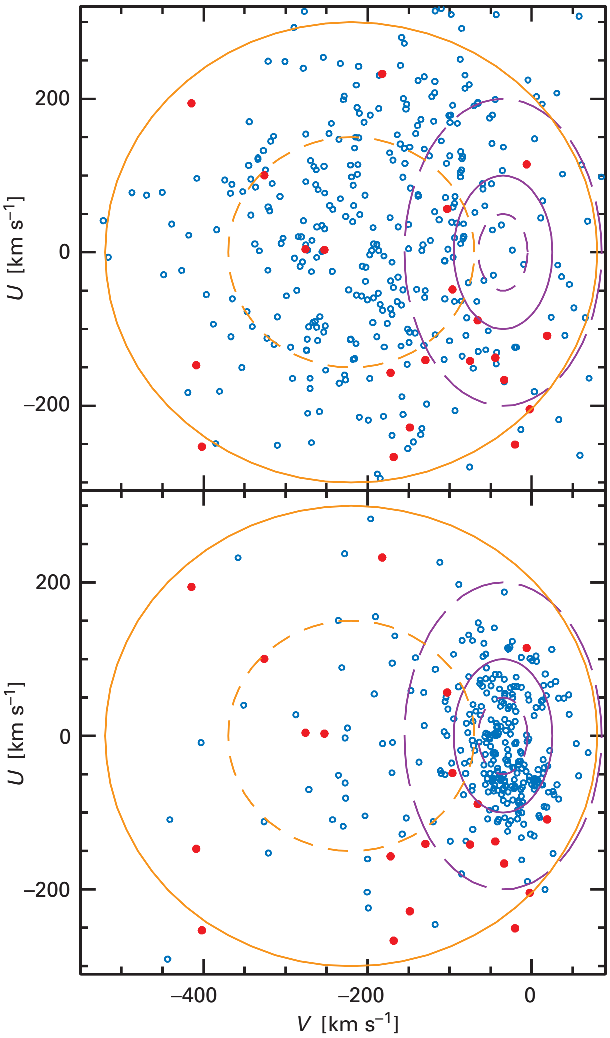

Fig. III.48: Distribution of the tangential velocities of white dwarfs. Black dots denote the objects observed, open circles the results of the Monte Carlo simulations. Members of the halo population (above) are located mainly within the large circles, those of the disk (below) within the small ellipses (1σ and 2σ limits, respectively).

ned a sample of about ten thousand white dwarfs that statistically have magnitudes, proper motions, and colors similar to the ones observed. Then they applied their galactic model to this group of stars, asking how many of them belong to the halo population due to their tangential velocity.

The Monte Carlo simulations showed that only about half of the white dwarfs observed are genuine halo members. The others belong to the disk (Fig. III.48). This reduces the mean number density of halo white dwarfs calculated in 2001 by a factor of 3.5 to a value of 3×10^{-5} per Mpc^3. The new value is in very good agreement with estimates obtained by others and also resolves the problem concerning the above-mentioned frequency of white dwarf progenitors. In future, the detection of additional white dwarfs will be very important in order to improve the statistics and to obtain a more accurate value of the number of these halo objects.

(A. Burkert)

IV Instrumental Development

The performance and the field of application of a telescope critically depend on the quality and efficiency of the measuring device installed in the focal plane. At MPIA, such scientific instruments are developed and built in its technical departments. Currently, several instruments are under construction, which will be used at ground-based observatories as well as in space telescopes.

The instruments are built in the workshops at MPIA, often in cooperation with companies from industry. The requirements set by the scientists frequently confront these firms with completely new tasks, the know-how gained in this way strengthening their competitive capacity on the global market.

Following is a summary of the MPIA's recent instruments and their actual status in the year under report.

Fig. IV.1: The prototype of PARSEC mounted in the MPE laboratory. (Image: MPE)

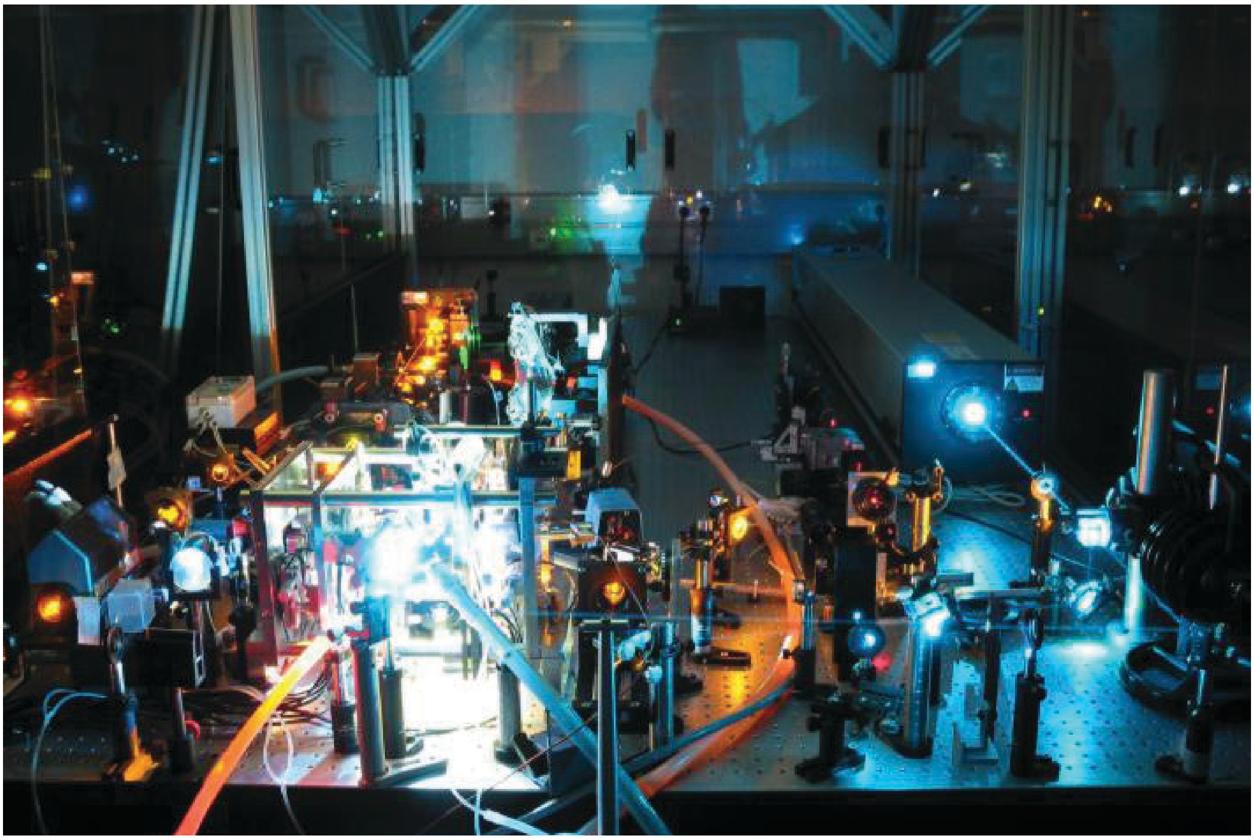

1. Adaptive Optics

In theory, the resolving power of a telescope, i.e., its capability to produce separate images of two objects lying close together, increases with the diameter of the primary mirror. In practice, however, atmospheric turbulences blur long-exposure images to such a degree that the resolution is one half to one arc second at its best, regardless of the mirror size. Astronomers and engineers at MPIA, together with colleagues from the MPI für extraterrestrische Physik (MPE), have built a so-called adaptive optics system for the near-infrared spectral range (ALFA) for the Calar Alto Observatory that corrects image fluctuations during the exposures (cf. Annual Report 2000, p. 31). In this way, the theoretically possible resolution, i.e. the diffraction limit, can be achieved.

On Calar Alto, it was demonstrated that ALFA can also be operated using an artificial laser guide star. Such an instrument consists of a laser pointed parallel to the telescope's optical axis towards the sky. At an altitude of about 90 kilometers, the laser beam excites atmospheric sodium atoms, which then start glowing. The emission typically extends over a cylindrical volume about one meter in diameter and seven kilometers long. The spot of light created in this way serves as a reference star for the adaptive optics system. The experience gained with this instrument will now be utilized at the ESO Very Large Telescope (VLT) and at the Large Binocular Telescope (LBT).

The VLT 8 m telescope YEPUN will be the first to be equipped with a **laser-guide-star device**. Here, a sodium laser, named **PARSEC**, will produce a continuous beam of 10 to 15 watts power. This instrument is being developed jointly by researchers at MPIA and MPE (Fig. IV.1). MPIA is contributing a so-called LIDAR (Light Detecting and Ranging) – a pulsed laser that can be used to measure the altitude of the atmospheric sodium layer and the concentration of sodium atoms there.

The LIDAR is based mainly on experience acquired with ALFA. It was shown that a laser guide- star can only be used efficiently during the observations if the atmospheric conditions are known in detail. Experiments with a LIDAR at the 3.5 m telescope on Calar Alto had turned out to be successful, so it was decided to build a similar device for PARSEC.

The LIDAR developed at MPIA is capable of measuring the altitude of the sodium layer with 150 m resolution and of determining the magnitude of the laser guide star independently from the adaptive optics. Acceptance by ESO will be in fall of 2003 in Garching. The first phase of commissioning will be early 2004 on Paranal. In the beginning, the LIDAR will be operated together with the NACO instrument (see below). In 2004, SINFONI, the second focal instrument on VLT-YEPUN, is planned to be put into operation. It is a 3D-spectrograph with an adaptive optics systems of its own that will use the laser guide star, too.

For the LBT, a somewhat different instrument is currently being tested – a **SCIDAR** (Scintillation Detection and Ranging), which helps to optimize the adaptive optics system of the LBT. Adaptive optics systems can only partially compensate image distortions due to atmospheric turbulences. This mostly affects objects outside the central correction axis of the adaptive optics. The strength of this so-called anisoplanicity effect depends mainly on the vertical structure of the atmospheric turbulence. If there are several bright stars in the field of view during an exposure with adaptive optics, the strength of this effect can be estimated afterwards to improve photometric and astrometric measurements. But bright stars are not always available and, furthermore, these estimates are highly uncertain. This is where SCIDAR will be put into action.

SCIDAR observes a binary star, producing a defocused image of it (actually it is an image in the pupil plane). From the intensities of the pupil images of both stars the vertical structure of the atmospheric turbulence can be determined up to an altitude of about 20 km. While measurements of the phase distortions over the pupil cannot yield information about the vertical structure of the turbulence, the strength of the scintillation depends on the distance between a turbulence layer and the observational plane. Thus, the brightness distribution over the pupil contains information on the vertical distribution of the turbulence.

The SCIDAR hardware was built at Steward Observatory while MPIA contributed the data analysis software. The instrument was successfully tested on the Vatican Advanced Technology Telescope. In mid-2004, it will be used during First Light on the LBT.

PYRAMIR

PYRAMIR is a new kind of wavefront sensor for the near infrared spectral range which will be used with ALFA. It is intended to replace the system's old tip-tilt sensor. The sensor will be completely reside within a dewar and mounted on the existing second sensor platform in ALFA.

The design of a pyramid wavefront sensor had been proposed for the first time in 1996. Its special feature is to create four pupil images which are then used to measure the gradient of the wavefront. This instrument has an important advantage over the customary Shack-Hartmann wavefront sensor in being able to control the amplification according to the observational conditions. Optically, this is achieved by a reflecting pyramid that splits the beam focused onto its tip into four parts. A zoom lens then creates four pupil images on the detector (Fig. IV.2).

PYRAMIR will be the first sensor of this kind worldwide operating in the near-infrared range. Thus, it will be working in a wavelength region where a highly efficient correction is achieved by the adaptive optics system. Theoretically, pyramid sensors should be able to work with fainter guide stars than comparable Shack-Hartman systems. However, up till now, no sensor exists to prove this in practice. Currently, PYRAMIR is the only project that will test its performance at a telescope. Because of its

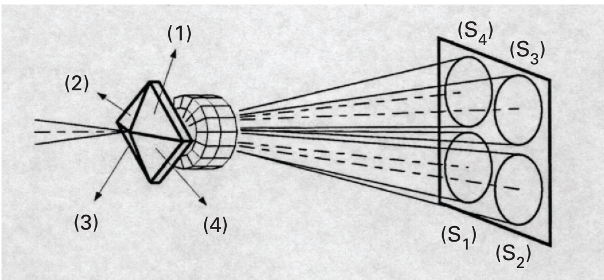

Fig. IV.2: The pyramid splits the beam focused onto its tip into four. A zoom lens then creates four pupil images on the detector.

higher sensitivity, PYRAMIR increases the sky coverage for certain classes of objects, such as young stars or highly reddened objects in general, in the Galactic plane from 7 percent to nearly 50 percent.

The internal design review of the project, taking place in December 2002, arrived at a positive result, with the restriction that the project has to be carried out as a technological development. The system is expected to be used in adaptive optics systems on 8 m class telescopes, such as the PLANET FINDER on VLT (see below). PYRAMIR entered the construction phase limited to one year. In spring 2004, it is planned to be put into operation on Calar Alto.

The PLANET-FINDER project CHEOPS

PLANET FINDER was announced by ESO as a VLT instrument of the second generation. An adaptive optics system of extremely high imaging quality is asked for that will be combined with an instrument achieving particularly high contrasts in the immediate vicinity of bright objects. In the end, this instrument is intended for the detection and imaging of extrasolar planets.

MPIA has assembled an international consortium of German, Italian, Swiss, Dutch and Portuguese institutes and in February 2002 submitted to ESO a preliminary proposal for such an instrument. It is called CHEOPS (Characterizing Extrasolar Planets by Opto-infrared Polarimetry and Spectroscopy). It records difference signals between star and planet and uses the different spectral properties of the two objects as well as their different degrees of polarization. A similar second proposal was submitted by a consortium led by the French. Thus ESO has asked both consortia to each perform a complete Phase-A study. The study started in March 2003 and will take 18 months. After that, a further selective review will take place.

Adaptive Optics as a Teaching Subject at the Universität Heidelberg

Because of the growing importance of adaptive optics MPIA, since winter semester 2002, offers a new experiment within the scope of the advanced practical course to all students of the Department of Physics and Astronomy at the Universität Heidelberg. During four afternoons, the students can set up a modern analyzer to examine the optical quality of light waves and determine optical aberrations such as, e.g., astigmatism and coma. The experiment is carried out in the newly established laboratory for adaptive optics at MPIA (Fig. IV.3).

(S. Hippler, M. Feldt, P. Bizenberger, W. Brandner, D. Butler, J. Costa, B. Grimm, Th. Henning, U. Neumann, W. Rix, R.-R. Rohloff, C. Unser)

Multiconjugate Adaptive Optics (MCAO)

Adaptive optics systems always need a reference star of a certain minimum brightness. Furthermore, optimum correction is only possible within a certain angle around this star. Beyond, the image becomes increasingly blurred. In the future, this limitation will be avoided by using so-called multiconjugate adaptive optics (MCAO).

To make this technique practicable for the first time, a special team was established at MPIA. On a long-term basis, a MCAO is also to provide the LBT with diffraction-limited images in the combined focus – not only in the near infrared range but also at wavelengths down to 800 nm. At an observing wavelength of 1 μm, the diffraction limit of the LBT is 9 milli-arc seconds. The goal is to get a diffraction-limited image over the entire field of view, which has a size of 1 arc minute.

With the classical adaptive optics, only one direction within the field of view is corrected. With MCAO, this technique is applied to several directions and reference stars, assuming the atmosphere can be represented by only a few thin turbulent layers.

During the next three years, MCAO will be coupled with the LBT LINC-NIRVANA camera (see below) that is also being built at MPIA. Light coming from one LBT mirror is divided by a beam-splitter. One part travels to a wavefront sensor, which controls the 672 actuators of the adaptive secondary mirror of the corresponding LBT primary mirror. The portion of light that passes the beam splitter is directed by two flexible mirrors with 349 actuators each and by several additional mirrors to the focus. The light beam coming from the second LBT primary mirror is subjected to the same procedure. Wave trains in phase then interfere in the joint focus.

In this instrument, a total of six wavefront sensors as well as six adaptive mirrors with a total of 2740 actuators will be used – a hitherto unique concept that will render the spatial resolution of ground-based telescopes almost independent of atmospheric influences over a large field of view. Moreover, the wavefront sensors' large fields of view of one to two arc minutes facilitate the selection of reference stars of sufficient brightness for the adaptive optics. This is crucial for conducting as many scientific projects as possible with this instrument.

(T. Herbst, D. Andersen, P. Bizenberger, H. Böhnhardt, W. Gässler, S. Kellner, Ch. Leinert, R. Ragazzoni, H.-W. Rix, R.-R. Rohloff, R. Soci, W. Xu)

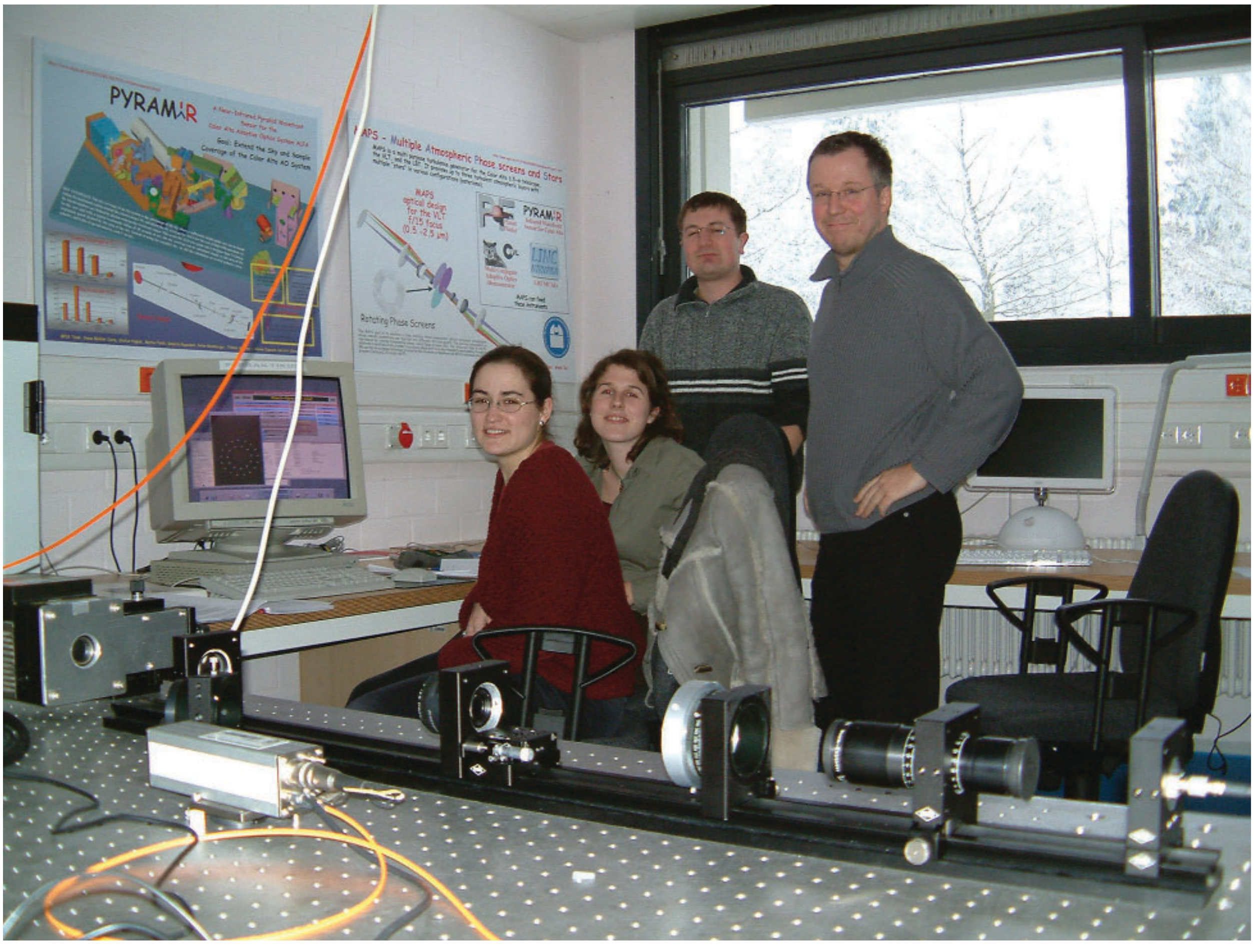

Fig. IV.3: Students attending the advanced practical course on adaptive optics in an MPIA laboratory.

2. Lucifer and Linc-Nirvana for the Large Binocular Telescope (LBT)

As mentioned in chapter I, MPIA, together with the MPI für extraterrestrische Physik in Garching, the MPI für Radioastronomie in Bonn, the Astrophysikalisches Institut Potsdam, and the Landessternwarte Heidelberg, will have a 25 percent share in costs and use of the Large Binocular Telescope, under the auspices of the LBT Beteiligungsgesellschaft (LBTB). Unlike all previously-built telescopes, the LBT will be equipped with two light-gathering mirrors of 8.4 m diameter each, fixed on a common mount. First light is planned for summer 2004.

In 2002, the telescope structure built in Italy was shipped to the US and subsequently reassembled in the telescope building. By the end of 2002, the rotating part of the azimuth structure was reconstructed while at the same time both primary mirrors were manufactured: grinding and polishing of the first mirror is complete; by the end of December, the mirror had successfully passed the verification tests. Now the second mirror blank is going to be finished.

Under the direction of the Landessternwarte Heidelberg, the German partners are building a pair of near-infrared spectrographs, called **Lucifer**, for the LBT. MPIA will supply the entire detector package and develop the overall design of the cooling system. Integration and tests of the instrument will also be carried out in the laboratories of MPIA. In addition, the MPI für extraterrestrische Physik in Garching, the Universität Bochum, and the Fachhochschule für Technik und Gestaltung in Mannheim are also involved in the Lucifer project.

In 2004, the first Lucifer will begin operations in the focal plane of the first mirror. Eighteen months later, the second, identical instrument will be put into operation at the focus of the second mirror. With Lucifer, both direct imaging and long-slit spectroscopy in the wavelength range between 0.85 and 2.45 μm will be possible. In order to reduce thermal background radiation of the instrument, Lucifer will be cooled to 77 K or even lower using liquid nitrogen. The following observing modes are planned:

- Seeing-limited direct imaging with a field of view of 4 arc minutes, long-slit spectroscopy with a slit length of 4 arc minutes, and multi-object spectroscopy.

- Diffraction-limited direct imaging with a field of view of 0.5 arc minutes and long-slit spectroscopy as well as
- Integral field spectroscopy.

With diffraction-limited imaging, the LBT provides excellent spatial resolution. Depending on the wavelength it is 0.031 arc seconds at 1.23 μm, 0.041 arc seconds at 1.65 μm, and 0.056 arc seconds at 2.2 μm. Corresponding to the observing mode, the cameras need to be exchanged in order to obtain the highest image quality for all seeing-limited imaging modes. Altogether, three cameras are planned with respective resolutions of 0.015 arc seconds, 0.12 arc seconds, and 0.25 arc seconds per pixel. The detector will be an infrared array with 2000 × 2000 pixels.

LUCIFER will be used in the near infrared mainly for observing faint objects, including, e.g., young galaxies at high redshifts. Astronomers also expect major progress in the spectroscopy of brown dwarfs, i.e., very faint red stars. Dusty disks around young stars and in the nuclei of active galaxies are also given high priority.

The beam combiner is being designed and constructed at MPIA while the Universität Köln is contributing the cryostat and the tip-tilt sensor. A team at the Institute, together with colleagues from Arcetri, is developing the adaptive optics system. In the year under report, the design of the cryo-mechanics was completed and the cryostat was ordered. Moreover, construction of several components, such as the filter wheels, the grating drive system, the N30 camera, and components of the MOS unit, is mostly completed. The detector has been delivered, too.

One of the most ambitious instruments on the LBT will be the LINC Fizeau-interferometer, which coherently combines the light arriving from both primary mirrors (Fig. IV.4), allowing unprecedented spatial resolution within a large field of view. Together with the large light-gathering power of both mirrors, this will make the LBT a leading observatory in the northern hemisphere. An in-

Fig. IV.4: Structure of the LBT (above) and the light path in the adaptive optics system, which is installed between both primary mirrors.

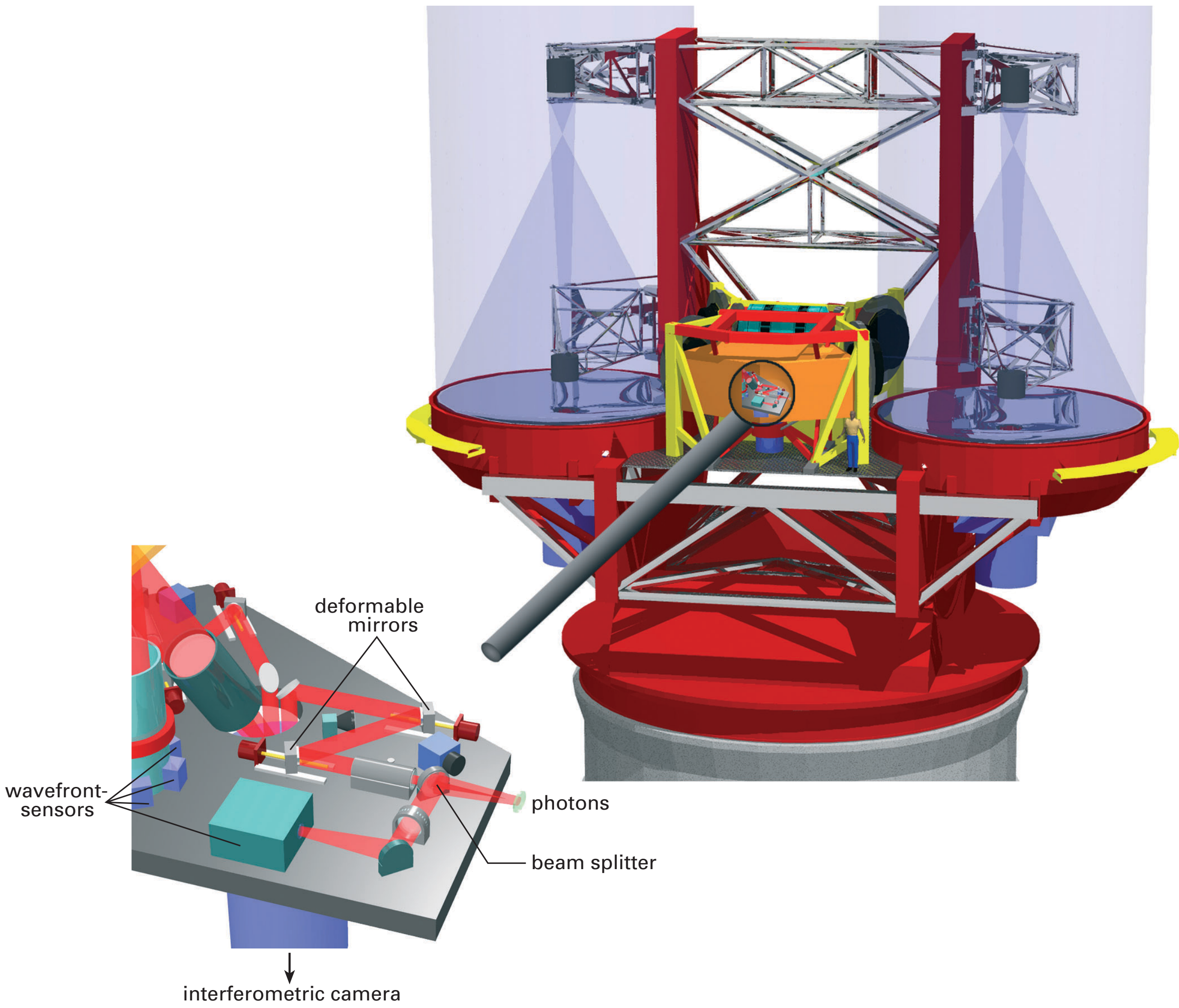

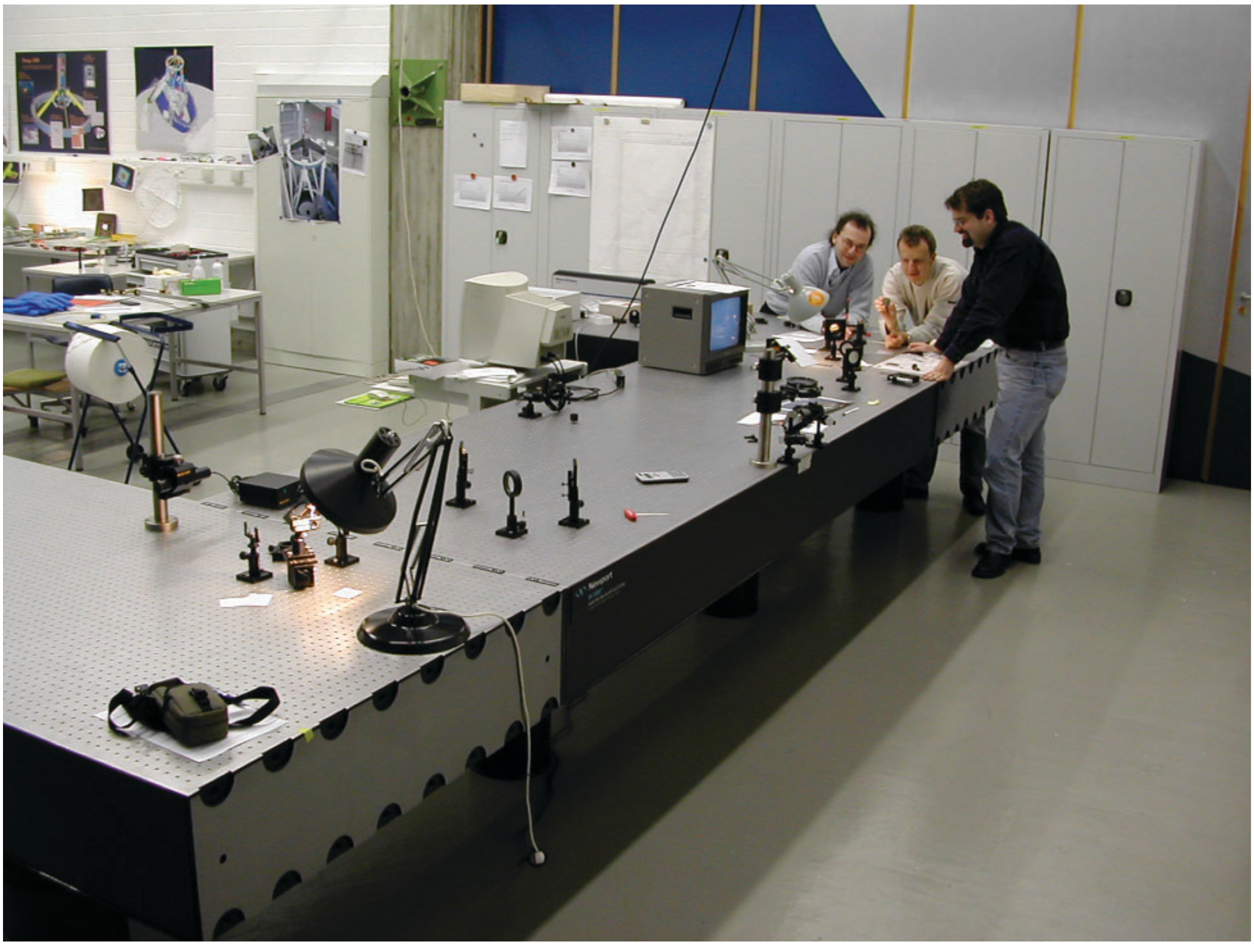

Fig. IV.5: The optical bench for testing the folded light path in the planned LINC instrument.

strument like this has never been built before and therefore requires an extremely demanding optical design. MPIA, forming a consortium with colleagues from the Universität Köln and the Astrophysical Institute in Arcetri, Italy, is developing the optics of the beam combiner.

With LINC, interferometry at wavelengths between 0.6 and 2.4 μm will be possible. This entire spectral range will be covered by two different detectors. For visible light, a CCD with pixel sizes of 9 to 12 μm will be used. For the near infrared between 1 and 2.4 μm, an infrared array with 2000 × 2000 pixels, each the size of 18 μm, is planned.

The interferometer will be operated together with an adaptive optics system, which will correct, depending on the wavelength, a field of view between 20 arc seconds (at 2 μm) and 5 arc seconds (at 0.7 μm). The ultimate resolution of LINC also depends on wavelength, lying between 0.02 arc seconds at 2 μm and 0.006 arc seconds at 0.7 μm.

LINC is developed in two stages. First, the diffraction limit is planned to be achieved with only one natural guide star; in a second stage (NIRVANA), the above-mentioned multiconjugate adaptive optics (MCAO) will be used also at wavelengths lower than 1 μm.

Astronomical observations will focus on compact objects, forming a long list ranging from the spatial extension of supernovae to the structure of protostellar disks to the search for extrasolar planets.

Large progress was made in the year under report. First, the project team was increased and now comprises 17 staff members, as was originally planned. This group completed the optical concept and proposed a preliminary design of the instrument. Furthermore, manufacturing of the first hardware components was started: In the optical laboratory of the Institute, the team installed a prototype of the folded light path, as it will later be realized at the telescope (Fig. IV.5). It was successfully tested, demonstrating the chosen layout to work well. Later, this set-up will be taken over for the prototype of the interferometer and be used to test the final hardware.

(T. Herbst, R. Lenzen, D. Andersen, H. Baumeister, P. Bizenberger, H. Bönhardt, F. Briegel, W, Gäsler, W. Laun, S. Ligori, C. Leinert, L. Mohr, R. Ragazzoni, H.-W. Rix, R.-R. Rohloff, R. Soci, R. A. Weiß, W. Xu)

3. OMEGA 2000 – a Wide Field Infrared Camera for Calar Alto

From the beginning, the Institute was heavily involved in infrared astronomy as is evidenced by the MAGIC as well as the OMEGA-PRIME and OMEGA-CASS instruments. The development of new cameras critically depends on the availability of infrared detectors. Recently, arrays with 2048 × 2048 pixels have become available. These are sensitive up to a wavelength of 2.4 μm and have a quantum efficiency of about 60 percent between 0.8 and 2.4 μm.

To keep Calar Alto at the forefront of infrared astronomy, MPIA decided to develop and build a new camera for the near infrared range. It will be similar to its forerunner OMEGA-PRIME, but its field of view will be five times larger with a size of 15 arc minutes×15 arc minutes, corresponding to a quarter of the size of the full moon. The instrument will be operated at the prime focus of the 3.5 m telescope where it will have an image scale of 0.45 arc seconds per pixel at a focal ratio of *f*/2.35.

In the year under report, the read-out electronics as well as the electronics controlling the motion of the filter wheels and of the external baffle were optimized. In addition, the development of a data reduction pipeline was started that will enable data reduction parallel to the data gathering. In January 2003, the instrument saw First Light (Fig. IV.6). First tests showed no major problems. In spring, OMEGA 2000 will be further optimized and from July on be made available to the general user, replacing the previous workhorse OMEGA-prime.

(H.-J. Röser, M. Alter, H. Baumeister, P. Bizenberger, A. Böhm, Fr. Briegel, R. Faßbender, B. Grimm, Z. Kovacs, W. Laun, U. Mall, R.-R. Rohloff, C. Storz, K. Zimmermann)

Fig. IV.6: First Light for OMEGA 2000.

4. LAICA – the Wide Field Camera for Calar Alto

In future, essential science will continue to come from wide field surveys searching for faint objects. This trend is increasingly taken into account by the Institute.

First, a wide field camera for the 2.2 m telescope on La Silla was built in collaboration with ESO. In 2000, MPIA decided to build the new OMEGA 2000 wide field infrared camera for Calar Alto. The third instrument of this kind is the Large Area Imager for Calar Alto, LAICA for short. It will work at the prime focus of the 3.5 m telescope, yielding an aberration-free field of 44 arc minutes (corresponding to a side length of 115 mm). In its focal plane, a mosaic of four CCDs is mounted, each having 4096 × 4096 pixels. The image scale will be 0.225 arc seconds per pixel (cf. Annual Report 1999, p.33).

For production reasons, the CCDs cannot be joined without gaps, thus leaving a space of about 50 mm width between them. Therefore, it is not possible to image a contiguous area of the sky in one shot. This can easily be compensated for by taking three more shots at different positions, thereby filling the gaps. A set of four images covers a contiguous field of one square degree, corresponding to about five times the area of the full moon.

In addition, two smaller CCDs are integrated into the focal plane for guiding purposes. In this way, image rotation, which may occur in long exposures, can be noted and corrected. In summer, this guiding system was successfully tested at the telescope.

For the moment, two filter sets are planned. The filter mounting resembles the magazine of a slide projector. It contains 20 filters that are taken out by a robot arm and placed into the light path.

Construction of LAICA started in early 1999. On 20 May 2001, it saw first light. Unfortunately, difficulties with the CCDs occurred subsequently that were due to production defects. New CCDs were ordered that will not be delivered before spring 2003.

(J. Fried, K.-H. Marien, F. Briegel, B. Grimm, R. Klein. C. Unser, K. Zimmermann).

5. NACO – the High-Resolution Infrared Camera for the VLT

At the end of 2001, First Light for the CONICA high-resolution infrared camera, developed and built under the leadership of MPIA, was one of the highlights of the year at the Institute. CONICA is operated together with the NAOS adaptive optics system, built by colleagues in France.

From the beginning, the instrument, renamed NACO, yielded astronomical images of unprecedented resolution that were enthusiastically taken up also by the international press (cf. Annual Report 2001, p. 13). During 2002, several improvements were made, particularly on the real-time computer software for the adaptive optics system and on the control software for NACO. In addition, the infrared wavefront sensor was put into operation. By various improvements on the optics and the compensation of static aberrations by the adaptive optics a Strehl ratio of more than 80 percent was achieved under optimal conditions in the K band.

Of the excellent scientific results, only two shall be mentioned here: For one thing, high-resolution images of the Galactic center were obtained that yielded an extremely high lower limit for the density of the central body lying at the very center of our Milky Way, implying that this body can only be a black hole (Fig. IV.7). For another thing, astronomers at MPIA and their colleagues observed the Arches star cluster located near to the Galactic center (Fig. IV.8). It is one of the most massive star clusters in the Milky Way, but cannot be observed in the visible spectral range because of dense dust clouds in the foreground that absorb its light. With NACO, Arches could be studied in the near-infrared range with unprecedented resolution. The scientific results will be reported in the next Annual Report.

(R. Lenzen, Becker, A. Böhm, M. Hartung, W. Laun, K. Meixner, Münch, R.-R. Rohloff, C. Storz, K. Wagner)

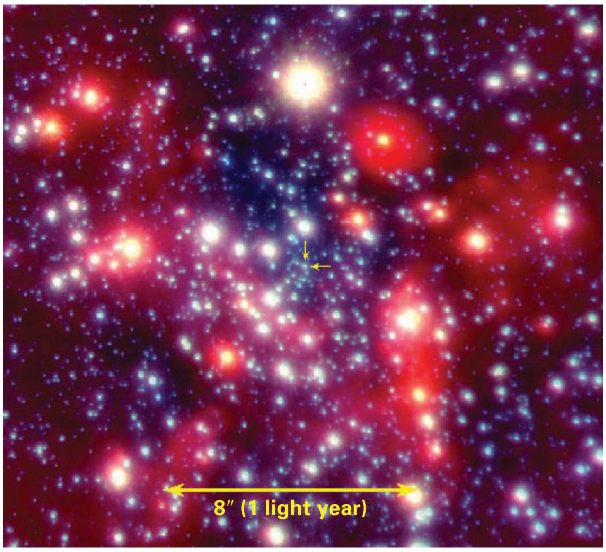

Fig. IV.7: The innermost region around the Galactic center, imaged with NACO in the near-infrared range.

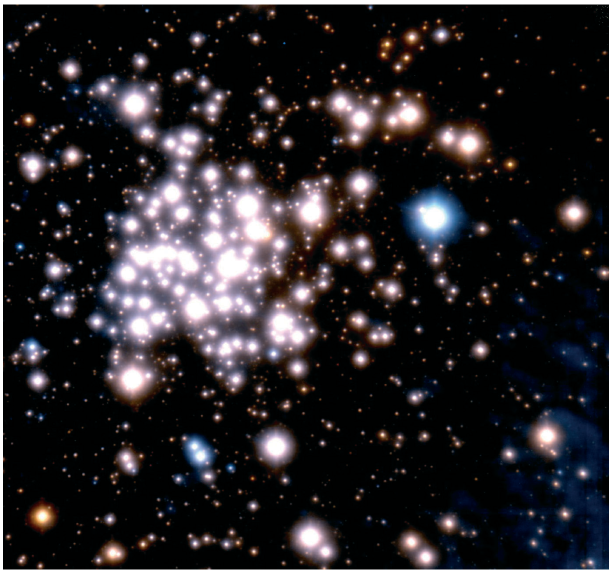

Fig. IV.8: The Arches star cluster near the Galactic center, imaged with NACO in the near-infrared range.

6. MIDI – an Infrared Interferometer for the VLT

Another highlight in the year under report was First Light for the MIDI interferometer on 15 December. MIDI is the first instrument worldwide enabling observations of this kind in the spectral range at 10 μm at large telescopes. It was built under the leadership of MPIA, together with colleagues from the Netherlands and France as well as from the Kiepenheuer-Institut in Freiburg and the Thüringische Landessternwarte Tautenburg.

Two of the large telescopes of the VLT, ANTU and MELIPAL, were successfully coupled interferometrically with a base line of 100 m, yielding first fringes. Among the first objects observed were the stars Z Canis Majoris, Epsilon Carinae and Eta Carinae. The results obtained fully met the expectations. So the goal aimed at was completely achieved. The functional performance of MIDI will be tested during 2003. For a detailed report see Chapter II.3.

(Ch. Leinert, U. Graser, A. Böhm, O. Chesneau, B. Grimm, T. M. Herbst, S. Hippler, R. Köhler, W. Laun, R. Lenzen, S. Ligori, R. J. Mathar, K. Meisenheimer, W. Morr, R. Mundt, U. Neumann, E. Pitz, F. Przygodda, Th. Rabzah, R.-R. Rohloff, P. Schuller, C. Storz, K. Wagner, K. Zimmermann)

7. PACS – the Infrared Camera and Spectrometer for HERSCHEL

In 2007, the European Space Agency (ESA) will launch the HERSCHEL far-infrared telescope (formerly called FIRST – Far-infrared and Submillimeter Space Telescope) as its fourth major "cornerstone" mission. The MPIA is partecipating to this mission.

HERSCHEL will be provided with a passively cooled 3.5 m mirror and three scientific instruments covering the wavelength range from 60 to 700 μm. These are being built by international consortia. One central issue of the research program will be the observation of protostellar dust clouds and protoplanetary disks. The Far-infrared and submillimeter emission of very distant young galaxies will also be detectable. MPIA is participating in the construction of one of the instruments, named PACS (Photoconductor Array Camera and Spectrometer). The PACS project is conducted under the leadership of the Max-Planck Institut für extraterrestrische Physik.

PACS is designed for photometric and spectrometric studies in the wavelength range between 60 and 210 μm. MPIA will significantly contribute to the development and characterization of the cameras and pre-amplifiers, as well as to the focal plane chopper and the data center. Based on experience acquired with ISO, the Institute will participate in the detailed planning of the structure of the HERSCHEL ground segment and, particularly, of the control center for PACS. The Institute will also be responsible for all aspects of the calibration of PACS before and during the flight.

In the year under report, encouraging progress was made. Together with the Carl Zeiss company, MPIA manufactured a model of the focal-plane chopper for PACS. A chopper is used for the following purpose: During infrared observations, a more or less strong confusing background signal can occur, caused by the thermal emission of the telescope and the sun shield. In order to eliminate this signal, the target object and a neighboring "empty" section of the sky are imaged alternately. The empty section provides the background that is later subtracted from the actual exposure. The alternating observation of two sections of the sky is achieved by installing a mirror in the light path that tips ("chops") to and fro up to ten times a second with high optical and mechanical precision.

Following preliminary experiments at the Fraunhofer-Labor für Betriebsfestigkeit in Darmstadt, the PACS-team celebrated the successfully concluded durability tests under cryo-vacuum conditions at the end of the year under report. This test, performed in a helium cryostat, proved the trouble-free operation of this important system of the PACS instrument over 650 million cycles. In this test, the three-year HERSCHEL mission was simulated in a period of four months by using a ten times higher sinus-modulated frequency instead of a square-wave-modulated one, allowing for a safety margin of a factor of two for the service life (Fig. IV.9).

This development was of benefit to the qualification model of the chopper that was assembled by the end of the year at Zeiss from components mostly built at MPIA. This chopper model will soon undergo the cold vibration tests simulating the rocket launch. The coils developed for the chopper were sold to Great Britain where they will be integrated into the HERSCHEL-SPIRE instrument. The position measuring system developed for the chopper by MPIA was accepted as a German patent at the end of the year. Major progress was also made in the development of the cold read-out electronics. All components developed at MPIA underwent functional tests.

(D. Lemke, S. Birkmann, R. Hofferbert, U. Grözinger, U. Klaas, Schmitt, R. Vavrek)

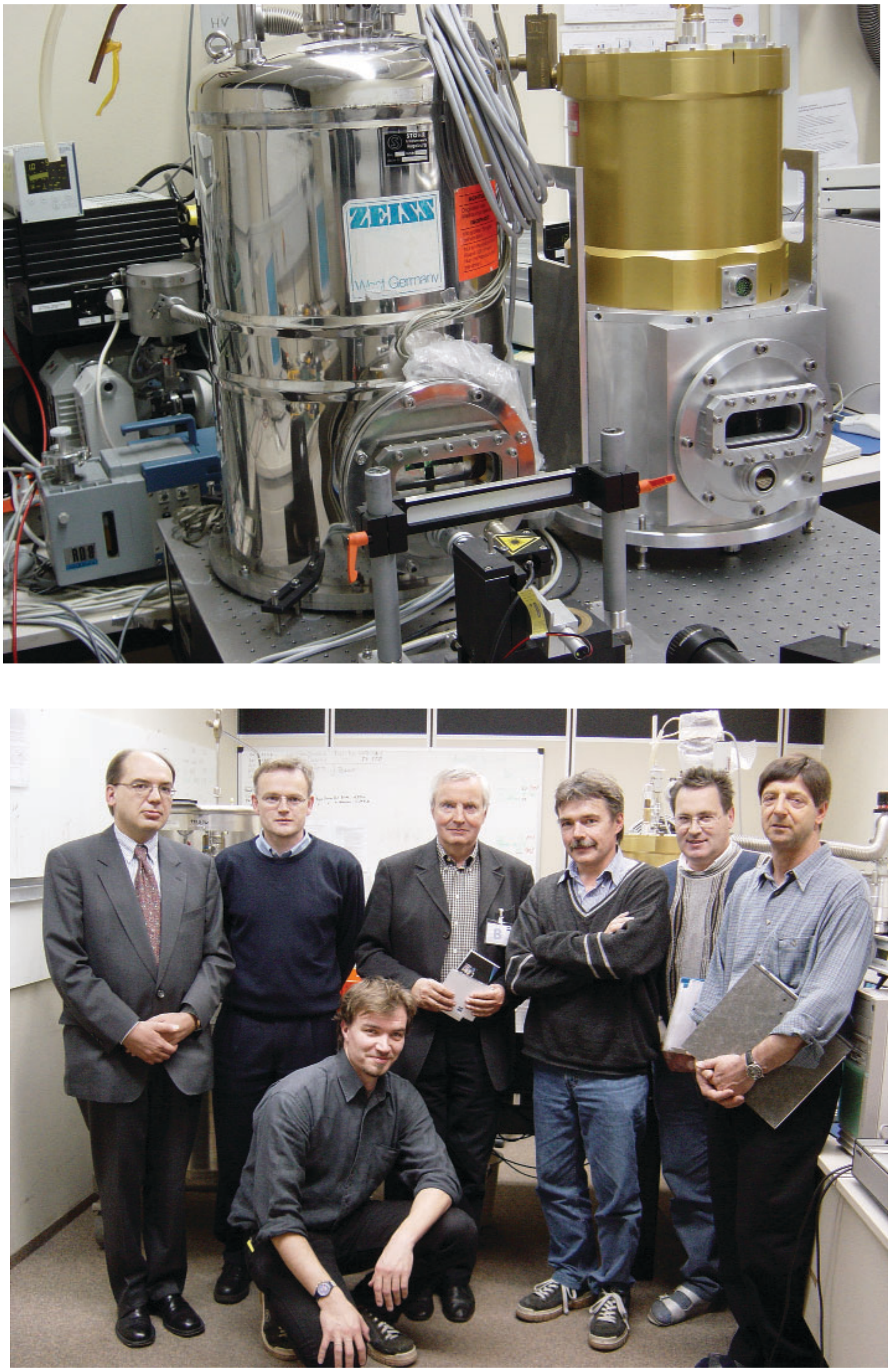

Fig. IV.9: a) This cryostat was used to test the durability of the focal-plane chopper in a cryo-vacuum at a temperature of -270 degrees Celsius. **b)** The team from the Zeiss company and from MPIA after a trouble-free run of 650 million cycles.

8. MIRI and NIRSPEC for the James Webb Space Telescope (formerly called Next Generation Space Telescope)

The successor to the HUBBLE Space Telescope is scheduled for launch in 2011: The James Webb Space Telescope (JWST) will be equipped with a folding primary mirror about 6 m across. It will mainly work in the infrared range, orbiting the sun at the Lagrange-point 2, at a distance of 1.5 million kilometers from Earth. The telescope cools down in the shadow of large solar cell panels to 45 Kelvin; an additional active cryo-system cools one of the scientific instruments to an operating temperature of 7 Kelvin. The European Space Agency ESA will significantly participate in the manufacture of the detector. Moreover, NASA and ESA decided to launch the JWST with the European rocket Ariane 5. The MPIA is partecipating to this mission.

Europe partakes in this large-scale project, among other things, by the development of two of the three focal-plane instruments. ESA will develop the NIRSPEC near-infrared spectrometer while the MIRI camera- and spectrometer instrument for the mid-infrared range will be built half by NASA and half by a European consortium. MPIA is a member of both Phase-A-study consortia for NIRSPEC as well as of the MIRI consortium. The Institute is focusing on the opto-mechanical positioners and the electronics for it. In addition, it is partaking in the definition of the scientific goals of MIRI and their translation into instrumental requirements.

In fall, the Phase-A-study for MIRI was completed and the report presented to ESA. MPIA took over the design of the filter wheel, the grating drive, the beam divider wheel, and the drive of the calibration mirror. All these components are subject to heavy demands on the operation in a cryo-vacuum, such as maximum reliability and precision, minimum power loss, and so on. The cryo-harnesses that will enable operation at 300, 35, and 7 Kelvin were designed, too. Here, the Institute can rely on its experience acquired with ISOPHOT and PACS. At the end of the year under report, the preliminary Phase B for MIRI began.

At this time, the Phase-A-studies for NIRSPEC were still underway. Here, MPIA made similar contributions to filter and grating wheels, to the focusing linear drives, to part of the control electronics, and to the cryo-harness (Fig. IV.10).

(D. Lemke, U. Grözinger, Th. Henning, R. Hofferbert, R.-R. Rohloff, K. Wagner)

Fig. IV.10: Prototype of a filter wheel for NIRSPEC. The wheel was designed computer-aided at the Institute and manufactured online with highest precision using a numerically controlled milling machine.

Staff

In Heidelberg

Director: Henning (Managing Didector), Rix

Scientists: Andersen, Bailer-Jones, Beetz (until 30.4.), Bell (since 1.9.), Birkle, Brandner (since 1.9.), Böhnhardt (since 1.10.), Burkert, Dehnen (until 30.6.), Del Burgo (1.9. until 30.11.), Drepper (1.9. until 31.10.), Feldt, Fried, Gässler (since 1.5.), Graser, Grebel, Haas, Heraudeau (until 30.9.), T. Herbst, Hotzel (until 28.2.), Huisken, Ilgner (1.3. until 30.9.), Jester (until 30.6.), Hippelein, Hofferbert, Klaas, Klahr (since 1.10.), Köhler (since 1.10.), Kranz (until 30.6.), Launhardt (since 1.10.), Leinert, Lemke, Lenzen, Ligori, Marien, Meisenheimer, Mundt, Naab (until 31.10.), Neckel (until 28.2.), Odenkirchen, Phleps, Ragazzoni, Röser, Staude, Stickel, Toth, Vavrek, Weiss (since 1.8.), R. Wolf, S. Wolf (until 31.1.), Wilke

Ph. D. Students: Apai (since 1.6.), Bertschik, Borch, Büchler, Dib, Geyer, Harbeck, Hartung (until 31.5.), Hempel, Jesseit, Khochfar, Kleinheinrich (until 31.3.), Kovács, Kranz (until 15.5.), Krause, Krdzalic (until 28.2.), Lamm, B. Lang (until 30.9.), Maier, Mühlhlbauer, Pascucci (since 1.7.), Przygodda, Puga, Rodmann (since 16.9.), Stolte, Walcher, Weiss (until 31.7.), Umbreit (since 1.4.), Wetzstein, Ziegler (until 30.06.)

Diploma Students and Student Assistants: Birkmann (since 13.5.), Drepper (until 28.2.), Egner, Fassbender (since 13.5.), Häring (since 1.3.), Häußler (since 16.10.), Schartmann (since 16.9.), Tschamber (until 23.4.), Tristram (since 1.12.), Zimer (until 30.6.), Mohr (until 28.2.), Kinder (since 1.9.)

Scientific Services: Bizenberger, Galperine (since 30.6.), Grözinger, Hofferbert, Laun, Mathar, Neumann, Quetz

Computers, Data Processing: Briegel, Helfert (until 30.4.), Hiller, Hippler, von Kuhlmann (von 16.6. until 15.7.), Rauh, Richter (since 1.9.), Storz, Tremmel, Zimmermann

Elektronis: Alter, Becker, Ehret, Grimm, Klein, Mall, Mohr (since 1.3.), Ridinger, Salm, Unser, Wagner, Westermann, Wrhel

Fine Mechanics: Böhm, Haffner (until 30.6.), Heitz, Meister, Meixner, Morr, Pihale, Sauer

Drawing Office: Baumeister, Ebert, Münch, Rohloff

Photo shop: Anders-Özçan

Graphic Artwork: Meißner-Dorn, Weckauf

Library: Dueck

Administration: Apfel, Flock (freigestellt until 31.3.), Gieser, Hartmann (until 30.11.), Heißler, Kellermann, Papousado, Schleich, Voss, Zähringer.

Secretariate: Bohm (since 1.10.), Goldberger (until 30.6.), Janssen-Bennynck, Koltes-Al-Zoubi (since 1.7.), Meng (since 1.7.), Silventoinen (until 31.10.).

Technical Services and Canteen: Behnke, Herz, M. Jung, Lang, Nauss, B. Witzel, F. Witzel, Zergiebel.

Trainees: Feinwerktechnik – Baumgärtner (since 1.9.), Lares (until 21.7.), Maurer, Rosenberger, Sauer, Stadler (since 1.9.), Petri; Konstruktion – Bender

Free Collaborator: Dr. Thomas Bührke

Scholarship Holders: Alvarez (since 1.6.), Butler, Caldwell (until 31.5.), Chesneau, Del Burgo (until 30.9.), Geyer (until 22.5.), Kranz (16.5. until 30.6.), Lee, Masciadri (since 1.9.), Pentericci, Prieto (since 1.9.), Soci (since 11.3.), Trujillo (since 1.9.)

Guests: Ábrahám, Ungarn (Nov./Dez.), Berro, Spanien (Dez.), Bodenheimer, USA (Dez.), Gallagher, USA (März-Juli/Nov.-Dez.), Garcia, Spanien (Feb.), W. Herbst, USA (Juni), Hiroshita, Japan (März), Hozumi. Japan (April-Dez.), Ionita, USA (Sept.), Januzzi, USA (Juni/Juli), Kiss, Ungarn (März), Kimball (Juli/Aug.), Kniazeva, Russland (Mai), Martinez-Delgado, Spanien (Sept.), Meyer, USA (Juli), Makarova, Russland (Nov.), Mellema, Niederlande (Mai/Juni), Melnikov, Usbekistan (Juni-Aug.) Mochizuki, Japan (Mai), Morel, Frankreich (April-Dez.), Morgan, USA (Juni/Juli), Mori, Japan (März) Naab, Deutschland (Nov./Dez.), Ofek, Israel (Juli/Aug.), O'Dell/USA (Jan./Okt.), Osmer, USA (Aug.), Patsis, Griechenland (Juli), Peng, USA (Juni-Juli und Sept.), Pilyugin, Ukraine (Juli/Aug.), Pizagno, USA (Aug), Powell (since Mai), Pramskij (August-Oktober), Pustilnik, Russland (März-April und Juli/Aug.), Rudnick, USA (Jan./Sept.), Schechter, USA (Juli), Schmitt, Deutschland (Okt.), Torres, Spanien (Jan.-März), C. Wolf, England (Sept.), S. Wolf, Deutschland (Okt./Nov.)

Due to regular international meetings at the MPIA further guests stood at the Institute for shorter periods, who are not listed here.

Co-operative Students: Boxermann (since 1.9.), Brunner (until 28.2.), Harth (until 28.2.), Hess (until 15.4.), Mahr (August/September), Wiese (März/April).

Calar Alto/Almeria

Local Directors: Gredel, Vives

Astronomy, Coordination: Thiele, Prada (until 31.7.), Frahm Astronomiy, Night Assistants: Aceituno, Aguirre, Alises, Guijarro, Hoyo, Pedraz

Telescope Techniques: Capel, Cardiel, De Guindos, García, Helmling, Henschke, L. Hernández, Raul López, Morante, Müller, W., Nunez, Parejo, Schachtebeck, Usero, Valverde, Wilhelmi

Technical Services: Aguila, A., Aguila M., Ariza, Barón, Carreno, Dominguez, Gómez, Góngora, Klee, Rosario Lopez, Marquez, Martinez, F. Restoy (until 31.1.), Romero, Saez, Sanchez, Tapia

Administration, Secretariate: M. Hernandez, M. J.Hernandez, M. I. López

Working Groops and Scientific Collaborations

Research Programmes

Brown Dwarfs
D. Apai, I. Pascucci, Th. Henning, W. Brandner. In collaboration with: ESO, Garching, Astrophysikalisches institut und Universitätssternwarte Jena, Thüringer Landessternwarte Tautenburg, University of Hawaii, Observatoire de Grenoble, Ecole Normale Superieure Lyon, University of Berkeley

Palomar 5
M. Odenkirchen, E.K. Grebel, W. Dehnen, H.-W. Rix. In Zusammenarbeit mit: ESO, Garching, Astronomisches Institut Potsdsm, Rensselaer Polytechnic Institute, University Seattle, Washington, Fermilab, Batavia, Yerkes Observatory, Chicago

Molecular Clouds under the Influence of External Radiation
O. Kessel-Deynet, A. Burkert.

Pre-protostellar Cores in Dark Clouds
O. Krause, D. Lemke, U. Klaas, L.V. Toth, M. Haas, M. Stickel, R. Vavrek, K. Wilke, U. Herbstmeier. In collaboration with: University of Helsinki, Finland, ESTEC, the Netherlands, ISO Data Center, Villafranca, Spain

Star Formation in Bright Spiral Galaxies
M. Haas, U. Klaas, D. Lemke. In collaboration with University of Hawaii, Royal Observatory Edinburgh, UK, Service d' Astrophysique Gif-sur-Yvette, France, ESTEC, Netherlands, ISO Data Center, Villafranca, Spain, Said Business School Oxford, UK, Imperial College London, UK, Caltech Pasadena, USA, University of Gainesville, Florida, USA

Exponential Distribution of the Stellar Density in Spiral Galaxies
A. D. Slyz, A. Burkert. In collaboration with University of Oxford, UK

Rotation of the DG Tauri Jet
F. Bacciotti, R. Mundt. In collaboration with: Dublin Institute of Advanced Studies, Irland, Thüringer Landessternwarte, Tautenburg, Landessternwarte Heidelberg

Luminosity Function of Galaxies, as derived from the COMBO-17 Survey
C. Wolf, K. Meisenheimer, H.-W. Rix, A. Borch, M. Kleinheinrich. In collaboration with: Universität Bonn, Imperial College London, UK, University of Oxford, UK

Hα Rotation Curves of Dwarf Galaxies and Dark Matter
E. d'Onghia. In collaboration with: University of Milano, Italy, SISSA/ISAS and Osservatorio di Trieste, Italy, Osservatorio di Brera-Merate, Italy

White Dwarfs and the Dark Matter Halo of the Galaxy
A. Burkert. In collaboration with: Universitat Politecnica de Catalunya, Barcelona

Variations of the Abundance of Elements in the Globular Cluster 47 Tuc
D. Harbeck, E. K. Grebel. In collaboration with: University of Santa Cruz, USA

Deep Studies of M 86 and its Surroundings in the Virgo Cluster
M. Stickel. In collaboration with: University of Ann Arbor, USA, University of Cambridge, UK, Vassar College Poughkeepsie, USA

CADIS
K. Meisenheimer, H. Hippelein, C. Maier, H.-J. Röser, E. Thommes, J. Fried, M. Kümmel, B. v. Kuhlmann, S. Phleps, C. Wolf

COMBO 17
K. Meisenheimer, C. Wolf, H.-W. Rix, A. Borch, M. Kleinheinrich. In collaboration with: Institute of Astronomy, Cambridge, UK, Institute of Astronomy, Edinburgh, UK, Imperial College, London, UK

Instrumental Projects

Adaptive Optics
Stefan Hippler, Markus Feldt, P. Bizenberger, D. Butler, J. Costa, B. Grimm, Th. Henning, U. Neumann, R. Ragazzoni, W. Rix, R.-R. Rohloff, C. Unser and all technical departments of MPIA and Calar Alto Observatory, in collaboration with MPI for extraterrestrial Physics, Garching, ESO, Garching, Osservatorio di Arcetri, Florence, Steward Observatory, Arizona, USA

CONICA
Rainer Lenzen, Becker, A. Böhm, M. Hartung, W. Laun, K. Meixner, Münch, R.-R. Rohloff, C. Storz, K. Wagner in collaboration with MPI for extraterrestrial Physics, Garching

LAICA
Joseph Fried, Karl-Heinz Marien, F. Briegel, B. Grimm, R. Klein, C. Unser, K. Zimmermann

MIDI
C. Leinert, U.Graser, O. Chesneau, B. Grimm, T. M. Herbst, S. Hippler, W. Laun, R. Lenzen, S. Ligori, R. J. Mathar, R. Mundt, U. Neumann, E. Pitz, F. Przygodda, R.-R. Rohloff, P. Schuller, C. Storz, K. Wagner, K. Zimmermann. In collaboration with ESO, Kiepenheuer-Institut für Sonnenphysik, Thüringer Landessternwarte Tautenburg, Astronomisches Institut, Universität Amsterdam, Sterrewacht Leiden/Leiden Observatory, Kapteyn Astronomical Institute, Netherlands Foundation for Research in Astronomy, Observatoire de la Côte d'Azur, Observatoire de Paris, Harvard-Smithsonian Center for Astrophysics, National Radio Astronomy Observatory)

OMEGA 2000
Hermann-Josef Röser, M. Alter, H. Baumeister, P. Bizenberger, A. Böhm, F. Briegel, R. Faßbender, B. Grimm, Z. Kovacs, W. Laun, U. Mall, R.-R. Rohloff, C. Storz, K. Zimmermann

PACS for HERSCHEL
Dietrich Lemke, S. Birkmann, R. Hofferbert, U. Grözinger, U. Klaas, Schmitt, R. Vavrek unter Federführung des MPI für extraterrestrische Physik, Garching. In collaboration with DLR, Berlin, Universität Kaiserslautern

LUCIFER for the LBT
Rainer Lenzen, Tom Herbst, H. Baumeister, P Bizenberger, B. Grimm, W. Laun,, R.-R. Rohloff, W. Xu. Coordination: Landessternwarte Heidelberg

LINC-NIRVANA for the LBT
Tom Herbst, D. Andersen, H. Baumeister, P.Bizenberger, H. Bönhardt, F. Briegel, W. Gässler, W. Laun, S. Ligori, C. Leinert, L. Mohr, R. Ragazzoni, H.-W. Rix, R.-.R Rohloff, R. Soci, R. A. Weiß, W. Xu

ISOPHOT Data Center
Dietrich Lemke, ISOPHOT-PI and the ISO-Group at the MPIA: C. del Burgo Diaz, M. Haas, P. Heraudeau, S. Hotzel, C. Kiss, U. Klaas, O. Krause, M. Stickel, R. Vavrek, K. Wilke

MIRI and NIRSPEC for the NGST
Dietrich Lemke, U. Grözinger, Th. Henning, R. Hofferbert, R.-R. Rohloff, K. Wagner

Collaboration with Industrial Firms

Calar Alto Observatory
DSD Dillinger Stahlbau GmbH, Saarlouis
PEP Modular Computers GmbH, Kaufbeuren
Loedige Gebäude Logistik GmbH, Paderborn
Demag Cranes and Components, S.A., Madrid
Ruetgers GmbH & Co. KG, Mannheim
ERT Refrigeration Technology GmbH, Hamburg

Laica
Filtrop AG, Balzers Liechtenstein
Reichmann Feinoptik, Brokdorf
Fairchild Imaging

Omega 2000
Barr Associates Ltd., USA.
Barr Associates, Inc, USA.
Rockwell Scientific, USA

Midi
AMI Doduco GmbH
AMS, Martinsried
B.E.S.T. Ventile und Fittinge GmbH
Baumer electric, Friedberg
BOC Edwards GmbH
Börsig, Neckarsulm
Bürklin, München
Colder Products GmbH
DNP Industriale SRL, Brugherio, Italien
Cryophysics GmbH, Darmstadt
Cryo-technics, Büttelborn
Danes, Fulda
Deckma, Rosengarten
Drollinger GmbH
Edmond Industrie Optik, Karlsruhe
Faulhaber, Schönaich
Faber Industrietechnik, Mannheim
Ferrofluidics, Nürtingen
Gerwah Präzisions GmbH, Grosswallstadt
Grulms Pneumatik, Grünstadt
Gudeco Elektronik, Neu-Anspach
Gutekunst, Metzingen
GVL Croengineering GmbH
Hommel Werkzeuge, Viernheim
Infrared Labs, Tucson, USA
Infrared Multilayer Laboratory, University of Reading
ISOLOC, Stuttgart
Knürr, Arnstorf
KOBOLD Messring GmbH
Lemo Elektronik, München
Leybold Vakuum GmbH
Linos Photonics, Göttingen
M-Industrieverpackung May
Mankiewicz, Hamburg
Marmor+Granit+Fliesen-Bank, Heidelberg
Melles-Griot, Bensheim
Merck Eurolab, Bruchsal
Metallschleiferei Christoph Höhnen
Möller, Frankfurt
Mörz Metallbearbeitungs GmbH
Mörz, Schallschutztechnik, Neuburg/Kammel
Newport, Darmstadt
OCLI, Santa Rosa, USA
Oxford Instruments, Wiesbaden
Pfeiffer Vacuum GmbH
Phoenix Contact, Blomberg
Physik Instrumente, Karlsruhe
Poligrat GmbH
Polytec, Waldbrunn
Präzisionsoptik Gera, Gera
RET Electronic, Rodgau
RETEC Instrumnents, Idstein
RS Components, Mörfelden
SHI Cryogenics Europe GmbH
Sika, Kaufungen
Sky Blue, München
Talema Elektronik, Germering
Taylor-Hobson, Wiesbaden
Telemeter Electronic, Donauwörth
VSYSTEMS, München
Wiebusch, Volkmarsen
Winkelman Hydraulik, Rödermark
Witzenmann GmbH
Zugck, Kälte-und Klimaanlagen

Prime
Kayser-Threde, Bremen
Focus Software Inc., Tucson, USA

Pacs
ABB Automation Products, Alzenau
Agilent (früher Hewlett-Packard), Böblingen
ANTEC, Kelkheim
Astrium, Friedrichshafen
Buerklin, München
Comtronic GmbH, Heiligkreuzsteinach
Cryophysics GmbH, Darmstadt
CSL, Liege (Belgien)
IMEC Leuven/Belgien
ITT Cannon, Dole Cedex (Frankreich)
Fraunhofer Institut für Betriebsfestigkeit, Darmstadt
Kayser-Threde, München
Kugler GmbH, Salem
Laboratorium für Elektronenmikroskopie Universität Karlsruhe, Karlsruhe
Leybold Vakuum Gmbh, Köln
Messer-Griesheim, Ludwigshafen
Rufenach Vertriebs GmbH, Heidelberg
Sacee International, Maintenon (Frankreich)
Spoerle Electronic, Dreieich
SolidTeam Informationssysteme GmbH, Sottrum
Stöhr Armaturen, Augsburg
Technologica, Sevilla (Spanien)
Trinos Vakuum-Systeme, Göttingen
TU Darmstadt FB Material- und Geowissenschaften Fachgebiet Chemische Analytik, Darmstadt
TU Darmstadt Kompetenzzentrum Materialcharakterisierung, Darmstadt
Vacuumschmelze, Hanau
Zeiss, Oberkochen

CCD Techniques
Analyt-MTC, Mühlheim
Fairchild Imaging Syst., USA
Heraeus, Hanau
ITOS GmbH, Mainz
Marconi Ltd., GB
Micro-Optronic-Messtechnik, Langebrück
Peltron GmbH, Fürth
Roth, Karlsruhe
Schäfter+Kirchhoff, Hamburg
Schott, Mainz
Steward Observatory, Tucson, Arizona, USA
Stöhr Armaturen, Augsburg
Tafelmeier, Rosenheim
Testo, Lenzkirch
WSM Armaturen, Rohrbach

Computer Equipment
asknet, Karlsruhe
Additive, Friedrichsdorf
Bechtle, Heilbronn
Cancom, Frankfurt
Creaso, Gilching
DELL, Langen
Gordion, Troisdorf
INMAC, Mainz
Kippdata, Bonn
Mizzi, Brühl
PROUT, Darmstadt
ProLogic, Wuppertal
PTC, Mannheim
Rufenach, Heidelberg
Schulz, München
Scientific Computers, Aachen
Transtec, Tübingen

Workshops
ABB (ehem. Hartmann + Braun), Alzenau
ADR, Paris
Agilent Technologies, Böblingen
Almet-AMB, Mannheim
Amphenol-Tuchel Electronics, Heilbronn
Angst+Pfister, Mörfelden
APE Elektronik, Kuppenheim
Arthur Henninger, Karlsruhe
Auer Paul GmbH, Mannheim
Baier Digitaldruck, Heidelberg
Barth, Leimen
Bectronic GmbH, Derschen
Best Power Technology, Erlangen
Beta Layout, Arbergen
Binder Magnete, Villingen-Schwenningen
Blaessinger, Stuttgart
Bohnenstiel, Heidelberg
Böllhoff, Winnenden

Börsig, Neckarsulm
Bubenzer Bremsen, Kirchen-Wehrbach
Bürklin, München
C&K Components, Neuried b. München
C.A.P. CNC + Coating Technik, Zell. a. H.
CAB, Karlsruhe
Cadillac-Plastic, Viernheim
Carl Roth, Karlsruhe
Cherry Mikroschalter, Auerbach
Christiani, Konstanz
Coating-Plast, Schriesheim
Com Pro, Stuttgart
Compumess Electronik, Unterschleissheim
Comtronic GmbH, Heiligkreuzsteinach
Conrad Electronic, Hirschau
Cryophysics, Darmstadt
Dannewitz, Linsengericht
Delta, Wuppertal
Deltron Components GmbH, Neuried b. München
DENC, Darmstadt
DMG-Service, Pfronten
Dürkes & Obermayer, Heidelberg
Dyna Systems NCH, Mörfelden-Walldorf
EBARA Pumpen, Dietzenbach
EBJ, Ladenburg
EBV-Electronik, Leonberg
EC Motion, Mönchengladbach
Edsyn Europa, Kreuzwertheim
EFH, Neidenstein
Eldon, Büttelborn
Elna Transformatoren, Sandhausen
elspec, Geretsried
ELV Electronik, Leer
ERNI, Adelberg
eurodis Enatechnik, Quickborn
EWF, Eppingen
Faber, Mannheim
Farben Specht, Bammental
Farnell Electronic Components, Deisenhofen
Farnell Electronic Services, Möglingen
FCT Electronic, München
Fels Spedition, Heidelberg
Fisba, St. Gallen
Fischer Elektronik, Lüdenscheid
FPS-Werkzeugmaschinen GmbH, Otterfing
Franke, Aalen
Fritz Faulhaber, Schönaich
Future Electronics Deutschland, Unterföhring
Ganter, Walldorf
Geier Metalle, Mannheim
GENOMA Normteile, Hameln
GLT, Pforzheim
Gould Nicolet Meßtechnik, Dietzenbach
Grandpair, Heidelberg
Grulms-Pneumatik, Grünstadt
GRW, Würzburg
Gummi Körner, Eppelheim
Gummi-Plast Schild, Gernsheim
Gutekunst, Pfalzgrafenweiler
Häcker, Weinsberg
Häfele Leiterplattentechnik, Schrießheim
Halm+Kolb, Stuttgart
Heidenhain, Traunreut
Helukabel, Hemmingen
Hema, Mannheim
Herz, Leister Geräte, Neuwied
Hewlett-Packard Direkt, Böblingen
Hilger und Kern, Mannheim
Hilma-Römheld GmbH, Hilchenbach
HM Industrieservice, Waghäusel
Hommel-Hercules Werkzeughandel, Viernheim
Hormuth, Heidelberg
Horst Göbel, Ludwigshafen
Horst Pfau, Mannheim
HOT Electronic, Taufkirchen
HTF Elektro, Mannheim
Huber + Suhner, Taufkirchen
Hummer+Rieß, Nürnberg
IBF Mikroelektronik, Oldenburg
Infrared Labs, Tucson, USA
Inkos, Reute/Breisgau
iSystem, Dachau
Jacobi Eloxal, Altlussheim
Jarmyn, Limburg
Joisten+Kettenbaum, Bergisch Gladbach
Kaufmann, Crailsheim
Kerb-Konus-Vertriebs-GmbH, Amberg
Kniel, Karlsruhe
Knürr, München
Lambda Electronics, Achern
Lemo Electronik, München
Lineartechnik Korb, Korb
LPKF CAD/CAM Systeme, Garbsen
Macrotron, München
Mädler, Stuttgart
Mankiewicz, Hamburg
Matsuo Electronics Europe, Eschborn
Matsushita Automation, Holzkirchen
Maxim Ges. f. elektronische integrierte Bausteine, Planegg
Menges electronic, Dortmund
Mentor, Erkrath
Metrofunkkabel-Union, Berlin
Mitsubishi-Electric, Weiterstadt
Mönninghoff, Bochum
MSC Vertriebs-GmbH, Stutensee
MTI, Baden-Baden
Munz, Lohmar
Nanotec, Finsing
Neust Schaltungselektronik, Ehringshausen - Katzenfurt
Newport, Darmstadt
Nickel Schalt- und Meßgeräte, Villingen-Schwenningen
Nies Electronic, Frankfurt
Noor, Viernheim
Nova Electronik, Pulheim
Oberhausen, Ketsch
Otto Faber, Mannheim
Otto Ganter, Furtwangen
OWIS GmbH, Staufen
Parametric Technology, Muenchen
Parcom, CH-Flurlingen
pbe Electronic, Elmshorn
Pfeiffer, Mannheim
Physik Instrumente, Waldbronn
Phytec Meßtechnik, Mainz
Phytron, Gröbenzell
Plastipol, Runkel
Präzisionsoptik Gera, Gera
PSI Tronix, Tulare, California, USA
Püschel Electronik, Mannheim
R.E.D. Regional-Electronic-Distribution, Rodgau-Jügesheim
Räder Gangl, München
Radiall, Rödermark
RALA, Ludwigshafen
Rau-Meßtechnik, Kelkheim
Reeg, Wiesloch
Reinhold Halbeck, Offenhausen
Reith, Mannheim
Retronic, Ronneburg
Riekert & Sprenger, Wertheim
Rittal-Werk, Herborn
Roland Häfele Leiterplattentechnik, Schriesheim
Roth, Karlsruhe
RS Components, Mörfelden-Walldorf
RSP-GmbH, Mannheim
Rudolf, Heidelberg
Rufenach Vertriebs-GmbH, Heidelberg
Rütgers, Mannheim
Rutronik, Ispringen
Sartorius, Ratingen
Sasco, Putzbrunn
Scantec, Planegg
Schaffner Elektronik, Karlsruhe
Schuricht, Fellbach-Schmiden
Schweizer Elektroisolierungsstoffe, Mannheim
SCT Servo Control Technology, Taunusstein
SE Spezial-Electronic, Bückeburg
Seifert mtm Systems, Ennepetal
Siemens IC-Center, Mannheim
Spaeter, Viernheim
Spindler & Hoyer, Göttingen
Spoerle Electronic, Dreieich
Stäubli, Bayreuth
Straschu Leiterplatten, Oldenburg
SUCO-Scheuffele, Bietigheim-Bissingen
Synatron, Hallbergmoos
Tandler, Brauen
THK, Düsseldorf
Thorlabs, Gruenberg
TMS Test- und Meßsysteme, Herxheim/Hayna
Tower Electronic Components, Schriesheim
TreNew Electronic, Pforzheim
TS-Optoelectronic, München
TWK-Elektronik, Karlsruhe
Vacuumschmelze, Hanau
VBE Baustoff+Eisen, Heidelberg
Vero Electronics, Bremen
VISION Engineering, Emmering
W. & W. Schenk, Maulbronn
WIKA, Klingenberg
Wikotec, Bramsche
Wilhelm Gassert, Schriesheim
Witter GmbH, Heidelberg
WS CAD Electronik, Berk Kirchen

Teaching Activities

Summer Term 2002

M. Haas: Far Infrared Astronomy (Lecture)

H. P. Gail, Chr. Leinert, D. Lemke, R. Mundt: Introduction into Astronomy and Astrophysics III (Seminar)

K. Meisenheimer, H.-J. Röser: Why are there Elliptical and Spiral Galaxies? (Seminar)

A. Burkert, B. Fuchs, A. Just, H. W. Rix, R. Spurzem, R. Wielen: Stellar Dynamics (Seminar)

The Astronomy Lecturers: Astronomical Colloquium

Winter Term 2002/2003

J. Krautter, D. Lemke, H. -J. Röser: : Introduction into Astronomy and Astrophysics III (Seminar)

A. Burkert, B. Fuchs, A. Just, H.-W. Rix, R. Spurzem, R. Wielen: Structure and Kinematics of Stellar Systems (Seminar)

H. P. Gail, Th. Henning, D. Lattard, M. Trieloff, W. M. Tscharnuter: Astromineralogy (Seminar)

J. G. Kirk, K. Meisenheimer, S. Wagner: Particle Acceleration and radiation Processes in Radio Galaxies (Seminar)

M. Haas: Präsentations – How to improve my lectures, papers, posters and (observing) proposals (Seminar)

The Astronomy Lecturers: Astronomical Colloquium

Organization of Conferences

E. K. Grebel: SDSS Spring Collaboration Meeting, MPIA, March 21. – 23.

H.-W. Rix: Workshop on Gravitational Lenses, Schloss Ringberg, July 15. – 19.

E. K. Grebel: Workshop on Chemical Evolution of Dwarf Galaxies – Present Statuts and Perspectives, Schloss Ringberg, Juy, 28. – August, 2.

A. Burkert: Workshop on Centers of Galaxies, chloss Ringberg, November, 10. – 15.

S. Hippler: Workshop and General Meeting of the EU Research and Training Network (RTN) – Adaptive Optics for Extremely Large Telescopes, Heidelberg, December.

Contributions to Conferences, Scientific and Public Lectures

C. Bailer-Jones: National Astronomy Meeting, Bristol (UK), April.(invited lecture); GAIA Photometry. Tartu, Estonia. Juli. (lecture); »GAIA Spectroscopy – Science and Technology«, Gressoney St. Jean, Italy, September (invited lecture); Astronomische Gesellschaft, Berlin, September (lecture); GAIA Classification Working Group Meeting. Heidelberg, December

E. F. Bell: Spectroscopic and Imaging Surveys for Cosmology Kick-off Meeting, University of Durham (UK), October

K. Birkle: Planetarium Mannheim. December (public lecture)

A. Burkert: University of Arizona, Tuscon, Kolloquium, März; III. Euroconference on Galaxy Evolution, Kiel. Juli; Univ ersity of California, Santa Cruz, August (colloquium); Conference on Galaxies and Chaos, Athen, Griechenland, September (invited lecture); Carnegie Centennial Symposium »Black Holes and Galaxies«, October, (invited review); TU Darmstadt, Colloquium, December

C. del Burgo: Conference »Exploiting the ISO Data Archive: Infrared Astronomy in the Internet Age«, Sigüenza, Spain, June: (lecture and poster)

E. K. Grebel: Colloquium, Ludwig-Maximilian-Universität München, January, Kernphysikalisches Seminar, Forschungszentrum, Karlsruhe, January; Colloquium Universität Basel, January; Astronomisches Kolloquium, Astronomische Institute der Universität Bonn, Februar; Hubble Science Legacy Tagung, Chicago (USA), April.

(invited review); Jahrestagung der Gleichstellungsbeauftragten der MPG, Mühlheim. April (lecture); Physikalisches Kolloquium, Universität Tübingen,. April; Hubble Science Legacy Tagung, Chicago (USA), April. (invited review); Jahrestagung der Gleichstellungsbeauftragten der MPG, Mühlheim. April (lecture); Physikalisches Kolloquium, Universität Tübingen,. April; 200th American Astronomical Society Meeting, Albuquerque (USA), Juni (lecture); Frontiers of Science, Irvine (USA), Juni: E. K. Grebel (invited review); III. Euroconference on Galaxy Evolution, Kiel. July (invited review); Astrophysikalisches Seminar, Astronomische Institute der Universität Bonn. October; Working Group for Relativistic Reference Frames for GAIA. Liège (Belgium). November: (lecture); GAIA Classification Working Group Meeting. Heidelberg, December

R. Gredel: Science with the GTC, Granada (Spain). February; LBT SAC Meeting, Bologna, May. (lecture); Spanish Astronomical Society, Toledo, Spain. August (lecture); SPIE Conference »Astronomical Telescopes and Instrumentation«, Waikoloa (Hawaii) August (lecture); NEON Sommer School, Asiago, September (lectures); OPTICON Board Meeting, Paris, September; Opticon Working Groop med-sized tels, Cambridge, UK, November

M. Haas: Conference »Exploiting the ISO Data Archive: Infrared Astronomy in the Internet Age«, Sigüenza, Spanien, Juni (invited lecture); Forum Astronomie, Bonn, December: (invited lecture)

D. Harbeck: SDSS Winter Workshop on Galaxy Spectra, Tucson, Arizona, Januar; SDSS Spring Collaboration Meeting, Heidelberg, March; Ringberg Workshop on the Chemical Evolution of Dwarf Galaxies. Schloss Ringberg, Tegernsee, July; CNO in the Universe. Conference , St. Luc, Switzerland, September

Th. Henning: University of Texas, Austin USA, März (Colloquium); Electromagnetic Light Scattering, Gainsville, Florida, USA, März (invited lecture); Max-Planck-Institut für Kernphysik, Heidelberg, April (Colloquium in Honour of E. Grün); Konference »Interaction of Starts with their Environment II«, Budapest, May: (invited lecture); Cornell University, Ithaka, USA, May (Colloquium); Laboratory Astrophysics Workshop, NASA Ames, USA, May (invited lecture); »Chemistry as a Diagnostic of Star Formation«, Waterloo, Canada, August (invited lecture)

S. Hippler SPIE Conference »Astronomical Telescopes and Instrumentation«, Waikoloa (Hawaii), August: (Poster); Mid-Term review des AO-ELT Research and Training Network. Marseille, October (invited lecture)

P. Héraudeau: Konference »Exploiting the ISO Data Archive: Infrared Astronomy in the Internet Age«, Sigüenza, Spanien, June (Poster)

U. Klaas: Konference »Exploiting the ISO Data Archive: Infrared Astronomy in the Internet Age«, Sigüenza, Spain, June (lecture); Meeting of the Astronomische Gesellschaft, Berlin, September: (Highlight Lecture); Konkoly Observatory, Budapest, October: (lecture); Rutherford Appleton Laboratory, Chilton, Dezember (lecture)

O. Krause: IAOC Workshop on »Star formation across the stellar mass spectrum«, La Serena, Chile, März: (lecture); Konference »Interaction of Starts with their Environment II«, Budapest, May: (Poster); Konference »Exploiting the ISO Data Archive: Infrared Astronomy in the Internet Age« , Sigüenza, Spanien, June (two Posters)

Ch. Leinert: SPIE Conference »Astronomical Telescopes and Instrumentation«, Waikoloa (Hawaii), August; JENAM, Porto (Portugal), September (invited lecture)

D. Lemke: Conference »Exploiting the ISO Data Archive: Infrared Astronomy in the Internet Age«, Sigüenza, Spanien, June; SPIE Conference »Astronomical Telescopes and Instrumentation« Waikoloa (Hawaii), August. (Poster)

H. Lee: Ringberg Workshop on the Chemical Evolution of Dwarf Galaxies. Schloss Ringberg, Tegernsee, July: (invited lecture); Astronomisches Institut, Ruhr-Universität Bochum. July. (invited lecture); ESO, Garching, August (invited lecture)

G. Mühlbauer Astronomische Schwerpunkte am MPIA – Instrumentierung und Forschung, MPIA, April: (lecture, Schiller International University Seminar)

L. Pentericci Galaxy Evolution: Theory and Observations. Cozumel (Mexico). April. (Poster); VII. Congresso Nazionale di Cosmologia. Rom (Italien). November (lecture); Radio Galaxies: Past, Present and Future. Leiden (Netherlands), November

M. Odenkirchen: SDSS Spring Collaboration Meeting, Heidelberg, März (lecture); 200th American Astronomical Society Meeting, Albuquerque (USA), June (Poster and Press conference); Conferenzce »New Horizons in Globular Cluster Astronomy«, Padua, June (Poster); Herbsttagung der Astronomischen Gesellschaft, Berlin, September: (Poster)

A. M. Quetz: Formation of Stars and Planets, MPIA, April (Conference, Schiller International University Seminar); Formation of Planetary Systems, Fachhochschule Zweibrücken, October (public lecture)

H.-W. Rix: The Very Large Telescope, Steward Observatory, Tuscon, USA, January: (public lecture); »Rotation Curves of SDSS Galaxies«, SDSS-Workshop, MPIA, Heidelberg, March; Das Bild des Kosmos, Universität Leipzig, April (Ringvorlesung); Physikalisches Kolloquium der Universität Jena, Mai (invited lecture); Galaxy Surveys, IAP, Paris, Junev(lecture); University of Leiden, Niederlande, Juli (invited lecture); (SPIE Conference, Science with the VLT, Waikoloa, Hawaii, August (Vortrag); »Die Entstehung von Galaxien und die Struktur des Universums«, 122. Versammlung der GDNÄ, Halle, September (invited lecture); Tidal Tales from the Sloan Digital Sky Survey, MPAE Kolloquium, Oktober (invited lecture); From WFI to HST: Galaxy Evolution with 2m Telescope, ESO Kolloquium, Garching, November (invited lecture)

H.-J. Röser NEON Sommerschool. Asiago, September: (lectures)

J. Staude: The Formation of Stars and Planets – School Lectures in Dresden (April), Halle and Dessau (June)

M. Stickel: Ringberg Workshop on the Virgo Cluster, Ringberg, April (lecture); Conference »Exploiting the ISO Data Archive: Infrared Astronomy in the Internet Age«, Sigüenza, Spain, Junie (invited lecture and Poster); SPIE Conference »Astronomical Telescopes and Instrumentation«, Waikoloa (Hawaii), August: (lecture); »The IGM/Galaxy Connection – The Distribution of Baryons at $z = 0$«, Boulder, Colorado, August (lecture)

A. Stolte: Euro Winterschool on »Observing with the VLTI«, Les Houches, France, February: (Poster); IAOC Workshop on Star formation across the stellar mass spectrum«, La Serena, Chile, März (lecture)

L. V. T'oth: Conferenz »Interaction of Starts with their Einvironment II«, Budapest, Mai: (Vortrag); Workshop »Super Shells and their Relationship with Massive Star Formation«, Nagoya, Japan, Juni (invited lecture)

K. Wilke: Konference »Exploiting the ISO Data Archive: Infrared Astronomy in the Internet Age«, Sigüenza, Spain, June: (lecture)

Service in Committees

C. Bailer-Jones: Member of the ESA Advisory Board for the development of the GAIA Satellite, menber of the GAIA Science Team, Chairman of the GAIA Working Groop »Classification«

A. Burkert: Chairman of the Mitarbeitervertreter der CPTS, Coordinator of the international Network »Planets« (founded november 1, 2002), Co-author of the Denkschrift Astronomie.

E. K. Grebel: member of the Student Selection committee at MPIA (until Oct. 2002), member of the PhD Advisory Council (PAC) at MPIA, member of the WBK at MPIA, Gleichstellungsbeauftragte at MPIA (until Juli 2002), Vice president of the Scientific Ernst Patzer Foundation, representative of the MPIA in the Collaboration Council of the Sloan Digital Sky Survey.

R. Gredel: member of the Calar Alto Program Committee, member of the OPTICON Working Groop »Future of medium-sized Telescopes«

Th. Henning: member of the DLR expert committee »Extraterrestrische Grundlagenforschung«, member of the Organizing Committee of the IAU Commission »Interstellar Matter«, member of the IAU working groop »Star Formation«, member of the ESO VLT Instrument Science Team for VISIR, member of the SOFIA Science Steering Committee, german representative in the Scientific Technical Committee of ESO, member of the ESO VLTI Steering Committee, DFG expert for Astronomy/Astrophysics, member of the Astronomy Working Group of ESA, member of the European ALMA Board, member of the Deutschen Akademie der Naturforscher Leopoldina, membero of the Scientific Oversight Committee of the Kiepenheuer Institut für Sonnenphysik, Freiburg.

U. Klaas: Co-Investigator of the ISOPHOT Consortium, Member of the ISO Active Archive Phase Coordination Committee, Co-Investigator of the HERSCHEL-PACS Consortium, member of the der HERSCHEL Calibration Steering Group

Chr. Leinert: Member of the ESO Working groop »Science Demonstration Time« for the VLTI, member of the »Working Group on Optical/IR Interferometry« in the Division IX of the IAU.

D. Lemke: Principal Investigator of the ISOPHOT Consortium, Co-Investigator in the HERSCHEL-PACS Consortium, Co-Investigator at NGST-MIRI, member of the expert committee Verbundforschung Astronomie, MPIA coordinator in the POE Network

M. Odenkirchen: member of the Calar Alto Program Committee

H.-W. Rix: member of the Scientific Oversight Committee at the Astrophysikalisches Institut Potsdam (AIP), member of the ESA Astronomy Working Group (AWG), member of the Board of the Large Binocular Telescope Corporation (LBTC), Chairman of the Board of the Large Binocular Telescope Beteiligungsgesellschaft (LBTB), member of the Board of OPTICON, member of the VLTI Steering Committee

H.-J. Röser: Secretary of the Calar Alto Program Committee, alo in charge of the allocation of MPG share of observing time at the 2.2 m Telescope on La Silla (together with R. Lenzen)

J. Staude: Member of the Jury for the national contest »Jugend forscht«

Publications

In Journals with Referee System:

Apai, D., Pascucci, I., Henning, T., Sterzik, M. F., Klein, R., Semenov, D., Günther, E. and Stecklum, B.: Probing Dust around Brown Dwarfs: The Naked LP 944-20 and the Disk of Chamaeleon Ha2. Astrophysical Journal 573 (2002), 115-117

Bacciotti, F., Ray, T. P., Mundt, R., Eislöffel, J. and Solf, J.: Hubble Space Telescope/STIS Spectroscopy of the Optical Outflow from DG Tauri: Indications for Rotation in the Initial Jet Channel. Astrophysical Journal 576 (2002), 222-231

Bailer-Jones, C. A. L.: Dust clouds or magnetic spots? Exploring the atmospheres of L dwarfs with time-resolved spectrophotometry. Astronomy and Astrophysics 389 (2002), 963-976

Bailer-Jones, C. A. L.: Determination of Stellar Parameters with GAIA. Astrophysics and Space Science 280 (2002), 21-29

Barrado y Navascués, D., Zapatero Osorio, M. R., Martín, E. L., Béjar, V. J. S., Rebolo, R. and Mundt, R.: Discovery of a very cool object with extraordinarily strong H-alpha emission. In: Astronomy and Astrophysics Letters 393 (2002), 85.

Barucci, A., Boehnhardt, H., Dotto, E., Doressoundiram, A., Romon, J., Lazzarin, M., Fornasier, S., de Berg, C., Tozzi, G. P., Delsanti, A., Hainaut, O., Barrera, L., Birkle, K., Meech, K., Ortiz, J. L., Sekiguchi, T., Thomas, N., Watanabe, J., West, R. M. and Davies, J. K.: Visible and near-infrared spectroscopy of the Centaur 32532 (2001 PT13). Astronomy and Astrophysics 392 (2002), 335-339

Bendo, G. J., Joseph, R. D., Wells, M., Gallais, P., Haas, M., Heras, A. M., Klaas, U., Laureijs, R. J., Leech, K., Lemke, D., Metcalfe, L., Rowan-Robinson, M., Schulz, B. and Telesco, C.: Dust Temperature in the Infrared Space Observatory Atlas of Bright Spiral Galaxies. Astronomical Journal 124 (2002), 1380-1392

Bendo, G. J., Joseph, R. D., Wells, M., Gallais, P., Haas, M., Heras, A. M., Klaas, U., Laureijs, R. J., Leech, K., Lemke, D., Metcalfe, L., Rowan-Robinson, M., Schulz, B. and Telesco, C.: An Infrared Space Observatory Atlas of Bright Spiral Galaxies. Astronomical Journal 123 (2002), 3067-3107

Bertschik, M. and Burkert, A.: Minor Mergers of Galaxies: Theory and Observations. Astrophysics and Space Science 281 (2002), 405-406

Boehnhardt, H., Delsanti, A., Barucci, A., Hainaut, O., Doressoundiram, A., Lazzarin, M., Barrera, L., de Bergh, C., Birkle, K., Dotto, E., Meech, K., Ortiz, J. E., Romon, J., Sekiguchi, T., Thomas, N., Tozzi, G. P., Watanabe, J., West, R. M.: ESO large program on physical studies of Transneptunian Object and Centaurs: Visible photometry. Astronomy and Astrophysics 395 (2002), 297-303

Böker, T., Laine, S., van der Marel, R. P., Sarzi, M., Rix, H.-W., Ho, L. C. and Shields, J. C.: A Hubble Space Telescope Census of Nuclear Star Clusters in Late-Type Spiral Galaxies. I. Observations and Image Analysis. Astronomical Journal 123 (2002), 1389-1410

Carilli, C. L., Harris, D. E., Pentericci, L., Röttgering, H. J. A., Miley, G. K., Kurk, J. D. and van Breugel, W.: The X-Ray-Radio Alignment in the z = 2.2 Radio Galaxy PKS 1138-262. Astrophysical Journal 567 (2002), 781-789

Chesneau, O. and Moffat, A. F. J.: Detecting Magnetic Fields in Rotationally Perturbed, Hot Stellar Winds. Publications of the Astronomical Society of the Pacific 114 (2002), 612-622

Dessart, L. and Chesneau, O.: Interferometric and spectroscopic monitoring of emission lines. Detection of CIRs in hot star winds. Astronomy and Astrophysics 395 (2002), 209-221

Dieball, A., Müller, H. and Grebel, E. K.: A statistical study of binary and multiple clusters in the LMC. Astronomy and Astrophysics 391 (2002), 547-564

Dieball, A., Mueller, H. and Grebel, E. K.: Binary and multiple clusters in the LMC (Dieball+, 2002). VizieR Online Data Catalog 339 (2002), 10547

Efremov, Y. N., Pustilnik, S. A., Kniazev, A. Y., Elmegreen, B. G., Larsen, S. S., Alfaro, E. J., Hodge, P. W., Pramsky, A. G. and Richtler, T.: 6-m telescope spectroscopic observations of the bubble complex in NGC 6946. Astronomy and Astrophysics 389 (2002), 855-870

Fan, X., Narayanan, V. K., Strauss, M. A., White, R. L., Becker, R. H., Pentericci, L. and Rix, H.-W.: Evolution of the Ionizing Background and the Epoch of Reionization from the Spectra of $z \sim 6$ Quasars. The Astronomical Journal 123 (2002), 1247-1257

Gray, M. E., Taylor, A. N., Meisenheimer, K., Dye, S., Wolf, C. and Thommes, E.: Probing the Distribution of Dark Matter in the A901/902 Supercluster with Weak Lensing. Astrophysical Journal 568 (2002), 141-162

Gutiérrez, C., López-Corredoira, M., Prada, F. and Eliche, M. C.: New Light and Shadows on Stephan's Quintet. Astrophysical Journal 579 (2002), 592-599

Gürtler, J., Klaas, U., Henning, T., Ábrahám, P., Lemke, D., Schreyer, K. and Lehmann, K.: Detection of Solid Ammonia, Methanol, and Methane with ISOPHOT. Astronomy and Astrophysics 390 (2002), 1075-1087

Haas, M., Klaas, U. and Bianchi, S.: The relation of PAH strength with cold dust in galaxies. Astronomy and Astrophysics 385 (2002), L23-L26

Hall, P. B., Anderson, S. F., Strauss, M. A., York, D. G., Richards, G. T., Fan, X., Knapp, G. R., Schneider, D. P., Vanden Berk, D. E., Geballe, T. R., Bauer, A. E., Becker, R. H., Davis, M., Rix, H.-W., Nichol, R. C., Bahcall, N. A., Brinkmann, J., Brunner, R., Connolly, A. J., Csabai, I., Doi, M., Fukugita, M., Gunn, J. E., Haiman, Z., Harvanek, M., Heckman, T. M., Hennessy, G. S., Inada, N., Ivezic, Z., Johnston, D., Kleinman, S., Krolik, J. H., Krzesinski, J., Kunszt, P. Z., Lamb, D. Q., Long, D. C., Lupton, R. H., Miknaitis, G., Munn, J. A., Narayanan, V. K., Neilsen, E., Newman, P. R., Nitta, A., Okamura, S., Pentericci, L., Pier, J. R., Schlegel, D. J., Snedden, S., Szalay, A. S., Thakar, A. R., Tsvetanov, Z., White, R. L.

and Zheng, W.: Unusual Broad Absorption Line Quasars from the Sloan Digital Sky Survey. Astrophysical Journal Supplement Series 141 (2002), 267-309

Handler, G., Weiss, W. W., Paunzen, E., Shobbrook, R. R., Garrido, R., Guzik, J. A., Hempel, A., Moalusi, M. B., Beach, T. E., Medupe, R., Chagnon, F., Matthews, J. M., Reegen, P. and Granzer, T.: The pulsational behaviour of the rapidly oscillating Ap star HD 122970 during two photometric multisite campaigns. Monthly Notices of the Royal Astronomical Society 330 (2002), 153-159

Hayward, S. A., Kim, S.-W. and Lee, H.: Dilatonic wormholes: Construction, operation, maintenance, and collapse to black holes. Physical Review D 65 (2002), 4003

Herbst, W., Hamilton, C. M., Vrba, F. J., Ibrahimov, M. A., Bailer-Jones, C. A. L., Mundt, R., Lamm, M., Mazeh, T., Webster, Z. T., Haisch, K. E., Williams, E. C., Rhodes, A. H., Balonek, T. J., Scholz, A. and Riffeser, A.: Fine Structure in the Circumstellar Environment of a Young, Solar-like Star: The Unique Eclipses of KH 15D. Publications of the Astronomical Society of the Pacific 114 (2002), 1167-1172

Herbst, W., Bailer-Jones, C. A. L., Mundt, R., Meisenheimer, K. and Wackerman, R.: Stellar rotation and variability in the Orion nebula clusters. Astronomy and Astrophysics 396 (2002), 513.

Ho, L. C., Sarzi, M., Rix, H.-W., Shields, J. C., Rudnick, G., Filippenko, A. V. and Barth, A. J.: An Efficient Strategy to Select Targets for Gasdynamical Measurements of Black Hole Masses Using the Hubble Space Telescope. Publications of the Astronomical Society of the Pacific 114 (2002), 137-143

Hotzel, S., Harju, J., Juvela, M., Mattila, K. and Haikala, L. K.: $C^{18}O$ abundance in the nearby globule Barnard 68. Astronomy and Astrophysics 391 (2002), 275-285

Hujeirat, A., Camenzind, M. and Burkert, A.: Comptonization and synchrotron emission in 2D accretion flows. I. A new numerical solver for the Kompaneets equation. Astronomy and Astrophysics 386 (2002), 757-762

Hujeirat, A., Camenzind, M. and Livio, M.: Ion-dominated plasma and the origin of jets in quasars. Astronomy and Astrophysics 394 (2002), L9-L13

Jesseit, R., Naab, T. and Burkert, A.: The Validity of the Adiabatic Contraction Approximation for Dark Matter Halos. Astrophysical Journal 571 (2002), L89-L92

Jester, S., Röser, H.-J., Meisenheimer, K. and Perley, R. A.: X-rays from the jet in 3C 273: Clues from the radio-optical spectra. Astronomy and Astrophysics 385 (2002), L27-L30

Juvela, M., Mattila, K., Lehtinen, K., Lemke, D., Laureijs, R. and Prusti, T.: Far-infrared and molecular line observations of Lynds 183 – Studies of cold gas and dust. Astronomy and Astrophysics 382 (2002), 583-599

Karachentsev, I. D., Sharina, M. E., Makarov, D. I., Dolphin, A. E., Grebel, E. K., Geisler, D., Guhathakurta, P., Hodge, P. W., Karachentseva, V. E., Sarajedini, A. and Seitzer, P.: The very local Hubble flow. Astronomy and Astrophysics 389 (2002), 812-824

Karachentsev, I. D., Sharina, M. E., Dolphin, A. E., Grebel, E. K., Geisler, D., Guhathakurta, P., Hodge, P. W., Karachentseva, V. E., Sarajedini, A. and Seitzer, P.: New distances to galaxies in the Centaurus A group. Astronomy and Astrophysics 385 (2002), 21-31

Karachentsev, I. D., Dolphin, A. E., Geisler, D., Grebel, E. K., Guhathakurta, P., Hodge, P. W., Karachentseva, V. E., Sarajedini, A., Seitzer, P. and Sharina, M. E.: The M 81 group of galaxies: New distances, kinematics and structure. Astronomy and Astrophysics 383 (2002), 125-136

Kasper, M. E., Feldt, M., Herbst, T. M., Hippler, S., Ott, T. and Tacconi-Garman, L. E.: Spatially Resolved Imaging Spectroscopy of T Tauri. Astrophysical Journal 568 (2002), 267-272

Kaufmann, P., Raulin, J.-P., Melo, A. M., Correia, E., Costa, J. E. R., de Castro, C. G. G., Silva, A. V. R., Yoshimori, M., Hudson, H. S., Gan, W. Q., Gary, D. E., Gallagher, P. T., Levato, H., Marun, A. and Rovira, M.: Solar Submillimeter and Gamma-Ray Burst Emission. Astrophysical Journal 574 (2002), 1059-1065

Keller, L. P., Hony, S., Bradley, J. P., Molster, F. J., Waters, L. B. F. M., Bouwman, J., de Koter, A., Brownlee, D. E., Flynn, G. J., Henning, T. and Mutschke, H.: Identification of Iron Sulphide Grains in Protoplanetary Disks. Nature 417 (2002), 148-150

Kemper, F., Jäger, C., Waters, L. B. F. M., Henning, T., Molster, F. J., Barlow, M. J., Lim, T. and de Koter, A.: Detection of carbonates in dust shells around evolved stars. Nature 415 (2002), 295-297

Kim, E., Einsel, C., Lee, H. M., Spurzem, R. and Lee, M. G.: Dynamical evolution of rotating stellar systems , II. Post-collapse, equal-mass system. Monthly Notices of the Royal Astronomical Society 334 (2002), 310-322

Kim, J. E. and Lee, H. M.: ZN orbifold compactifications in AdS6 with a Gauss-Bonnet term. Physical Review D 65 (2002), 6008

Kiss, C. and T'oth, L. V.: Cold Cores of the Cepheus Flare Region. PADEU 12 (2002), 85.

Klaas, U. and Walker, H. J.: ISOPHOT far-infrared photometry of NGC 3079. Astronomy and Astrophysics 391 (2002), 911-915

Koch, A. and Edvardsson, B.: Europium abundances in F and G disk dwarfs. Astronomy and Astrophysics 381 (2002), 500-506

Koch-Miramond, L., Haas, M., Pantin, E., Podsiadlowski, P., Naylor, T. and Sauvage, M.: Determination of limits on disc masses around six pulsars at 15 and 90 μm. Astronomy and Astrophysics 387 (2002), 233-239

Koehler, R. and Petr-Gotzens, M. G.: Close binaries in the Eta Chamaeleontis cluster. Astronomical Journal 124 (2002), 2899-2904

Launhardt, R., Zylka, R., and Mezger, P. G.: The nuclear bulge of the Galaxy. III. Large-scale physical characteristics of stars and interstellar matter. Astronomy and Astrophysics 384 (2002), 112-139

Leh'ar, J., Falco, E. E., Kochanek, C. S., McLeod, B. A., Munoz, J. A., Impey, C. D., Rix, H-W., Keeton, C. R. and Peng, D. C. Y.: Erratum: »Hubble Space Telescope Observations of 10 Two-Image Gravitational Lenses«. Astrophysical Journal 571 (2002), 1021-1021

Leinert, C., Ábrahám, P., Acosta-Pulido, J., Lemke, D. and

Siebenmorgen, R.: Mid-infrared spectrum of the Zodiacal light observed with ISOPHOT. Astronomy and Astrophysics 393 (2002), 1073-1079

Makarova, L. N., Karachentsev, I. D., Grebel, E. K. and Barsunova, O. Y.: Surface photometry of new nearby dwarf galaxies. Astronomy and Astrophysics 384 (2002), 72-80

Makhmutov, V. S., Kaufmann, P., Costa, J. E. R., Lagrotta, P. R., Magun, A., Arzner, K., Bazilevskaya, G. A. and Shea, M. A.: Great solar bursts of October 19, 22 and 23, 1989. Advances in Space Research 29 (2002), 2101-2104

Marchesini, D., D'Onghia, E., Chincarini, G., Firmani, C., Conconi, P., Molinari, E. and Zacchei, A.: Ha-alpha Rotation Curves: The Soft Core Question. Astrophysical Journal 575 (2002), 801-813.

Markwick, A. J., Ilgner, M., Millar, T. J. and Henning, T.: Molecular distributions in the inner regions of protostellar disks. Astronomy and Astrophysics 385 (2002), 632-646

McKay, T. A., Sheldon, E. S., Johnston, D., Grebel, E. K., Prada, F., Rix, H.-W., Bahcall, N. A., Brinkmann, J., Csabai, I., Fukugita, M., Lamb, D. Q. and York, D. G.: Dynamical Confirmation of Sloan Digital Sky Survey Weak-lensing Scaling Laws. Astrophysical Journal 571 (2002), L85-L88

Meusinger, H., Scholz, R.-D., Irwin, M. and Lehmann, H.: QSOs from the variability and proper motion survey in the M3 field. Astronomy and Astrophysics 392 (2002), 851-863

Meusinger, H. and Brunzendorf, J.: A QSO survey via optical variability and zero proper motion in the M 92 field. II. Narrow emission line galaxies. Astronomy and Astrophysics 390 (2002), 879-890

Miceli, A., Lamb, D. Q., Zucker, D., Covey, K., Dembicky, J. and Hastings, N. C.: GRB 020531 – optical observations. GRB Circular Network 1416 (2002), 1

Moffat, A. F. J., Corcoran, M. F., Stevens, I. R., Skalkowski, G., Marchenko, S. V., Mücke, A., Ptak, A., Koribalski, B. S., Brenneman, L., Mushotzky, R., Pittard, J. M., Pollock, A. M. T. and Brandner, W.: Galactic Starburst NGC 3603 from X-Rays to Radio. Astrophysical Journal 573 (2002), 191-198

Müller, T. G., Hotzel, S. and Stickel, M.: Solar system objects in the ISOPHOT 170 μm serendipity survey. Astronomy and Astrophysics 389 (2002), 665-679

Nedialkov, P., Orio, M., Birkle, K., Conselice, C., Della Valle, M., Greiner, J., Magnier, E. and Tikhonov, N. A.: First Optical Identification of a Supersoft X-ray Source in M 31. Astronomy and Astrophysics 389 (2002), 339-345

Neuhäuser, R., Guenther, E. W., Alves, J., Grosso, N., Leinert, C., Ratzka, T., Ott, T., Mugrauer, M., Comeron, F., Eckart, A. and Brandner, W.: Deep infrared imaging and spectroscopy of the nearby late M-dwarf DENIS-P J104814-395606. Astronomische Nachrichten 323 (2002), 447-452

Neuhäuser, R., Brandner, W., Alves, J., Joergens, V. and Comerón, F.: HST, VLT, and NTT imaging search for wide companions to bona-fide and candidate brown dwarfs in the Cha I dark cloud. Astronomy and Astrophysics 384 (2002), 999-1011

Newberg, H. J., Yanny, B., Rockosi, C., Grebel, E. K., Rix, H.-W., Brinkmann, J., Csabai, I., Hennessy, G., Hindsley, R. B., Ibata, R., Ivezic, Z., Lamb, D., Nash, E. T., Odenkirchen, M., Rave, H. A., Schneider, D. P., Smith, J. A., Stolte, A., York, D. G., Stoughton, C., Lupton, R. H., Bernardi, M., Blanton, M. R., Burles, S., Castander, F. J., Connolly, A. J., Eisenstein, D. J., Frieman, J. A., Hennessy, G. S., Kent, S., Kunszt, P. Z., Lee, B. C., Meiksin, A., Munn, J. A., Newberg, H. J., Nichol, R. C., Nicinski, T., Pier, J. R., Richards, G. T., Richmond, M. W., Schlegel, D. J., Strauss, M. A., SubbaRao, M., Szalay, A. S., Thakar, A. R., Tucker, D. L., Vanden Berk, D. E., Adelman, J. K., Anderson, J. E., Jr., Anderson, S. F., Annis, J., Bahcall, N. A., Bakken, J. A., Bartelmann, M., Bastian, S., Bauer, A., Berman, E., Böhringer, H., Boroski, W. N., Bracker, S., Briegel, C., Briggs, J. W., Brinkmann, J., Brunner, R., Carey, L., Carr, M. A., Chen, B., Christian, D., Colestock, P. L., Crocker, J. H., Csabai, I., Czarapata, P. C., Dalcanton, J., Davidsen, A. F., Davis, J. E., Dehnen, W., Dodelson, S., Doi, M., Dombeck, T., Donahue, M., Ellman, N., Elms, B. R., Evans, M. L., Eyer, L., Fan, X., Federwitz, G. R., Friedman, S., Fukugita, M., Gal, R., Gillespie, B., Glazebrook, K., Gray, J., Greenawalt, B., Greene, G., Gunn, J. E., de Haas, E., Haiman, Z., Haldeman, M., Hall, P. B., Hamabe, M., Hansen, B., Harris, F. H., Harris, H., Harvanek, M., Hawley, S. L., Hayes, J. J. E., Heckman, T. M., Helmi, A., Henden, A., Hogan, C. J., Hogg, D. W., Holmgren, D. J., Holtzman, J., Huang, C.-H., Hull, C., Ichikawa, S.-I., Ichikawa, T., Johnston, D. E., Kauffmann, G., Kim, R. S. J., Kimball, T., Kinney, E., Klaene, M., Kleinman, S. J., Klypin, A., Knapp, G. R., Korienek, J., Krolik, J., Kron, R. G., Krzesinski, J., Lamb, D. Q., Leger, R. F., Limmongkol, S., Lindenmeyer, C., Long, D. C., Loomis, C., Loveday, J., MacKinnon, B., Mannery, E. J., Mantsch, P. M., Margon, B., McGehee, P., McKay, T. A., McLean, B., Menou, K., Merelli, A., Mo, H. J., Monet, D. G., Nakamura, O., Narayanan, V. K., Nash, T., Neilsen, E. H., Jr., Newman, P. R., Nitta, A., Okada, N., Okamura, S., Ostriker, J. P., Owen, R., Pauls, A. G., Peoples, J., Peterson, R. S., Petravick, D., Pope, A., Pordes, R., Postman, M., Prosapio, A., Quinn, T. R., Rechenmacher, R., Rivetta, C. H., Rockosi, C. M., Rosner, R., Ruthmansdorfer, K., Sandford, D., Schneider, D. P., Scranton, R., Sekiguchi, M., Sergey, G., Sheth, R., Shimasaku, K., Smee, S., Snedden, S. A., Stebbins, A., Stubbs, C., Szapudi, I. and Szkody, P.: The Ghost of Sagittarius and Lumps in the Halo of the Milky Way Sloan Digital Sky Survey: Early Data Release. Astrophysical Journal {\bf 569} (2002), 245-274

O'Dell, C. R., Balick, B., Hajian, A. R., Henney, W. J. and Burkert, A.: Knots in Nearby Planetary Nebulae. Astronomical Journal 123 (2002), 3329-3347

Odenkirchen, M., Grebel, E. K., Dehnen, W., Rix, H.-W. and Cudworth, K. M.: Kinematic Study of the Disrupting Globular Cluster Palomar 5 Using VLT Spectra. The Astronomical Journal, 124 (2002), 1497-1510

Odenkirchen, M. and Soubiran, C.: NGC 6994 – clearly not a physical stellar ensemble. Astronomy and Astrophysics 383 (2002), 163-170

Ofek, E. O., Rix, H.-W., Maoz, D. and Prada, F.: A survey for large-separation lensed FIRST quasars – II. Magnification bias and redshift distribution. Monthly Notice of the Royal Astronomical Society, 337 (2002), 1163-1168

Orio, M., Harbeck, D., Gallagher, J. and Woodward, C.: V838 Monocerotis. International Astronomical Union Circular 7892 (2002), 1

Paunzen, E., Handler, G., Weiss, W. W., Nesvacil, N., Hempel, A., Romero-Colmenero, E., Vuthela, F. F., Reegen, P., Shobbrook, R. R. and Kilkenny, D.: On the Period-Luminosity-Colour-Metallicity relation and the pulsational characteristics of lambda Bootis type stars. Astronomy and Astrophysics 392 (2002), 515-528

Peng, C. Y., Ho, L. C., Impey, C. D. and Rix, H.-W.: Detailed Structural Decomposition of Galaxy Images. The Astronomical Journal 124 (2002), 266-293

Pentericci, L., Fan, X., Rix, H.-W., Strauss, M. A., Narayanan, V. K., Richards, G. T., Schneider, D. P., Krolik, J., Heckman, T., Brinkmann, J., Lamb, D. Q. and Szokoly, G. P.: VLT Optical and Near-Infrared Observations of the $z = 6.28$ Quasar SDSS J1030+0524. Astronomical Journal 123 (2002), 2151-2158

Pentericci, L., Kurk, J. D., Carilli, C. L., Harris, D. E., Miley, G. K. and Röttgering, H. J. A.: A Chandra study of X-ray sources in the field of the $z = 2.16$ radio galaxy MRC 1138-262. Astronomy and Astrophysics 396 (2002), 109-115

Poppe, T., Blum, J. and Henning, T.: Experiments on dust aggregation and their relevance to space missions. Advances in Space Research 29 (2002), S. 763-771.

Potter, D., Martín, E. L., Cushing, M. C., Baudoz, P., Brandner, W., Guyon, O. and Neuhäuser, R.: Hokupa'a-Gemini Discovery of Two Ultracool Companions to the Young Star HD 130948. Astrophysical Journal 567 (2002), S. L133-L136

Prada, F. and Burkert, A.: The Fundamental Line of the Local Group Satellites. Astrophysical Journal 564 (2002), S. L73-L76.

Pustilnik, S. A., Kniazev, A. Y., Masegosa, J., Márquez, I. M., Pramskij, A. G. and Ugryumov, A. V.: The metallicities of UM 151, UM 408 and A 1228+12 revisited. Astronomy and Astrophysics 389 (2002), S. 779-786

Pustilnik, S. A., Kniazev, A. Y., Lipovetsky, V. A. and Ugryumov, A. V.: Blue compact galaxies from SBS. VizieR Online Data Catalog 337 (2002), 30024

Quinten, M., Kreibig, U., Henning, T. and Mutschke, H.: Wavelength-dependent Optical Extinction of Carbonaceous Particles in Atmospheric Aerosols and Interstellar Dust. Applied Optics 41 (2002), S. 7102-7113

Rockosi, C. M., Odenkirchen, M., Grebel, E. K., Dehnen, W., Cudworth, K. M., Gunn, J. E., York, D. G., Brinkmann, J., Hennessy, G. S. and Ivezic, Z.: A Matched-Filter Analysis of the Tidal Tails of the Globular Cluster Palomar 5. Astronomical Journal 124 (2002), 349-363

Sahai, R., Brillant, S., Livio, M., Grebel, E. K., Brandner, W., Tingay, S. and Nyman, L.-Å. Proper Motions in the Knotty, Bipolar Jet in Henize 2-90. Astrophysical Journal 573 (2002), L123-L127

Salzer, J. J., Gronwall, C., Sarajedini, V. L., Lipovetsky, V. A., Kniazev, A., Moody, J. W., Boroson, T. A., Thuan, T. X., Izotov, Y. I., Herrero, J. L. and Frattare, L. M.: The KPNO International Spectroscopic Survey. III. [O III]-selected Survey List. Astronomical Journal 123 (2002), 1292-1306

Sarajedini, A., Grebel, E. K., Dolphin, A. E., Seitzer, P., Geisler, D., Guhathakurta, P., Hodge, P. W., Karachentsev, I. D., Karachentseva, V. E. and Sharina, M. E.: The Stellar Populations of the Cetus Dwarf Spheroidal Galaxy. Astrophysical Journal 567 (2002), 915-921

Sarzi, M., Rix, H.-W., Shields, J. C., McIntosh, D. H., Ho, L. C., Rudnick, G., Filippenko, A. V., Sargent, W. L. W. and Barth, A. J.: Limits on the Mass of the Central Black Hole in 16 Nearby Bulges. Astrophysical Journal 567 (2002), 237-246

Schödel, R., Ott, T., Genzel, R., Hofmann, R., Lehnert, M., Eckart, A., Mouawad, N., Alexander, T., Reid, M. J., Lenzen, R., Hartung, M., Lacombe, F., Rouan, D., Gendron, E., Rousset, G., Lagrange, A.-M., Brandner, W., Ageorges, N., Lidman, C., Moorwood, A. F. M., Spyromilio, J., Hubin, N. and Menten, K. M.: A star in a 15.2-year orbit around the supermassive black hole at the centre of the Milky Way. Nature 419 (2002), S. 694-696.

Schrempel, F., Jäger, C., Fabian, D., Dorschner, J., Henning, T. and Wesch, W.: Study of the amorphization process of MgSiO2 by ion irridation as a form of dust processing in astrophysical environments. NIM B 191 (2002), 411-415

Schreyer, K., Henning, T., van der Tak, F. F. S., Boonman, A. M. S. and van Dishoeck, E. F.: The Young Intermediate-mass Stellar Object AFGL 490 – A disk Surrounded by a Cold Envelope. Astronomy and Astrophysics 394 (2002), 561-583

Schulz, B., Huth, S., Laureijs, R. J., Acosta-Pulido, J. A., Braun, M., Castaneda, H. O., Cohen, M., Cornwall, L., Gabriel, C., Hammersley, P., Heinrichsen, I., Klaas, U., Lemke, D., Müller, T., Osip, D., Román-Fernández, P. and Telesco, C.: ISOPHOT – Photometric Calibration of Point Sources. Astronomy and Astrophysics 381 (2002), 1110-1130.

Slyz, A. D., Devriendt, J. E. G., Silk, J. and Burkert, A.: Forming stars on a viscous time-scale: the key to exponential stellar profiles in disc galaxies? Monthly Notices of the Royal Astronomical Society 333 (2002), 894-910

Smith, G. H. and Burkert, A.: On the Low-Mass End of the Globular Cluster Luminosity Function. Astrophysical Journal 578 (2002), L51-L54.

Stecklum, B., Brandl, B., Henning, T., Pascucci, I., Hayward, T. L. and Wilson, J. C.: High Resolution Mid-infrared Imaging of W3(OH). Astronomy and Astrophysics 392 (2002), 1025-1029

Steinacker, J., Bacmann, A. and Henning, T.: Application of Adaptive Multi-Frequency Grids to Three-Dimensional Astrophysical Radiative Transfer. J. Quant. Spectr. Rad. Transf. 75 (2002), 765-786

Stickel, M., Klaas, U., Lemke, D. and Mattila, K.: Far-Infrared Emission from Intracluster Dust in Abell Clusters. Astronomy and Astrophysics 383 (2002), 367-383

Stolte, A., Grebel, E. K., Brandner, W. and Figer, D. F.: The mass function of the Arches cluster from Gemini adaptive optics data. Astronomy and Astrophysics 394 (2002), 459-478

Stoughton, C., Lupton, R. H., Bernardi, M., Blanton, M. R., Burles, S., Castander, F. J., Connolly, A. J., Eisenstein, D. J., Frieman, J. A., Hennessy, G. S., Hindsley, R. B., Ivezic, Z., Kent, S., Kunszt, P. Z., Lee, B. C., Meiksin, A., Munn, J. A., Newberg, H. J., Nichol, R. C., Nicinski, T., Pier, J. R., Richards, G. T., Richmond, M. W., Schlegel, D. J., Smith, J. A., Strauss, M. A., SubbaRao, M., Szalay, A. S., Thakar, A. R., Tucker, D. L., Vanden Berk, D. E., Yanny, B., Adelman, J. K., Anderson, J. E., Jr., Anderson, S. F., Annis, J., Bahcall, N. A., Bakken, J. A., Bartelmann, M., Bastian, S., Bauer, A., Berman, E., Boehringer, H., Boroski, W. N., Bracker, S., Briegel, C., Briggs, J. W., Brinkmann, J., Brunner, R., Carey, L., Carr, M. A., Chen, B., Christian, D., Colestock, P. L., Crocker, J. H., Csabai, I., Czarapata, P. C., Dalcanton, J., Davidsen, A. F., Davis, J. E., Dehnen, W., Dodelson, S., Doi, M., Dombeck, T., Donahue, M., Ellman, N., Elms, B. R., Evans, M. L., Eyer, L., Fan, X., Federwitz, G. R., Friedman, S., Fukugita, M., Gal, R., Gillespie, B., Glazebrook, K., Gray, J., Grebel, E. K., Greenawalt, B., Greene, G., Gunn, J. E., de Haas, E., Haiman, Z., Haldeman, M., Hall, P. B., Hamabe, M., Hansen, B., Harris, F. H., Harris, H., Harvanek, M., Hawley, S. L., Hayes, J. J. E., Heckman, T. M., Helmi, A., Henden, A., Hogan, C. J., Hogg, D. W., Holmgren, D. J., Holtzman, J., Huang, C.-H., Hull, C., Ichikawa, S.-I., Ichikawa, T., Johnston, D. E., Kauffmann, G., Kim, R. S. J., Kimball, T., Kinney, E., Klaene, M., Kleinman, S. J., Klypin, A., Knapp, G. R., Korienek, J., Krolik, J., Kron, R. G., Krzesinski, J., Lamb, D. Q., Leger, R. F., Limmongkol, S., Lindenmeyer, C., Long, D. C., Loomis, C., Loveday, J., MacKinnon, B., Mannery, E. J., Mantsch, P. M., Margon, B., McGehee, P., McKay, T. A., McLean, B., Menou, K., Merelli, A., Mo, H. J., Monet, D. G., Nakamura, O., Narayanan, V. K., Nash, T., Neilsen, E. H., Jr., Newman, P. R., Nitta, A., Odenkirchen, M., Okada, N., Okamura, S., Ostriker, J. P., Owen, R., Pauls, A. G., Peoples, J., Peterson, R. S., Petravick, D., Pope, A., Pordes, R., Postman, M., Prosapio, A., Quinn, T. R., Rechenmacher, R., Rivetta, C. H., Rix, H.-W., Rockosi, C. M., Rosner, R., Ruthmansdorfer, K., Sandford, D., Schneider, D. P., Scranton, R., Sekiguchi, M., Sergey, G., Sheth, R., Shimasaku, K., Smee, S., Snedden, S. A., Stebbins, A., Stubbs, C., Szapudi, I., Szkody, P., Szokoly, G. P., Tabachnik, S., Tsvetanov, Z., Uomoto, A., Vogeley, M. S., Voges, W., Waddell, P., Walterbos, R., Wang, S.-i., Watanabe, M., Weinberg, D. H., White, R. L., White, S. D. M., Wilhite, B., Wolfe, D., Yasuda, N., York, D. G., Zehavi, I. and Zheng, W.: Sloan Digital Sky Survey: Early Data Release. In: The Astronomical Journal, Vol. 123 (2002), 485-548

Torres, S., García-Berro, E., Burkert, A. and Isern, J.: High-proper-motion white dwarfs and halo dark matter. Monthly Notices of the Royal Astronomical Society 33} (2002), 971-978

Tóth, L. V., Kiss, C., Juvela, M., Stickel, M., Lisenfeld, U. and Hotzel, S.: Extending the limits of globule detection. ISOPHOT Serendipity Survey observations of interstellar clouds II. Astronomy and Astrophysics 395 (2002), 663-667

Tuffs, R. J., Popescu, C. C., Pierini, D., Völk, H. J., Hippelein, H., Leech, K., Metcalfe, L., Heinrichsen, I. and Xu, C.: Erratum: »Far-Infrared Photometry of a Statistical Sample of Late-Type Virgo Cluster Galaxies«. Astrophysical Journal Supplement Series 140 (2002), 609-609

Tuffs, R. J., Popescu, C. C., Pierini, D., Völk, H. J., Hippelein, H., Leech, K., Metcalfe, L., Heinrichsen, I. and Xu, C.: Far-Infrared Photometry of a Statistical Sample of Late-Type Virgo Cluster Galaxies. Astrophysical Journal Supplement Series 139 (2002), 37-79

Venemans, B. P., Kurk, J. D., Miley, G. K., Röttgering, H. J. A., van Breugel, W., Carilli, C. L., De Breuck, C., Ford, H., Heckman, T., McCarthy, P. and Pentericci, L.: The Most Distant Structure of Galaxies Known: A Protocluster at $z = 4.1$. Astrophysical Journal 569 (2002), L11-L14

Villar-Martín, M., Vernet, J., di Serego Alighieri, S., Fosbury, R., Pentericci, L., Cohen, M., Goodrich, R. and Humphrey, A.: Giant low surface brightness haloes in distant radio galaxies: USS0828+193. Monthly Notices of the Royal Astronomical Society 336 (2002), 436-444

Winn, J. N., Kochanek, C. S., McLeod, B. A., Falco, E. E., Impey, C. D. and Rix, H.-W.: PKS 1830-211: A Face-on Spiral Galaxy Lens. Astrophysical Journal 575 (2002), 103-110

Woitas, J., Eislöffel, J., Mundt, R. and Ray, T. P.: The Environment of FS Tauri Observed with Hubble Space Telescope Wide Field Planetary Camera 2 in Narrowband Emission Line Filters. Astrophysical Journal 564 (2002), 834-838

Wolf, S., Voshchinnikov, N. V. and Henning, T.: Multiple scattering of polarized radiation by non-spherical grains: First results. Astronomy and Astrophysics 385 (2002), 365-376

Wolf, S., Gueth, F., Henning, T. and Kley, W.: Detecting Planets in Protoplanetary Disks: A Prospective Study. Astrophysical Journal 566 (2002), L97-L99

Young, O. R. C., Meixner, M. M., Fong, D., Haas, M., Rudolf, A. L. and Tielens, A. G. G. M.: Testing Models of Low-Excitation Photodissociation Regions with Far-Infrared Observations of Reflection Neublae. Astrophysical Journal 578 (2002), 885-896

Zapatero Osorio, M. R., Béjar, V. J. S., Martín, E. L., Rebolo, R., Navascués, D. B., Mundt, R., Eislöffel, J. and Caballero, J. A.: A Methane, Isolated, Planetary-Mass Object in Orion. Astrophysical Journal 578 (2002), 536-542

Zaritsky, D., Harris, J., Thompson, I. B., Grebel, E. K. and Massey, P.: The Magellanic Clouds Photomtric Survey: The Small Magellanic Cloud Stellar Catalog and Extinction Map. Astronomical Journal 123 (2002), 855-872.

In Conference Proceedings

Ábrahám, P., Moor, A., Kiss, C., Héraudeau, P. and del Burgo, C.: Circumstellar dust around main-sequence stars: what can we learn from the ISOPHOT archive? In: C. Gry et al. (eds.), Exploiting the ISO Data Archive: Infrared Astronomy in the Internet Age SP-511. ESA, Vilspa (2002), 129-132.

Alvarez, C. A. and Hoare, M. G.: Near-IR Speckle Imaging of Massive YSOs. In: Crowther, P. E. (ed.): Near-IR Speckle Imaging of Massive YSOs. Hot Star Workshop III: The Earliest Stages of Massive Star Birth., ASP Conference Proceedings 267. Astronomical Society of the Pacific, San Francisco (2002), 335

Andersen, D. R. and Bershady, M. A.: Dense-Pak Halpha Velocity Fields of Face-On Disk Galaxies. In: Bulletin of the American Astronomical Society. American Astronomical Society Meeting 201, Washington, D.C. (2002), 68.05

Andersen, D. R. and Bershady, M. A.: The Intrinsic Ellipticity of Spiral Disks. In: Athanassoula, E., Bosma, A., Mujica, R. (eds.), Disks of Galaxies: Kinematics, Dynamics and Perurbations 275. Astron. Society of the Pacific, San Francisco (2002), 39-42

Apai, D., Henning, T. and Stecklum, B.: High-Resolution Near-IR Study of Regions of Massive Star Formation. In: Crowther, P. A. (ed.): High-Resolution Near-IR Study of Regions of Massive Star Formation. Hot Star Workshop III: The Earliest Stages of Massive Star Birth., Conference Proceedings 267. Astronomical Society of the Pacific, San Francisco, USA (2002), 337

Bacciotti, F., Ray, T. P., Mundt, R., Eislöffel, J. and Solf, J.: High Angular Resolution Analyses of Herbig-Haro Jets. In: High Angular Resolution Analyses of Herbig-Haro Jets. The Origins of Stars and Planets: The VLT View. Proceedings of the ESO Workshop, ESO, (2002), 253-258

Bailer-Jones, C. A. L.: Automated stellar classification for large surveys: a review of methods and results. In: Gupta, R., Singh, H. P., Bailer-Jones, C. A. L. (eds.), Automated Data Analysis in Astronomy, Narosa Publishing House, New Delhi (2002), 83-98

Bailer-Jones, C. A. L., Gupta, R. and Singh, H. P.: An introduction to artificial neural networks. In: Gupta, R., Singh, H. P., Bailer-Jones, C. A. L. (eds.), Automated Data Analysis in Astronomy, Narosa Publishing House, New Delhi (2002), 51-68

Bailer-Jones, D. M. and Bailer-Jones, C. A. L.: Modelling data: Analogies in neural networks, simulated annealing and genetic algorithms. In: Magnani, L. (ed.): Model-based Reasoning, Kluwer/Plenum, Dordrecht (2002), 85-102

Barrado Y Navascués, D., Zapatero Osorio, M. R., Béjar, V., Rebolo, R., Martín, E. L., Mundt, R. and Bailer-Jones, C. A. L.: VLT/FORS Spectroscopy in s; Orionis: Isolated Planetary Mass Candidate Members. In: The VLT View. The Origins of Stars and Planets, Proceedings of the ESO Workshop. ESO, (2002), 195-200

Baumann, O., Röser, H.-J., Tschamber, C., Hawkins, M. R. S. and MacGillivray, H.: Deep Photographic Clusters Survey - DPCS. In: Borgani, S., Mezzetti, M., Valdarnini, R. (eds.), Tracing cosmic evolution with galaxy clusters, ASP Conference Series 268. Astronomical Society of the Pacific, San Francisco (2002), 333-334

Beckwith, S. V. W., Rix, H.-W., Peng, C., McIntosh, D., Caldwell, J., Meisenheimer, K., Wolf, C., Wisotzki, L., Borch, A., Haeussler, B., Barden, M. and Collaboration, G.: Galaxy Evolution from Morphology and SEDs (GEMS): a large, multi-color mosaic with HST's Advanced Camera for Surveys. American Astronomical Society Meeting 201. (2002). #32.08

Bershady, M. A., Verheijen, M. and Andersen, D. R.: WIYN Integral-Field Kinematics of Disk Galaxies. In: Athanassoula, E., Bosma, A., Mujica, R. (eds.), Disks of Galaxies: Kinematics, Dynamics and Perurbations, 275. Astronomical Society of the Pacific, San Francisco (2002), S. 43-46.

Bertschik, M. and Burkert, A.: Minor Mergers of Galaxies: Theory vs. Observations. Galaxy evolution, theory and observations. In: The Origins of Stars and Planets: The VLT View, Proceedings of the ESO Workshop. The VLT View ESO (2002), 7

Burkert, A. M. and Bodenheimer, P.: Core Collapse and the Formation of Binaries. In: Proceedings of the ESO Workshop The Origins of Stars and Planets: The VLT View. ESO (2002), 101-104

Butler, D., Ku, J. and Swanson, T.: Loop Heat Pipes and Capillary Pumped Loops-An Applications Perspective. In: AIP Conf. Proc. 608: Space Technology and Applications International Forum, (2002), 49

Datta, S., Pittroff, L., Guhathakurta, P., Grebel, E. and Harbeck, D.: Keck Spectroscopy of Red Giants in the M 31 dSph Satellites: Chemical Abundance Spread. In: American Astronomical Society Meeting 201, (2002), #14.14

Davies, R. I., Bonaccini, D., Rabien, S., Hackenberg, W., Ott, T., Hippler, S., Neumann, U., Barden, M., Lehnert, M., Eisenhauer, F. and Genzel, R.: Multi-Conjugate Adaptive Optics with Laser Guide Stars. In: Scientific Drivers for ESO Future VLT/VLTI, Proceedings of the ESO Workshop ESO (2002), 158

del Burgo, C. et al.: The far-infrared signature of dust in high-latitude regions. In: Exploiting the ISO Data Archive. Infrared Astronomy in the Internet Age (2002), 18

del Burgo, C., Héraudeau, P. and Ábrahám, P.: Re-analysed steps of the ISOPHOT calibration scheme: reset interval correction, transient correction, and by-passing sky light subtraction. In: C. Gry et al. (eds.), Exploiting the ISO Data Archive – Infrared Astronomy in the Internet, SP-511. ESA (2002), 339-342

del Burgo, C., Héraudeau, P. et al.: Improved calibration strategy for faint objects. In: Improved calibration strategy for faint objects. Exploiting the ISO Data Archive. Infrared Astronomy in the Internet Age (2002), 17

del Burgo, C., Laureijs, R. J., Ábraháam, P. and Kiss, C.: Far-infrared colours of high-latitude dust regions. In: C. Gry et al., (eds.), Exploiting the ISO Data Archive: Infrared Astronomy in the Internet Age, SP-511. ESA, Vilspa (2002), 195-198

Edgar, M. L., Zmuidzinas, J., Harris, A. I., Erickson, N. R., Colgan, S. W. J. and Haas, M. R.: CASIMIR, A High Resolution, Submillimeter, Heterodyne Spectrometer for Airborne Astronomy. In: American Astronomical Society Meeting, 200 (2002)

Fan, X., Narayanan, V. K., Strauss, M. A., Lupton, R. H., Becker, R. H., White, R. L., Pentericci, L. and Rix, H.-W.: z = 6 Quasars from the SDSS: Probing the End of the Dark Ages. In: ESO (ed.): Light of the Universe: The Most Luminous Celestial Objects and their Use for Cosmology. Lighthouses of the Universe: Proceedings of the MPA/ESO, Springer-Verlag series »ESO Astrophysics Symposia«, (2002), 309

Feldt, M., Puga, E., Weiß, A. R. and Hippler, S.: The Massive Star Forming Region S106. In: Crowther, P. A. (ed.): Hot Star Workshop III: The Earliest Stages of Massive Star Birth, ASP Conference Proceedings 267. Astronomical Society of the Pacific, San Francisco (2002), 367

Flynn, G. J., Henning, T., Keller, L. P. and Mutschke, H.: Infrared Spectroscopy of Cosmic Dust. In: Optics of Cosmic Dust (2002), S. 37

Grady, C., Woodgate, B., Stapelfeldt, K., Padgett, D., Stecklum, B., Henning, T., Grinin, V., Quirrenbach, A. and Clampin, M.: HST/STIS Coronagraphic Imaging of the Disk of DM Tauri. American Astronomical Society Meeting 201 (2002)

Grady, C. A., Woodgate, B., Stapelfeldt, K., Padgett, D., Stecklum, B., Henning, T., Grinin, V., Quirrenbach, A., Clampin, M., Wassel, E., Rhodes, J., Paliunas, P. and Brinkmann, J.: Coronagraphic Imaging of DL Tau and CW Tau with HST/STIS and the Goddard Fabry-Perot at Apache Point Observatory. American Astronomical Society Meeting 200 (2002)

Grebel, E. K., Brandner, W. (eds.): Modes of Star Formation and the Origin of Field Populations. ASP conference series 285. Astronomical Society of the Pacific, San Francisco (2002)

Grebel, E. K., Odenkirchen, M. and Harbeck, D.: The Structure of the Sextans Dwarf Spheroidal Galaxy From SDSS Data. In: American Astronomical Society Meeting 200. American Astronomical Society,(2002)

Guenther, E., Joergens, V., Torres, G., Neuhäuser, R., Fernández, M. and Mundt, R.: Preparing for the VLTI: A Search for Pre-Main Sequence Spectroscopic Binaries. In: The Origins of Stars and Planets: The VLT View. Proceedings of the ESO Workshop. ESO (2002), S. 431-436

Haas, M.: Distant dust – high redshift in the ISO archive. In: Exploiting the ISO Data Archive. Infrared Astronomy in the Internet Age, (2002), 27

Haas, M.: Luminous Dust Emission in Active Galaxies as Seen by ISO. In: C. Gry et al. (eds.): Exploiting the ISO Data Archive – Infrared Astronomy in the Internet Age, SP-511. ESA (2002), 257-262

Haas, M. and Klaas, U.: What powers the PAH emission in galaxies? In: Exploiting the ISO Data Archive. Infrared Astronomy in the Internet Age, SP-511. ESA, (2002), 283-284

Hamilton, C. M., Herbst, W., Rhodes, A., Bailer-Jones, C. A. L., Mundt, R., Vrba, F. J., Mazeh, T., von Hippel, T., Crowe, R., Ibrimahov, M., Haisch, K., Webster, Z. and Scholz, A.: Detection of Significant Structure in the Circumstellar Disk of a Pre-Main Sequence Star. In: American Astronomical Society Meeting 200. American Astronomical Society (2002)

Handler, G., Weiss, W. W., Shobbrook, R. R., Garrido, R., Paunzen, E., Hempel, A., Moalusi, M. B., Anguma, S. K., Kalebwe, P. C., Guzik, J. A., Beach, T. E., Me Dupe, R., Chagnon, F., Matthews, J. M., Reegen, P. and Granzer, T.: Multi-site observations of rapidly oscillating Ap stars: HD 99563 and HD 122970. In: ASP Conf. Ser. 256: Observational Aspects of Pulsating B- and A Stars (2002), 109

Harbeck, D.-R.: Chemical Inhomogeneities in the Old Stellar Populations of the Local Group. In: American Astronomical Society Meeting 201 (2002), #108.04

Harbeck, D., Smith, G. H. and Grebel, E. K.: External Enrichment Processes in 47 Tuc? American Astronomical Society Meeting 200, American Astronomical Society (2002)

Hegyi, S., Horváth, C., Németh, I., Keresztesi, M., Hegyi, A., Kovács, Z., Diósy, T., Kabai, S. and Bérczi, S.: Solar Panel and Electric Power System of Hunveyor-2 University Lander: Experiments for Various Planetary Insolations. In: Experiments for Various Planetary Insolations. 33rd Annual Lunar and Planetary Science Conference, Lunar and Planetary Institute Conference Abstracts 33. LPI (2002), 1124

Henning, T.: Nanoparticles in Space and the Laboratory. In: Salama, F. (ed.): Nanoparticles in Space and the Laboratory. NASA Laboratory Astrophysics Workshop, Book of Abstracts of the NASA LAW NASA-Ames Research Center (2002), 51

Henning, T., Feldt, M. and Stecklum, B.: High-Resolution Studies of Massive Star-Forming Regions. In: Hot Star Workshop III: The Earliest Stages of Massive Star Birth. ASP Conference Ser. 267. Astronomical Society of the Pacific, San Francisco (2002), S. 153-164.

Héraudeau, P., del Burgo, C., Stickel, M., Efstathiou, A., Rowan-Robinson, M., Oliver, S., Kiss, C., Ábrahám, P., Klaas, U. and Lemke, D.: The European Large Area ISO Survey: 90 microns number counts. In: C. Gry et al. (eds.), Exploiting the ISO Data Archive – Infrared Astronomy in the Internet Age, SP-511. ESA, Vilspa (2002), 325-330

Jeon, Y.-B., Kim, S.-L., Lee, H. and Lee, M. G.: Time Series CCD Photometry of the Globular Cluster M 53. In: ASP Conf. Ser. 259: IAU Colloq. 185: Radial and Nonradial Pulsations as Probes of Stellar Physics (2002), 140

Joergens, V., Guenther, E., Neuhäuser, R., Comerón, F., Huélamo, N., Alves, J. and Brandner, W.: Multiplicity of Young Brown Dwarfs in Cha I. In: The Origins of Stars and Planets: The VLT View. Proceedings of the ESO Workshop (2002), 127

Kemper, F., Jäger, C., Waters, L. B. F. M., Henning, T., Molster, F. J., Barlow, M. J., Lim, T. and de Koter, A.: Carbonates in Dust Shells Around Evolved Stars. In: Lunar and Planetary Institute Conference Abstracts, 33 (2002), 1193

Kessel-Deynet, O. and Burkert, A.: Dynamics of Molecular Clouds Under the Influence of Ionizing Radiation from Young Massive Stars. In: Revista Mexicana de Astronomia y Astrofisica Conference Series, 12 (2002), 25-26

Kimball, A. E., McKay, T. A., Rix, H.-W., Grebel, E. and Sheldon, E. S.: Population Studies of Galaxies Satellites in the Sloan Digital Sky Survey. In: American Astronomical Society Meeting 201. AAS, (2002), #13.07.

Kiss, C., Ábrahám, P., Klaas, U., Lemke, D., del Burgo, C. and Héraudeau, P.: An archive survey of cirrus structures with ISOPHOT. In: C. Gry et al. (eds.), Exploiting the ISO Data Archive - Infrared Astronomy in the Internet Age, SP-511. ESA, Vilspa (2002), 189-194.

Klaas, U., Haas, M., Richards, P. J., Walker, H. H. and Wilke, K.: Extragalactic Research with ISOPHOT Pipeline Products. In: C. Gry et al. (eds.), Exploiting the ISO Data Archive – Infrared Astronomy in the Internet Age, SP-511. ESA, Vilspa (2002), S. 247-250

Kleinheinrich, M., Erben, T., Meisenheimer, K., Rix, H.-W., Schirmer, M., Schneider, P. and Wolf, C.: Galaxy-Galaxy Lensing in the COMBO-17 Survey. In: Avila-Reese, V., Firmani, C., Frank, C., Allen, C. (eds.), Galaxy evolution, theory and observations, RevMexAA (2002), 34

Klessen, R. S.: Mass Spectra from Turbulent Fragmentation. In: The Origins of Stars and Planets: The VLT View. Proceedings of the ESO Workshop. (2002), 61-66

Kraft, S., Van Hoof, C. A., Katterloher, R. O., Rosenthal, D., Rumitz, M., Grözinger, U., Hofferbert, R. and Beeman, W.: Qualification status of the stressed photoconductor arrays for the PACS instrument aboard Herschel. In: Berghmans, F., Taylor, E. W. (eds.), Photonics for Space and Radiation Environments II. Remote Sensing, 4547. SPIE (2002), 374-385

Kranz, T., Slyz, A. D. and Rix, H.-W.: The Stellar Mass Density within Spiral Galaxy Disks. In: Athanassoula, E., Bosma, A., Mujica, R. (eds.), Disks of Galaxies: Kinematics, Dynamics and Perturbations, Astronomical Society of the Pacific, San Francisco (2002), S. 35-38

Krause, O., Lisenfeld, U., Stickel, M., Lemke, D. and Klaas, U.: ISOPHOT's Serendipity Survey unveils an unusual ULIRG. In: C. Gry et al. (eds.), Exploiting the ISO Data Archive – Infrared Astronomy in the Internet Age, SP-511}. ESA, Vilspa (2002), 285-288.

Krause, O., Vavrek, R., Lemke, D., T\'oth, L. V., Klaas, U. and Stickel, M.: Cold dust in luminous star forming regions. In: Kiss, C. (ed.): Interaction of stars with their environment II. Budapest (2002)

Krause, O., Vavrek, R., Lemke, D., Tóth, L. V., Klaas, U. and Stickel, M.: Follow-up studies of very young intermediate and high mass star forming regions detected by the ISOPHOT Serendipity Survey. In: C. Gry et al. (eds.), Exploiting the ISO Data Archive – Infrared Astronomy in the Internet Age, SP-511. ESA, Vilspa (2002), 133-136

Kümmel, M. W., Heidt, J., Wagner, S. J., Appenzeller, I. et al.: Number counts and Angular Correlation functions for the FORS Deep Field. In: Deep Fields. ESO Astrophysics Symposia, Springer, Heidelberg (2002), 159

Kurk, J. D., Pentericci, L., Röttgering, H. J. A. and Miley, G. K.: Observations of Radio Galaxy MRC 1138-262: Merging Galaxies Embedded in a Giant Ly alpha Halo. In: Revista Mexicana de Astronomia y Astrofisica Conference Series, 13 (2002), 191-195

Kurk, J. D., Venemans, B. P., Röttgering, H. J. A., Miley, G. K. and Pentericci, L.: A Search for High Redshift Clusters Associated with Radio Galaxies at $2 < z < 4$. In: ASP Conf. Ser. 268: Tracing Cosmic Evolution with Galaxy Clusters (2002), 19

Launhardt, R., Stecklum, B. and Sargent, A. I.: A Close View on the Protoplanetary Disk in the Bok Globule CB 26. In: Alves, J. F., McCaughrean, M. J. (eds.), The Origins of Stars and Planets: The VLT View., ESO (2002), 319-324

Lee, H., Grebel, E. K. and Hodge, P. W.: The Chemical Abundances of Southern Dwarf Irregular Galaxies. In: American Astronomical Society Meeting {\bf 201}. (2002), \#14.21.

Ligori, S., Herbst, T. M. and Robberto, M.: Thermal IR imaging of W51-IRS2. In: Crowther, P. A. (ed.): Hot Star Workshop III: The Earliest Stages of Massive Star Birth. Astronomical Society of the Pacific, San Francisco (2002), S. 383-384.

Llamas, J. I., Mutschke, H., Clément, D. and Henning, T.: Laboratory in-situ infrared spectroscopy of carbon nanoparticles. In: C. Gry et al. (eds.), Exploiting the ISO Data Archive - Infrared Astronomy in the Internet Age, SP-511. ESA (2002), S. 49

Maier, C. M.: Mapping Acidalia Mensa: Redefining Northern Plains Units and Possible Deformation History. In: Lunar and Planetary Institute Conference Abstracts, 33 (2002), 1360

Martin, E. L., Zapatero Osorio, M. R., Bejar, V. J. S., Rebolo, R., Barrado y Navascues, D., Mundt, R., Eisloffel, J. and Caballero, J. A.: Direct Imaging and Spectroscopy of a Young Jupiter-like Object. American Astronomical Society Meeting 200, (2002)

Meisenheimer, K., Maier, C. M., Hippelein, H., Roeser, H.-J., Fried, J., Kümmel, M., von Kuhlmann, B., Phleps, S., Rix, H. W. et al.: The CADIS search for Lyman-α Galaxies. In: ESO Astrophysics Symposia, Springer, Heidelberg (2002)

Meyer, M. R., Backman, D., Beckwith, S. V. W., Brooke, T. Y., Carpenter, J. M., Cohen, M., Gorti, U., Henning, T., Hillenbrand, L. A., Hines, D., Hollenbach, D., Lunine, J., Malhotra, R., Mamajek, E., Morris, P., Najita, J., Padgett, D. L., Soderblom, D., Stauffer, J., Strom, S. E., Watson, D., Weidenschilling, S. and Young, E.: The Formation and Evolution of Planetary Systems: SIRTF Legacy Science in the VLT Era. In: The Origins of Stars and Planets: The VLT View. Proceedings of the ESO Workshop 2001, (2002), 463

Moór, A., Ábrahám, P., Kiss, C., Héraudeau, P. and del Burgo, C.: A full scale photometric investigation of the ISOPHOT minimap mode. In: C. Gry et al. (eds.), Exploiting the ISO Data Archive – Infrared Astronomy in the Internet Age, SP-511. ESA, Vilspa (2002), 353-356

Neuhäuser, R., Guenther, E., Brandner, W., Húelamo, N., Ott, T., Alves, J., Cómeron, F., Cuby, J.-G. and Eckart, A.: Direct Imaging and Spectroscopy of Substellar Companions Next to Young Nearby Stars in TWA. In: The

Origins of Stars and Planets: The VLT View. Proceedings of the ESO Workshop (2002), 383

Odenkirchen, M., Grebel, E. K., Dehnen, W., Rix, H. W., Rockosi, C. M., Newberg, H. and Yanny, B.: The Extended Tails of Palomar 5: A Ten Degree Arc of Globular Cluster Tidal Debris. American Astronomical Society Meeting 200 (2002)

Pentericci, L., Kurk, J. D., Röttgering, H. J. A., Miley, G. K. and Venemans, B. P.: The Population of Galaxies in the Forming Cluster around the Radio Galaxy MRC 1138-262 at z = 2.2. In: ASP Conf. Ser. 268: Tracing Cosmic Evolution with Galaxy Clusters (2002), S. 23

Rabien, S., Davies, R. I., Ott, T., Hippler, S. and Neumann, U.: PARSEC: the laser for the VLT. In: Tyson, R. K., Bonaccini, D., Roggemann, M. C. (eds.), PARSEC: Adaptive Optics Systems and Technology II, Proc. SPIE 4494. (2002), 325-335

Ray, T. P. and Mundt, R.: Exploring the Central Engines of Young Stars. In: Revista Mexicana de Astronomia y Astrofísica Conference Series, 13 (2002), 83-89

Richards, P. J. and Klaas, U.: Development of the ISOPHOT Pipeline during the Active Archive Phase. In: Exploiting the ISO Data Archive. Infrared Astronomy in the Internet Age, SP-511. ESA, Vilspa (2002), 357-360

Robberto, M., Beckwith, S. V. W., Ligori, S., Herbst, T. M., Custo, A., Boccacci, P. and Bertero, M.: Mid-IR Imaging of the BN/KL Region. In: Henney, W. J., Franco, J., Martos, M., Pena, M. (eds.), Revista Mexicana de Astronomía y Astrofísica Conference Series. Ionized Gaseous Nebulae, 12. Instituto de Astronomía, Universidad Nacional Aut\'onoma de M\'exico, Mexico City, Mexico (2002), 40-40

Singh, H. P., Bailer-Jones, C. A. L. and Gupta, R.: Principal component analysis and its application to stellar spectra. In: Gupta, R., Singh, H. P., Bailer-Jones, C. A. L. (eds.), Automated Data Analysis in Astronomy, Narosa Publishing House, New Delhi (2002), 69-82

Soderblom, D., Meyer, M. R., Backman, D., Beckwith, S. V. W., Brooke, T. Y., Carpenter, J. M., Cohen, M., Gorti, U., Henning, T., Hillenbrand, L. A., Hines, D., Hollenbach, D., Kim, S., Lunine, J., Malhotra, R., Mamajek, E., Moro-Martin, A., Morris, P., Najita, J., Padgett, D. L., Stauffer, J., Strom, S. E., Watson, D., Weidenschilling, S., Wolf, S. and Young, E.: Formation and Evolution of Planetary Systems: A SIRTF Legacy Science Program Progess Report. American Astronomical Society Meeting 201 (2002)

Stecklum, B., Brandl, B., Feldt, M., Henning, T., Linz, H. and Pascucci, I.: Infrared Observation of Hot Cores: Based on observations collected at the European Southern Observatory, La Silla, Chile. In: The Origins of Stars and Planets: The VLT View. Proceedings of the ESO Workshop. ESO (2002), 225-230

Stickel, M.: The complex far-infrared morphology of M86. In: C. Gry et al. (eds.), Exploiting the ISO Data Archive: Infrared Astronomy in the Internet Age, SP-511. ESA, Vilspa (2002), 289-292

Stickel, M., Lemke, D., Klaas, U., Krause, O., Tóth, L. V., Vavrek, R. and Hotzel, S.: The Scientific Potential of the ISOPHOT Serendipity Sky Survey. In: C. Gry et al. (eds.), Exploiting the ISO Data Archive: Infrared Astronomy in the Internet Age, SP-511}. ESA, Vilspa (2002), 169-176

Stickel, M., Lemke, D., Klaas, U., Krause, O., Vavrek, R., Tóth, L. V. and Hotzel, S.: Multi-Wavelength Data Mining of the ISOPHOT Serendipity Sky Survey. In: Astronomical Telescopes and Instrumentation.. 4847. SPIE, Waikoloa (2002)

Stolte, A., Grebel, E. K., Brandner, W. and Figer, D. F.: Infrared Imaging of the Arches Cluster – Adaptive Optics in the densest region of the Milky Way. In: Grebel, E. K., Geisler, D., Minniti, D. (eds.), Extragalactic Star Clusters. IAU Symp. 207, ASP Conference Series, Astronomical Society of the Pacific, San Francisco (2002), 132

Stolte, A., Grebel, E. K., Brandner, W. and Figer, D. F.: Mass Function of the Arches Cluster from Gemini Adaptive Optics Data. In: De Buizer, J. M. (ed.): Galactic Star Formation Across the Stellar Mass Spectrum. IAOC Workshop, ASP Conference Series, Astronomical Society of the Pacific (2002)

Stolte, A., Grebel, E. K., Brandner, W., Iwamuro, F., Maihara, T. and Motohara, K.: The IMF in Young Massive Star Forming Regions. In: Alves, J., McCoughrean, M. J. (eds.), The Origins of Stars and Planets: The VLT View. ESO Astrophysics Symposium XXVII, European Southern Observatory (2002)

Stolte, A., Ibata, R., Rix, H.-W., Yanny, B. and Ivezic, Z.: Constraints on the Sagittarius Dwarf Galaxy's Tidal Stream. In: Brandner, W., Grebel, E. K. (eds.), Modes of Star Formation and the Origin of Field Star Populations. MPIA Workshop, ASP Conference Series, Astronomical Society of the Pacific, San Francisco (2002), 195

Tuffs, R. J., Popescu, C. C., H.J., V., Pierini, D., Hippelein, H. and al..: ISOPHOT observations of Late-Type Virgo Cluster Galaxies. In: ISOPHOT observations of Late-Type Virgo Cluster Galaxies. ASP Conference Series 268 (2002), 447

Waters, L. B. F. M., Leinert, C., Graser, U., Perrin, G., Lopez, B. and Jaffe, W.: The Scientific Potential of MIDI in the 20 Micron Window. In: Scientific Drivers for ESO Future VLT/VLTI Instrumentation, Proc. of the ESO Workshop, ESO (2002), 314

Wilke, K., Stickel, M., Haas, M., Herbstmeier, U., Klaas, U. and Lemke, D.: The Small Magellanic Cloud in the Far Infrared: New ISO Results. In: C. Gry et al. (eds.), Exploiting the ISO Data Archive: Infrared Astronomy in the Internet Age. SP-511. ESA, Vilspa (2002), 235-238.

Wolf, S., Henning, T. and D'Angelo, G.: Detecting Gaps in Protoplanetary Disks with MIDI at the VLTI. In: The Origins of Stars and Planets: The VLT View. Proceedings of the ESO Workshop, ESO (2002), 325

Xu, W. and Seifert, W.: Optical glasses with high NIR transmission. In: Astronomical Telescopes and Instrumentation 2002: Ground-based Telescopes and Instrumentation, 4842. Bellingham, WA, USA (2002)

Zheng, W., Ford, H., Tsvetanov, Z., Davidsen, A., Szalay, A., Kruk, J., Hartig, G., Stockman, P., Postman, M., Rix, H.-W., Lenzen, R. and Shu, P.: Search for the First Quasars and Supernovae. In: Lighthouses of the Universe: The

Most Luminous Celestial Objects and their Use for Cosmology, Proceedings of the MPIA/ESO. Springer-Verlag series »ESO Astrophysics Symposia« (2002), 323

Popular Articles

Brandner, W., Rousset, G., Lenzen, R., Hubin, N., Lacombe, F., Hofmann, R., Moorwood, A., Lagrange, A.-M., Gendron, E., Hartung, M., Puget, P., Ageorges, N., Biereichel, P., Bouy, H., Charton, J., Dumont, G., Fusco, T., Jung, Y., Lehnert, M., Lizon, J.-L., Monnet, G., Mouillet, D., Moutou, C., Rabaud, D., Röhrle, C., Skole, S., Spyromilio, J., Storz, C., Tacconi-Garman, L. and Zins, G.: NAOS+CONICA at YEPUN: first VLT adaptive optics system sees first light. The ESO Messenger 107 (2002), 1.

Bührke, T. and Lenzen, R.: NAOS-CONICA. Die neue Höchstleistungskamera am VLT. Sterne und Weltraum 4 (2002), 24

Harbeck, D., Grebel, E. K. and Smith, G. H.: Evidence for external enrichment processes in the globular cluster 47 Tuc? The Messenger 108 (2002), 26

Hofferbert, R.: Infrarot-Astronomie am Lagrangepunkt L2. Ein neuer Höhenrekord für CRYOPERM? VACumschau – Firmenzeitschrift der Vakuumschmelze Hanau (2002), 8-9

Lemke, D.: Größer, schneller, tiefer... Sterne und Weltraum 12 (2002), 26-30

Meisenheimer, K. and Wolf, C.: COMBO-17: Fifty thousand galaxies at a glance. Astronomy and Geophysics 43 (2002), 15-13

Meisenheimer, K. and Wolf, C.: Zehntausende Galaxien auf einen Blick. Sterne und Weltraum 1 (2002), 22-30

Pentericci, L., Rix, H. W., Fan, X. and Strauss, M.: The VLT and the most distant quasars. The ESO Messenger 108 (2002), 24

Staude, J.: Berge auf Planeten und Monden. In: Der Berg. H. Gercke (ed.), Heidelberger Kunstverein, Kehrer Verlag, Heideberg (2002), 16-21

Staude, J.: Die Bilder der Astronomen. In: B. Zimmer: Ursprung Auge Farbe Welten. Wienand Verlag, Köln (2002), 168-179

Diploma Theses

Drepper, Sabine: Stellare Dichtestruktur der Milchstraße. Ruprecht-Karls-Universität, Heidelberg

Tschamber, Carsten: Verification of distant galaxy cluster using Wide Field Imager data. Ruprecht-Karls-Universität, Heidelberg

Doctoral Theses

Maier, Christian: Emission Line Galaxies from CADIS: High-Redshift Lyman-alpha Galaxies and Metal Poor Galaxies at Medium Redshift. Ruprecht-Karls-Universität, Heidelberg.

Patents

Krause, O. Grözinger, U., Böhm, A. Lemke, D.: German Patent Application 10036910 (2002) Position Sensor

Heidelberg – City map

The Max Planck Society

The Max Planck Society for the Promotion of Sciences was founded in 1948. In succession to the Kaiser Wilhelm Society, which was founded in 1911, the Max Planck Society operates at present 78 Institutes and other facilities dedicated to basic and applied research. With an annual budget of around 1.25 billion € in the year 2001, the Max Planck Society has about 12000 employees, of which one quarter are scientists. In addition, annually about 7000 junior and visiting scientists are working at the Institutes of the Max Planck Society.

The goal of the Max Planck Society is to promote centers of excellence at the forefront of the international scientific research. To this end, the Institutes of the Society are equipped with adequate tools and put into the hands of outstanding scientists, who have a high degree of autonomy in their scientific work.

Max-Planck-Gesellschaft zur Förderung der Wissenschaften
Public Relations Office
Hofgartenstr. 8
D-80539 München

Tel.: 0049-89-2108-1275 or -1277
Fax: 0049-89-2108-1207
Internet: http://www.mpg.de

MAX-PLANCK-GESELLSCHAFT